KU LEUVEN

FACULTY OF
ENGINEERING SCIENCE

Extraction and characterization of extracellular polymeric substances from various wastewater treatment sludges

Vedran Vangramberen

Thesis submitted for the degree of
Master of Science in
Chemical Engineering, option
Product Engineering

Supervisors:
Prof. dr. ir. Ilse Smets
Prof. dr. ir. Peter Van Puyvelde

Assessors:
Prof. dr. ir. Florence Vermeire
ir. Huiyu Chen

Assistant-supervisors:
dr. ir. Anja Vananroye
ir. Hannah Vanhoof

Academic year 2024 – 2025

Preface

The past five years of becoming a chemical engineer have been an incredible journey, in which I had the privilege to tackle some interesting projects, to collaborate with many intelligent and wonderful people and to develop myself. In this journey, I truly discovered my passion for research. This master thesis might be the end of my master's degree, but I hope it may serve as a beginning for my further research-oriented career. All of this was enabled by some inspiring people, to whom I would like to show my gratitude.

First of all, I would like to thank my promoters prof. dr. ir. Peter Van Puyvelde and prof. dr. ir. Ilse Smets creating a thesis topic, sitting in both SMaRT and CREaS divisions. It was a pleasure to collaborate with both of them, as our meetings made me experience a combination of so many brilliant ideas and the passion to investigate them, which even further sparked the flame in me to make the best out of this project. Thank you for the constructive guidance, feedback and support which kept me on the right track throughout the year. Without them, this thesis would not have been what it is today.
My appreciation also goes towards my assistant-supervisors dr. ir. Anja Vananroye and ir. Hannah Vanhoof, for their unlimited support in- and outside the lab. Their doors were always open for me, to ask questions or report problems regarding my results, while also making time for correcting and guiding me when needed. Their knowledge and ideas assured my advancement throughout the year, while the freedom they provided also enabled me to define the destiny of this work myself. I could not have imagined better assistant-supervisors.

Next, I would like to show my gratitude towards everyone in the SMaRT and CREaS labs, who supported me all year round. Being able to work in two labs full of intelligent people really encouraged me to make as much out of the thesis as possible. I would also like show my appreciation to my assessors prof. dr. ir. Florence Vermeire and ir. Huiyu Chen for making time to read and evaluate this work.

Finally, the most important people in my life, my friends, family and partner in life, Shawn. Thank you for all of your support and help during the past five years. Without you, I would not have become the person I am today.

Vedran Vangramberen

Contents

Abstract

High-quality liquid water is one of the most precious goods on earth, which must be preserved at all costs. Companies and municipalities contribute to this goal by treating their wastewater before disposing it in nature. However, while avoiding the pollution of natural waters, another waste stream arises, namely excess sludge produced during biological wastewater treatment. To date, no large-scale application of this stream has been found, as most is either disposed of or incinerated. With the shift towards a circular economy in mind, research on possible applications of this stream is of utmost importance. One component of this waste sludge that shows potential for various applications is the extracellular polymeric substances (EPS), a complex mixture of different biopolymers that act as a glue, keeping sludge aggregates together. Their complex composition results in a versatile material that can be used for many applications, some of which utilize their ability to form hydrogels. However, a whole process must be followed before EPS can be applied.

First, the EPS must be obtained from the waste sludge using a specific extraction protocol. Standardization of this extraction is important, as different protocols result in a different composition of the extracted EPS. Hence, four extraction protocols are applied to the same biomass to compare the extracted EPS and visualize the effects of varying the extraction protocol. This comparison enables the selection of the optimal protocol, which is applied in the remainder of this work.

In the second step, the EPS must be chemically characterized, as they are known to depend on many external factors. The chemical fingerprints of EPS extracted from four different industrial sludge samples are determined via Nuclear Magnetic Resonance, Raman, and Fourier-Transform Infrared Spectroscopy and are compared to each other to get a notion of the effects of different operating conditions on the EPS. Comparisons are made between EPS from granular and floccular sludges, as well as salt-adapted and non salt-adapted sludges. EPS are also extracted from three pure cultures, which are then compared to the industrial sludges as well.

After these two steps, one possible application of EPS is studied, specifically its use as a hydrogel. An attempt is made to link the chemical composition of EPS to the rheological characteristics and gelation behavior of hydrogels made from them. To facilitate this, EPS-based hydrogels are compared to two model polysaccharides, namely alginate and κ-carrageenan. It is expected that the gelation of EPS hydrogels is more complex than that of the model systems due to the EPS being composed of various biomolecules, including proteins, polysaccharides, and lipids. No definite conclusions could be made due to the EPS's complex composition.

List of Figures

List of Tables

List of Abbreviations, Symbols and Chemical species

Abbreviations

3D-EEM	Three-Dimensional Excitation-Emission Matrix
AGS	Aerobic Granular Sludge
ALE	Alginate-Like Exopolymers
ANAMMOX	ANaerobic AMMonium OXidizing
AnGS	Anaerobic Granular Sludge
APHA	American Public Health Association
AOB	Ammonium Oxidizing Bacteria
BOD	Biochemical Oxygen Demand
CER	Cation Exchange Resin
CLSM	Confocal Laser Scanning Microscopy
CSTR	Continuous Stirred Tank Reactor
E. coli	*Escherichia coli*
eEPS	extractable Extracellular Polymeric Substances
EGSB	Expanded Granular Sludge Blanket
EPS	Extracellular Polymeric Substances
FTIR	Fourier Transform InfraRed spectroscopy
GFP	Green Fluorescent Protein
HRT	Hydraulic Retention Time
ICP-MS	Inductively Coupled Plasma Mass Spectrometer
ICP-OES	Inductively Coupled Plasma Optical Emission Spectrometer
LVER	Linear ViscoElastic Regime
MBR	Membrane BioReactor
MLSS	Mixed Liquor Suspended Solids
MLVSS	Mixed Liquor Volatile Suspended Solids
MWCO	Molecular Weight Cut Off
NASA	North American Space Agency
NMR	Nuclear Magnetic Resonance

NOB	Nitrite Oxidizing Bacteria
OLR	Organic Loading Rate
PHA	PolyHydroxyAlkanoate
PFR	Plug Flow Reactor
SBR	Sequential Batch Reactor
SEM	Scanning Electron Microscopy
SDS-PAGE	Sodium Dodecyl Sulfate PolyAcrylamide Gel Electrophoresis
SGBR	Static Granular Bed Reactor
TOC	Total Organic Concent
TS	Total Solids
TSS	Total Suspended Solids
UASB	Upflow Anaerobic Sludge Blanket
VMM	Vlaamse Milieumaatschappij
VS	Volatile Solids
WRRF	Water Resource Recovery Facility
WWTP	WasteWater Treatment Plant

Symbols

g	Free-fall acceleration	$[m/s^2]$
G'	Storage modulus	[Pa]
G"	Loss modulus	[Pa]

Chemical species

Ca^{2+}	Calcium cation
Cu^{2+}	Copper cation
CH_4	Methane
CO_2	Carbon dioxide
H_2	Hydrogen gas
HCl	Hydrogen Chloride
H_2S	Hydrogen sulfide
K^+	Potassium cation
N_2	Nitrogen gas
Na^+	Sodium cation
NaCl	Sodium chloride
Na_2CO_3	Sodium carbonate
$Na_2C_2O_4$	Sodium oxalate
NaOH	Sodium hydroxide
Ni^{2+}	Nickel cation
NO_2^-	Nitrite anion
NO_3^-	Nitrate anion
Pb^{2+}	Lead cation
PETG	Polyethylene terephthalate glycol
PO_4^{3-}	Phosphate anion
O_2	Oxygen gas
SO_4^{2-}	Sulphate anion
Zn^{2+}	Zinc cation

Chapter 1

Introduction

According to the North American Space Agency (NASA), liquid water is one of the three enablers of life [151]. Not only aquatic fauna and flora rely on water of sufficient quality to survive, it is also important for industrial processes, especially for the final product quality [52, 119, 165, 193]. To ensure a high environmental water quality, many governments have implemented rules for wastewater discharge [38, 210, 216].

Despite both physical processes, such as sedimentation and UV-radiation, and chemical processes, like chlorination [23, 198, 235], being employed to treat wastewater, biochemical processes, in which activated sludge is added to the wastewater, are applied most often due to their low cost [48, 150]. Organisms inside the sludge remove the pollutants from the wastewater by using them as an energy source [73]. The main downside of this treatment is the production of vast amounts of excess sludge, without any added value as most is either disposed or incinerated [46, 223].

With the transition to a circular economy, possible uses of such a waste stream must be considered [111, 158]. Apart from the organisms, sludge also contains other constituents, among which the extracellular polymeric substances or EPS [133, 155]. The EPS are a mixture of various biopolymers including polysaccharides and proteins [87] and show potential for replacing chemical polymers as well as utilization as hydrogel for heavy metal uptake [157]. As these applications require pure EPS, the sludge must undergo an extraction process, which is not straightforward as no standardized method has been reported in literature [59, 213]. As the extraction protocol influences the extracted EPS composition, it is important to standardize the extraction method [59, 67].

Another difficulty with EPS is that their composition depends on both the organisms inside the sludge, as well as their environment, resulting in possible variability in composition over time [182]. Hence, it is important to characterize the EPS before further processing, as differences in EPS composition might affect their final usability. This can be at various levels of complexity, ranging from very general tests that determine the total protein content [135] to more precise tests that can

distinguish different proteins [50], for example, by molecular fingerprinting [91, 146]. A comparison of the fingerprints of EPS from different sources can induce a better understanding of which EPS or which organisms are dominating in a particular system.

This master thesis first investigates four different extraction protocols to select the optimal method to be applied in the remainder of this work. Next, EPS are extracted from several sources, ranging from pure cultures to more complex industrial sludge samples, and their chemical fingerprints are compared. Finally, the EPS from industrial sludges are also compared to two model systems, sodium alginate and κ-carrageenan, which are often used in hydrogel applications. Their chemical and thermal properties are determined, as well as their rheological behavior, which is important for the application of EPS as a hydrogel. An attempt is made to link the mechanical properties of the EPS hydrogels to their chemical fingerprints based on the observations of the model systems.

Chapter 2

Literature study

Going from a wastewater treatment plant (WWTP) to characterized extracellular polymeric substances (EPS) is challenging, as numerous factors in this process can influence the final results. Therefore, the current literature study focuses on the crucial steps in this process.

Section 2.1 provides a general introduction to wastewater treatment plants (WWTPs). Next, **Section 2.2** focuses on the two most important distinctions for wastewater treatment which are relevant in this paper: aerobic versus anaerobic processes and floccular versus granular sludge. **Section 2.3** then covers the applicability of sludge systems for treating highly saline wastewaters, along with their associated difficulties. Afterwards, **Section 2.4** gives a detailed overview of the EPS extraction methods. An overview of the possible characterization methods is given in **Section 2.5**. Finally, **Section 2.6** discusses several current and future applications of EPS, with the focus being put on utilizing EPS as a hydrogel. **Section 2.7** draws a conclusion to this literature review.

2.1 General introduction to industrial wastewater treatment plants

According to the North American Space Agency (NASA), liquid water is one of the three key ingredients that make life possible, besides chemistry and energy [151]. Not only do aquatic fauna and flora rely on water of sufficient quality to survive, as poor water quality can disturb an entire ecosystem [52, 165], but industrial processes also require sufficient water quality, as it influences the final product quality [119, 193]. Hence, high-quality water in its liquid form must be preserved at all costs.

This goal is already reflected in the policies of several governments and local agencies, as specific guidelines or obligations regarding wastewater discharge are imposed [38, 210]. An example is given by the *Act on the protection of the surface waters against pollution*, imposed by the Flanders Environment Agency [216], prohibiting companies from discharging wastewater containing high concentrations of pollutants

without any permit. Hence, companies must treat wastewater to remove pollutants with a minimal efficiency and until the concentration is below a certain maximum level [212]. To comply with all these criteria, companies treat their wastewater thoroughly by installing a wastewater treatment plant (WWTP), of which a general overview is provided in the next section.

2.1.1 Primary, secondary and tertiary wastewater treatment

As shown in Figure 2.1, a WWTP consists of four distinct segments: namely, pretreatment, primary, secondary, and tertiary treatment [150]. Each segment focuses on the removal of specific contaminants and pollutants from the wastewater.

The first step in the WWTP is pretreatment, in which large debris, such as paper and plastics, present in the wastewater are removed, thereby reducing the risk of damage to the equipment in the remainder of the plant. This section mainly consists of screens and sieves with different opening sizes [212].

The next stage is the primary treatment, during which sand and grit are removed through sedimentation and oils and greases through flotation, both physical processes [198]. Calculations by Iyare showed that microplastics as small as 27 μm can also be removed via these mechanisms [97]. Both processes rely on a difference in density and in size of the particles or agglomerates to be removed as the main driving forces. During these processes, part of the biochemical oxygen demand (BOD, biodegradable organic material) and total suspended solids (TSS, material floating in the wastewater) are also removed, including both smaller debris and large clumps of organisms.

After removing larger debris, oils, fats, and sand, the secondary treatment commences. This stage of the WWTP is the primary focus of the remainder of this current study. This stage is the only one in which the pollutants are removed biologically [48, 150]. A microbiological community containing multiple species of bacteria, archaea, protozoa, and metazoa are added to the wastewater to form an activated sludge mixture. According to Garnaey *et al.*, activated sludge can be seen as *"a bacterial biomass suspension (that) is responsible for the removal of pollutants"* [73]. The organisms present in the sludge break down the pollutants in the wastewater biochemically. Several different setups for secondary wastewater treatment exist, with one distinction being made between aerobic and anaerobic treatment.

The final stage of the WWTP is tertiary treatment, in which micropollutants, such as non-biodegradable organic matter, pharmaceuticals, microplastics, as well as residual microorganisms are removed [229]. Tertiary treatment is performed when the discharge norms are not met after secondary treatment or when very high water quality is required, such as for water reuse [235]. Similar to secondary wastewater treatment, various methods exist for tertiary treatment, including physical methods, such as sand filtration [56, 86] and UV-radiation [176, 235], as well as chemical methods like chlorination [23, 235] and ozonation [4, 220, 222].

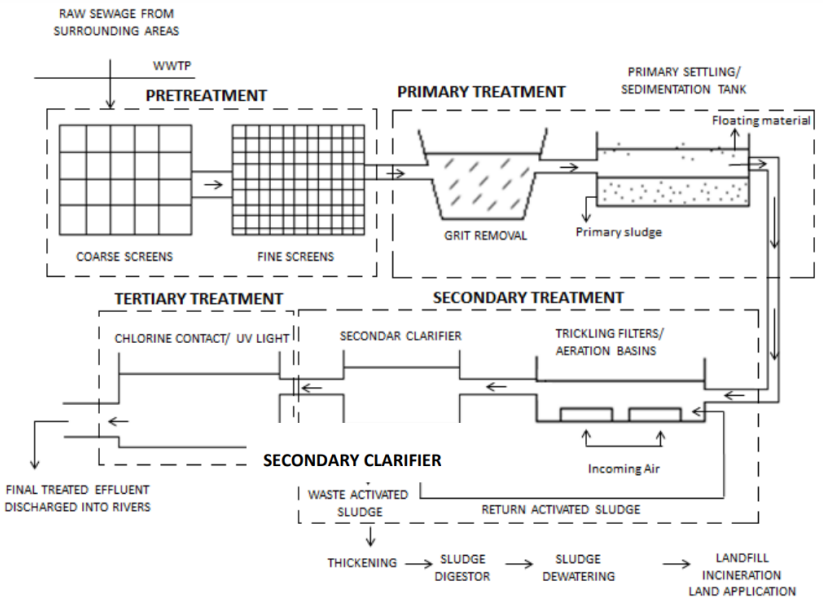

FIGURE 2.1: General overview of a wastewater treatment plant, with the different stages of treatment indicated. Taken from Naidoo *et al.* (2013) [150].

2.2 Distinctions in biological wastewater treatment

Secondary, or biological wastewater treatment can be performed under various conditions, each with its own specific requirements and specifications. The most important distinction, as already mentioned in the previous section, is between aerobic and anaerobic processes. Another possible differentiation, focusing more on the sludge morphology, is between granular sludge and floccular sludge systems. This section covers both differences, as they are addressed later in this work.

2.2.1 Aerobic versus anaerobic processes

As established in the previous subsection, the main distinction to be made for biological (secondary) wastewater treatment is between aerobic and anaerobic processes. During aerobic treatment, oxygen gas (O_2) serves as an electron acceptor for the organisms in the activated sludge, enabling the oxidation reactions happening in the reactor [191]. One of the most important difficulties of O_2 is its poor solubility in (fresh) water, being only $1.22 \cdot 10^{-3}$ $\frac{\text{mol}}{\text{L}}$ at atmospheric pressure [227]. It is also beneficial for aerobic processes to have a homogeneous oxygen concentration throughout the reactor. For these reasons, mixed reactors are most often employed, as these provide better aeration [98]. During anaerobic processes, nitrate (NO_3^-), sulfate (SO_4^{2-}), and the biomass itself, act as electron acceptors [64, 144, 233]. Both aerobic and anaerobic processes are equally important during the removal of organic carbon, nitrogen and phosphorus components, as discussed in the paragraphs below, which is why activated sludge often contains both types of organisms.

Carbon removal Carbon can be removed both aerobically and anaerobically. During aerobic treatment, the organic pollutants present in the wastewater are oxidized to carbon dioxide (CO_2) [104]. This results in the release of energy, which can be utilized for intracellular processes, cell multiplication, or the synthesis of more biological material, such as excess sludge [46, 114, 174]. This is accomplished by aerobic, heterotrophic bacteria like *Pseudomonas* and *Alcaligenes* species [12]. Anaerobic systems can also degrade organic materials. In this process, a mixture of methane (CH_4) and CO_2, known as biogas, is formed in a four-stage process consisting of hydrolysis, acidogenesis, acetogenesis, and methanogenesis step [144]. The first three steps are performed by facultative anaerobic bacteria, like *Firmicutes*, *Bacteroidetes*, and *Syntrophomonas*, while the final step is mostly carried out by archaea, including *Methanosaeta* and *Methanosarcina* [152]. Anaerobic carbon removal also results in the formation of excess sludge, albeit in lower quantities than aerobic treatment [46].

Nitrogen removal Nitrogen is removed via a combination of an aerobic and anaerobic step. Oxygen must be supplied during the nitrification [184], in which ammonium (NH_4^+) is oxidized to nitrate (NO_3^-) using a two-step process. First, ammonium oxidizing bacteria (AOB), such as the *Nitrosomonas* and *Nitrosospira* genera, oxidize the NH_4^+ to nitrite (NO_2^-) [11], followed by the oxidation of NO_2^- to NO_3^-, by nitrite oxidizing bacteria (NOB), including *Nitrobacter* or *Nitrococcus* [168]. During the anaerobic part of the process, denitrifiers such as *Azoarcus communis* and *Dietzia maris* utilize the produced NO_3^- as an oxidant to break down organic matter, converting it into energy and nitrogen gas (N_2) [184]. During this process, the absence of O_2 must be ensured, as it inhibits the expression and activity of most nitrogen-reducing proteins, even at concentrations as low as 0.1 mg O_2 per liter [136].

Phosphorus removal Also during biological phosphorus removal, an aerobic step is required, in which polyhydroxyalkanoates (PHAs) are oxidized using O_2 to form polyphosphate structures [22]. This step uses inorganic phosphate (PO_4^{3-}) present in the wastewater as a PO_4^{3-} source, resulting in its removal from the wastewater, which is necessary as excessively high phosphate concentrations in water bodies can lead to eutrophication of the flora [106]. This aerobic step must be preceded by an anaerobic one, in which the required PHAs are formed [22]. Bacteria like *Candidatus* Phosphoribacter, previously known as *Tetrasphaera*, are the dominant organisms for biological phosphorus removal [194].

2.2.2 Floccular versus granular sludge

Activated sludge, used during biological wastewater treatment, can be divided into two categories: the more conventional floccular sludge and the granular sludge. Instead of considering the types of biochemical processes taking place, the focus is now put on the sludge morphology.

Figure 2.2 shows obvious differences between granular sludge, characterized by larger and more closely packed aggregates (a and b), and floccular systems, con-

taining smaller and looser aggregates (c and d) [108]. This difference in size and packing density leads to different behavior of the sludges when employed in a WWTP. Defining granular sludge can be rather difficult, as the definition of larger and more closely packed is quite subjective. For this reason, its definition for aerobic treatment was established after the first aerobic granular sludge workshop, held in Delft in 2004 [45], as *"Granules making up aerobic granular activated sludge are to be understood as aggregates of microbial origin, which do not coagulate under reduced hydrodynamic shear, and which settle significantly faster than activated sludge flocs."* [45].

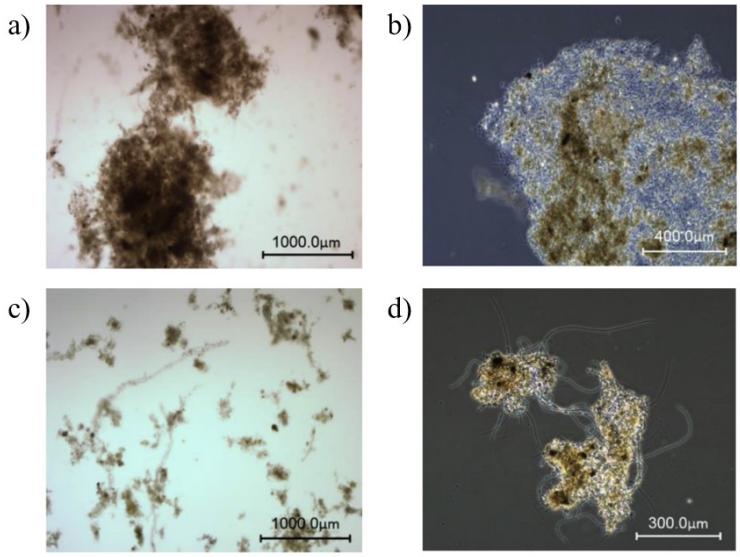

FIGURE 2.2: Microscopic images of granular sludge (a and b) and floccular sludge (c and d). Taken from Krysiak-Baltyn *et al.* (2019) [108].

Due to the difference in morphology, granular sludge behaves differently compared to the more conventional floccular sludge. The first difference is visible after the biological treatment when the formed sludge must be removed from the effluent. This is usually carried out in a secondary settling tank, where treated water is removed from the top, while the sludge sediments and becomes more concentrated [161]. However, such a settler can be expensive and very space-consuming since a large surface area is desired. Hence, granular sludge systems with a settling rate up to 5.7 times higher than floccular sludge are used preferably, as these require a smaller surface area [45, 236]. This difference in settling rate is a direct effect of the larger size and density of the granules [43]. Another advantage of granular sludge is its lower excess sludge production, compared to floccular sludges [40], which is important the disposal of this waste stream can account for up to half of the running costs of a wastewater treatment plant [156].

Granulation also induces changes in the microbiological structure of the sludge, as Krysiak-Baltyn *et al.* found that the surface of sludge granules has sulfur-enriched zones, compared to flocs made with the same sewage feed [108]. Santegoeds *et al.*

also discovered in their research that gradients in sulfate-reducing bacteria exist in granular sludges [181].
Pronk even found that granular sludge has the ability to combine aerobic and anaerobic processes into one granule, as oxygen can only penetrate into the outer layers of the granules, but not into the inner part due to the resistance of diffusion [167]. Therefore, aerobic organisms can be found in the outer layers of the granule, while anaerobic organisms are more commonly found more towards the center [44, 225]. For the less compact floccular sludge, the aggregate size and compactness are too low to form such gradients [167].
In anaerobic treatment processes, the granule structure also facilitates the degradation of pollutants in the wastewater by inducing a syntrophic symbiosis between the organisms inside the granule. Some sludge organisms use the byproducts of other organisms' metabolism as their primary food source. Hence, the presence of all these organisms close to each other facilitates following the whole metabolic pathway [192]. Figure 2.3 from Hulshoff Pol *et al.* [94] shows the typical layered structure of anaerobic granular sludge schematically, as proposed by MacLeod *et al.* [138]. The hydrogen gas (H_2) producing acidogens are located in the outer layers of the granule, while the middle layer consists of a range of methanogenic archaea, such as *Methanosarcina*, *Methanococcales*, and *Methanospirillum*-like organisms, which both produce and consume H_2 [81]. Finally, the *Methanosaeta* archaea, which produce biogas from either acetate or H_2 and CO_2 and are oxygen-sensitive, are mostly abundant in the center of the granules [186].

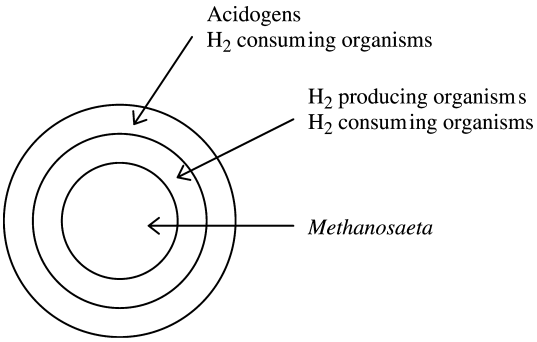

Figure 2.3: Typical layered structure, observed in anaerobic granular sludge [138]. Taken from Hulshoff Pol *et. al* (2004) [94].

The granule also serves as a protective layer for the microorganisms in the sludge against environmental dangers, like predators, extreme pH and highly salinity [192].

Importance of extracellular polymeric substances in aggregation

Sludge aggregates do not only contain microorganisms, as can be seen in Figure 2.4 [155]. Other components, such as filamentous organisms and extracellular polymeric substances (EPS), are also present inside the granule [133]. A balanced combination of these species facilitates the formation of flocs and granules [128]. The EPS, the primary focus of the remainder of this work, serve as a glue, keeping the different

sludge components tightly together. Hence, the importance of EPS for the formation and properties of sludge flocs and granules cannot be underestimated [133].

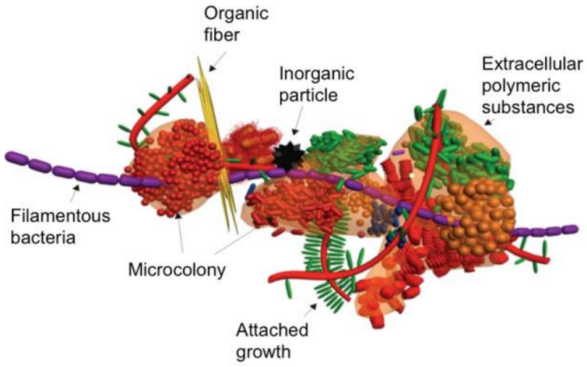

FIGURE 2.4: Different components present in activated sludge aggregates. Taken from Nielsen (2012) [155].

EPS are a mixture of many polymeric substances, including polysaccharides, proteins and nucleic acids, like DNA, as well as humic acids and lipids [87]. They play an essential role in the advantages of aggregated sludge, such as its increased settleability and protection from pollutants in the wastewater, such as heavy metals or other exogenous toxic compounds [209]. They also affect the sludge adsorption ability, adhesion, dewaterability and stability [129, 153]. Induced by the appropriate wastewater composition and operational conditions, sludge flocs can be transformed into granules, which can be seen as more intensified aggregates.

Settlability and granule formation
Sludge settlability depends on the size and density of the aggregates. The higher both values, the higher the settling rate [43]. EPS improve the settlability by decreasing the surface charge of the different organisms in a granule, thereby decreasing intercellular repulsion, enabling the formation of larger aggregates. Additionally, other interactions between different proteins and polysaccharides, like hydrogen bonds and hydrophobic interactions, also promote the formation of larger aggregates [89, 231]. This aggregation depends on both the composition and the amount of EPS produced, which in turn depend on the operating conditions, as well as the type of microorganisms present in the bioreactor [163, 199]. Liu *et al.* found that proteins are the most dominant component of the EPS and that an increased protein concentration leads to an easier formation of sludge granules or aggregates [129]. He also observed that granular sludge contains more EPS than floccular sludges, indicating that granule formation requires a certain amount of EPS. He also discovered that anaerobic granules produce more EPS than aerobic ones. Lastly, he also realized that more hydrophobic EPS result in better sludge aggregation [129].
Ni *et al.* conducted a similar comparison as Liu *et al.*, specifically focusing on the formation of granules in anaerobic ammonium oxidating (anammox) sludge. They observed that anammox sludge produces more EPS compared to other anaerobic and

aerobic sludges, and that so-called *"low-enriched granules"* exhibit greater granule strength and therefore better stability. These granules are characterized by proteins being spread out throughout the entire granule, while cells are most abundant in the outer layer [153].

Protection from harsh environments
EPS can also enhance the performance of sludges when used to remove pollutants from harsh environments [209]. The EPS act as a protective barrier for the microorganisms against heavy metals and toxic compounds, like phenol or other aromatics [74, 99, 189]. Proteins are the primary constituents of the EPS that provide this protection, as they contain negatively charged functional groups, such as hydroxyl and carboxyl groups [27]. These functional groups then chelate the heavy metal ions in the wastewater, thereby preventing direct contact between the microorganisms and the heavy metals [232]. Highly saline wastewater streams can also be seen as harsh environments for the sludge. As such streams are relatively common in industry, they are covered in Section 2.3.

Other effects of EPS
EPS directly affect the stability of biofilms by influencing the microbial adhesion and the formation of a matrix structure. More hydrophobic EPS are known to stabilize the biofilm made [27, 131, 132].
As higher dewaterability leads to a lower final sludge volume, it is an important parameter for waste sludge disposal. Hydrophilic groups in the EPS, like hydroxyl and carboxyl groups, can attract water, decreasing the sludge dewaterability [162].
Lastly, according to research by Liu *et al.*, EPS can also improve phosphorus removal from wastewater, as inorganic phosphorus can be contained in the EPS from aerobic granular sludge [130].

2.2.3 Applications of granular sludge

Most research on granular sludge has been conducted on aerobic granular sludge (AGS). AGS can be used to remove organic compounds from wastewater from breweries, papermaking and the dairy industry, as well as to treat landfill leachates [70]. The technology can even be used to treat wastewater rich in phenol, at concentrations up to 833 $\frac{\text{mg}}{\text{L}}$ [99]. AGS is versatile, as it can remove carbon-based pollutants, as well as nitrogen and phosphorus, from wastewater. However, at the industrial scale, AGS systems still encounter some difficulties due to the high aeration costs and mass transfer problems within the granules [70]. Both factors result in an increased difficulty in treating wastewater with a high organic loading. For those waters, it is preferable to replace the AGS system with an Upflow Anaerobic Sludge Blanket (UASB) reactor, which contains Anaerobic Granular Sludge (AnGS). The advantages of UASB reactors include their ability to produce methane (CH_4) without requiring aeration [70]. The UASB reactor exhibits high efficiency, even at high organic loading, which is why it is often used as an alternative to conventional aerated systems [122].

Upflow Anaerobic Sludge Blanket (UASB) reactor as an application of anaerobic granular sludge

The Upflow Anaerobic Sludge Blanket (UASB) reactor was established by Lettinga *et al.* in 1980 [118]. This type of reactor has evolved to become the most cost-effective method for treating industrial wastewater with high organic loading ($\geq 5\frac{\text{kg}}{\text{m}^3\cdot\text{day}}$) on an industrial scale [35, 215].

A basic overview of a UASB is shown in Figure 2.5 [35]. Prior to the system startup, the column is seeded with an inoculum of anaerobic granular sludge. The influent wastewater enters the bottom of the reactor. This stream then flows upwards, carrying the lighter dispersed particles to the effluent of the reactor. Hence, spontaneous granulation plays a crucial role, as sufficiently fast sedimentation of the sludge is required to remain in the reactor [35]. The formation of sludge granules and flocs that are heavy enough to settle to the bottom of the tank is promoted. In this way, a dense sludge bed is formed, where most of the biochemical reactions occur [35].
As the reactor runs anaerobically, the carbon-based pollutants present in the influent are reduced to form biogas, a mixture of CH_4 and CO_2 [9]. These gases are separated from the sludge mixture using a gas-liquid-solid separator. The baffles are used to avoid sludge particles flowing out of the reactor. One of the key reasons for the success of the UASB is its combination of simplicity and effectivity, leading to its use in many sectors, ranging from tanneries and food processing to metal mining [103].

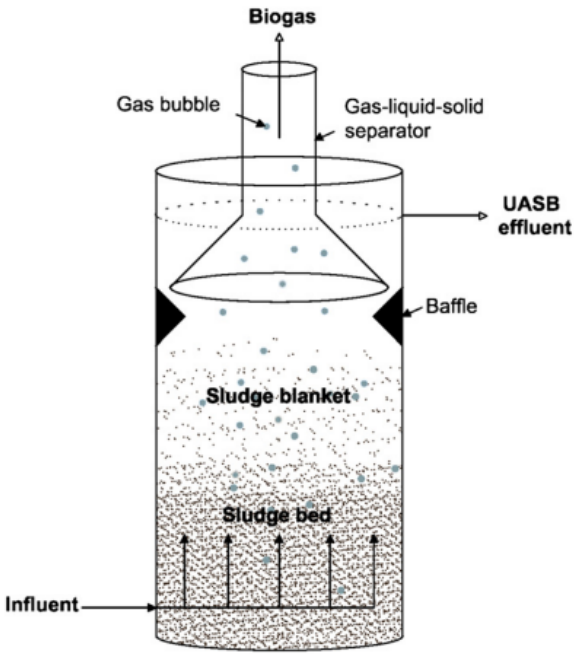

FIGURE 2.5: Schematic overview of a typical upflow anaerobic sludge blanket (UASB) reactor. Taken from Chong *et. al* (2012) [35].

To ensure the proper functioning of a UASB reactor, strict operational conditions, like temperature, hydraulic retention time (HRT) and organic loading rate (OLR), are maintained. Other key parameters, such as pH and total organic carbon (TOC) removal, are continuously monitored, as they provide valuable insights into the bioreactor's performance. pH values between 6 and 8 are desired for the good activity of most bacteria and archaea in the sludge [103].

The use of a UASB reactor has several advantages over more conventional, aerobic treatment, such as eliminating the aeration costs and producing up to twelve times less excess sludge [46]. Another advantage is that part of the energy from the biomass can be recovered via the CH_4 present in the biogas [9]. The reactor also requires a relatively low footprint to operate while still maintaining a high efficiency in treating wastewater with a high loading [35, 215]. However, UASB reactors also have disadvantages, such as the long acclimatization time required compared to floccular sludge and the lower efficiency in removing organic matter, including pathogens and nutrients, compared to aerobic processes [35]. The latter has led to further studies being conducted to improve the UASB's effluent quality. Two other disadvantages are the heating requirements, as anaerobic processes require higher temperatures, and the potential production of unpleasant odors, due to the formation of hydrogen sulfide (H_2S) [35].

2.3 Sludge systems for treating highly saline streams

Approximately 5 % of the wastewater is considered saline, with salinity ranging from 15 to 150 $\frac{g}{L}$ [112, 116]. These wastewater streams originate from various industries, including seafood processing, textile industry, tanneries, dairy, and pharmaceutical industry [68, 226]. Wastewater with a higher salt concentration, up to 80 $\frac{g}{L}$ NaCl, is referred to as hypersaline. Such streams are mainly produced during the tanning of chromium and the pickling of food [115]. For a municipal WWTP, the influent salt concentrations are typically much lower, with values ranging from 0.013 to 0.020 $\frac{g}{L}$ for potassium ions (K^+) and from 0.05 to 0.25 $\frac{g}{L}$ for sodium ions (Na^+) [7].

To treat these saline streams, UASB reactors similar to those discussed in Section 2.2.3 can be used. The anaerobic operation of the UASB reactor is preferred when treating saline streams contaminated with persistent products. The advantages discussed in Section 2.2.3 remain applicable here [226]. However, high salinity also imposes several problems, which require attention.

2.3.1 Problems of highly saline wastewater treatment

The first problem associated with highly saline wastewater is its increased density compared to non-saline wastewater, which is caused by the presence of salts [115]. This results in a smaller density difference between the sludge and the wastewater, which is the driving force behind sedimentation. Even more problems arise when viewed from a cellular perspective, as cells generally experience osmotic stress [115].

The highly saline environment can lead to plasmolysis due to the increase in osmotic pressure [68]. High concentrations of monovalent salts are also known to inhibit methanogens in anaerobic granular sludge (AnGS) [204]. High salinity often leads to more difficult granule formation or even granule disruption in the UASB reactor [204] because the filamentous bacteria, which form the backbone of the granule, are more susceptible to plasmolysis at high salt concentrations [110]. The lower amounts of filamentous bacteria lead to the formation of smaller flocs rather than sludge granules. In addition, the high sodium ion (Na^+) concentration in the environment causes the expulsion of calcium ions (Ca^{2+}) from within the granule, resulting in a decreased granule strength and size. These Ca^{2+} ions contribute to stabilizing the granule structure by enabling the formation of compact and dense aggregates [127]. Therefore, a highly saline environment can lead to smaller granule or floc sizes by destabilizing them, which can even result in washout [95].

Two brief examples of the problems encountered in the industries treating highly saline wastewater are given. The textile industry generates a hypersaline wastewater stream with concentrations of up to 100 $\frac{g}{L}$ or approximately 10 % NaCl. After testing, it was found that granular sludge, not adapted to saline wastewater, could be used for salt concentrations lower than 3 % [226]. At higher salinities, the system was inhibited. When using a culture with higher salt tolerance, this border can be increased to 15 % [82]. The second example considers the tanning process applied to leather, which results in a hypersaline wastewater stream containing 1 to 10 % NaCl, as well as numerous other chemicals, including collagen and heavy metals, such as zinc and lead [226]. For this industry, it is challenging to use activated sludge systems that are not specifically adapted to the high salt concentration, as the salt concentration in the influent of the treatment system varies over time [115]. Although some slight adaptation to salt is possible for the activated sludge system, as shown in the example above, the variable salt concentration results in the non-usability of general activated sludge systems [115]. Halotolerant bacteria, which can tolerate saline environments, are therefore still preferred for the tannery industry [195].

2.3.2 Solutions for problems of saline wastewater treatment

Ample research has been conducted to enhance the performance of UASB reactors in treating highly saline streams. The different attempted methods are mentioned in this section.

Adding specific salts

Although it may appear counterintuitive, the addition of specific salts can mitigate the detrimental effects of high salt concentrations encountered during saline wastewater treatment. Gagliano *et al.* found that the addition of potassium salts leads to the cellular uptake of these potassium ions, resulting in a smaller osmotic pressure difference between the intracellular and extracellular environments [68, 224], which reduces the cytotoxic effects, especially for methanogens [58, 217]. The addition of extra multivalent ions, such as Ca^{2+}, to the influent of the reactor did not improve

the performance, despite playing a significant role in increasing the granule strength. No granulation was possible due to the filamentous *Methanosaeta harundinacea* bacteria, which serve as the granule's backbone, being insufficiently present. The addition of Ca^{2+} ions did not resolve this absence [68].

Changing the reactor setup
Another solution for treating highly saline wastewater is to change the reactor setup from a UASB to a membrane bioreactor (MBR). An MBR tends to exhibit greater stability and a higher removal rate of organic matter when high salt concentrations are present in the reactor influent [65, 149]. The most significant advantage of an MBR over conventional systems is its ability to prevent the sludge washout from the bioreactor during degranulation [115]. However, MBRs cannot always be applied, as some sludge types can lead to extensive membrane fouling [212].

Sludge acclimatization
Since the addition of salts has only a limited effect on the operation of the UASB reactor, research has focused on acclimatizing conventional sludge to higher salt concentrations. Xiao and Roberts demonstrated that acclimatization is possible when using municipal wastewater sludge to treat wastewater from fish processes [226]. Other studies demonstrated that granulation is also possible for some saline wastewater treatment systems [20, 203]. Buenano-Vargas observed that non salt-adapted sludge disintegrates when exposed to a saline feed stream, after which new granules are formed, resulting in an improved process performance. The process returns to its initial state after three months. The microbiological character of the sludge also remains unchanged during this process. Hence, the granules might be stabilized by the formation of different types of EPS, which protect the cells inside the granules from the harsh, highly saline environment [20]. This hypothesis can be verified by performing an extensive characterization of the EPS present in the granular sludge.

2.4 Extraction of Extracellular Polymeric Substances from sludge

As already mentioned in Section 2.2.2, EPS consist of different biological macromolecules, such as proteins and polysaccharides, and act as a glue keeping the sludge components together [87]. The previous sections have demonstrated the importance of EPS in sludge from wastewater treatment, indicating the added value of characterizing them. As sludge contains constituents other than EPS as well, they must be extracted before their usage and characterization. To enable correct EPS characterization, the extraction process should be selective for EPS, should not alter its composition and should have a high yield [72]. It is also undesirable that microorganisms, like bacteria are lysed during the extraction method, as this will result in the contamination of EPS with intracellular components.
To date, no standardized EPS extraction method has been given in the literature [59, 213]. Therefore, an overview of the most important extraction protocols is given.

2.4.1 Current extraction methods

Heat extraction, by Horan and Eccles [92]
This method was developed by Horan and Eccles in 1986 and is also used in the work of van Dierdonck [92, 213]. The method uses only heat to extract the extractable extracellular polymeric substances. Sludge is centrifuged, after which it is put in a 100 mM Tromethylamine/HCl buffer for 1 hour at 80℃. The mixture is then centrifuged again, and the EPS are collected in the supernatant. Afterwards, the different EPS components are precipitated using isopropanol [213].

Extraction using a cation exchange resin, by Frølund *et al.* [67]
Another EPS extraction method was developed by Frølund *et al.* in 1996 and utilizes a cation exchange resin (CER) [67]. In their research, the authors used different concentrations of CER and different mixing intensities. Larger amounts of extract are observed with a higher CER concentration and more intensive mixing. The extracted EPS mainly consisted of proteins, but also significant amounts of humic compounds, polysaccharides, uronic acids, and DNA contributed substantially to the EPS. The composition of the extract depends on the process parameters, as the ratio of proteins to carbohydrates varied from 3.9 to 5.1 when varying the mixing time. Prolonged mixing also resulted in a higher amount of cell lysis. However, it did not affect the final extracted EPS too much, as only 10 to 15 % of the extract was considered intracellular material [67]. This extraction method is also used in the PhD thesis of Van den Broek, to extract EPS from two different sludges, yielding similar results [211].

Sodium oxalate extraction, by Sajjad and Kim [179]
Another method, developed by Sajjad and Kim in 2016, uses sodium oxalate ($Na_2C_2O_4$) for the extraction of EPS from aerobic activated sludge [179]. The authors expect the method to be effective due to a combination of Na^+ expelling some multivalent ions, such as Mg^{2+} and Ca^{2+}, from the sludge and the oxalate ions forming a strong complex with these ions. In their research, granular sludge is added to a $Na_2C_2O_4$ solution at different concentrations for different mixing times. The extract contains proteins, polysaccharides and humic substances. The composition was highly dependent on the operating conditions, such as the $Na_2C_2O_4$ concentration, mixing time, and speed. They also observed that prolonged contact led to cell lysis, as the amount of DNA present in the extract doubled when mixing for 1 hour compared to 2 hours [179].

Overview of different extraction methods, by Felz [59]
Felz provides an overview of six commonly used extraction methods, applying all of them to aerobic granular sludge from a pilot wastewater treatment plant (WWTP) in Utrecht, the Netherlands [59]. The methods he compares are extraction using centrifugation [126], sonication [57], EDTA [126], formamide and sodium hydroxide [2], formaldehyde and sodium hydroxide [126] and, finally, extraction using high temperature and sodium carbonate [124]. Felz observed that the extraction using

heat and sodium carbonate (Na_2CO_3) is the only one that can completely destroy the EPS structure in the granules. In this way, more EPS can be extracted from the granules, which is, of course, desired. For the other methods, sonication was the only one that had an effect on the granules' shape after extraction. On the other hand, he also observed that the extraction protocol affects the amount and composition of the extracted EPS, with the extractions using formaldehyde, formamide, and the heat and sodium extraction yielding the most EPS. Alkaline conditions appear to ameliorate the extraction. However, it is also observed that cells are more prone to lysis at higher pH levels [19]. Hence, the higher mass of extracted EPS is possibly a result of them being contaminated with intracellular components, which is not verified in Felz's study [59]. The extraction using heat and Na_2CO_3 is employed as the first extraction protocol to obtain EPS from different sludge samples in this work.

Most of these studies are individual ones conducted on a laboratory scale. The various works are also not entirely representative of all types of sludge, as the efficiency of the different methods most likely depends on the granule composition, which in itself depends on its microbial content. Therefore, selecting an optimal extraction method can be challenging, which is why it is necessary to try different extraction protocols and compare them.

The use of other chemicals, like urea, sodium chloride, or a combination of both, for EPS extraction can also be justified. Urea is known to disrupt hydrogen bonds, which can reduce the interaction between EPS components, such as proteins and polysaccharides [141]. It is a potential cleaning chemical for membranes used in reverse osmosis, as it can destabilize the biofilm that forms on the membrane surface [180]. The extraction of EPS from granular sludge shows similarities to this process, which is why urea could also be utilized for this purpose. It must be noted, however, that urea is also known to cause cell lysis [170], which makes it less optimal for EPS extraction.

The effect of NaCl has already been discussed, as high concentrations of NaCl can reduce the granule strength, potentially leading to its disruption [204]. Different components of the sludge granule can be separated more easily in this method. Using sodium chloride will therefore also be tried as an extraction method. However, possible cell lysis must also be taken into account for this extraction method.

2.4.2 Difficulties with Extracellular polymeric substances extraction

Although various extraction methods have been explored, many difficulties with EPS extraction remain. First of all, the extraction methods are likely to contaminate the extracted EPS with intracellular material. This concern has already been outed for both physical and chemical extraction processes, such as sonication, sodium hydroxide, high shear during mixing, EDTA and CER [59, 67, 83, 126]. Hence, it is

important to verify the presence of intracellular components in the extracted EPS, using, for example, 2-keto-3-deoxyoctonate or glucose-6-phosphate dehydrogenase, which are markers for cell lysis [2, 50]. Another difficulty arises from the fact that the initial EPS concentration and composition is unknown. Because of this, one cannot determine an absolute yield or the efficiency of the extraction nor guarantee that the extracted EPS are representative of the actual EPS content of the granular sludge. The composition of the extracted EPS is also known to be affected by the extraction protocol [27, 37, 59, 240].

Sajjad states that physical methods have detrimental effects, including low EPS yield and protein denaturation at elevated temperatures [179]. The use of chemicals results in higher yields; however, the extract may be contaminated with the reagents, which is also not beneficial for characterizing the EPS. For instance, EDTA is known to interact with proteins, leading to erroneous results when determining the protein content. Apart from this side effect, Metzger *et al.* have also proven that the EDTA extraction leads to a misleadingly high yield, caused by the fact that around 40 % of the EDTA used in the extraction resides in the EPS [146]. Using CER avoids these disadvantages; however, due to the high amounts of CER and the high mixing rates required for an effective extraction, it is a more costly extraction process [67].

Another difficulty of EPS extraction is that differences in the extraction protocol, such as varying concentrations of chemicals, mixing times, and intensities, result in different compositions of the extracted EPS [67, 179]. Therefore, it is important to apply the same extraction method when comparing extracts from different sludges.

2.5 Characterization of Extracellular Polymeric Substances

Knowledge of the exact composition and functionality of the extracted EPS is crucial to determine the effectiveness of the extraction process and for its future valorization. Therefore, the current section provides an overview of typical EPS characterization methods found in literature. This chapter mainly serves as an overview of these methods; less focus is put on their working principles.

2.5.1 General tests: focus on the type of molecule

The first type of characterization methods determine the amount of a specific type of biomolecule in the EPS. These methods are typically not only used to study EPS, but also to determine properties of wastewater effluent quality. The total amount of polysaccharides can be determined by the phenol-sulfuric acid assay developed by Dubois in 1951 [51], while the total protein content is determined by the method of Lowry, developed in the same year [135]. Both methods require a standard, namely D-glucose and bovine serum albumin, respectively. To determine the amount of nucleic acids in a sample, the method of Burton can be used [24, 50]. Other

standardized methods are given by the American Public Health Association (APHA) [6]. These primarily consider the determination of solids in a sample, including the total solids (TS), volatile solids (VS), mixed liquor suspended solids (MLSS) and mixed liquor volatile suspended solids (MLVSS).

Besides the methods given above, also other methods exist [50, 211, 213]. For example, Dai *et al.* used the Filon-hydroxybenzene method (also applying bovine serum albumin as a standard) to determine the protein content and the Anthrone-sulfuric acid colorimetric method to determine the protein and carbohydrate composition [42]. To determine the humic acid content, dichromate titration was employed. Additionally, test kits, such as the 2D-Quant Kit by Amersham Biosciences, can be used to determine the protein content [188].

Another test that can be performed is a hydrophobicity test. During the test, granules at a concentration of 2.5 $\frac{g}{L}$ MLVSS are put in a two-phase mixture containing one polar and one apolar liquid. The hydrophobicity can then be determined by comparing the absorbance of the polar, aqueous phase before and after the addition of the sludge. This test does not directly determine the sludge's EPS composition, but determines its relative hydrophobicity [213].

Colorimetric methods also determine concentrations of specific biomolecules, such as total protein and polysaccharide concentration. However, they exhibit a lot of interference between different EPS components, leading to inaccurate results [59, 157].

It is clear that only general information is obtained from the characterization methods mentioned in this section. To gain a deeper understanding of the various (bio)molecules present in the extracted EPS, more specific tests are required.

2.5.2 Towards improved characterization

In general, it can be concluded that no single test is able to characterize the EPS entirely. Therefore, a combination of characterization methods should be employed, ranging from three-dimensional excitation-emission matrix (3D-EEM) to Mass Spectrometry (MS), as well as Nuclear Magnetic Resonance (NMR) and Raman and Fourier Transform Infrared spectrometry (FTIR). Additionally, molecular genetic techniques are helpful in this process [157, 187]. The remainder of this chapter gives an overview of the methods used in literature.

Mass spectrometry (MS)
Dubé used Mass Spectrometry (MS) to specifically determine which proteins were present in anaerobic granular sludge (AnGS) from three industrial WWTPs [50]. First, the extracted EPS in solution were sent through a sodium dodecyl sulfate polyacrylamide gel electrophoresis (SDS-PAGE) step to separate the proteins, followed by sending the most prominent bands to a mass spectrometer for their characterization. Forty-five proteins were characterized, all having a molecular weight between 26 and

89 kDa. Other studies, however, showed molecular weights greater than or equal to 235 kDa [14, 61, 221].
MS was also used to look at the inorganic fraction of the EPS. D'Abzac confirmed the presence of metals in the EPS from four AnGS samples using inductively coupled plasma mass spectrometry (ICP-MS) [41]. These metals are an important constituent of the EPS, as they can account for up to 77 % of its dry weight and can have an effect on the EPS properties. He characterized the mineral content by digesting the sludge granule using a mixture of nitric and hydrochloric acid. After digestion, the remains were added to ultrapure water and filtered, followed by analyzing it using an inductively coupled plasma optical emission spectrometer (ICP-OES) and an inductively coupled plasma mass spectrometer (ICP-MS) [41].

Three-dimensional excitation-emission matrix (3D-EEM)
Three-dimensional excitation-emission matrix (3D-EEM) combines excitation and emission of a sample against electromagnetic radiation in the UV-VIS region (200-400 nm for excitation, 280-550 nm for emission) to identify the characteristics of a sample [32]. Depending on the combination of these two, aromatic protein-like, fulvic acid-like, humic acid-like and microbial by-product-like substances can be differentiated [42, 119]. In this way, a deeper understanding of the biopolymers within a sample can be formed. The primary disadvantage of this characterization method is that only qualitative results are obtained [32].

Fourier Transform Infrared Spectrometry (FTIR)
During a Fourier Transform Infrared Spectrometry (FTIR) measurement, infrared light with a wavenumber between 4000 and 400 cm^{-1} (wavelength from 2500 to 25000 nm) is sent through the sample, which can absorb this light at specific frequencies, corresponding to the vibrational frequencies of its chemical bonds. By measuring the absorbance of the IR light as a function of the frequency (or wavenumber), an idea can be formed on which bonds are present in the sample [91].
In their study from 2012, Zhu *et al.* identified the dominant spectral bands in aerobic granular sludge [237]. Similar research was already performed by Schmidt and Flemming in 1998 [185]. However, they used FTIR to study microorganisms in a biofilm without having to destroy the different organisms in it. They also identified four regions in the FTIR spectrum, corresponding to fatty acids, proteins, polysaccharides and a fourth "mixed" region. Each region has characteristic wavelengths at which infrared radiation is absorbed. This table can be found in Appendix C.1.1 [185].

Raman spectrometry
Raman spectroscopy uses a monochromatic laser that induces light scattering when interacting with the sample. The Raman spectrum is determined from the inelastically scattered light, which is shifted in frequency compared to the monochromatic laser [21]. The method can determine the functional groups, as well as the conformation and intermolecular interactions of materials in the sample [101]. Past studies have demonstrated the difference in protein-to-polysaccharide ratio between loosely bound EPS and tightly bound EPS, using a combination of Raman and FTIR

spectroscopy [34]. Elleuch *et al.* have compiled a table (Table C.2, Appendix C.1.2), listing several characteristic wavenumbers and their corresponding biomolecule [55]. A similar table was created by Wagner *et al.* in their study of EPS from biofilms [218].

Nuclear magnetic resonance (NMR)
Nuclear Magnetic Resonance (NMR) has been used in the past to gain a deeper understanding of the composition and structure of EPS in biofilms [77, 146]. The method uses a magnetic field to alter the electron spin level of specific atoms in the material [228]. When placing EPS in an external magnetic field and exposing it to electromagnetic waves, some frequencies of the energy are absorbed, while others are not. These energies correspond to the energy differences required for electrons to transition from one spin level to another. The amount of energy required depends on both the atom and its surroundings. The different amounts of energy required for electrons to transition from one energy level to another can be detected as a chemical shift δ, expressed in ppm [228].
Gonzalez-Gil *et al.* compared the ^{1}H-NMR of the EPS extracted from anaerobic granules to those of different polysaccharides (alginate, gellan and xanthan) and found some similarities between the EPS and these model systems [77]. Both EPS and model systems showed peaks in regions between 3.2 and 5.6 ppm. This region can be divided into two separate regions: one from 3.2 to 4.4 ppm, corresponding to H-atoms from sugar rings, and one from 4.4 to 5.6 ppm, corresponding to anomeric H-atoms [1]. In their research, Metzger *et al.* investigated the amount of EPS extracted from bacterial and fungal species using different extraction methods via ^{13}C-NMR [146]. They determined that on average proteins made up 70 % of the carbon content of the extracted EPS. They also discovered that the apparent EPS yields obtained using EDTA extractions are higher than the actual ones, as 40 % of the EDTA used in the extraction process resides inside the extracted EPS [146].

2.6 Valorization of extracellular polymeric substances as raw material

Both aerobic and anaerobic wastewater treatment processes generate excess sludge. Up to 15 % of the influent BOD is converted to this biomass for anaerobic processes, while this can be as high as 60 % for aerobic processes [46]. To date, most of this excess sludge is being disposed of or incinerated; its use on land is not performed extensively anymore due to the potential risks to human and animal health [223]. The disposal comes with a significant cost, accounting for approximately half of the total operational cost of a WWTP [156]. Together with the urge of society to become more circular, the disposal of waste sludge is making place for the recovery of valuable materials, such as the biopolymers inside the EPS [157]. Replacing conventional oil-based polymers with these bio-based EPS from sludge increases the circularity of a WWTP, inducing its shift towards becoming a Water Resource Recovery Facility (WRRF) [187, 214]. Knowing that the yearly production of waste sludge in municipal wastewater treatment alone is equal to 45 million tons of dry

weight [62], vast amounts of EPS could be obtained. Having an understanding of the composition of the EPS present in the granular sludge opens up a whole new world of possible applications, which have been investigated over the last 15 years and form the subject of this final section.

2.6.1 Waste sludge as a resource

Karakas *et al.* researched the use of aerobic granular sludge (AGS) in the construction sector, posing that the EPS from AGS can be added to cement to enhance curing [102, 157]. This statement is based on the fact that sodium alginate, which is a polysaccharide, enhances cement curing [238]. As the behavior of the polysaccharides in EPS might resemble that of alginate, it is plausible that EPS also enhance the curing of cement [102]. The production of polyhydroxyalkanoates (PHAs) is also considered in their work, as AGS systems show potential for the recovery of PHAs [102]. These polymers can then be used in films, bags, and bottles, replacing fossil fuel-based plastics [171].

Extracted EPS also show potential to function as surface coating, increasing the water resistance of hydrophilic surfaces [123]. In this application, the amphiphilic character of the EPS, caused by the presence of both carbohydrates and lipids in the EPS, is exploited. The EPS could be used in the paper industry, where a hydrophobic film is desired on top of the paper to enhance its water resistance. Within the film, the hydrophilic parts of the EPS tend to interact with the hydrophilic cellulose fibers of the paper, while the hydrophobic parts sit closer to the paper-air interface [59, 123]. EPS can be used not only to create hydrophobic coatings, but also to reduce the flammability of a material [111] or to increase its resistance to corrosion [105, 230].

EPS also show potential for use in ion-exchange membranes with selectivity towards monovalent ions. The idea arose from the research of Gagliano *et al.*, who observed that EPS from anaerobic granular sludge (AnGS) of saline wastewater treatment can resist a high concentration of Na^+ in the environment by adsorbing these ions [69]. The EPS can selectively allow other cations, such as K^+, to diffuse through the matrix while stopping Na^+ to a larger extent [205]. Based on this observation, Sudmalis *et al.* constructed a cation exchange membrane using AnGS EPS [205]. The obtained membrane showed a higher selectivity towards K^+ ions compared to Na^+ ions. The selectivity factor for potassium over sodium was equal to 1.3 for the EPS-based membrane. This performance was compared to a membrane made with alginate, which had an even higher factor of 1.9, indicating that polysaccharides and EPS may be suitable materials for cation exchange membranes. However, the efficiency of the membranes was lower than that of conventional cation exchange membranes. Nevertheless, EPS show the potential to specifically select one ion, which is not yet possible for conventional membranes [61].

2.6.2 Using EPS as a hydrogel

EPS can also be used to create hydrogels, possessing specific properties. By comparing EPS hydrogels with hydrogels of model systems, some new fields of application may emerge, such as their use as a thickening agent [134]. This section covers two applications of EPS hydrogels: pollutant adsorption and the release of agricultural species into the soil.

EPS can be used as adsorbents for toxic species, such as microplastics [117], both organic and inorganic pollutants [41], and heavy metals [41, 159]. Pagliaccia performed extensive research on the adsorption capacity of heavy metal ions (Pb^{2+}, Cu^{2+}, Ni^{2+} and Zn^{2+}) in hydrogels made from EPS extracted from anammox sludge [159]. The EPS can adsorb heavy metal ions due to the presence of numerous polar functional groups, including carboxyl, hydroxyl, and amine groups [120]. As the EPS from anammox sludge are rich in protein, they are an ideal candidate for heavy metal adsorption [159]. However, it must be considered that different ions compete for the same functional groups. The effect of having different heavy metal ions in a mixture on the adsorption is not investigated yet. This process could even be taken one step further, as the EPS might be able to reduce metal ions back to metal nanoparticles, such that heavy metals can not only be adsorbed but also recovered from wastewater streams [15, 134].

EPS can also be used as a hydrogel in agriculture. Here, the gel can be loaded with nutrients, after which it is put in the soil [157]. EPS hydrogels can absorb nutrients from the soil when the concentration of nutrients is higher in the soil than in the gel. When the soil is depleted of nutrients, the hydrogel releases the nutrients together with water into the soil, achieving a controlled nutrient release [157]. This application could serve as a biodegradable alternative to the current systems of polyacrylic acid and polyacrylamide gels [160]. However, it should be mentioned that high concentrations of sodium and chlorine are considered cytotoxic to crops. Therefore, the EPS extraction and hydrogel formation must be performed without chemicals containing the two species (such as NaOH, Na_2CO_3, and HCl). However, this does not significantly affect the final characteristics of the obtained hydrogels [157]. Before commercializing this application, the potential risks of using these EPS to animal and human health must be considered [223].

Apart from the application areas mentioned above, it can also be helpful to compare EPS hydrogels with model system hydrogels, like alginate and κ-carrageenan. In this way, the possible replacement of these model systems with the EPS from different sludge sources can be studied. In this process, the mechanical properties of these gels are crucial, which is why they must determined, using, for example, rheology. Performing rheological measurements on EPS hydrogels can enhance their understanding, thereby increasing their potential valorization in industries not previously considered [157].

2.7 Conclusions

Wastewater treatment is divided into four distinct steps: pretreatment, primary, secondary, and tertiary wastewater treatment. During the secondary or biological wastewater treatment, sludge is used to remove pollutants from the wastewater. The three most important pollutants removed via secondary wastewater treatment are carbon-, nitrogen- and phosphorous-based components. Three distinctions of such wastewater treatment processes can be made: aerobic versus anaerobic processes, freshwater versus saline wastewater treatment and granular versus floccular sludge processes. Independent of which process is occurring in the wastewater treatment plant (WWTP), large amounts of excess sludge are produced, which are mainly disposed of or incinerated up to this date. With the transition to a circular economy, possible uses of this waste stream must be considered. An interesting component of this sludge are the extracellular polymeric substances (EPS). These EPS consist of many different biological molecules, such as proteins, polysaccharides, lipids, and others, acting as a glue keeping the sludge together. They show potential in future applications, ranging from replacing oil-based polymers to adsorbing heavy metals as a hydrogel.

However, before employing these EPS, they must be extracted from the sludge. Here, the first problem arises because no standardized method has been found in the literature yet. No perfect extraction method exists to this day, as every method has its advantages and disadvantages. Both physical and chemical extraction methods have been employed in the literature, all resulting in different yields and compositions of the extracted EPS. Even when changing parameters like the mixing time and speed, the extracted EPS composition varies. It is thus crucial to standardize the extraction method to minimize the variability between EPS extracted in different batches. Therefore, Chapter 5 discusses the selection of the optimal extraction method based on qualitative and quantitative criteria. An equilibrium between feasibility and performance forms the basis of the decision-making process.

After the extraction process, the extracted EPS can be characterized. Similar to the extraction, no standardized method has been found in the literature yet. Different characterization methods for EPS were covered, including tests that enable molecular fingerprinting, such as NMR, FTIR and Raman spectroscopy. Even these methods cannot fully characterize EPS. However, combining several techniques can enhance the understanding of extracted EPS.

Chapter 3

Problem statement and research outline

3.1 Research objectives

The primary objective of this thesis is to investigate the differences in characteristics of EPS from various sources. To do this in a structured manner, the scheme shown in Figure 3.1 is followed. First, the biomass undergoes an extraction process to obtain only the EPS fraction, which is then characterized using different tests. After comparing the EPS from different sources to each other, a comparison is also made with two model systems, in an attempt to link the rheological behavior of the EPS and their gelation to their chemical characteristics. The model systems chosen in this work are sodium alginate and κ-carrageenan, two polysaccharides, and are also compared to one another.

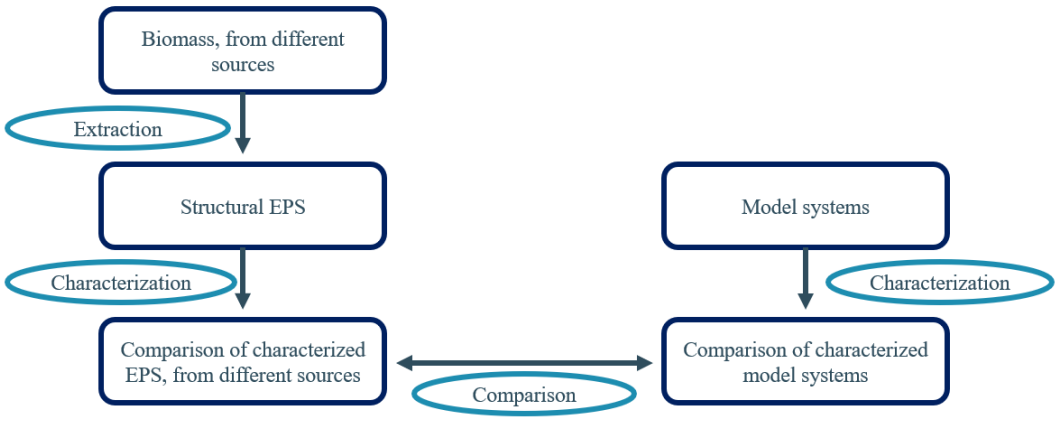

FIGURE 3.1: Schematic overview of the experimental procedures followed in this work, starting from EPS extraction from biomass, to EPS characterization and comparison with model systems. In this work, the biomass refers to both industrial sludge samples, as well as lab-grown pure cultures.

It is important to focus on the extraction methods first before proceeding with the EPS characterization. As shown in the literature study, it is important to maintain a constant extraction protocol throughout the entire thesis. To make a decision on which method to use, a qualitative and quantitative comparison is made between four extraction protocols: (1) heat and sodium carbonate, (2) sodium chloride, (3) urea, and (4) a combination of sodium chloride and urea extractions. Several aspects, ranging from feasibility to amount of extracted EPS, are determined for each extraction method, allowing the selection of the optimal extraction method.

Next, the EPS extracted from different sources are compared, according to the scheme in Figure 3.2. First of all, a comparison is made between the EPS from pure cultures of two denitrifiers, *Azoarcus communis* and *Dietzia maris* (H1). Afterwards, the EPS from these strains are compared to EPS extracted from Enhanced Biological Phosphate removal (EBPR) granules (H2). The two pure cultures serve as a reference, containing only one type of bacteria, resulting in a less complex EPS composition. The granules should also contain bacteria similar to the two denitrifiers, as the granule is used for both nitrogen and phosphorus removal. Next, EPS extracted from non saline-adapted sludge and the same sludge after salt adaptation are compared to see how the EPS characteristics change (H3a). Finally, a comparison is made between salt-adapted granular sludge and floccular sludge (H3b), which are ultimately compared to the fungal species *Aspergillus oryzae*. All comparisons are made using fingerprinting methods, such as NMR, FTIR and Raman spectrometry.

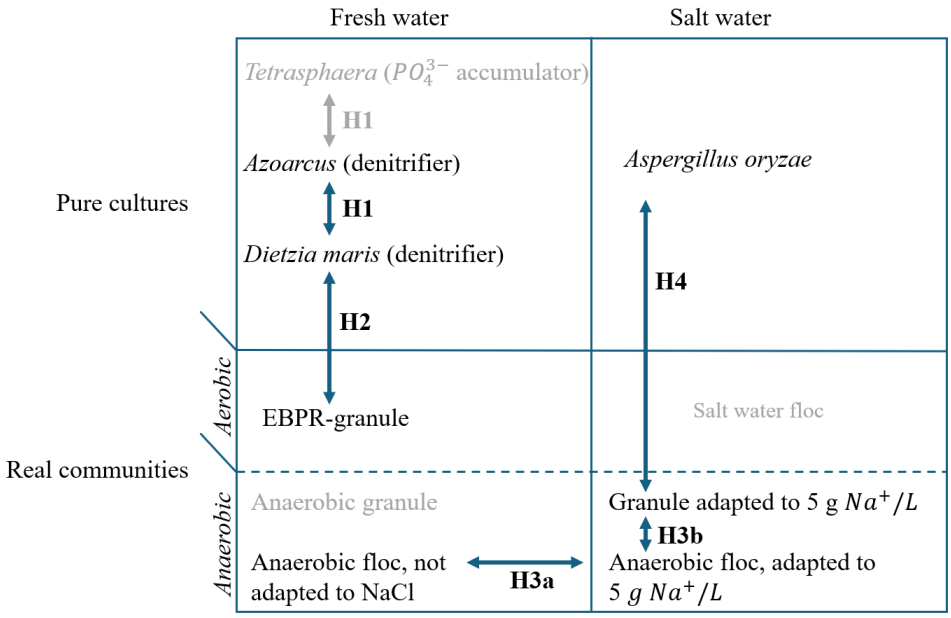

Figure 3.2: Schematic overview of the different sources for biomass, of which the EPS can be extracted and characterized to get an idea of the effect of operating conditions on the EPS present in wastewater sludge. The grayed-out names are not discussed in this work, all others are.

The ultimate goal of this thesis is to explore the valorization of EPS by examining their application as a hydrogel. The EPS are compared to two model systems: sodium alginate and κ-carrageenan, which are currently often employed in hydrogels. Firstly, the fingerprinting methods are used to compare the chemical structure of the EPS and the model systems to determine if similar functional groups are present in both. Secondly, a rheological characterization of hydrogels made from both is performed to compare the mechanical behavior of EPS-based and model system hydrogels. Finally, an attempt is made to link the mechanical behavior of EPS-based hydrogels to their chemical characteristics by extrapolating the results of the model systems to the EPS.

3.2 Thesis outline

With the exact research objectives in mind, the outline of the remainder of this work is presented.

Chapter 4 shows all of the different materials and methods used in this thesis, following the flow of obtaining the EPS from different sludges, shown in Figure 3.1, starting with the different biomass sources and ending with the extraction and characterization methods.

In **Chapter 5**, the four different extraction methods are compared by making a balance between the following criteria: feasibility, amount of material extracted, organic content of the material, NMR results and cell lysis. Based on which extraction method gives the optimal results, the extraction method used in the remaining chapters is selected.

Next, **Chapter 6** deals with the characterization of the EPS, as EPS from different sources will be fingerprinted using NMR, FTIR and Raman spectroscopy. A comparison is made between the fingerprints of EPS from different sources, ranging from pure cultures, acting as a reference system, to more complex industrial sludges. To keep the comparisons as structured as possible, Figure 3.2 is closely followed.

Furthermore, **Chapter 7** compares the EPS extracted from industrial sludge samples to two model systems, sodium alginate and κ-carraggeenan, which are both polysaccharides. Both chemical fingerprints and rheological tests are performed on both model systems and the different EPS. The rheological measurements enable a comparison of the mechanical properties of the EPS gels with those of the model system hydrogels to determine whether the gelling behavior of EPS closely resembles that of the known model systems. An attempt is made to link the differences in the rheological behavior of the EPS-based hydrogels to their chemical composition.

Finally, **Chapter 8** wraps up this work by giving an overview of the most important conclusions of this thesis while also providing some future prospects.

Chapter 4

Materials and methods

The current chapter discusses the different sources for EPS used, the extraction methods performed, and the various characterization methods applied on the EPS. Finally, the methodology to make hydrogels from extracted EPS is explained.

4.1 Industrial sludges as EPS sources

EPS are extracted from three different types of sludge in this work.
The first sludge is floccular in nature and collected from a full-scale municipal wastewater treatment plant, near Leuven (BE), and is further referred to as "non salt-adapted floccular sludge". The second is granular sludge from an anaerobic wastewater treatment plant treating saline wastewater, the so-called "salt-adapted granular sludge". The last sludge is Enhanced Biological Phosphorous Removal (EBPR) granular sludge, from a full scale municipal wastewater treatment plant near Utrecht (NL). It consists of millimeter sized granules from an aerobic process treating non-saline wastewater, and is referred to as "EBPR granular sludge".

To allow comparison with the "salt-adapted granular sludge, the "non salt-adapted floccular sludge" is adapted to a higher salt concentration, by loading the original sludge into a 1,15 L UASB reactor at a concentration of 6 $\frac{g}{L}$ volatile solids. As influent, 47.9 mL of artificial wastewater containing NaCl (Acros Organics, Belgium) at a concentration of 5 $\frac{g}{L}$ Na^+ is fed to the reactor every hour, resulting in an average residence time of 24 h. The UASB reactor is run for 105 days and kept at 37 ℃ throughout the process, such that the initial sludge is adapted to a saline environment. More details on this salt adaptation can be found in the work of L. Mertens [145].

4.2 Reference pure cultures as EPS source

Four different bacterial reference cultures are grown to collect EPS. As more is known about these cultures, the resulting EPS is expected to be more consistent and more easily characterizable. The cultures involved are *Aspergillus oryzae*, *Escherichia coli*

and *Azoarcus communis* and *Dietzia maris*. The cultivations in this work have been carried out by ir. L. Parret, mr. K. Simoens, and Lien Mertens.

4.2.1 *Aspergillus oryzae* growth

Spores of *Aspergillus oryzae* (*A. oryzae*) are grown on a Petri dish (**Ø** 92 mm, Sarstedt, Germany), covered with agar (VWR Chemicals, USA) for five days, at 37 ℃. Then, 20 mL of demineralized water is added on top of the agar, and the grown fungi are removed from the plate by scraping. The obtained suspension, which contains the fungi, is poured from the dish into a 50 mL falcon tube and stored at -18 ℃ until further usage.

To grow fungal pellets, 10 mL of the aforementioned fungal suspension is dosed into a 1 L erlenmeyer containing 500 mL of a watery potato dextrose broth medium, with the potato dextrose broth (Thermo Fischer Scientific, USA) at a concentration of 24 $\frac{g}{L}$ and NaCl ($\geq$ 99.5 %, Acros Organics, Belgium) at a concentration of 5 $\frac{g}{L}$ Na^+. The Erlenmeyer is put in an incubator, and is shaken at 200 rpm and 37 ℃ for at least one day to allow the formation of millimeter sized pellets. The pellets are then put in a 50mL falcon tube and stored at 4 ℃ until further use.

4.2.2 *Escherichia coli* growth

Escherichia coli CM2588, containing the *pSunny* plasmid are grown in Lysogen Broth medium, containing 10 $\frac{g}{L}$ Tryptone (Thermo Fischer Scientific, USA), 5 $\frac{g}{L}$ Gibco^{TM} Bacto^{TM} Yeast Extract (Thermo Fischer Scientific, USA) and 10 $\frac{g}{L}$ NaCl ($\geq$ 99.5 %, Acros Organics, Belgium). The flask containing the biomass and medium is shaken overnight at 200 rpm, at 37 ℃, after which the mixture is centrifuged for five minutes at 5000g, at room temperature. The pellet, containing the cells is used for the further tests, the supernatant is discarded. All centrifugations in this work are carried out using the Eppendorf Centrifuge 5810 R, by Eppendorf (Hamburg, Germany). The pellet is put in a 50 mL falcon tube and refrigerated at 4 ℃ until further usage.

4.2.3 *Azoarcus communis* and *Dietzia maris* growth

Azoarcus communis and *Dietzia maris* bacteria are grown from a preculture in a 250 mL flask, with 100 mL of Tryptone Soy broth medium, containing 2.994 g of Tryptone Soy broth powder (Thermo Fischer Scientific, USA) and demiwater. The flask is shaken for 24 h at 220 rpm and 30 ℃, after which the contents of the flask are distributed over five 1 L erlenmeyers, containing 500 mL of fresh medium, made with 14.97 g of the same Tryptone Soy broth and demiwater. The flasks are incubated at 30 ℃ and shaken for 36 h at 220 rpm. Finally, the mixture is centrifuged for 5 minutes at 5000g, at room temperature to collect the pellet, used for the further experiments. The supernatant is discarded.

4.3 Extraction of extracellular material

Four different extraction processes are applied to at least one of the EPS sources, namely (1) extraction with heat and sodium carbonate, (2) extraction with sodium chloride, (3) extraction with sodium chloride and urea, and (4) extration with urea. The extraction procedures are discussed in detail in the subsections below. Prior to each extraction, the biomass containing the EPS is subjected to three washing steps to remove impurities. A falcon tube is filled with the biomass and 50 mL of demineralized water, and shaken manually until the content is fully dispersed. Then, centrifugation is performed three times at 5000g for 5 min at room temperature. In between two centrifugation steps, the supernatant is discarded, demiwater is added, and the biomass is redispersed by shaking. After the third centrifugation, the wet biomass is collected from the bottom of the tube and used in the extraction processes.

4.3.1 Extraction process 1: heat and sodium carbonate

The extraction protocol using heat and sodium carbonate provides heat according to the bain-marie principle (see Figure 4.1) and is taken from Felz [59].
0.25 g of Na_2CO_3 (> 99 %, Sigma Aldrich, USA) is added to 50 mL of ultrapure (milliQ) water in a 250 mL baffled flask containing a magnetic stirring bar. To this solution, 3 g of wet, washed biomass is added. Next, the flask is covered with aluminum foil and partially submerged in a 1L beaker containing 150 mL of demiwater, which is preheated to 80 ℃ on a magnetic heating plate. The setup is covered with aluminum foil to prevent water evaporation. The biomass mixture is stirred at 400 rpm for 35 min at 80 ℃. Hereafter, the setup is allowed to cool down after which the mixture is entirely poured in a 50 mL centrifugation tube and centrifuged for 20 min at 4000g and 4 ℃. The supernatant, containing the extracted EPS, is collected, while the remaining pellet is discarded as biological waste.

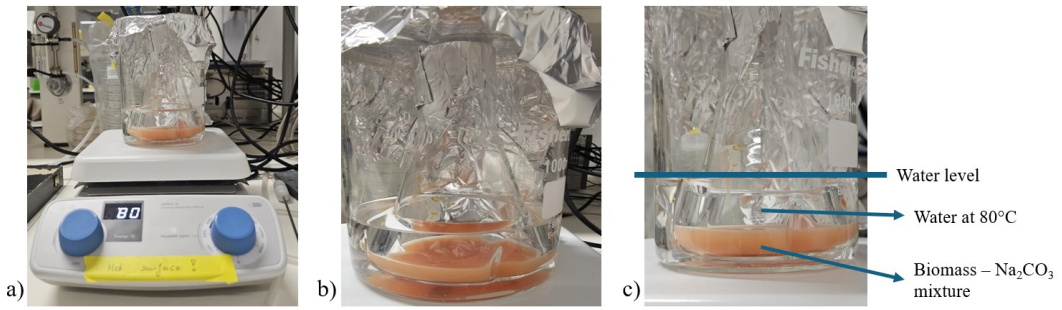

FIGURE 4.1: Set-up used for the heat and sodium carbonate extraction process, following the bain-marie principle, applied on *Dietzia maris*. **a)** 250 mL baffled flask containing 50 mL of the biomass-Na_2CO_3 mixture, inside a 1 L beaker, containing 150 mL of water, on top of a heated magnetic stirrer. **b)** The baffled flask inside the beaker. **c)** Contents of the 1 L beaker. It is important for the bain-marie principle that the water level is higher than the level of the biomass-Na_2CO_3 mixture.

In a next step, the supernatant is put in a Vivaspin Turbo 15 centrifugation tube (Sartorius, Germany), containing a dialysis membrane, with a molecular weight cut off (MWCO) of 3 kDa. The contents are centrifuged until most water has passed the membrane. Next, ultrapure water is added and the whole is centrifuged once more until most of the newly added water has passed the membrane. Later on, this step was replaced by the membrane dialysis explained in Section 4.3.5: *EPS purification*, due to the fact that this membrane centrifugation was insufficiently able to remove low molecular weight components from the extract (see Chapter 5).

4.3.2 Extraction process 2: sodium chloride

50 mL of a NaCl solution, containing 100 $\frac{g}{L}$ Na^+, made with 12.23 g sodium chloride ($\geq$ 99 %, Thermo Fisher Scientific, USA) and ultrapure water is put in a 250 mL baffled flask, together with a magnetic stirring bar. Three grams of wet, washed biomass is then added to this baffled flask. Next, the contents are stirred at 400 rpm for 120 minutes, after which the whole is added to a 50 mL falcon tube and centrifuged for 20 minutes at 4000g, at 4 °C. The supernatant, containing the extracted EPS is collected, the remaining pellet is discarded.

4.3.3 Extraction process 3: sodium chloride and urea

18.02 g of urea ($\geq$ 98 %, suitable for cell culture, Sigma-Aldrich, USA) and 2.94 g of NaCl ($\geq$ 99 %, Thermo Fischer Scientific, USA) are put in a 250 mL baffled flask, and is filled up to 50 mL using demiwater. 3 g of wet, washed biomass is added to this baffled flask, after which the contents are stirred at 400 rpm for 120 minutes. After this, the whole is centrifuged for 20 minutes at 4000g, at 4 °C. The supernatant, containing the extracted EPS, is collected, the remaining pellet is discarded.

This extraction protocol is based on the fact that hydrogels can be destabilized by shielding the hydrogen bonds between the different molecules in the hydrogel. Na^+ ions also induce ion exchange with the ions in the hydrogel, destabilizing it. Bose *et al.* used a similar protocol to extract proteins from *Acheta domesticus* [16].

4.3.4 Extraction process 4: urea

18.02 g of ureum ($\geq$ 98 %, suitable for cell culture, Sigma-Aldrich, USA) are put in a 250 mL baffled flask, and is filled up to 50 mL using demiwater. 3 g of wet, washed biomass is added to this baffled flask, after which the contents are stirred at 400 rpm for 120 minutes. After this, the whole is centrifuged for 20 minutes at 4000g, at 4 °C. The supernatant, containing the extracted EPS is collected, the remaining pellet is discarded.

Hence, this extraction method is very similar to extraction method 3, with the sole difference being the exclusion of NaCl.

4.3.5 EPS purification

To purify the supernatants from the different extraction processes, the remaining reagents are removed using membrane centrifugation or membrane dialysis. As explained before, the membrane centrifugation was unable to remove the low molecular weight species sufficiently, which is why the membrane dialysis is performed on most extracted EPS.
The membrane dialysis uses a Spectra/Por dialysis membrane with a molecular weight cut-off of 3.5 kDa (Spectrum Laboratories Inc., USA). This membrane is activated by soaking it first in Technisolv denatured ethanol ($\geq$ 99 %, VWR Chemicals, USA) for 30 minutes, followed by 90 minutes in ultrapure water. The membrane is then closed at one side using a clip, after which the supernatant is poured into the membrane, that is finally closed at the top too with another clip. The activated membrane containing the supernatant is then put in 20 L ultrapure water and the dialysate conductivity is monitored over time. The water is replaced multiple times, until the increase in conductivity of the dialysate is less than 0.1 $\frac{\mu \text{S cm}}{\text{h}}$. The supernatant is then poured into a 50 mL falcon tube and heated to 60 ℃ in an oven until most water has evaporated. The final traces of water are removed by applying vacuum to the oven at 60 ℃ for at least 60 h or by freeze drying (Telstar LyoQuest-85 PLUS, Spain) at a pressure of 0.100 mbar and a condensor temperature of -80 ℃ for 48 to 72 h, after freezing the samples at -18 ℃ in 15 mL or 50 mL falcon tubes in a regular freezer. As a result, solid EPS are obtained.

4.4 EPS characterization methods

As is clear from the literature review, characterizing the extracted EPS is challenging. Therefore, multiple characterization techniques need to be combined and applied to gain fundamental insights. A correct interpretation of the reference model systems is necessary to serve as a reference framework for interpreting the industrial samples. Crucial in that respect is the possible cell lysis during the extraction as this will affect the composition of the extracted EPS drastically. The methodology to determine whether cell lysis takes place, is discussed in Section 4.4.1. In Section 4.4.2 the thermal and gravimetrical analysis methods are discussed, while Section 4.4.3 covers the chemical analysis methods.

4.4.1 Quantification of cell lysis from *Escherichia coli*

The amount of cell lysis is determined by applying the extraction protocols to *Escherichia coli* containing green fluorescent protein (GFP). To quantify this concentration, UV-VIS spectrometry is performed, using the Infinite M200 Pro plate reader (Tecan, Switzerland). The extracted material is first filtered, using a 0.2 μm PES filter (Macherey-Nagel GmbH & Co., Germany), after which 200 μL of the filtered extract is put in the plate reader.

Both absorbance (at 395 and 480 nm) and excitation-emission tests (at 488 nm and 510 nm) are performed on the extracts. Also 200 μL of the solutions used in the extraction processes is put in the plate reader, acting as a reference. For each test, the bandwidth of the light is 9 nm and 25 flashes are used. All tests are performed in triplicate.

4.4.2 Thermal characterization methods

Quantification of total and volatile solids in wet biomass

As mentioned above, all extraction methods start from wet biomass. To get an idea on how much organic material is present in this wet material, the amount of total solids (TS) and volatile solids (VS) is determined. TS corresponds to the sum of the organic material in the pellets and the inorganics like salts, while VS only considers the organic material.

To determine the TS, 0.5 g of wet pellets is put in a Binder ED 400 Lab oven (Binder GmbH, Germany) at 105 ℃ for 2 h. The TS content is determined as the difference of the pan mass after drying at 105 ℃ and the initial pan mass. Afterwards, the pan is put into a Nabertherm LE/4/11/R6 muffle oven (Nabertherm, Germany), operating at 550 ℃ for 2 h. The VS are determined as the difference in pan mass before and after the 2 h at 550 ℃.

Thermogravimetric analysis (TGA)

Samples with a mass between 5 and 10 mg are prepared in an aluminum pan, which is loaded into a TGA Q500 V20.13 Build 39 (TA Instruments, Belgium) thermogravimetric analyser, using a platinum sample holder. The temperature is increased from 20 ℃ to 550 ℃ at a rates of 5 and 10 ℃ per minute. Finally, the temperature is kept at 550 ℃ for 5 minutes. During heating, the weight loss is monitored as a function of temperature, which can provide insight on the volatile components present in the samples as well as the degradation profile of the sample.

Differential Scanning Calorimetry (DSC)

Samples with a mass between 5 and 10 mg are put in an aluminum DSC pan, covered with a non-hermetic lid and loaded into a DSC Q2000 V24.11 Build 124 (TA instruments, Belgium) to carry out the differential scanning calorimetry (DSC) tests. For all tests, a reference DSC pan with non-hermetic lid with a mass of 52.31 mg is used.
After equilibration at 25 ℃, the temperature is increased to 190 ℃ at 5 ℃ per minute, followed by 5 minutes at this temperature. Next, the temperature is lowered to -80 ℃ at 5 ℃ per minute, followed by five minutes at -80 ℃. The two final steps are then repeated once.

4.4.3 Chemical Tests

FTIR, Raman and NMR spectrometry are performed on both model systems and extracted EPS to get more insights on the chemical composition and structure of these samples.

Fourier-Transform InfraRed spectroscopy (FTIR)

FTIR spectroscopy is used to determine the different chemical bonds and functional groups present in the different model systems and EPS samples.

FTIR spectra of the extracted EPS and model systems are obtained by compressing a small volume of sample into a Spectrum 100 spectrometer (PerkinElmer Life & Analytical Sciences, USA). The absorbance of infrared radiation is measured and depicted as a function of the wavenumber of the infrared radiation, to obtain insights on the functional groups present in the sample.

Raman spectroscopy

A small amount of sample is loaded into the DXR3 Flex Raman spectrometer (Thermo Scientific, USA), covering the full laser area to determine its Raman spectrum. The laser has a wavelength of 785 nm, a maximal power of 150 mW, and a spectral range from 50 to 3250 cm^{-1}. The lower limit is used to avoid Rayleigh scattering to be dominant in the data. For the measurements, the spectrum is given from 50 to 2000 cm^{-1}. The spot size used during the tests is on average 3 μm, made possible via a 20X long working distance objective.

The inelastic light scattering, measured by the Raman spectrometer, gives information complementary to that obtained via FTIR, as chemical bonds active in Raman are often inactive in FTIR and vice versa.

Nuclear Magnetic Resonance (NMR)

Nuclear Magnetic Resonance (NMR) tests are performed on both the model systems and the extracted EPS to get insight in the molecular arrangements of the molecules inside the samples.

10 mg of sample is put in a small vial, to which 750 μL of deuterium oxide ($\geq$ 99.95 %, Thermo Fischer Scientific, USA) is added, after which the whole is mixed until the sample has fully dissolved in the D_2O. Once the vial contents appear homogeneous, 500 μL of the mixture is put in an NMR-tube, with 5 mm diameter, made for NMR tests at 400 MHz (Sigma-Aldrich, USA) using a glass Pasteur pipette. The NMR-tube is then loaded into a Bruker Avance III HD 400, containing a Bruker Ascend^{TM} 400 magnet, equipped with a 5 mm PABBO BB (31P-109Ag)/19F-1H/D SmartProbe with z-gradients and ATM accessory for Automatic Tuning and Matching. The apparatus operates at 400 MHz.

4.5 Hydrogel formation

As a possible application, the extracted EPS are used to make hydrogels. The mechanical strength (and hence, the quality) of the obtained hydrogels is rheologically determined and compared to well-known reference hydrogels.
Rheological tests are carried out on hydrogels made of κ-carrageenan (TCI Chemicals, Japan) and sodium alginate, from brown algae (Sigma Aldrich, USA), as well as on hydrogels made of extracted EPS. To keep the variability in the hydrogel formation as low as possible, hydrogels of the model systems and the EPS are made in a similar fashion, the only difference being the size of the gels made. This is important, as the available amounts of extracted EPS are much lower than those of κ-carrageenan and sodium alginate.

Hydrogel formation - model systems

The different hydrogels are made using a hydrogel base, which is poured inside a 3D-printed mold. The whole is put in a salt solution to induce the gelation of the hydrogel base, as the cations of the salts induce physical crosslinking. Like this, firm hydrogels are formed.

To make the hydrogel bases of κ-carrageenan, various amounts of the model system are put in 20 mL of a 0.01 M sodium hydroxide solution (NaOH), made by combining 2 mL of 0.1000 M NaOH solution (VWR Chemicals, USA) with 18 mL of ultrapure water. The amounts needed to make mixtures with κ-carrageenan content, ranging from 1.0 to 2.5 wt%, can be found in Table 4.1. The mixture is then put in a water bath (bain-marie principle), heated to 80 ℃ to enable the incorporation of the κ-carrageenan into the NaOH solution. Once fully incorporated, the hydrogel base is cooled down, after which it is poured into the molds.

For the hydrogels of sodium alginate, different amounts of the model systems are put in 20 mL of a 0.1000M NaOH solution (VWR Chemicals, USA), to obtain hydrogel bases with sodium alginate content ranging from 1.0 to 2.5 wt% (see Table 4.1). The mixture is stirred at room temperature, until a homogeneous consistency is achieved, after which the molds are filled.

Table 4.1: Different amounts of sodium alginate or κ-carrageenan needed to obtain hydrogel bases with the desired concentration of model system.

Desired concentration model systems [wt%]	Volume NaOH [mL]	Mass model system [g]
1.0	20	0.202
1.5	20	0.304
2.0	20	0.408
2.5	20	0.513

These hydrogel bases are then poured into a 3D-printed mold, based on the protocol made by Pagliaccia [157]. All 3D-models discussed are made with the Shapr3D software package (https://www.shapr3D.com/), and exported to .stl-files. These are converted to G-code using the Ultimaker Cura software, Version 5.9.2. The molds in this work are made using polyethylene terephthalate glycol (PETG), instead of the more conventional PLA, due to the undesired swelling and degradation of PLA when put in water [166]. The molds are printed using the Creality Ender 3 V3 KE, by Ultimaker (Shenzhen, China) with a plate temperature of 75 °C and a nozzle temperature of 235 °C. The infill of the print is set to 100 %. A picture of the different pieces is shown in Figure 4.2a. As visible on the figure, the mold consists of two caps and one ring, in which the hydrogel is formed. The dimensions used in the 3D-design are given in Figure A.1 and A.2, in Appendix A.1.

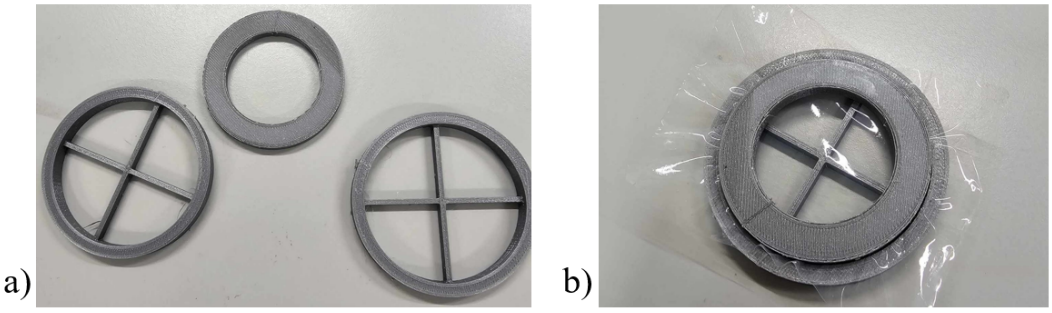

FIGURE 4.2: 3D-printed mold to make hydrogels of the model systems: **a)** The 3D-printed mold consists of two caps and one annular ring. The design of the molds is based on the work of Pagliaccia [157]. **b)** As an intermediate step in the formation of the hydrogels, a dialysis membrane is put in between one of the caps and the ring.

To form the hydrogels, an activated dialysis membrane (Spectrum Laboratories Inc., USA), that is cut open, is put between one cap and the annular ring. Like this, a configuration as shown is Figure 4.2b is obtained. Next, the hydrogel base is poured inside the ring, a second dialysis membrane sheet is put on top of it and the whole is closed of using the second cap. The system is then kept horizontally and at a constant height inside a salt solution for 36 h, using a clamp as shown in Figure 4.3. Different solutions of potassium chloride ($\geq$ 99 %, Acros Organics, Belgium), calcium chloride ($\geq$ 99 %, Sigma-Aldrich, USA) or combinations of the two are used, with the concentrations of the salts varying from 0.01 to 0.1 M. The salt solution is replaced four times in the formation of the hydrogel.

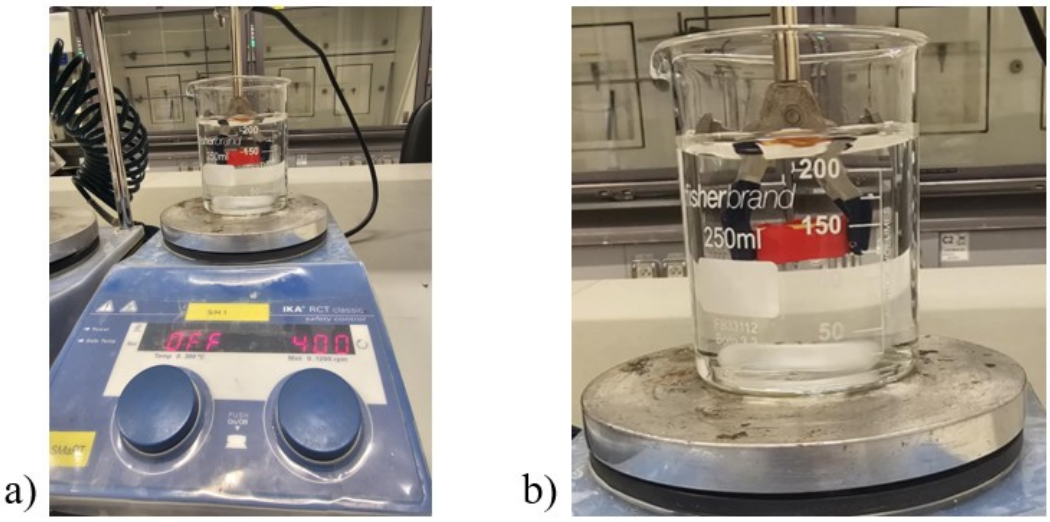

Figure 4.3: Experimental setup used to make the different hydrogels. The mold containing the hydrogel base is kept horizontally in a salt solution for 36 h in order to crosslink.

Hydrogel formation - extracted EPS

EPS extracted from different sludge samples are put in a small vial, after which 0.1000 M NaOH solution is added to it, to obtain hydrogel bases with EPS concentrations of 2 and 5 wt%. The volume of the hydrogel base is kept close to 1 mL. The whole is mixed using a magnetic stirrer, until all EPS has dissolved.

The hydrogel base is then poured in a 3D-printed mold, based on the paper of Pagliaccia [157]. A picture of the mold is shown in Figure 4.4, while the dimensions used in the 3D-design are given in Figure A.3 and A.4, in Appendix A.1. Also in this case, the mold is made of PETG instead of the more conventional PLA.

The assembly of the hydrogel base inside the mold is exactly the same as discussed before. Once assembled, the whole is kept inside a salt bath, containing potassium chloride ($\geq$ 99 %, Acros Organics, Belgium) and calcium chloride ($\geq$ 99 %, Sigma-Aldrich, USA) at a concentration of 0.1 M, for 96 h, to ensure that as much ions as possible have had the chance to diffuse into the hydrogel base. This is also done because the EPS hydrogels tend to have a lower strength and moduli, such that it is desired to keep the hydrogels longer in the salt solution, to enable as much physical crosslinking as possible.

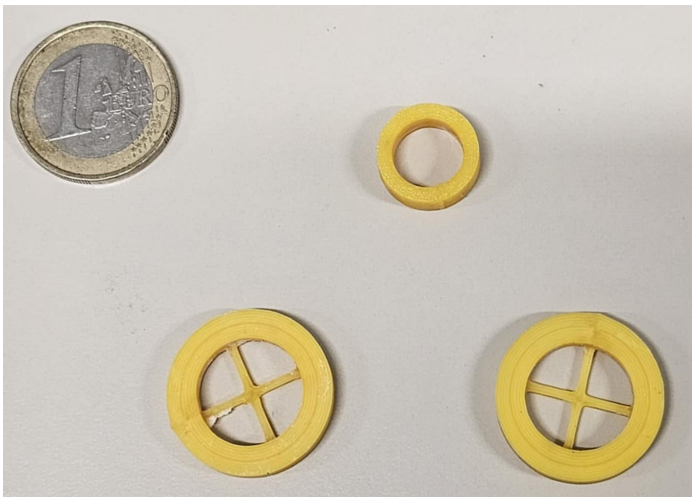

FIGURE 4.4: 3D-printed mold to make hydrogels of EPS. The design of the molds is based on the work of Pagliaccia [157]. The mold consists of one annular ring and two caps, with the 1 euro coin acting as a reference for the mold's size.

4.6 Rheological tests on hydrogels

4.6.1 Model system hydrogels

Rheological tests on the model systems hydrogels are performed on a stress controlled AR-G2 rheometer (TA Instruments, Antwerp, Belgium), using a 25 mm disposable parallel plate geometry. The bottom Peltier plate is set to 20 ℃ and is connected to a water bath. Sand paper is added to the top and bottom geometries to minimize slip between them and the hydrogel.

Time sweeps are performed at a strain of 0.01 % and an angular frequency of 1 $\frac{\text{rad}}{\text{s}}$ for 30 minutes, to check the time dependency of the storage and loss modulus of the gel. Via amplitude sweeps, from 0.001 % to 100 % and at an angular frequency of 1 $\frac{\text{rad}}{\text{s}}$, the linear visco-elastic regime (LVER) is determined, as the point where the moduli deviate more than 5 % from the initial value. The frequency dependent behavior of the moduli is determined via a frequency sweep, in which the oscillation amplitude is kept at 0.01 %, while decreasing the oscillation frequency stepwise from 100 to 0.1 $\frac{\text{rad}}{\text{s}}$. The oscillation amplitude is selected such that it is located in the linear viscoelastic regime, as confirmed by the amplitude sweeps, provided in Appendix A.2.

For all dynamic tests, the conditioning time is set to 5 s, while the sampling time is equal to 1 cycle. As the different hydrogels have varying thickness, the top plate geometry is lowered until it touches the sample and a normal force of 1 N is reached. At this point, the experiment is started.

4.6.2 EPS hydrogels

All rheological tests on hydrogels made of EPS are performed on a stress-controlled Discovery HR-3 rheometer (TA Instruments, Antwerp, Belgium), using an 8 mm disposable parallel plate geometry as top geometry and a Peltier plate as bottom geometry. The temperature is kept constant at 20 ℃ by connecting the bottom Peltier plate geometry to a water bath. Sand paper is added to the top and bottom geometries to minimize slip between them and the hydrogel.

Amplitude sweeps from 0.001 % to 100 % strain at an angular frequency of 10 $\frac{\text{rad}}{\text{s}}$ are measured to obtain the linear visco-elastic regime (LVER). This is defined as the point where the moduli deviate more than 5 % from the initial value. The frequency is increased compared to the model system hydrogels as the EPS hydrogels are generally weaker and show smaller moduli, resulting in a lower torque. By increasing the angular frequency, a better signal-to-noise ratio on the measured torque is obtained. The frequency behavior of the moduli of the hydrogels is determined via a frequency sweep, with an oscillation amplitude is kept at 5 % and a frequency decreasing from 100 to 0.1 $\frac{\text{rad}}{\text{s}}$. The oscillation amplitude is increased to enhance the signal-to-noise ratio for the measured torque, while still being sufficiently small to be inside the LVER, which is verified by the amplitude sweeps, provided in Appendix A.2.

For all dynamic tests, the conditioning time is set to 5 s, while the sampling time is equal to 1 cycle. The sample is loaded on the top geometry after which it is lowered until the top plate's surface is fully covered. Next, the geometry is lowered to 1200 μm, after which the sample is scraped for the first time. The gap is then further lowered to 1000 μm, which is the gap height for all experiments, and is kept constant throughout the measurements. At this point, the experiment is started.

Chapter 5

Extraction of EPS

The first part of this work discusses the extraction process to obtain EPS from various types of biomass. As concluded in the literature survey, no standardized method has been proposed yet. Therefore, four different extraction routes are compared in this section; being extraction using (1) heat and sodium carbonate (Na_2CO_3), (2) NaCl, (3) urea and (4) a combination of NaCl and urea. The first method is chosen since Felz suggested that this method results in the highest EPS yield [59]. The extraction method using urea and NaCl has already been used by Bose *et al.* to extract protein from crickets [16]. The last three methods are based on the principles of hydrogel disruption, as their integrity can be attributed to both hydrogen bonds and ionic interactions. Selectively disrupting one or both of these mechanisms reduces the hydrogel's integrity, facilitating the extraction of EPS components from different sources.

Comparing the methods is quite challenging and requires both qualitative and quantitative measurements. Therefore, five criteria are used to select the optimal extraction method, which are (1) the amount of extracted EPS, (2) the organic matter present in the EPS, (3) the duration of the extraction method, (4) the quality of the Nuclear Magnetic Resonance (NMR) spectrum, and (5) the amount of cell lysis. NMR is the preferred characterization method, as it only requires 10 mg of EPS. The extraction protocol should prevent cell lysis in the initial biomass, such that a pure EPS fraction can be isolated. Hence, cell lysis is selected as the fifth criterion, as it can be quantified by applying each extraction protocol to *Escherichia coli* (*E. coli*) containing Green Fluorescent Protein (GFP). The concentration of GFP in the extracted EPS is a measure of the extent of cell lysis for each extraction method. Lower degrees of cell lysis are preferred, as the contamination of EPS with intracellular material is undesired.

The protocols discussed in this chapter are meant to be applied on various industrial sludges throughout the remainder of this work, each containing a distinct and complex mixture of biological, chemical, and biochemical components that depends on many external factors [182]. It is possible that different samples of the same batch of sludge contain EPS with a different composition. To minimize the variability

between the different biomass samples, each extraction protocol is performed on pellets of the fungal species *Aspergillus oryzae* (*A. oryzae*). These pellets have a more controlled content, as they only contain one microbial species that forms a more reproducible EPS matrix when grown under the same conditions.

5.1 Methodology

A. oryzae pellets are grown according to the protocol shown in Section 4.2. The four extraction methods described in Section 4.3 are applied to the pellets. The quantification method of cell lysis from *Escherichia coli*, as described in Section 4.4.1 and the determination of the total and volatile solids, from Section 4.4.2 are applied as well. Finally, NMR and TGA analysis are performed as characterization methods, following the protocols outlined in Sections 4.4.2 and 4.4.3.

5.2 Results

5.2.1 Extracted mass and its organic fraction - TGA analysis

First, the extraction using heat and Na_2CO_3 is applied to 3 g of wet pellets of *A. oryzae*, from which only 22 mg of EPS is extracted. The organic fraction of the biomass is determined as the decrease in mass between 200 °C and 550 °C, based on the suggestion by Chen *et al.* [33]. Even though the authors state that the degradation of carbohydrates already begins at 164 °C, the starting point in this work is set at 200 °C, to avoid the inclusion of the thermal degradation of urea, which occurs between 135 and 190 °C [219], in the determined organic fraction. With this definition, the TGA curve in Figure 5.1 shows that only 10 % of the EPS extracted with heat and Na_2CO_3 is organic, as the weight decreases from 80 % to 70 % between 200 and 550 °C. The curve clearly shows a gradual decrease of mass between 200 and 550 °C, which can be attributed to the degradation of the EPS. The most significant decrease, however, is visible between 100 and 150 °C, which can be attributed to the residual water present in the extracted EPS, even after drying in the vacuum oven for over 48 hours. At the end of the test, approximately 70 % of the initial mass remains, corresponding to the inorganic material present in the sample. This includes (part of) the Na_2CO_3 used for the extraction, as well as the ions initially present inside the pellets.

When comparing the TGA results of all four extraction methods, as shown in Figure 5.2, it becomes clear that extraction with NaCl results in an extract containing 75 % organic material. For the extraction with urea and a combination of urea and NaCl, these values equal 57 % and 38 %, respectively. The degradation profiles show that the EPS extracted with urea displays a relatively large decrease in mass between 150 and 200 °C, compared to those extracted with NaCl and Na_2CO_3, which can be attributed to the presence of residual urea in the extract [219].

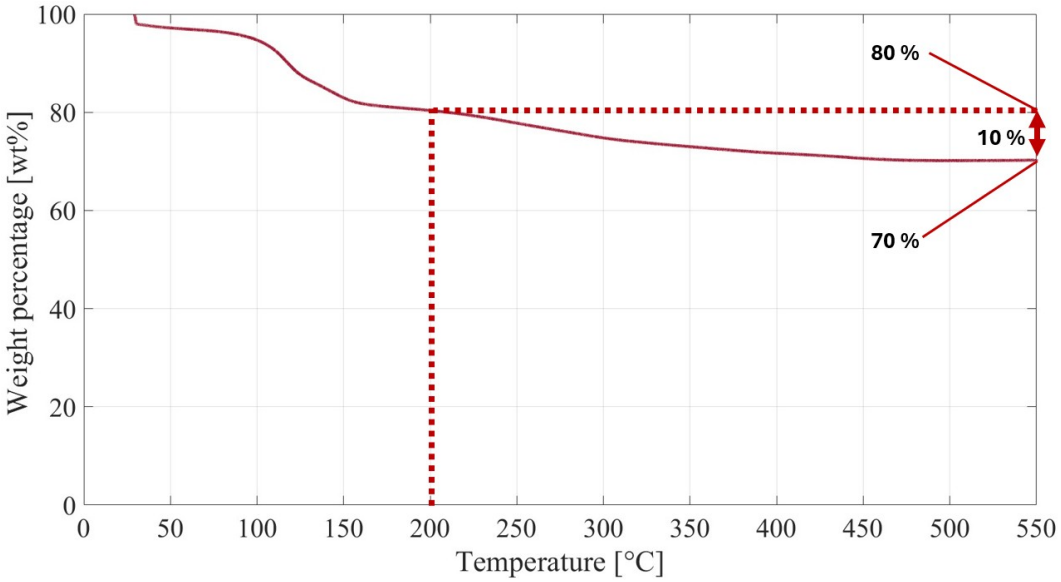

FIGURE 5.1: TGA-curve of EPS extracted from *Aspergillus oryzae*, using heat and sodium carbonate. The weight is plotted as a function of the temperature, expressed as percentage of the initial weight of the sample at 25 ℃.

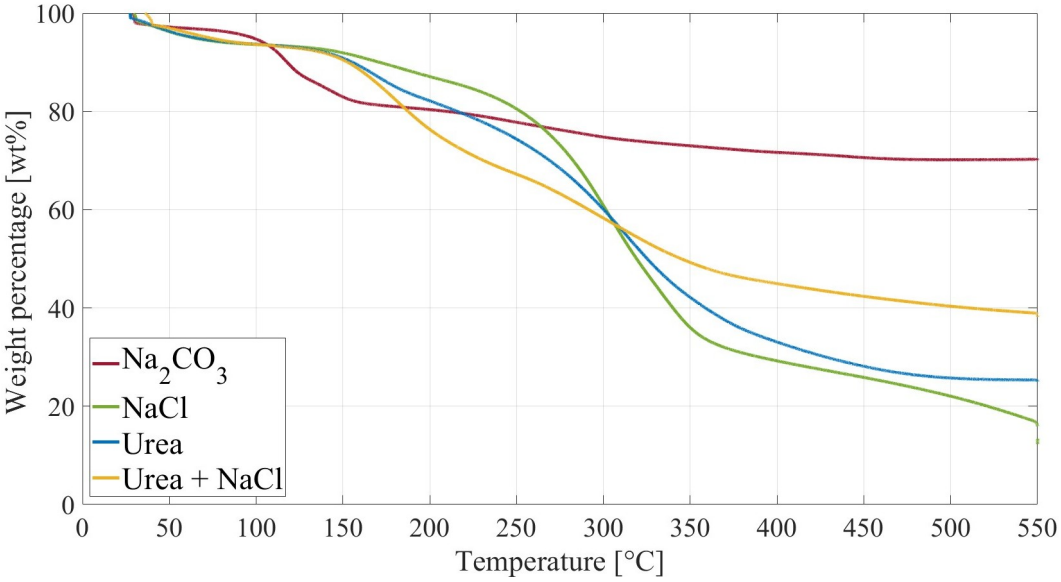

FIGURE 5.2: TGA-curve of EPS extracted from *Aspergillus oryzae*, using the four different characterization methods, discussed in Section 4.3: (1) heat and Na_2CO_3, (2) NaCl, (3) urea and NaCl and (4) urea. The weight is plotted as a function of the temperature, expressed as percentage of the initial weight of the sample at 25 ℃.

5.2.2 Organic EPS characteristics - NMR

The ^{1}H-NMR spectrum of the EPS extracted with Na_2CO_3 is given in Figure 5.3. Multiple peaks are observed in the spectrum, most of which are rather small and narrow. The most prominent peak in Figure 5.3, located at a shift of 4.646 ppm, is attributed to the residual water, still present in the EPS after drying [8]. Most of the peaks lay in the regions between 3.7 and 3.3 ppm, corresponding to H-atoms from the sugar rings [1] and between 2 and 0 ppm. To identify the peaks, the NMR peaks website (https://nmrpeaks.com/) is used. For the peak at 8.319 ppm, formic acid is identified as the closest match, at a NMR shift of 8.26 ppm. This value is confirmed by Babij *et al.* [8]. It is unlikely that this molecule is present in the extracted EPS on its own, as no formic acid is used during the extraction. However, molecules similar to formic acid, containing a carboxylic acid group, are expected to be present in the extracted EPS, as such groups are found in free fatty acids, as well as in individual amino acids and proteins containing aspartic or glutamic acids, and in humic acids.

For the other regions, it is too tedious to look at all possible molecules that could result in peaks. Therefore, an NMR table (see Figure C.1, in Appendix C.1.3) showing the typical chemical shifts for some common chemical bonds is used [202]. The region between 3.7 and 3.3 ppm possibly corresponds to bonds such as alcohol, ether and ester bonds, typically seen in organic molecules, like sugars. This corresponds to the statement of Abeygunawardana *et al.* as the region is located completely within the so-called "sugar ring" region, discussed in their paper [1]. Also halide bonds, like organic chloride and bromide bonds, have characteristic shifts in this region. These are less often observed in biomolecules like proteins and polysaccharides [39], which are the most prominent molecules in EPS [80, 189], but can occur in lipids as halogenated fatty acids [47]. However, these are mostly originating from marine sources, such that halide bonds are expected to have a negligible contribution to the NMR spectrum shown in Figure 5.3. The shift between 2 and 0 ppm, on the other hand, is most likely caused by saturated alkanes, alcohols, and amine groups [202], which also occur in the biomolecules mentioned earlier.

NMR spectroscopy is also carried out on EPS extracted using the NaCl extraction as well as the urea and NaCl extraction method. No NMR spectrum of the EPS extracted via the urea extraction protocol was determined, as the amount of EPS was too low to obtain a sufficiently high-quality NMR spectrum. The spectra of the EPS extracted using the other two methods are provided in Figures B.1 and B.2, in Appendix B.2, while the regions between 4 and 3 ppm, as well as between 2 and 0 ppm are provided in Figure 5.4. Both spectra look similar to each other for NMR shifts above 2.5 ppm. The spectrum of the EPS extracted using urea and NaCl (Figure B.2) shows less pronounced and wider peaks at lower phase shifts compared to the spectrum of EPS obtained using the NaCl extraction (Figure B.1). Both spectra in Appendix B.2 show a large peak around a shift of 2.069 ppm, which could be assigned to molecules containing an acetate-like structure in them [8]. This peak is not visible in the spectrum of the EPS extracted with heat and Na_2CO_3 (Figure

5.3), which does show two peaks at 2.55 and 1.779 ppm, which are not visible on the two spectra in Figures B.1 and B.2. Also these peaks can be attributed to amine and alcohol structures [202].
All three NMR spectra indicate that the majority of the peaks are located in the regions between 4 and 3 ppm and between 2 and 0 ppm. Hence, Figure 5.4 gives a comparison of these regions for the three spectra. The NMR spectra of the EPS extracted using NaCl (2), and urea and NaCl (3) show the strongest similarities, as they both show a broad peak covering almost the entire region between 4 and 3 ppm. This is strikingly different from the spectrum of the EPS extracted with heat and Na_2CO_3 (1), which shows many peaks close to each other between 3.7 and 3.6 ppm, as well as four peaks around 3.5 and 3.4 ppm. These peaks are likely to be caused by low-molecular-weight species [201]. The presence of high-molecular-weight EPS is confirmed as well, by the broad peaks observed between 2 and 0 ppm. Hence, in the case of the EPS extracted using heat and Na_2CO_3, the membrane centrifugation used to separate the EPS from the low-molecular-weight species is unable to purify the EPS sufficiently. For this reason, a membrane dialysis must be performed to purify EPS extracted using heat and Na_2CO_3.

Although it is clear that the composition of the extracted EPS depends on the selected extraction protocol, as confirmed by literature [27, 37, 59, 240], all spectra show the presence of EPS, irrespective of the extraction method. The presence of the low-molecular-weight species in the EPS extracted using heat and Na_2CO_3 is problematic. Nevertheless, based on the observation that the NMR spectra of the EPS from the other two extraction protocols do not show low molecular weight species, it is expected that this problem will be resolved by using membrane dialysis to purify the EPS. Nevertheless, this statement is not confirmed in this work. Hence, no definite conclusion can be drawn regarding the extraction protocol preference, based on the NMR results.

5.2.3 Ease of extraction

The ease of extraction is a rather subjective property and is quantified by the time required to perform an extraction. For the heat and Na_2CO_3 extraction, this time equals 6 hours, consisting of 35 minutes for the extraction, 20 minutes for the centrifugation, and 5 hours for the centrifugation dialysis. For the other methods, a much longer time is required as the membrane dialysis step alone already requires 48 hours.

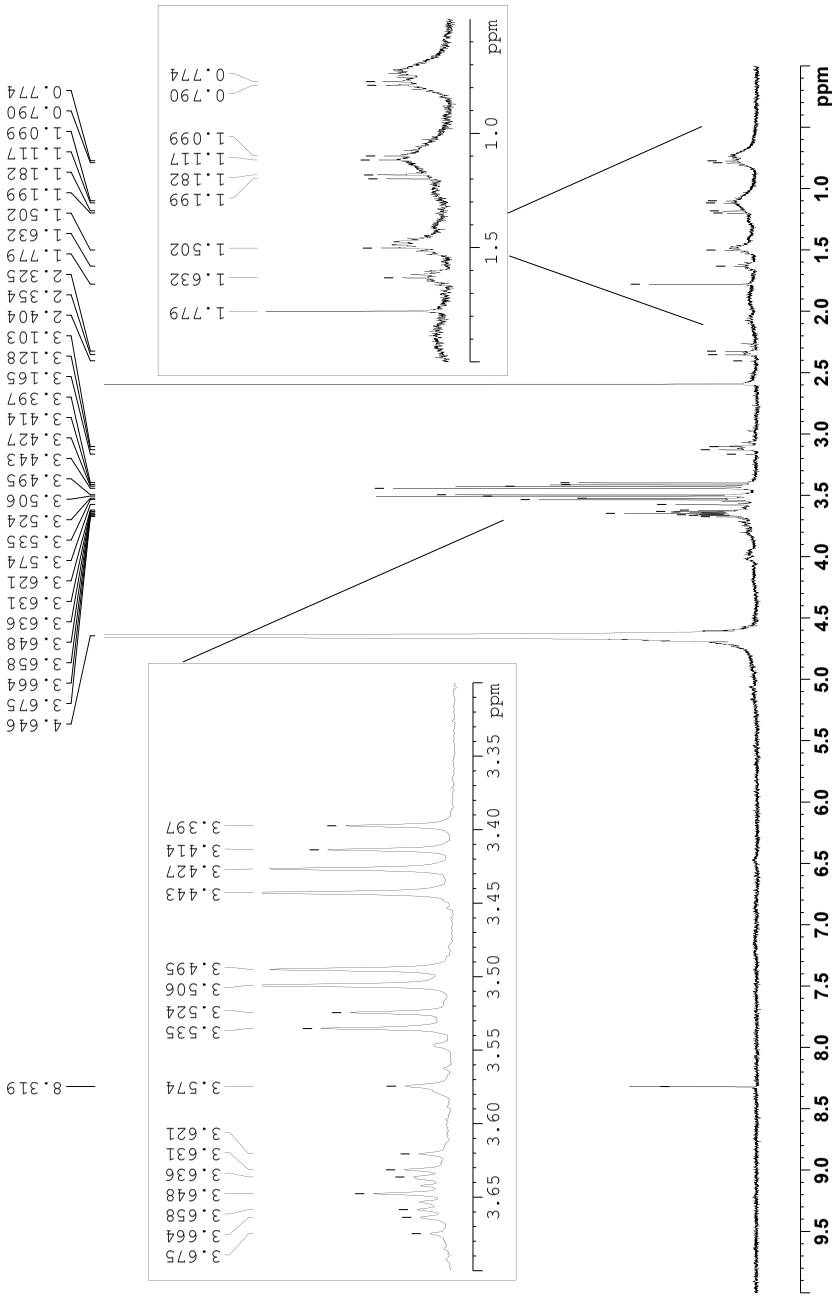

Figure 5.3: ^{1}H-NMR spectrum of EPS extracted from *Aspergillus oryzae*, using heat and sodium carbonate. The spectrum is made using the TopSpin software package (Bruker, United States of America).

FIGURE 5.4: ^{1}H-NMR spectrum of EPS extracted from *Aspergillus oryzae*, using (1) heat and sodium carbonate, (2) NaCl and (3) urea and NaCl, zoomed in between 4 and 3 ppm, and between 2 an 0 ppm. The spectrum is made using the TopSpin software package (Bruker, United States of America).

5.2.4 Extent of cell lysis

Finally, the extent of cell lysis is determined via excitation-emission spectroscopy. Each extraction protocol is applied to *Escherichia coli* (*E. coli*) containing green fluorescent protein (GFP), after which the extract is put in a plate reader to determine its absorbance and excitation/emission parameters. The amount of green fluorescent protein in the extract is a direct indicator of the extent of cell lysis, which can be quantified by measuring the amount of light absorbed or emitted by the extract at the characteristic wavelengths of GFP. These measurements should be directly proportional to the concentration of GFP in the extract.

Figure 5.5 illustrates the differences in color between the EPS extracted from the *Escherichia coli* containing GFP, according to the four protocols. A bright yellow color can be observed for the EPS extracted with heat and Na_2CO_3 (a), indicating the greatest extent of cell lysis. A hint of yellow is also visible on the extracts from the urea (c) and urea and sodium chloride protocols (d). In contrast, the sodium chloride extraction shows the lowest amount of yellow (b). To quantify these observations, the extracts are filtered, and UV-VIS measurements are performed, of which the absorbance and excitation-emission results are given in Tables 5.1 to 5.3, at 395, 480, and 488-510 nm, respectively. The tables also show the values of the references, which are the solutions used to carry out the extraction. These results confirm the observations with the naked eye, as the absorption data at 395 and 480 nm wavelengths both show the most significant difference between the extract and the reference for the heat and Na_2CO_3 extraction method. The smallest difference is observed for the NaCl extraction, while the other two extractions show similar results.

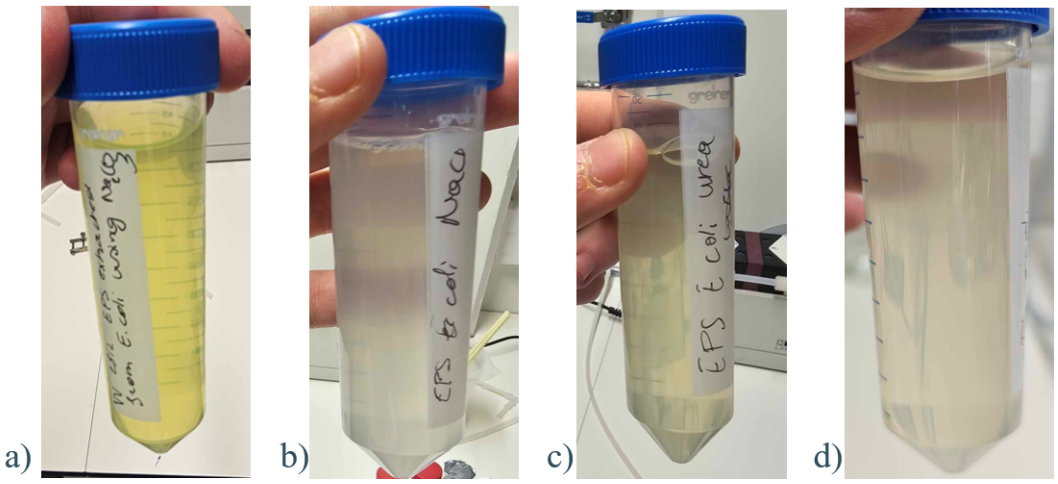

Figure 5.5: Supernatant of the extraction methods, applied on *Escherichia coli* containing Green Fluorescent Protein. **a)** Heat and sodium carbonate extraction **b)** Sodium chloride extraction **c)** Urea extraction **d)** Urea and sodium chloride extraction

TABLE 5.1: Absorbance data of the extract from the four different extraction methods, applied on *Escherichia coli* containing green fluorescent protein, at a wavelength of 395 nm. For each row, the reference is the solution used to extract the EPS during the respective extraction protocol.

Extraction protocol	Extract absorbance [-]	Reference absorbance [-]	**Difference [-]**
Heat and Na_2CO_3	0.4127	0.0426	**0.3701**
NaCl	0.0643	0.0429	**0.0214**
Urea	0.1350	0.0443	**0.0907**
Urea and NaCl	0.1194	0.0453	**0.0741**

TABLE 5.2: Absorbance data of the extract from the four different extraction methods, applied on *Escherichia coli* containing green fluorescent protein, at a wavelength of 480 nm. For each row, the reference is the solution used to extract the EPS during the respective extraction protocol.

Extraction protocol	Extract absorbance [-]	Reference absorbance [-]	**Difference [-]**
Heat and Na_2CO_3	0.1588	0.0370	**0.1218**
NaCl	0.0473	0.0376	**0.0097**
Urea	0.0721	0.0386	**0.0335**
Urea and NaCl	0.0565	0.0397	**0.0168**

TABLE 5.3: Excitation-emission data of the extract from the four different extraction methods, applied on *Escherichia coli* containing green fluorescent protein, at wavelengths of 488 and 510 nm. For each row, the reference is the solution used to extract the EPS during the respective extraction protocol.

Extraction protocol	Extract emission [-]	Reference emission [-]	**Difference [-]**
Heat and Na_2CO_3	1797	811.33	**895.67**
NaCl	454.67	903	**-448.33**
Urea	520	798.33	**-278.33**
Urea and NaCl	217	670	**-453.00**

5.3 Discussion

The different extraction methods are compared in Table 5.4, based on the five aforementioned criteria. When considering the relative amount of organic matter present inside the EPS, it is clear that the extracts only contain between 0.63 and 3.38 mg of organic matter, which equals only 1 ‰ of the wet weight used in the extraction process. However, the wet weight is not entirely representative of the amount of biological material in the initial biomass, as it also includes water and inorganic salts. Therefore, the volatile solids (VS) content of the *A. oryzae* pellets is determined (see Appendix B) and appears to be, on average, 19.5 mg of VS per 1 g of initial wet pellets. Hence, the amount of extracted organic matter remains relatively low (between 1 and 5.7 %), but it is at least higher than the 1 ‰ assumed previously.

Next, a comment has to be made regarding the extraction time for the heat and Na_2CO_3. As mentioned earlier, the NMR spectrum of the EPS extracted using this protocol shows bands around 3.5 and 3.4 ppm, which appear to have the characteristics of low-molecular-weight species [201]. These are, of course, undesired, as the final extract should only contain extracellular polymers with higher molar masses. Hence, membrane centrifugation is insufficiently able to remove molecules with low molar mass from the extracted EPS; therefore, a membrane dialysis step is also preferred for this extraction. This increases the extraction time required for the heat and Na_2CO_3 extraction from 6 h to 36 h.

The most notable difference is observed in cell lysis, as the difference between the reference solution and the extracted EPS is more than four times larger for the heat-Na_2CO_3 extraction compared to the other extraction protocols, resulting in the contamination of the extracellular polymers with intracellular ones. Depending on the kind of research or application, this can be more or less problematic. When focusing on the more fundamental scale, to identify the different types of biomolecules inside the EPS, cell lyss is undesired, as only the **extracellular** components are in focus. When a more application-oriented research is performed, cell lysis is less important, as the extracted material is only intended to be used in a specific application. In this case, the distinction between intracellular material and extracellular material becomes less important, as in this case, the term 'EPS-based biomaterial' comes more into play, as used by Le *et al.* [111].

A critical remark regarding the cell lysis data is that *Escherichia coli* bacteria are known to lyse easily, when subjected to a temperature of 80 °C, due to cell wall disruption [173]. As a result, large amounts of cells are lysed during the extraction protocol using heat and Na_2CO_3, resulting in the release of GFP in the extract, which is also visible in Figure 5.5a. The thermal cell lysis behavior of *E. coli* may not be representative of the different organisms in the various sludge samples. Nevertheless, it is expected that the high temperatures and alkaline conditions used in the heat and Na_2CO_3 extraction would induce more cell lysis compared to the other extraction protocols [90].

In addition, the UV-VIS data may not accurately reflect the true extent of cell lysis due to possible protein denaturation of GFP caused by the heat, salts, and urea used in the extraction protocols. However, Alkaabi *et al.* found that GFP denaturation is only significant at pH values below 6.5 [5]. For higher pH values, as applicable during the extraction protocols used in this work (see Appendix B.3 for the determination of the pH during the heat and Na_2CO_3 extraction method, which is confirmed by Le *et al.* [111]), GFP appeared to be relatively stable against temperature- and urea-based denaturation. Based on their results, the relative intensity of the GFP after both the urea, and heat and Na_2CO_3 extraction processes is expected to be approximately 60 % of the original GFP intensity, keeping the ratio between the differences shown in Tables 5.1 to 5.3 constant. Stepanenko *et al.* observed that NaCl also influences the absorption of GFP, with 2.5 M of NaCl resulting in a 35 % lower absorption at 480 nm [200]. Although the UV-VIS data may not be entirely representative of the actual degree of cell lysis, some general insights can still be obtained from the results in Tables 5.1 to 5.3. A more conclusive result on the extent of cell lysis could be obtained by using 2-keto-3-deoxyoctonate or glucose-6-phosphate dehydrogenase as markers of cell lysis [2, 50].

From the five criteria shown in Table 5.4, the optimal extraction protocol can be determined. The column representing the NMR results is omitted as no results were particularly outstanding. The table clearly shows that the long extraction time is the only disadvantage of the NaCl extraction method. All the other results appear to be as good or even better than the other extraction protocols. Therefore, the NaCl extraction is selected as the most optimal one. Also the heat and Na_2CO_3 scores well on all criteria, except for the very poor result of the cell lysis. Although it is one of the protocols most often applied in literature for EPS extraction, it does not appear to be the most optimal one. However, in order to make the most comparable conclusions, the heat and Na_2CO_3 extraction method is applied for all extractions throughout the remaining chapters of this work.

TABLE 5.4: Comparison table of the different extraction methods (++) is excellent, (+) is good, (±) is average, (-) is poor, (- -) is very poor.

	Extracted material [mg]	Organic material [mg]	Extraction time [h]	Cell lysis
Heat and Na_2CO_3	22.0	2.22	6 (36)	- -
NaCl	4.5	3.36	48	+
Urea	1.1	0.63	48	±
Urea and NaCl	5.0	1.91	48	±

5.4 Conclusions

In this chapter, a comparison was made between four different extraction protocols based on the amount of material extracted, the organic fraction of the extract, the duration of the extraction, the NMR spectra of the obtained EPS, and the extent of cell lysis.

The amounts of extracted EPS range from 1.1 to 22 mg of material, which appears to be very low considering that 3 g of initial wet biomass are used in each protocol. When taking into account the organic fractions, it is observed that the extracts contain only between 0.63 and 3.36 mg of biological material. However, as 1 g of wet biomass only contains 19.5 mg of volatile solids, the obtained values are not dramatically low, ranging from 1.0 to 5.7 percent of the total volatile solids in the sample.

The most drastic differences are observed in the cell lysis, as the absorbance at 395 and 480 nm of the EPS extracted using heat and Na_2CO_3 are more than four times larger than those of the other methods, indicating the largest extent of cell lysis. The absorption values of the NaCl extract are the lowest.

The extraction time appeared to be rather similar, as the heat and Na_2CO_3 extraction also requires a membrane dialysis to remove the low-molecular-weight species from the extracted EPS, resulting in an extraction time of 36 h, which is slightly less than the 48 h needed for the three other extractions. The NMR results did not show significant differences between the different protocols.

Based on these results, the NaCl extraction is categorized as the most optimal extraction protocol. However, as the heat and Na_2CO_3 method is most often applied in literature, it is selected as the extraction method applied throughout the remainder of this work. From this chapter, it is thus clear that the EPS extracted using this method are a mixture of extracellular and intracellular components, such that the term EPS-based materials is a better representation of the material obtained after the extraction protocol.

Chapter 6

Comparison of EPS from different sources: from pure cultures to full-scale sludges

Chapter 6 gives a comparison of the characteristics of EPS extracted from various sources. Three pure cultures, being *Azoarcus communis*, *Dietzia maris* and *Aspergillus oryzae*, are compared to commercial sludges as sources for EPS.
Azoarcus communis are aerobic bacteria that are found in different natural sources, such as roots of plants or soil and can fixate N_2 to form NH_3 [239]. They produce amyloid-like adhesins, which are important glycoproteins for aggregate formation [109]. *Azoarcus* is a common denitrifier in conventional wastewater systems. Denitrifiers convert nitrate (NO_3^-) to nitrogen gas (N_2) while consuming organic carbon components in the absence of oxygen [184].
Dietzia maris are also aerobic bacteria extracted from both soil and carp fish [164] and are also known to produce extracellular amyloids [100]. *Dietzia maris* bacteria can be found in activated sludge from wastewater treatment, where they also act as denitrifiers [197].
Aspergillus oryzae are aerobic filamentous fungi used in food products that require fermentation in their production, like sake and soy sauce [107, 234]. They can be grown into millimeter-sized pellets in a saline environment under shear [154].

Apart from the pure cultures, EPS are also extracted from full-scale sludges (indicated as "real communities" in Figure 6.1), from both aerobic and anaerobic processes, as well as from fresh water and salt water applications.

A schematic overview of all the possible sources for EPS is provided in Figure 6.1. The ones in black are discussed in this work, while the ones in grey are added to complete the overview. They are not covered due to their unavailability within the regular master thesis time frame. The EPS extracted from several sources are mutually compared, as indicated by the different arrows, to gain fundamental insights into the relationships between the EPS characteristics and their sources.

First, a comparison (**H1**) is made between two of the aforementioned pure cultures: *Azoarcus communis* and *Dietzia maris*, both aerobic bacteria used in fresh water applications. Each bacterium is expected to produce EPS with a specific, yet similar composition, as their cellular processes are also expected to be similar.
In the second comparison (**H2**), these two pure cultures are compared to the full-scale community in the EBPR-granule. Both pure cultures and the EBPR-granule are grown aerobically in fresh water applications. Where the pure cultures only contain one type of bacteria, the full-scale communities are a mixture consisting of multiple bacterial species, as well as other microorganisms [133, 155]. The denitrifiers are expected to be among the dominating organisms in the EBPR-granule, as the sludge is used for carbon, nitrogen, and phosphorus removal from municipal wastewater from the city of Utrecht. The EPS characteristics of the two denitrifiers are, therefore, expected to be reflected in those of the EBPR-granule.
Next, a comparison (**H3a**) is made between floccular sludge from fresh water before and after adaptation to saline conditions. As discussed in Section 2.3, it is expected that the saline environment will affect the EPS composition, as it makes aggregation more difficult, necessitating the production of different EPS to counteract this change. The increased salt concentration of the environment also increases the osmolarity surrounding the microorganisms, resulting in a shift in the dominant bacteria, which induces a change in the EPS composition after salt adaptation.
The salt-adapted floccular sludge is compared to salt-adapted granular sludge (**H3b**), as both come from anaerobic processes in a saline environment. Granules are denser and larger aggregates than flocs. A more in-depth overview of the (morphological) differences between granular and floccular sludge is found in Section 2.2.2. As both sludges are used in an anaerobic process treating saline wastewaters, no significant differences in the EPS characteristics of the salt-adapted granular and floccular sludge are expected.
Finally, EPS from *Aspergillus oryzae* and salt-adapted granular sludge are compared (**H4**), as both can form aggregate-like structures in saline environments. It is expected that the EPS extracted from the salt-adapted granular sludge are more complex than that of *Aspergillus oryzae*, due to the greater variety of microorganisms present in it.

Based on the comparisons given in Figure 6.1, five hypotheses are proposed:

H1) EPS fingerprints/signatures of two denitrifiers are expected to be similar, as their cellular processes are also similar.

H2) EPS signatures from EBPR-granules are expected to show similarities to those from denitrifiers because they are one of the dominant species in these granules.

H3) EPS signature within a community changes when acclimating to higher salt concentration because the dominant species changes. More specifically: *H3a) EPS signatures are expected to be different before and after salt adaptation of the sludge.* and *H3b) EPS signatures of two salt-adapted sludges are expected to be similar.*

H4) EPS signature of salt-tolerant aerobic fungus is different from EPS signature of anaerobic salt-adapted granule community, due to its different microbiological complexity.

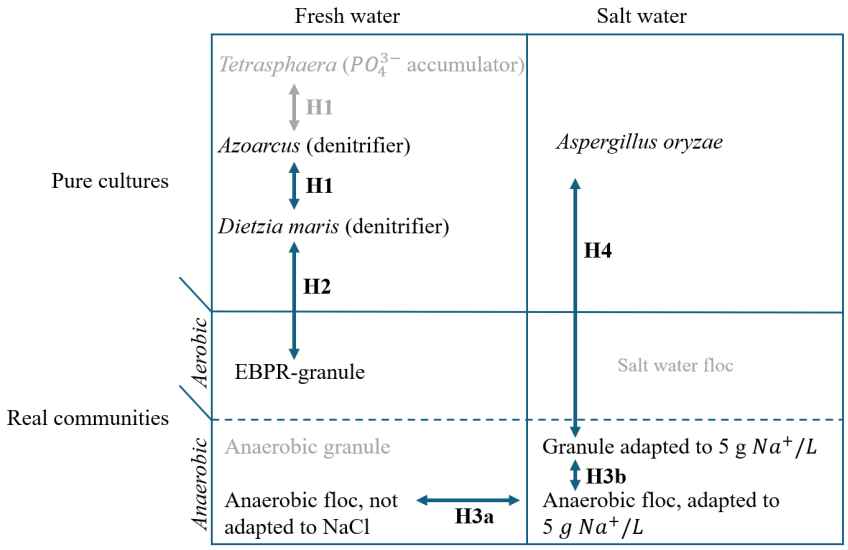

FIGURE 6.1: Schematic overview of the different sources for biomass, of which the EPS is extracted and characterized. The sources in black are discussed in this work, the ones in grey are not.

6.1 Methodology

This chapter discusses the extraction and characterization of EPS from all biomass samples mentioned in Sections 4.1 and 4.2, except *Escherichia coli*. The EPS are extracted according to the heat and sodium carbonate extraction protocol, as outlined in Section 4.3.1, and characterized using NMR, FTIR and Raman spectroscopy, as well as thermogravimetric analysis, as discussed in Sections 4.4.2 and 4.4.3.

6.2 Results and discussion

Here, the five hypotheses previously mentioned are verified and the most important differences in the extracted EPS of each type of biomass are highlighted. The focus is put on the interpretation of the FTIR spectra, as these contain the most information on the differences in EPS composition.

6.2.1 *Azoarcus communis* vs. *Dietzia maris*: two denitrifiers (H1)

As visible in Figure 6.2, the EPS extracted from *Azoarcus communis* and *Dietzia maris* have a distinctly different appearance. Where the *Azoarcus communis* have brownish-yellow colored EPS, the EPS from *Dietzia maris* are bright pink, indicating that they likely do not have an identical composition.

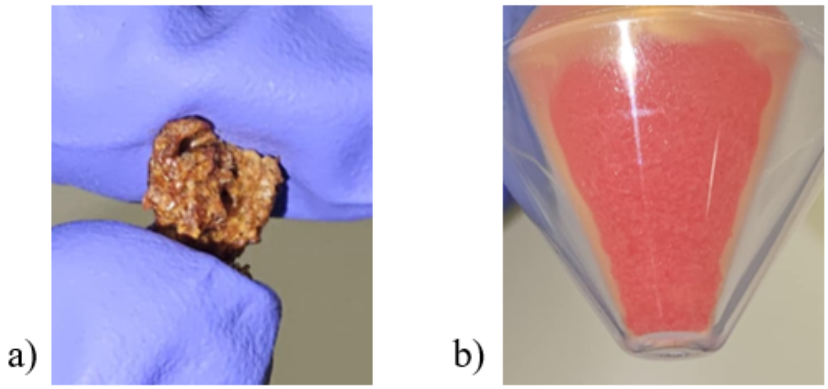

Figure 6.2: EPS extracted from two denitrifiers, using the heat and Na_2CO_3 extraction method **a)** EPS from *Azoarcus communis* **b)** EPS from *Dietzia maris*.

In contrast to their appearance, the Raman spectra of both extracted EPS, given in Figure 6.3, do not exhibit significant differences. The only differences are the small peaks at 1154 and 1513 cm^{-1}, which are only visible in the Raman spectrum of *Dietzia maris*. These two peaks can be attributed to the presence of carotenoids [218], which are natural pigments that contribute to the bright pink color of the extracted EPS [53, 78]. Goswami *et al.* confirmed that the carotenoid canthaxanthin is produced by *Dietzia maris*, validating the obtained peaks in the Raman spectrum. Peaks at 485 and 601 cm^{-1} are visible in both spectra and can be attributed to carbohydrates, like polysaccharides, according to Table C.2 in Appendix C.1.2 [55]. No assignments for the peaks at 790 and 1553 cm^{-1} could be found in this table, but they can be attributed to nucleic acids and tryptophan, respectively [18, 206].

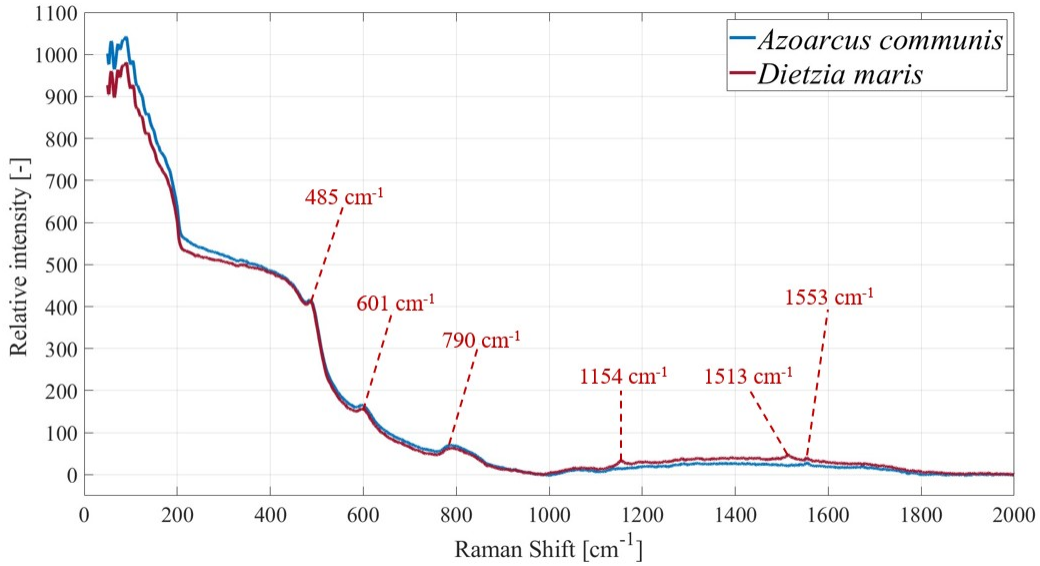

Figure 6.3: Raman spectra of EPS extracted from *Azoarcus communis* and *Dietzia maris* using the heat and sodium carbonate extraction method.

The FTIR spectra of the two denitrifiers also appear to be very similar, both containing a large water peak between 3500 and 2500 cm^{-1} and with most other peaks at the same location. The most significant difference visible is between the two peaks at 2920 and 2851 cm^{-1}, possibly caused by the more prominent presence of fatty acids in the EPS from *Dietzia maris* [185]. Raman spectroscopy could not confirm this, as lipids typically have characteristic peaks at Raman shifts greater than 2000 cm^{-1}. The peak at 1232 cm^{-1} in the FTIR spectra in Figure 6.4, which is possibly caused by P−O or P=O bonds from phosphates [185], could indicate a higher presence of phospholipids in the EPS from *Azoarcus communis*, explaining the more slime-like consistency of the EPS from this strain. As these form a significant component of the cell membrane, this could indicate a higher amount of cell lysis for *Azoarcus communis* compared to *Dietzia maris*. This is not confirmed by the fatty acid peaks however, as the spectrum of *Azoarcus communis* exhibits smaller peaks at 2920 and 2851 cm^{-1}. The peak at 1042 cm^{-1} can be attributed to polysaccharides and indicates a higher amount present in the EPS of *Dietzia maris*. This is confirmed by the NMR data, shown in Figures 6.5 and 6.6, as the polysaccharide region, ranging from 4.4 to 3.2 ppm [1], contributes to 45 % of the total area under the NMR-curve, excluding the water peak for *Azoarcus communis*, while this value equals 56 % for *Dietzia maris*. Based on the FTIR spectra given in Figure 6.4, the two bacteria produce similar biomolecules, albeit with different compositions.

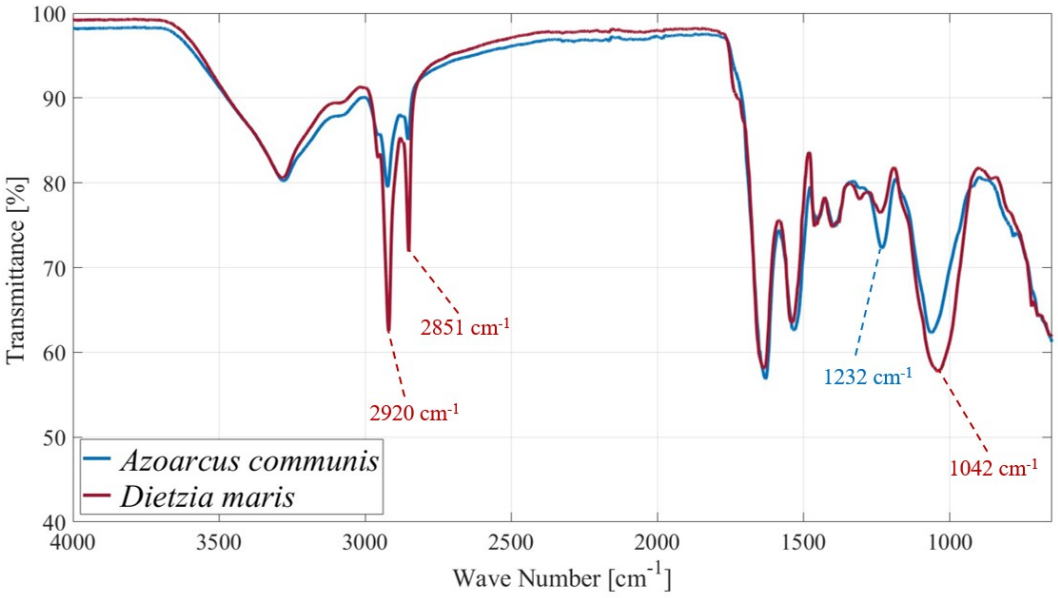

FIGURE 6.4: FTIR spectra of EPS extracted from *Azoarcus communis* and *Dietzia maris* using the heat and sodium carbonate extraction method.

The differences in the EPS content between the two bacterial strains are more prominent in their respective NMR spectra (Figures 6.5 and 6.6), as they display 34 peaks for *Dietzia maris* compared to 21 for *Azoarcus communis*, indicating that both samples contain different biomolecules. The EPS from *Azoarcus communis* show a greater intensity of peaks between 2.0 and 1.0 ppm, which can be attributed to methylated sugars [85, 137]. No explanation has been found for the difference in peak density between 5.5 and 6.0 ppm, due to the general difficulty of performing NMR on extracted EPS. Due to the complex and unknown composition of EPS, it is challenging to assign peaks at specific locations to a particular molecule [77]. Most knowledge comes from comparing EPS to model polysaccharides and examining the similarities between the two [85]. For proteins and lipids, peaks below 3.2 ppm were observed by Gonzalez-Gil *et al.*, but no specific peak values and their corresponding biomolecule were provided [77]. This makes it challenging to analyse the ^{1}H-NMR spectra of the EPS. One of the only regions that has been identified is the sugar ring region, which ranges from 4.4 to 3.2 ppm, as reported by Abeygunawardana *et al.* in their research on the NMR spectra of bacterial polysaccharides [1]. This region can be assigned to the polysaccharides present in the EPS, which is why it can be used to obtain an understanding of the relative contribution of polysaccharides to the EPS content. This is done in a similar fashion to that described before for all the remaining comparisons, by determining the ratio of the area below the curve in the sugar ring region to the total integral under the NMR spectrum, excluding the large water peak around 4.7 ppm.

Determining the ^{13}C-NMR spectrum of the EPS would have been an alternative to gather a more comprehensive understanding of the different biomolecules present in EPS. Metzger *et al.* were able to characterize the characteristic peaks for biomolecules different than polysaccharides, such as proteins. However, it was impossible to determine this spectrum for all EPS sources, due to the sample mass being required, which was unavailable for the EPS due to their scarcity [146].

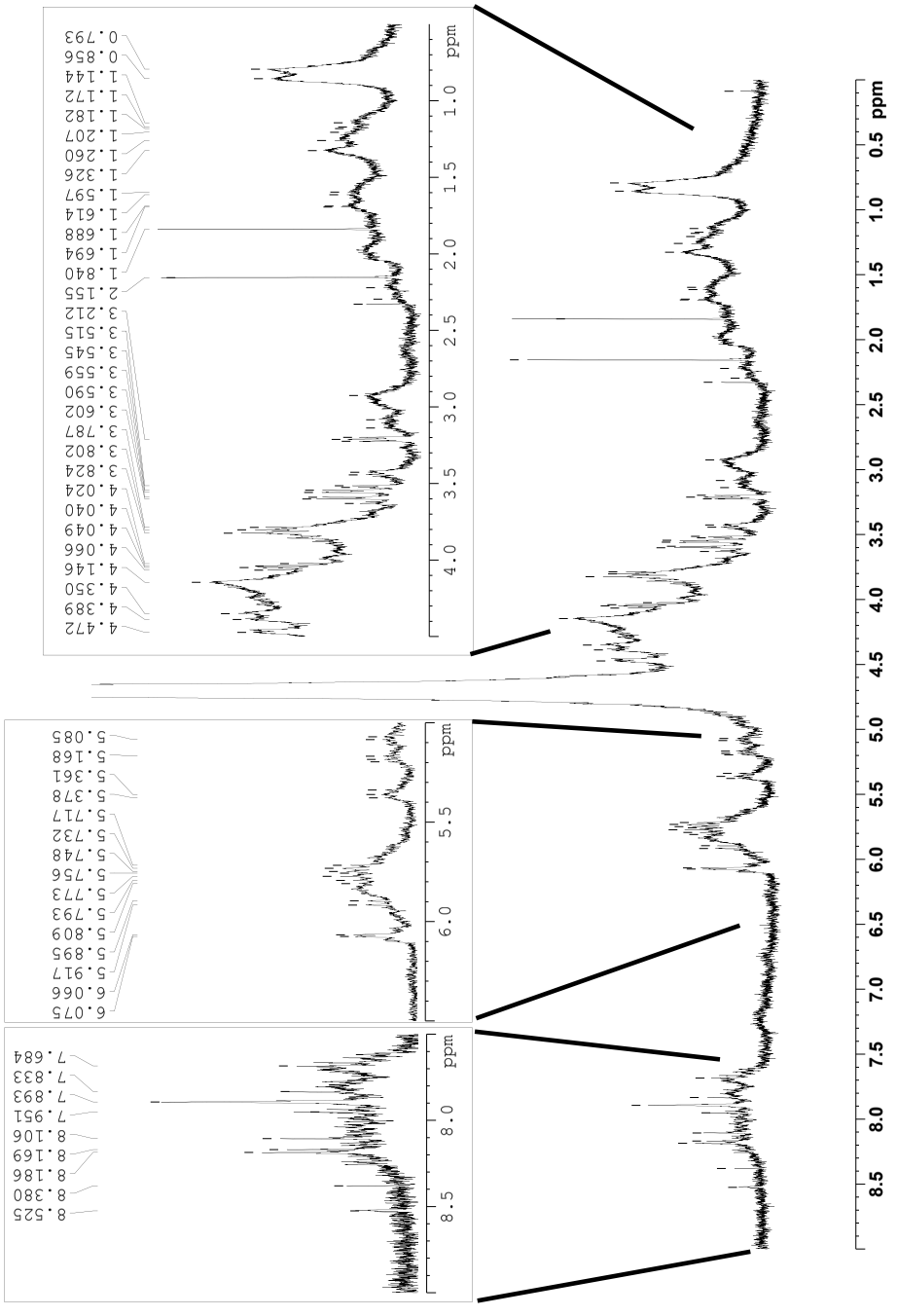

FIGURE 6.5: ^{1}H-NMR spectrum of EPS extracted from *Azoarcus communis*, using the heat and sodium carbonate method. The spectrum is made using the TopSpin software package (Bruker, United States of America).

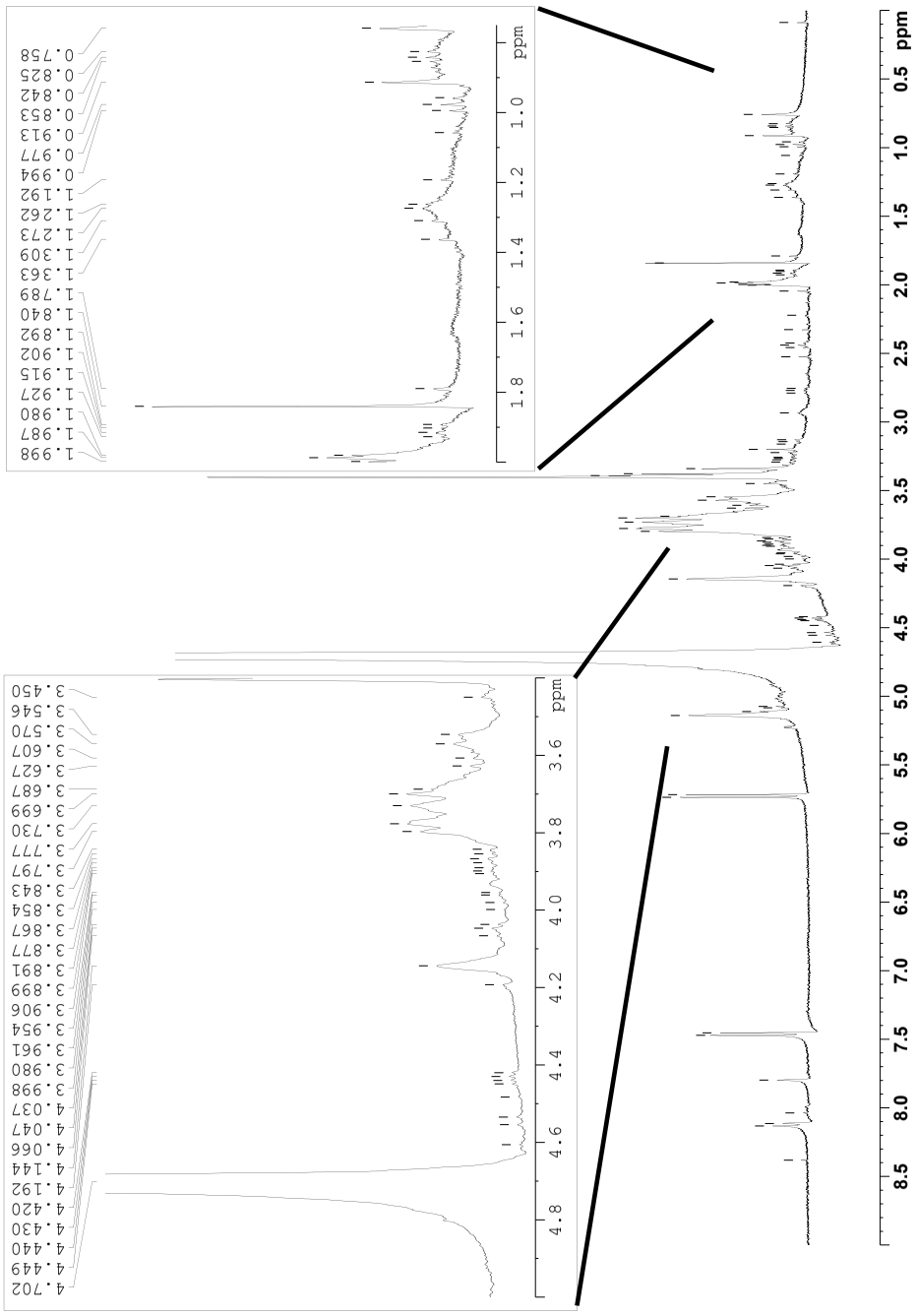

Figure 6.6: ^{1}H-NMR spectrum of EPS extracted from *Dietzia maris*, using the heat and sodium carbonate method. The spectrum is made using the TopSpin software package (Bruker, United States of America).

A final characterization method to determine differences in EPS composition utilizes thermogravimetric analysis (TGA), which provides information on the presence and release of volatile components from the EPS. TGA data of both *Azoarcus communis* and *Dietzia maris* are shown in Figure 6.7. As stated by Chen *et al.*, each type of biomolecule has its specific window of thermal degradation, being 164-497 ℃ for polysaccharides, 209-309 ℃ for proteins and 200-635 ℃ for lipids [33]. Extracting information from the TGA is difficult due to the overlap of these ranges. Unless distinct zones can be observed in the degradation profile, it is difficult to draw conclusions from the TGA data only.

The degradation profile of *Azoarcus communis* in Figure 6.7 shows three different ranges, each with an increasingly steeper slope, estimated visually as 150-235 ℃, 235-290 ℃ and 290-315 ℃. Around 315 ℃, an inflection point can be observed, after which the slopes of both curves are more similar. For *Dietzia maris*, such regions are less clear, as the change in slope appears more gradual. Hence, linking each range to specific biomolecules is impossible as the complete composition of the EPS is not known. For this reason, the TGA results of the comparisons made in the following sections are provided in Appendix D.3 and are only mentioned if significant differences are visible.

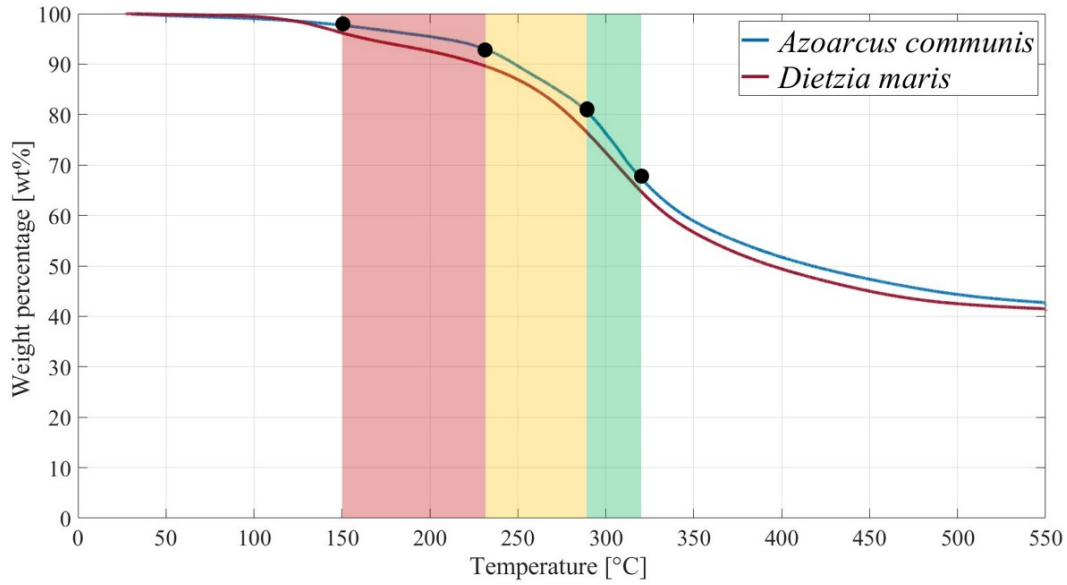

FIGURE 6.7: TGA data of EPS extracted from *Azoarcus communis* and *Dietzia maris* using the heat and sodium carbonate extraction method.

6.2.2 Denitrifiers vs. EBPR-granule (H2)

As the EBPR-granule is used for both phosphorus and nitrogen removal, the denitrifiers are assumed to be among the dominating organisms in the granules. Hence, the EPS from the two denitrifiers and the EBPR-granule are expected to exhibit similar chemical characteristics.

Figure 6.8 shows a comparison between the Raman spectra of the three samples, indicating that the EPS from the EBPR granular sludge most closely resemble the EPS from *Azoarcus communis*. No small peaks are observed at 1154 and 1553 cm^{-1}, indicating the absence of carotenoids, which are present in the EPS from *Dietzia maris*. Apart from these, the peaks around 485, 601, 790 and 1553 cm^{-1} are present in all three spectra, having approximately the same magnitude.

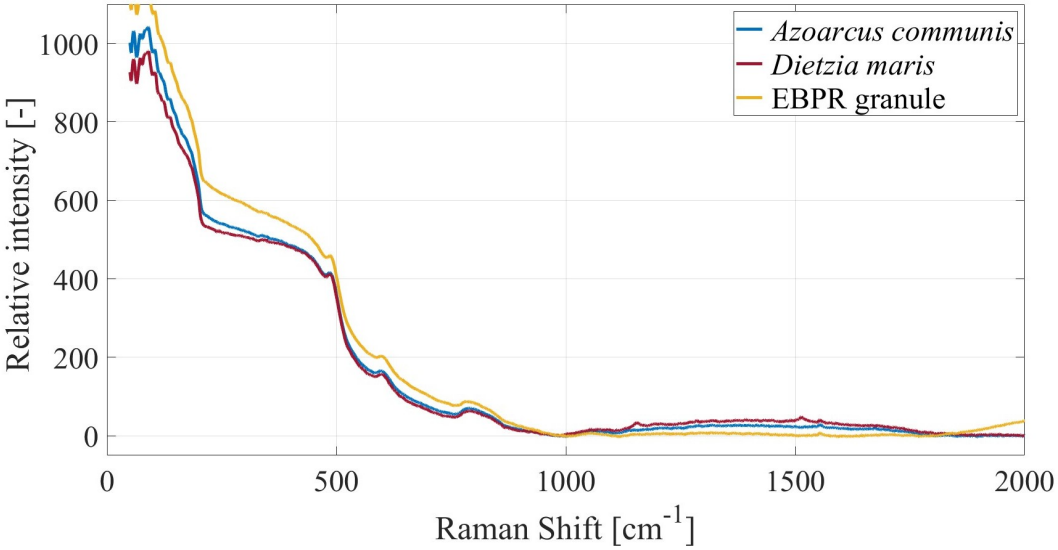

Figure 6.8: Raman spectrum of EPS extracted from *Azoarcus communis*, *Dietzia maris* and EBPR granular sludge, using the heat and sodium carbonate extraction method

Figure 6.9 shows that the FTIR spectrum of the EBPR-granule EPS exhibits peaks at locations similar to the two denitrifiers. However, the peaks appear to differ in intensity (i.e. the much less pronounced peaks around 2900 cm^{-1} in the EBPR-granule spectrum) such that the ratios of different biomolecules might differ. For this reason, a comparison is made of the size of the most important peaks, indicated by the arrows on Figure 6.9, by taking the integral between the curve and a manually introduced baseline (see Figure D.1 in Appendix D.1 for an example), for the regions between 2950 and 2850 cm^{-1}, 1700 and 1450 cm^{-1} and 1200 and 900 cm^{-1}, representing the fatty acids, proteins, and polysaccharides, respectively [157, 185].

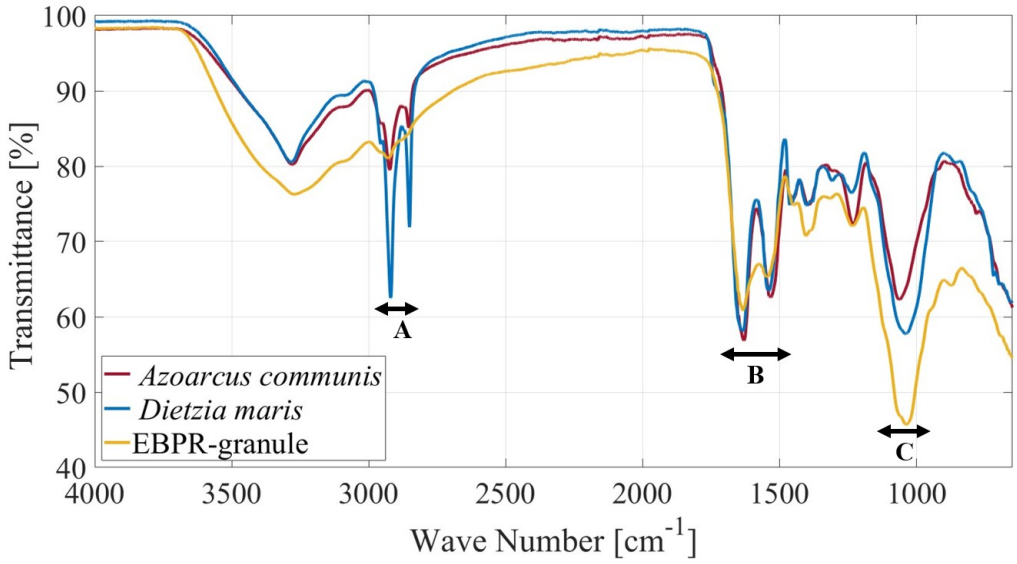

FIGURE 6.9: FTIR spectra of EPS extracted from *Azoarcus communis*, *Dietzia maris* and Enhanced Biological Phosphorous removal granular sludge using the heat and sodium carbonate extraction. The A, B and C regions are the regions from which the integrals are taken to determine the ratio of fatty acids (2950 and 2850 cm^{-1}), proteins (1700 and 1450 cm^{-1}) and polysaccharides (1200 and 900 cm^{-1}).

The area between the FTIR spectrum and the baseline is determined using numerical integration via the trapezoid rule. When normalizing the different areas by dividing them by the total area of the three peaks, the results in Table 6.1 are obtained, showing that the fatty acids are the most limited fractions of the EPS for all three sources. The protein and polysaccharide content differ substantially for each sample, with the polysaccharide-to-protein ratio being equal to 0.59 for the EPS from *Azoarcus communis*, 0.84 for the *Dietzia maris*, and 0.98 for that from EBPR-granule. The community in the EBPR-granule thus produces a larger fraction of polysaccharides as EPS compared to the pure cultures. Guibaud *et al.* obtained similar results in their comparison of the complexation ability of EPS from activated sludge to that of EPS of pure cultures isolated from the same activated sludge [80]. They observed that EPS extracted from all isolated strains show a smaller polysaccharide-to-protein ratio (ranging from 0.038 to 0.192) compared to those extracted from the activated sludge (0.42). The results presented here are similar to those provided by Guibaud *et al.*. However, the changes observed here are not as significant as in Guibaud *et al.*'s work, as the largest decrease in polysaccharide-to-protein ratio observed is between the EBPR-granule and *Azoarcus communis*, where it decreases by a factor of 1.65 (from 0.98 to 0.59), while in the paper of Guibaud *et al.*, the changes are a factor of 2.16 or larger. This difference could result from the different methods used for determining the protein and polysaccharide content. In this work, the FTIR spectrum is integrated for the corresponding characteristic region. On the other hand, Guibaud *et al.* used methods explained in the literature study, more specifically the adapted Lowry and modified Dubois method, to determine the absolute amounts of protein

and polysaccharides in the EPS [51, 80, 135]. The method used in this work remains helpful in obtaining general trends (sample A has a larger polysaccharide-to-protein ratio than sample B). However, exact quantitative results are impossible to obtain. Another possible reason for the minor differences in this work is the use of granular sludge for the comparison, as such sludge is known to contain a larger protein fraction [2, 129, 189] compared to floccular sludges, used by Guibaud *et al.* [80]. Nevertheless, the observed trends remain similar.

Table 6.1: Normalized surface area between the baseline and the FTIR spectrum of EPS extracted from *Azoarcus communis*, *Dietzia maris* and the EBPR-granule. In each row, the area is normalized by dividing the area by the total area, between the three peaks and baselines.

Sample name	Relative area fatty acids [%]	Relative area proteins [%]	Relative area polysaccharides [%]
Azoarcus communis	11	56	33
Dietzia maris	18	44	37
EBPR-granule	4	48	47

Another observation of the FTIR and Raman spectra of the EPS from the EBPR-granule is that they do not show a particularly high amount of phosphates or other bonds containing phosphorus. The EBPR-granule removes phosphates from wastewater by storing them intracellularly as polyphosphate [147]. However, other authors state that the phosphates mainly accumulate extracellularly on the granule surface in dedicated phosphate granules [29], so it is plausible to assume that the EPS would contain some phosphorus-based materials as well. Nevertheless, this is not observed in the EPS from the EBPR-granule as the peaks in the Raman spectrum of the EBPR-granule around 495 and 790 cm^{-1} are approximately the same size as those of the two bacteria (see Figure 6.8 in Appendix D.2.1). Both of these peaks indicate the presence of PO_4 bonds [55, 175]. The FTIR spectrum, given in Figure 6.9, does not exhibit significantly larger peaks at 1240 and 1222 cm^{-1} either, which are characteristic for these phosphorus-containing molecules [55, 185]. Apart from the absence of the extracellular phosphate granules, a possible explanation for the absence of phosphates in the extracted EPS is their relatively low solubility in water at basic conditions, as the polyphosphate structures are mostly phosphates of Ca^{2+}, Mg^{2+} and K^{+} [29], resulting in the accumulation of the polyphosphate granules in the pellet from the extraction protocol. This was not determined experimentally, however.

Comparing the ^{1}H-NMR data of the EPS extracted from the EBPR-granule (see Figure 6.11) to that of the two denitrifiers (Figures 6.5 and 6.6), it is directly observed that the peaks present in the spectrum of the EPS from the EBPR-granule are much less detailed than the peaks in the spectra of the other two. Where the spectra of *Azoarcus communis* and *Dietzia maris* show many narrow peaks, only seven peaks are visible in the NMR spectrum of the EPS from the EBPR-granule, with one caused

by residual water. When integrating the signal in the polysaccharide region for these samples (excluding the water peak), it is observed that these are equal to 45 %, 56 % and 55 % of the total integral of the EPS from *Azoarcus communis*, *Dietzia maris* and EBPR-granular sludge, respectively, which does not entirely correspond to the relative areas of the polysaccharides, found in the fourth column of Table 6.1. This could be ascribed to the fact that the FTIR and NMR look at different atoms in the molecules, as the bonds in the polysaccharide region of the FTIR are mainly looking at C−O bonds, while the ^{1}H-NMR looks at the hydrogen atoms in the molecules.

The thermogravimetric analyses of the EPS from the two denitrifiers and the EBPR-granule are given in Figure 6.10 and show the steepest decrease in mass between 150 and 250 ℃ for the EBPR-granule, indicating a higher presence of polysaccharides, confirming the FTIR and Raman results [33]. Apart from this, not much can be concluded from the remaining parts of the degradation, as they follow a similar pattern at temperatures above 300 ℃.

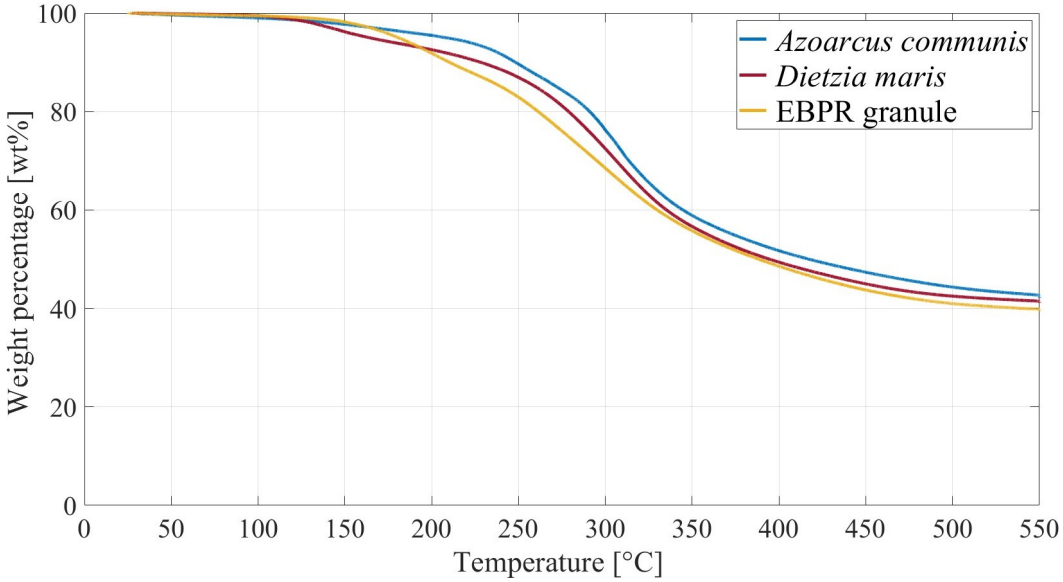

FIGURE 6.10: Thermogravimetric analyses of EPS extracted from *Azoarcus communis*, *Dietzia maris* and EBPR-granule using the heat and sodium carbonate extraction method.

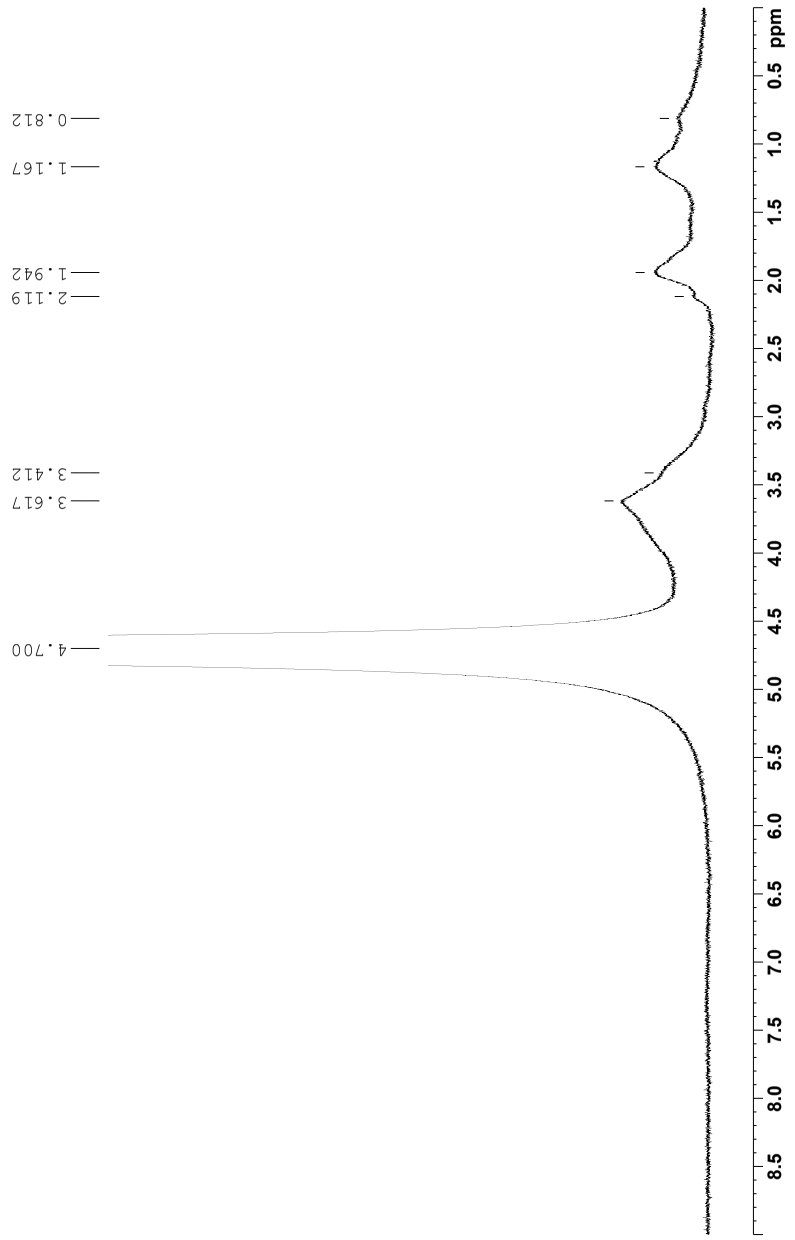

Figure 6.11: ^{1}H-NMR spectrum of EPS extracted from EBPR-granular sludge, using the heat and sodium carbonate method. The spectrum is made using the TopSpin software package (Bruker, United States of America).

6.2.3 Floccular sludge: before and after salt adaptation (H3a)

It is expected that organisms in the sludge produce more and different EPS when exposed to a more saline environment, to protect themselves from the higher osmotic pressure. The halophiles and other more salt-tolerant organisms are also expected to become more dominant in the sludge, as the increased osmolarity impacts them less than non-halophilic or non-halotolerant cells.

The Raman spectra of the floccular sludge before and after salt adaptation are given in Figure D.2 in Appendix D.2.1 and show no significant differences. Broad peaks are observed around Raman shifts of 800 and 1050 cm^{-1}, while narrower nods appear at 485 and 600 cm^{-1}. Except for the shift at 800 cm^{-1}, these correspond to the typical macromolecules found in EPS, as listed in Table C.2 in Appendix C.1.2 [55]. According to Risi *et al.*, the peak around 800 cm^{-1} corresponds to the symmetric stretch vibration of O−P−O bonds present in phosphates [175].

The FTIR spectra of both EPS samples are shown in Figure 6.12 and show minor differences between the EPS before and after salt adaptation. The most significant differences are again observed for the peaks at 2920 and 2851 cm^{-1}, where the salt-adapted floccular sludge exhibits more distinct peaks. The same holds for the peaks at 1630 and 1541 cm^{-1}, while the peak at 1042 cm^{-1} appears larger for the floccular sludge before adaptation. These regions represent fatty acids, proteins, and polysaccharides, respectively, of which the relative contributions are shown in Table 6.2, determined in the same way as those in Section 6.2.2.

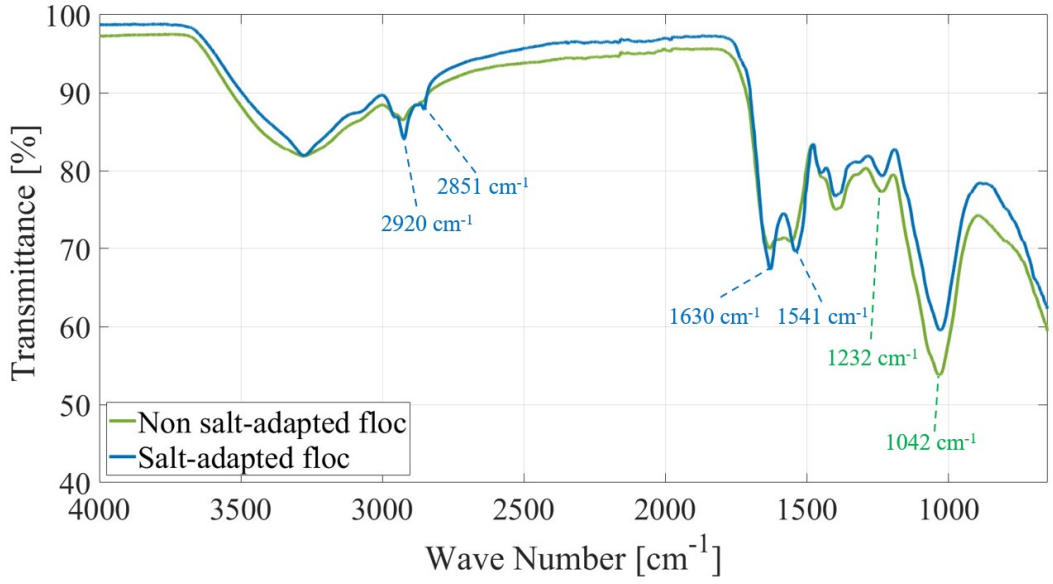

FIGURE 6.12: FTIR spectrum of EPS extracted from floccular sludge, before and after salt adaptation, obtained using the heat and sodium carbonate extraction method.

Table 6.2 shows that the polysaccharides and proteins have larger contributions compared to fatty acids. The ratio of the relative area of polysaccharides to that of proteins is determined as 1.18 (52/44) before and 1.33 (52/39) after salt adaptation, indicating an increase in polysaccharide contribution after salt adaptation.
Fatty acids make a larger contribution to the sludge EPS after salt adaptation, as their relative importance increases by a factor of 2.25 (from 4 % to 9 %). A possible cause of this higher contribution is a greater extent of cell lysis, which would result in an increased amount of phospholipids in the extracted EPS. However, if this were the case, also a larger peak would have to be observed in the FTIR spectrum of the salt-adapted floc around 1240 and 1222 cm^{-1}, as these regions represent the phosphate bonds [185]. Looking back at Figure 6.12, no clear difference is observed. A similar observation can be made by looking at the region between 400 and 500 cm^{-1} in the Raman spectra given in Figure D.2. Hence, it is not expected that the increased fatty acid content is caused by cell lysis. Another possible explanation for the higher fatty acid content is that more hydrophobic EPS facilitate biomass aggregation [189], compensating for the more difficult aggregation caused by the more saline environment. Because a better aggregation promotes easier settling and the better settling flocs are washed out less, the sludge remaining in the reactor is expected to contain more aggregation-facilitating fatty acids.

Table 6.2: Normalized surface area between the baseline and FTIR spectrum of EPS extracted from floccular sludge before and after salt adaptation. In each row, the area is normalized by dividing the area by the total area, between the three peaks and baselines.

Sample name	Relative area fatty acids [-]	Relative area proteins [-]	Relative area polysaccharides [-]
Before salt adaptation	4	44	52
After salt adaptation	9	39	52

As shown in Figures 6.13 and 6.14, both ^{1}H-NMR spectra exhibit very broad peaks located in similar regions. The peaks at NMR shifts smaller than 5 ppm do not overlap exactly, but some are relatively close to each other (i.e. 1.997 vs. 1.990 ppm and 0.832 vs. 0.812 ppm). The relative amount of polysaccharides is, once again, determined by calculating the ratio of the area below the NMR spectrum between 4.4 and 3.2 ppm and that of the entire spectrum, excluding the vast water peak at 4.70 ppm. This is determined to be 53 % before and 35 % after salt adaptation, contradicting the FTIR results in the fourth column of Table 6.2 for the floccular sludge after salt adaptation. Again, this difference is most likely caused by the different approaches of the two methods used to determine the relative amount of polysaccharides.

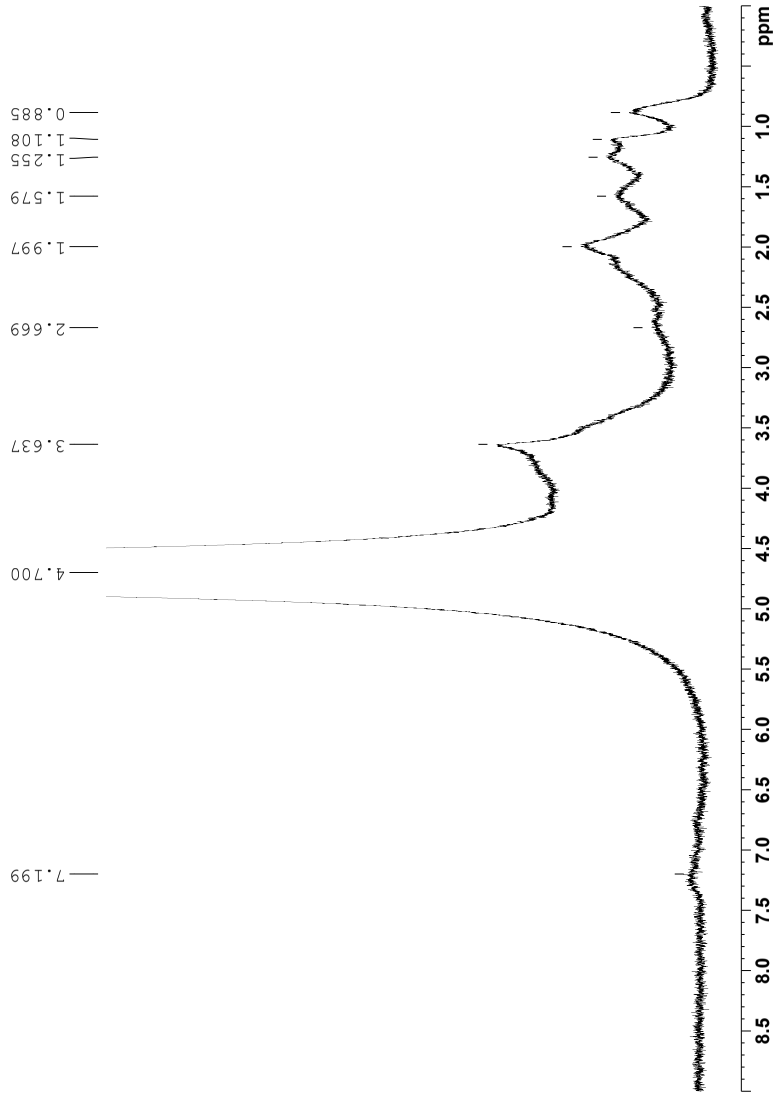

FIGURE 6.13: ^{1}H-NMR spectrum of EPS extracted from floccular sludge, before salt adaptation, using the heat and sodium carbonate method. The spectrum is made using the TopSpin software package (Bruker, United States of America).

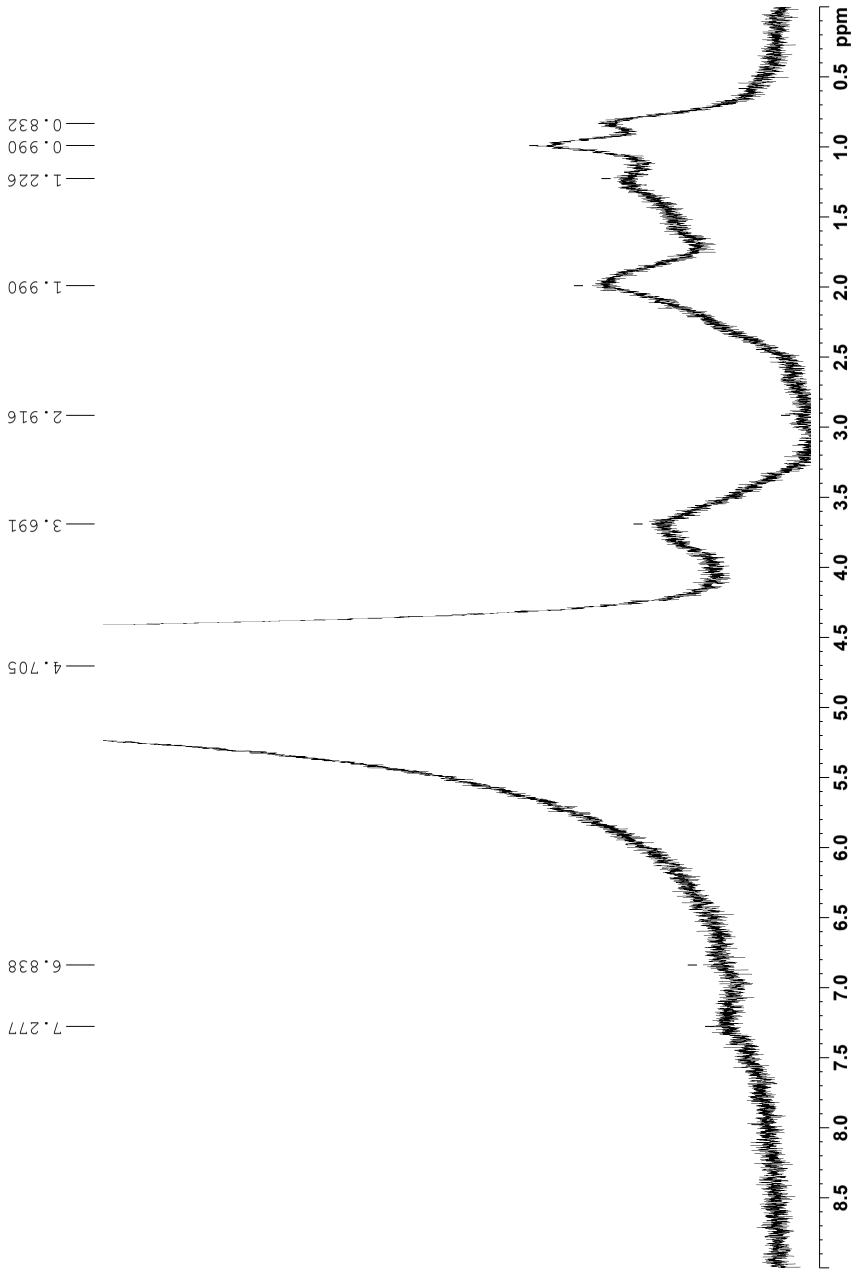

Figure 6.14: ^{1}H-NMR spectrum of EPS extracted from floccular sludge, adapted to 5 $\frac{g}{L}$, using the heat and sodium carbonate method. The spectrum is made using the TopSpin software package (Bruker, United States of America).

The region between 150 and 200 ℃ of the TGA in Figure D.5 in Appendix D.3 shows a steeper slope for the EPS from floccular sludge after salt adaptation compared to the EPS before adaptation. However, due to the higher amount of water present in the EPS from floccular sludge before salt adaptation (represented by the drop in mass between 25 and 150 ℃) and due to the broad temperature range in which polysaccharides show degradation (160-497 ℃ [33]), no definite conclusions can be made solely based on the TGA data.

Chen *et al.* also observed an increase in polysaccharide-to-protein ratio in the EPS after salt adaptation of sludge in an anaerobic reactor with an influent salt concentration of 5 $\frac{g}{L}$ Na^+, the same value as used in this work [31]. This was also confirmed by Guo *et al.* in their work on MBRs [31, 84]. However, this effect only occurs at salt concentrations up to 10 $\frac{g}{L}$ Na^+, while at higher concentrations, the polysaccharide-to-protein ratio converges again towards its initial value. The increase in this ratio results from Na^+ ions residing inside the granule, binding to the proteins in the EPS and bringing bound water along with them. This process of "salting in" results in an increased solubility of the proteins [20, 30]. The sludge components appear to counter this effect by producing extra fatty acids. Reid *et al.* also found that the amount of polysaccharides in EPS increases more than that of proteins when the chloride concentration in the treated wastewater is increased [172]. Gagliano *et al.* investigated the EPS components in anaerobic granular sludge applied in saline wastewater treatment at salt concentrations of 5 and 20 $\frac{g}{L}$ [69]. They observed that glycoconjugates (polysaccharide-like molecules) serve as a protective barrier for the methanogens inside the sludge at both salt concentrations. As the salt adaptation in this work is carried out in an anaerobic environment as well, the polysaccharide content in the extracted EPS is expected to increase after the salt adaptation [69].

6.2.4 Salt-adapted floc vs. Salt-adapted granule (H3b)

The EPS from salt-adapted floccular and granular sludge are expected to show similarities, as they are both employed to treat saline wastewater anaerobically. The Raman spectra of the salt-adapted sludges, provided in Figure D.3 in Appendix D.2.1, clearly show similar results for both EPSs. The curves practically overlap in the region between 500 and 2000 cm^{-1}, which contains most of the information on the chemical bonds present inside the EPS.

The FTIR spectra of the EPS from the two salt-adapted sludges are given in Figure 6.15 and show again peaks at similar locations, indicating that similar biomolecules are present in the EPS. However, where the peaks at 1056 cm^{-1} are comparable in size, the difference is more striking for the peaks at 1400, 1545, and 1635 cm^{-1}. The peaks at 1545 and 1635 belong to the protein region, as mentioned before, while the peak at 1400 can be attributed to the C−O bending of the carboxylate ions ($R-COO^-$) in the sludge [185]. These could result from the presence of glutamic and aspartic acid amino acids in the protein, as well as polysaccharides, fatty acids, and humic acids, impeding the assignment of this peak to one specific biomolecule.

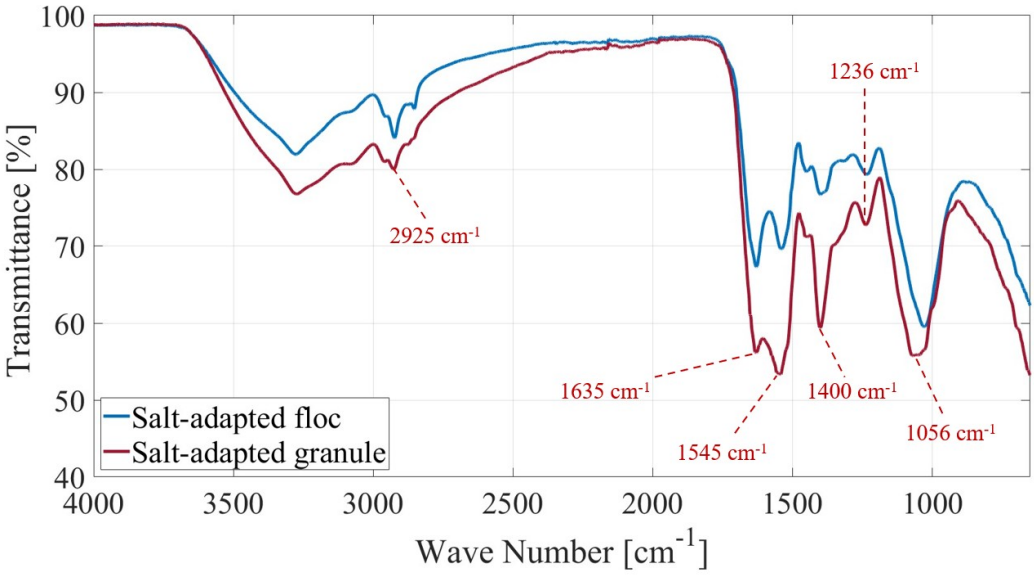

Figure 6.15: FTIR spectra of EPS extracted from salt-adapted granular and floccular sludge, obtained using the heat and sodium carbonate extraction method.

Similarly to earlier, the ratio of fatty acids, proteins, and polysaccharides is calculated by determining the area between the curve and a baseline for the same regions as discussed before. These results are shown in Table 6.3. The EPS from salt-adapted granular sludge contain relatively more proteins than the floccular sludge, as the ratio of the relative polysaccharide area and that of the proteins equals 0.70 for salt-adapted granular and 1.33 for salt-adapted floccular sludge. This could indicate that a lower polysaccharide-to-protein ratio results in easier aggregation and granulation, which was already concluded by Liu *et al.* [129].

Table 6.3: Normalized surface area between the baseline and FTIR spectrum of EPS extracted from salt-adapted granular and floccular sludge. In each row, the area is normalized by dividing the area by the total area, between the three peaks and baselines.

Sample name	Relative area fatty acids [-]	Relative area proteins [-]	Relative area polysaccharides [-]
Salt-adapted granule	5	56	39
Salt-adapted floc	9	39	52

The NMR spectra of the salt-adapted floc and salt-adapted granule are given in Figures 6.16 and 6.14, respectively. The most remarkable difference is in the number of peaks, which is much larger for the salt-adapted granule. Where some peaks are observed at shifts larger than 6.5 ppm for the salt-adapted granule, barely any peaks are visible in that range on the spectrum of the salt-adapted floc. The water peak at 4.7 ppm is also much narrower for the salt-adapted granule than

that of the salt-adapted floccular sludge. The area beneath the spectrum also appears larger inside the polysaccharide region (4.4−3.2 ppm) for the salt-adapted granule compared to the floc. However, also the area beneath the curve at the regions outside the polysaccharide region appears larger. The ratio of this area and the total area, excluding the water peak, results in a value of 33 % for the granular and 35 % for the floccular sludge, which differs from the FTIR results in Table 6.3.

The most striking difference between the EPS from the salt-adapted granular and floccular sludge is the smaller polysaccharide-to-protein ratio in the salt-adapted granule. The fact that a higher protein content facilitates granulation was already demonstrated by Peng *et al.*, who observed that proteins are the most important factor facilitating granulation [163]. Liu *et al.* observed that the proteins can neutralize the negative charge of EPS, thereby inducing better aggregation of microorganisms, which results in a more stable granule [129].

A similar observation was made by Adav and Lee, who observed a 4 to 7-fold decrease in the polysaccharide-to-protein ratio in EPS extracted from aerobic granular sludge compared to floccular sludge [2]. However, in that work, formamide and sodium hydroxide were used to extract the EPS, which might be a reason for the larger increase in protein content. It is important to mention that sodium hydroxide solubilizes a larger fraction of the EPS, while on the other hand, it also degrades some of the EPS, which is undesired [17]. Later, Adav *et al.* also observed that a protein-rich core is present in several types of granular sludge, embedded in a backbone of β-polysaccharides [3]. In their work, Sheng *et al.* propose that more hydrophobic EPS (i.e., some proteins) induce better granulation, resulting in an increased settlability of the sludge [189]. In this regard, the relative presence of hydrophobic fatty acids is expected to be higher in the salt-adapted granule than in the salt-adapted floc. However, the results in Table 6.3 show the opposite, with the relative area of the fatty acids being smaller for the granular sludge. Hence, it is expected, although not confirmed, that the hydrophobic regions in proteins (and polysaccharides) contribute more to the granulation process, compared to fatty acids.

Floccular and granular sludge EPS clearly contain different ratios of proteins and polysaccharides. It is hypothesized that two separate processes induce this difference. First, as discussed in the previous section, salt adaptation results in the production of glycoconjugates that act as a protective barrier for the microorganisms within the sludge community. In this way, salt-adapted flocs are formed. In the second step, these protected microorganisms are able to produce (glyco)proteins to enhance the granulation, which was already observed by Boleij *et al.* [13]. The glycoproteins are can be characterized in the FTIR spectra by their crossed-β-sheets, which display peaks around 1630 cm^{-1} [190]. Figure 6.15 confirms this hypothesis, as the FTIR spectrum of the salt-adapted granule exhibits a larger peak at a wavenumber of 1635 cm^{-1}. This hypothesis cannot be confirmed using the Raman and FTIR data, however, indicating that a more extensive chemical characterization is required to characterize the EPS more completely.

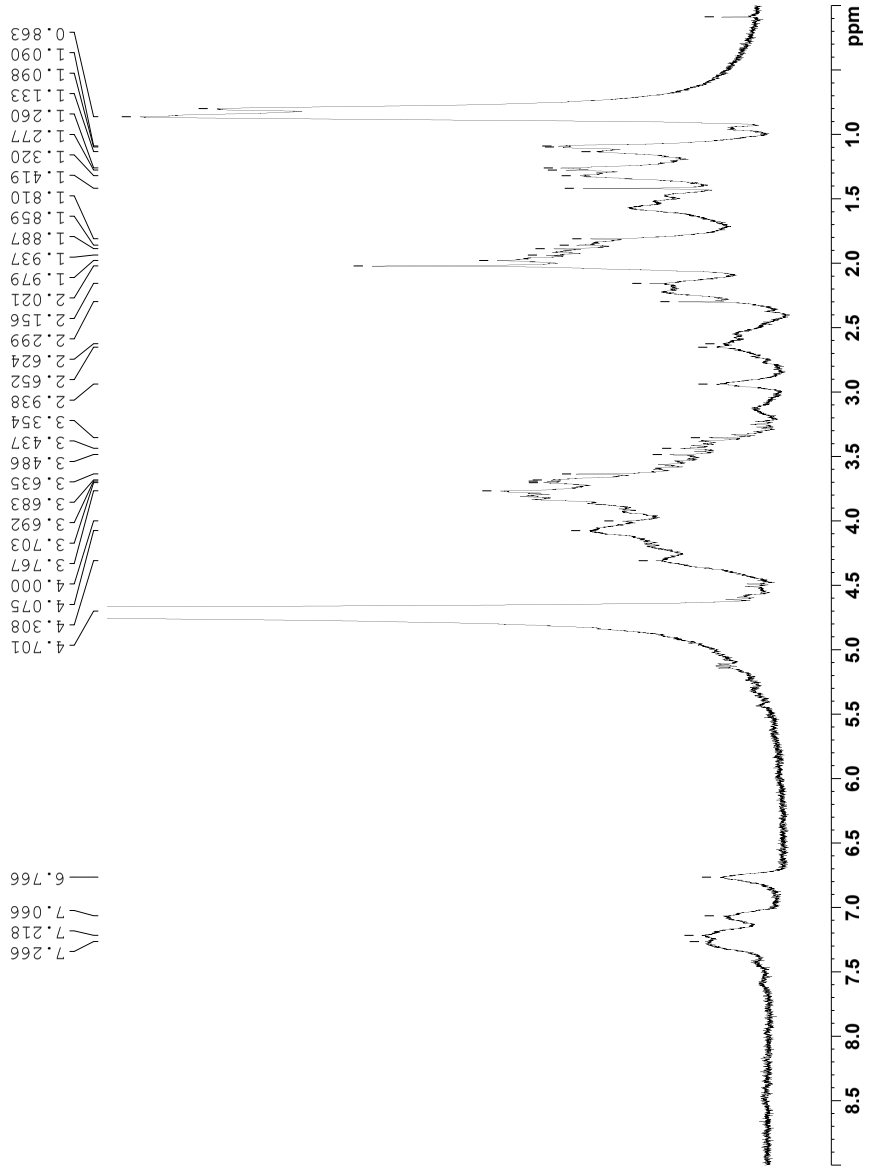

Figure 6.16: ^{1}H-NMR spectrum of EPS extracted from salt-adapted granular sludge, using the heat and sodium carbonate method. The spectrum is made using the TopSpin software package (Bruker, United States of America).

6.2.5 Salt-adapted granule vs. salt-adapted fungus (H4)

A final comparison is made between the salt-adapted granular sludge and the EPS from pellets of the fungal species *Aspergillus oryzae* (*A. oryzae*). The EPS from the fungus are expected to be less complex than those of the granule, as the fungus only contains a single species. Even larger differences in EPS composition are expected to be present due to the differences in dominating organisms in the two sources of biomass. Where prokaryotic bacteria and archaea dominate the community inside the salt-adapted granular sludge, eukaryotic fungi dominate the *A. oryzae* pellets, as these are the only organisms present in them [36, 66].

The FTIR spectra of EPS from both sources are given in Figure 6.17 and show clear differences between both spectra, such as a much larger peak in the polysaccharide (1200-900 cm^{-1}) and fatty acid region (2950-2850 cm^{-1}) for the *Aspergillus oryzae*. At the same time, the salt-adapted granular sludge exhibits a larger protein region (1700-1400 cm^{-1}) and peak at 1400 cm^{-1}.

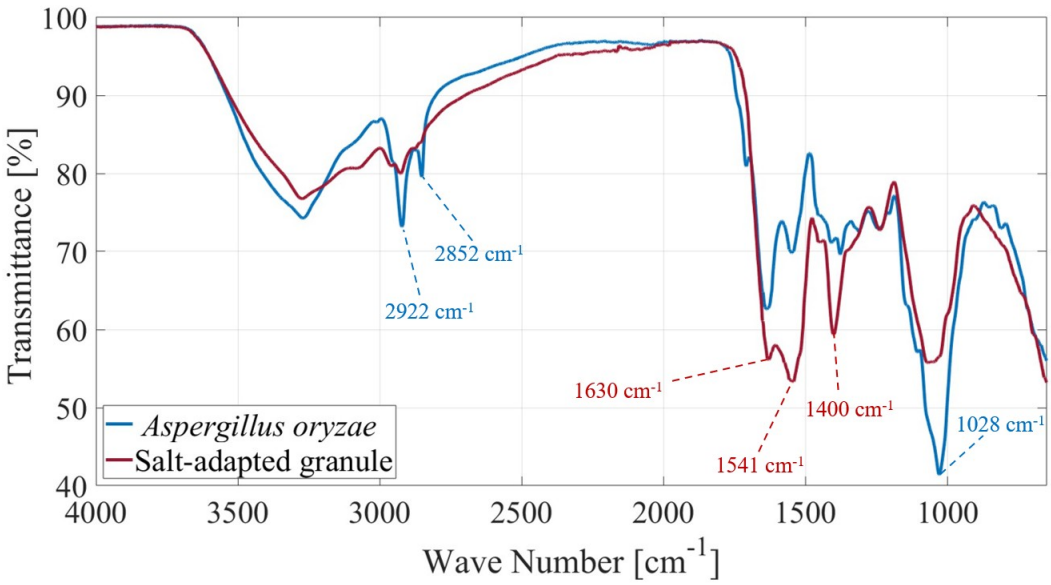

FIGURE 6.17: FTIR spectra of EPS extracted from *Aspergillus oryzae* and salt-adapted granular sludge, obtained using the heat and sodium carbonate extraction method.

The results of the peak intensity analysis in Table 6.4 indicate that fatty acids again contribute to the lowest surface area of the three biomolecules. For the *A. oryzae*, the ratio of the polysaccharide-to-protein area is much larger (2.31) compared to the salt-adapted granule (0.70), indicating that the role of polysaccharides is larger in the EPS from *A. oryzae*. Another important difference is observed in the protein-to-fatty acid ratio, which is much smaller for the *A. oryzae* than for the salt-adapted granule, indicating the relatively lower importance of fatty acids in the salt-adapted granule.

Table 6.4: Normalized surface area between the baseline and FTIR spectrum of EPS extracted from *Aspergillus oryzae* and salt-adapted granular sludge. In each row, the area is normalized by dividing the area by the total area, between the three peaks and baselines.

Sample name	Relative area fatty acids [-]	Relative area proteins [-]	Relative area polysaccharides [-]
Aspergillus oryzae	14	26	60
Salt-adapted granule	5	56	39

The complete NMR spectra of both EPS sources are shown in Figure 5.3 in Chapter 5 and Figure 6.16. Figure 6.18 focuses on the region between 4.5 and 0 ppm, in which most peaks are located. Again, the spectrum of the EPS from the salt-adapted granular sludge (1) appears to be more complex than that of the EPS from *Aspergillus oryzae* (2), as more peaks are observed, confirming the initially expected complex composition of the salt-adapted granular sludge's EPS. The peaks in the former spectrum are also significantly broader, compared to most peaks present in the latter. The ratio of the area beneath the curve for the polysaccharides to that of the total curve (without the water peak) are not compared in this case, as the peaks in the sugar region of the *A. oryzae* represent low-molecular-weight species, as observed in Chapter 5. Hence, determining this ratio would yield erroneous results.

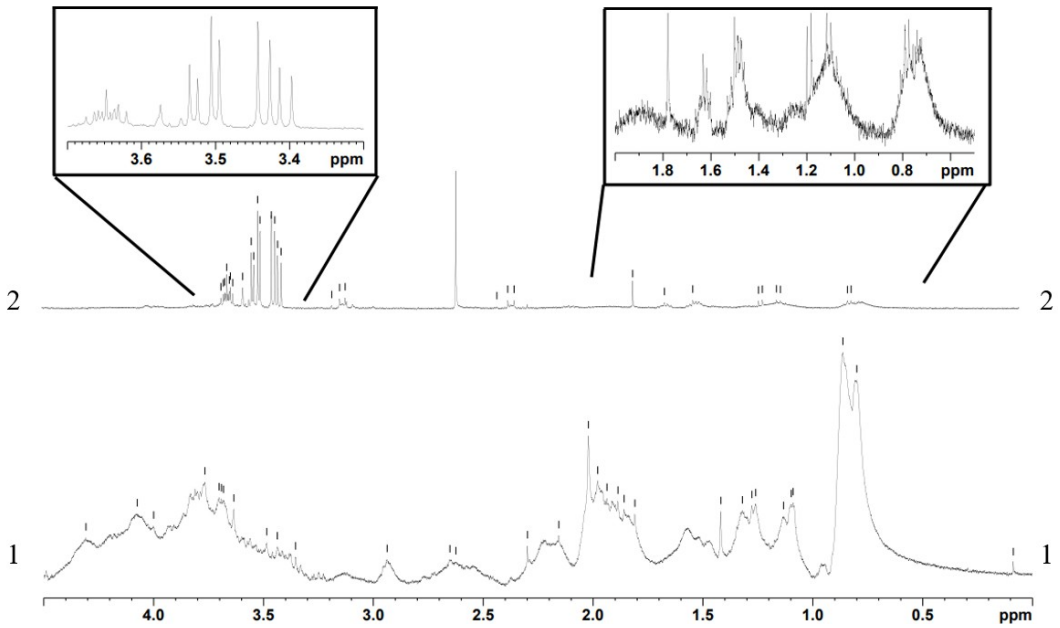

Figure 6.18: NMR spectra of EPS extracted from salt-adapted granular sludge (1) and *Aspergillus oryzae* (2), obtained using the heat and sodium carbonate extraction method. The spectra are made using the TopSpin software package (Bruker, United States of America).

The FTIR results indicate that polysaccharides contribute to a larger extent to the EPS of *Aspergillus oryzae* compared to that of salt-adapted granular sludge. This observation is likely the result of the combination of two different effects. First, the salt-adapted granular sludge is expected to show a greater amount of proteins in the EPS due to their contribution to the granulation process. On the other hand, growing the *Aspergillus oryzae* in potato dextrose broth results in EPS containing fewer proteins, such that the relative contribution of polysaccharides is larger for the *A. oryzae* [129]. From the frequent use of *Aspergillus* species to produce extracellular polysaccharides [10], it can also be assumed that the EPS of *Aspergillus oryzae* have a high polysaccharide content. These effects outweigh the observation that EPS from pure cultures tend to have a lower polysaccharide-to-protein ratio, as reported by Guibaud *et al.* [80]. The observed differences are also assumed to be caused by the difference in pure cultures used for the comparisons, as Guibaud *et al.* used prokaryotic bacteria for the comparison, while this thesis used a eukaryotic fungus.

6.2.6 EBPR-granule vs. salt-adapted granule

For completeness, EPS from the non salt-adapted EBPR-granule and from the salt-adapted granule are compared to study the effects of salt adaptation on the EPS fingerprints. Figure D.4 in Appendix D.2.1 shows that the Raman spectra of EPS extracted from both sludges practically overlap, so no significant differences are observed between the two spectra.

The FTIR spectra of the two EPS samples are provided in Figure 6.19, with Table 6.5 showing the relative areas between the curves and the baselines, which are used to determine the relative amounts of proteins and polysaccharides. When comparing the two, it is clear that the salt-adapted granule has a higher protein content than the EBPR granule, which contradicts the observations made in Section 6.2.3. The NMR data confirms this, as polysaccharides make up a larger fraction of the EBPR-granule EPS (55 %), compared to that of the salt-adapted granule (33 %). However, in this case, the EBPR granular sludge and the salt-adapted granular sludge are expected to have completely different dominating organisms, as the former is an aerobic granule, while the latter is an anaerobic granule. Hence, their comparison does not provide much added value compared to those given in the previous sections.

Table 6.5: Normalized surface area between the baseline and FTIR spectrum of EPS extracted from the EBPR-granule and salt-adapted granular sludge. In each row, the area is normalized by dividing the area by the total area, between the three peaks and baselines.

Sample name	Relative area fatty acids [-]	Relative area proteins [-]	Relative area polysaccharides [-]
EBPR-granule	4	48	47
Salt-adapted granule	5	56	39

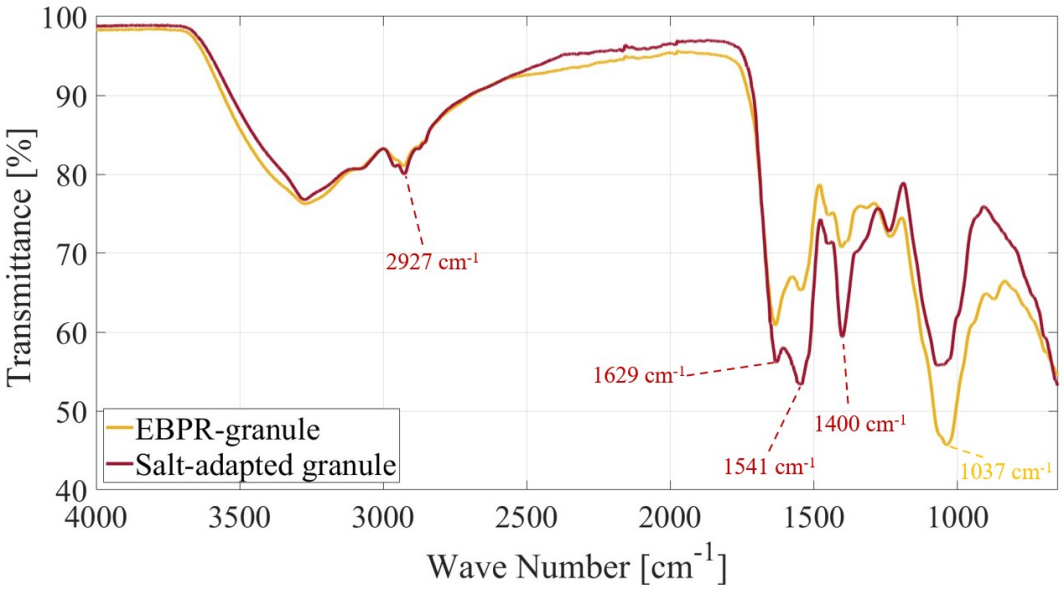

Figure 6.19: FTIR spectra of EPS extracted from *Aspergillus oryzae* and salt-adapted granular sludge, obtained using the heat and sodium carbonate extraction method.

6.3 Conclusions

In this chapter, five comparisons were made between EPS extracted from different sources, ranging from pure cultures to industrial sludge samples containing a plethora of different microbiological organisms.

When comparing the EPS fingerprints of *Azoarcus communis* and *Dietzia maris*, the Raman spectra appear very similar, except for two small peaks at 1154 and 1513 cm^{-1} present in the spectrum of *Dietzia maris*. These indicate the presence of carotenoids, which are biological pigments that contribute to the bright pink color of the EPS from *Dietzia maris*. The FTIR data indicate that each bacterium produces similar biomolecules in its EPS, albeit in varying relative amounts. The EPS from *Dietzia maris* appear to contain more fatty acids, while EPS from *Azoarcus communis* contain more phospholipids and have a smaller polysaccharides-to-protein ratio. The NMR spectra suggest that the EPS from the two strains do not only contain different relative amounts of the biopolymers, but that there is also more diversity within the different biomolecule groups. However, due to the complexity of the NMR spectra, no specific molecules could be identified in either of the two sludge EPSs. These observations contradict *Hypothesis H1*, as the EPS appear to be clearly strain-dependent, even though their cellular processes are similar.

When comparing the two bacterial strains to EPS extracted from an EBPR granule, it is found that the granule EPS are more complex and have a significantly larger

polysaccharide-to-protein ratio, as shown in the FTIR and NMR data. The Raman data appear similar to those of the two denitrifiers, with the absence of peaks at 1154 and 1513 cm^{-1} indicating the absence of carotenoids. Also in this case, the *Hypothesis H2*, proposed at the beginning of this chapter, is disproved, as the composition of the granule EPS is much more complex and has different biopolymer fractions compared to those of the isolated strains.

Another comparison was made between EPS from floccular sludge before and after adaptation to 5 $\frac{g}{L}$ Na^+. Here, the adaptation to salts leads to an increase in polysaccharide-to-protein ratio due to the proteins' salting in, induced by the Na^+ ions migrating towards the charged proteins and dragging water molecules with them in the process, resulting in a lower adhesion of the protein fraction to the EPS matrix. Glycoconjugates, which are polysaccharide-like molecules, are also known to act as a protective barrier for the microorganisms inside the sludge, shielding them from the higher salt concentration in the environment. This further explains the observed increase in the polysaccharide-to-protein ratio after salt adaptation. This observation confirms *Hypothesis H3a*, as the salt adaptation clearly affects the EPS composition.

The differences in EPS composition between salt-adapted granular and salt-adapted floccular sludge were also investigated. Here, a higher protein content is observed in both FTIR and NMR results of the granular sludge, while the Raman results do not show significant differences. These observations contradict *Hypothesis H3b*, which stated that the EPS signatures of the two salt-adapted sludge EPSs would be similar.

Lastly, a comparison was made between salt-adapted granular sludge and the salt-adapted aerobic fungus *Aspergillus oryzae*, showing that the aerobic fungus produces a larger relative amount of polysaccharides than the salt-adapted sludge, contradicting the observations made between the EPS from the two denitrifiers and EBPR-granule. However, this is likely attributed to specific characteristics of the *Aspergillus oryzae* fungus, confirming *Hypothesis H4*.

Chapter 7

EPS-based vs. model systems' hydrogels: towards EPS valorization

As a possible application of EPS extracted from wastewater treatment sludge, EPS-based hydrogels are developed and compared to the hydrogels of two model systems. The hydrogel-like behavior of EPS has already been demonstrated in literature by Sheng *et al.* [189]. Two polysaccharides, sodium alginate and κ-carrageenan, whose chemical structures are depicted in Figures 7.1 and 7.2, respectively, are selected as model systems. Their hydrogels are considered ionic hydrogels, as cations induce physical crosslinks between the different molecules. For the EPS-based hydrogels, the gelation is expected to be more complex and dependent on the chemical characteristics of the extracted EPS [59]. Where possible, the rheological behavior of EPS hydrogels is linked to their chemical characteristics.

Salts of alginic acid, often simply referred to as alginates, are polymeric polysaccharides extracted from brown seaweed and consist of β-D-mannuronic and α-L-guluronic acid monomers (see Figure 7.1) [113, 157], and are known to undergo a sol-gel transition in the presence of divalent ions like Ca^{2+} [49, 137]. They are mainly used in the medical and pharmaceutical fields due to their resemblance to extracellular matrices, making them suitable materials for wound healing hydrogels and the encapsulation of pharmaceutical ingredients [75]. Alginates' gelation is often described using the egg-box model, in which divalent ions are incorporated into sequential guluronic acid monomers to form strong physical crosslinks [79]. Mannuronic acid monomers do not contribute to the formation of crosslinks [137]. Although alginate can also form hydrogels by lowering the pH below 3.38, ionic crosslinking is more commonly used, especially in industrial applications [49]. Alginate's relatively easy gelation and the great understanding of the polymer make it an ideal model system for the comparison with EPS [49, 59, 113].
κ-carrageenan is also a biological polymeric polysaccharide extracted from red seaweeds, that differentiates itself from alginate by its sulphonate ($-OSO_3H$) groups

(see Figure 7.2) [177]. It is most often employed in the food industry as a gelling agent and thickener, as well as in the production of pharmaceuticals and cosmetics [26]. The gelation of κ-carrageenan is a two-step process, requiring both cooling and ionic crosslinkers, most often K^+ and Ca^{2+}. Its ability to gelate with monovalent ions distinguishes it from alginate, requiring multivalent ions. The cooling process induces the transition from a coil to a helix structure, while the ions promote aggregation of the helices, forming the physical crosslinks [26, 169]. As its gelation mechanism is distinctly different from that of alginates, using different functional groups, it is an interesting alternative model system for the comparison with EPS hydrogels [157].

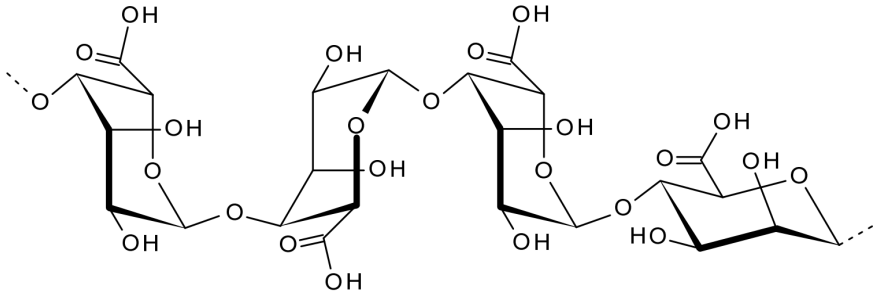

FIGURE 7.1: Lewis-structure of alginic acid. The figure shows three consecutive guluronic acid monomers (left), followed by one mannuronic acid monomer (right). Taken from Geetha Bai and Tuvikene [71].

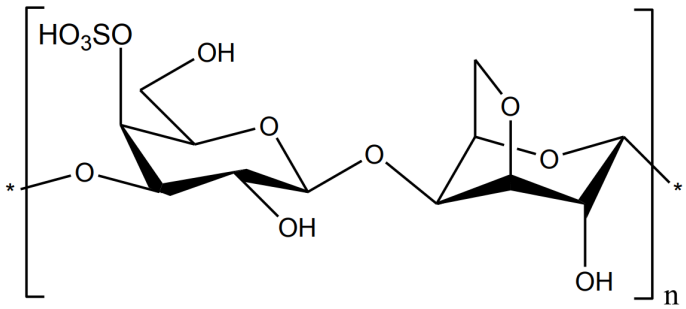

FIGURE 7.2: Lewis structure of κ-carrageenan. Taken from Solov'eva *et al.* [196].

7.1 Methodology

EPS from the sources mentioned in Section 4.1 are extracted using the heat and sodium carbonate extraction method provided in Section 4.3. Hydrogels are then made from the sludge EPS (at concentrations of 2 and 5 wt%) and the model systems (at concentrations of 1 and 2.5 wt%), as described in Section 4.5. The rheological characterization presented in Section 4.6 allows a comparison of the mechanical properties of the hydrogels. Finally, these are compared to the chemical characteristics of the EPS, obtained using the protocols from Section 4.4.3, in an attempt to relate the rheological properties of the EPS to their chemical structure.

7.2 Results

First, the chemical properties of the two model systems are discussed and compared to those of the extracted EPS, determined in Chapter 6. Next, the rheological properties of the model systems' and EPS-based hydrogels are compared, after which the gelation mechanisms of the two model systems are given and linked to their rheological properties. Finally, the relationships between the rheological properties and the chemical characteristics of the EPS are unraveled.

7.2.1 Chemical characterization

Model systems

FTIR spectra of sodium alginate and κ-carrageenan are shown in Figure 7.3. The spectrum of sodium alginate exhibits the three expected peaks in the spectrum, located at 1600 (C=O bond in the carboxylic acid group), 1400 (C−OH and O−C−O of the carboxylate ion) and 1028 cm^{-1} (C−O and C−C bonds of the pyranose ring) [54, 76, 185]. The small peak at 2927 cm^{-1} can be attributed to the C−H stretch in the main chain [143]. Note that this peak was attributed to the fatty acids in the previous chapter, as proposed by Pagliaccia and Schmitt and Flemming [157, 185]. The peaks at 1224 and 842 cm^{-1}, only present in the spectrum of κ-carrageenan, are caused by the presence of sulphate groups, while the peak at 926 cm^{-1} is most likely caused by 3,6-anhydro-d-galactose residues [76]. Similar to alginate, the peak at 1035 cm^{-1} results from the C−O and C−C bonds of the pyranose ring. The closest match for the peak at 1637 cm^{-1} was found by Tecson *et al.*, who attributed a peak at 1625 cm^{-1} to the presence of residual water in the sample [207], which is confirmed via TGA for the κ-carrageenan used in this work (data not shown).

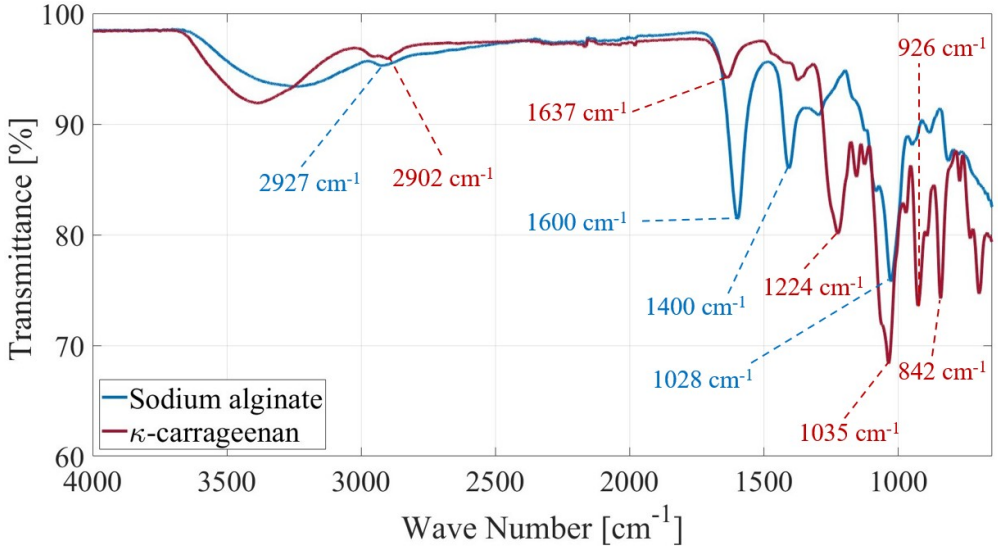

FIGURE 7.3: FTIR spectra of sodium alginate and κ-carrgeenan, with the different characteristic peaks indicated in the same color as the respective spectrum.

The Raman spectra of sodium alginate and κ-carrageenan are shown in Figure 7.4. The spectrum of κ-carrageenan shows a single peak at 848 cm^{-1}, caused by the C−O−SO_3H-group, as well as a combination of two peaks at 1043 and 1087 cm^{-1}, due to the identical 3,6-anhydro-d-galactose residues as before [140].
More peaks are distinguished in the Raman spectrum of sodium alginate compared to κ-carrageenan, for instance, at 808, 885, 952, 1092, and 1414 cm^{-1}. The first three peaks correspond to the stretching of C−C and C−O bonds, as well as C−C−H and C−C−O bending, while the last two are caused by glycosidic ring breathing and symmetric carboxylate stretching vibration, respectively. The peak at 1305 cm^{-1} also results from the carboxylate's stretching vibration [183].

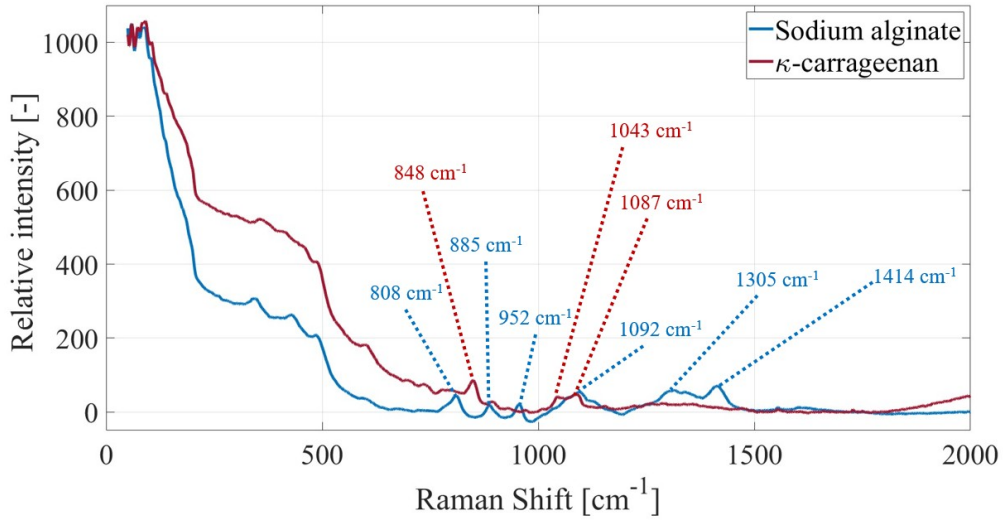

FIGURE 7.4: Raman spectra of sodium alginate and κ-carrageenan, with the different characteristic peaks indicated in the same color as the respective spectrum.

The ^{1}H-NMR spectrum of sodium alginate, shown in Figure 7.5, exhibits a large peak at 4.701 ppm, corresponding to residual water in the sample. Most of the spectrum is focused between 4.7 and 3.5 ppm, in the so-called sugar ring region discussed by Abeygunawardana *et al.* [1], which is expected as sodium alginate consists of sugar ring monomers. According to the table of Steurs (Figure C.1, Appendix C.1.3), chemical shifts in this region correspond to ether, alcohol and ester bonds, which are present in the Lewis structure from Figure 7.1 [202]. Additionally, three smaller, but very narrow peaks are observed at 8.384, 1.844 and 1.112 ppm, related to formic acid-like (typical NMR shift at 8.26 ppm) and alcohol-related structures [8, 202].
The ^{1}H-NMR spectrum of κ-carrageenan, provided in Figure 7.6, indicates that most of the spectrum is located between 4.4 and 3.2 ppm, as expected [1]. The results are similar to those reported by Hu *et al.*, who also observed the most prominent peaks between 4 and 3.5 ppm [93]. The peak at 2.150 ppm might be caused by acetate-containing molecules (with the typical NMR shift of allyl acetate and glycol diacetate in D_2O at 2.13 and 2.12 ppm, respectively [8]). The peak around 1.833 ppm possibly corresponds to alcohol bonds (see Figure C.1) [202].

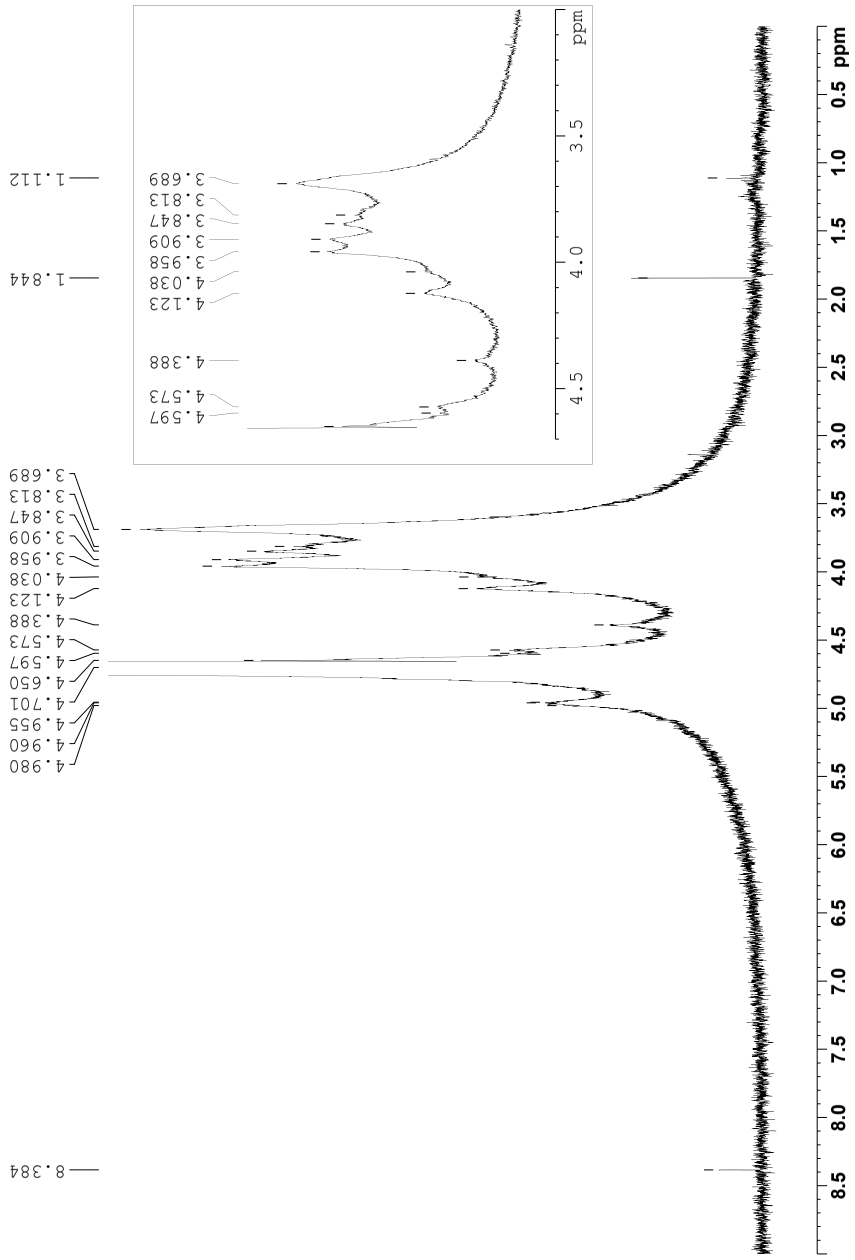

FIGURE 7.5: ^{1}H-NMR spectrum of sodium alginate. The spectrum is made using the TopSpin software package (Bruker, USA).

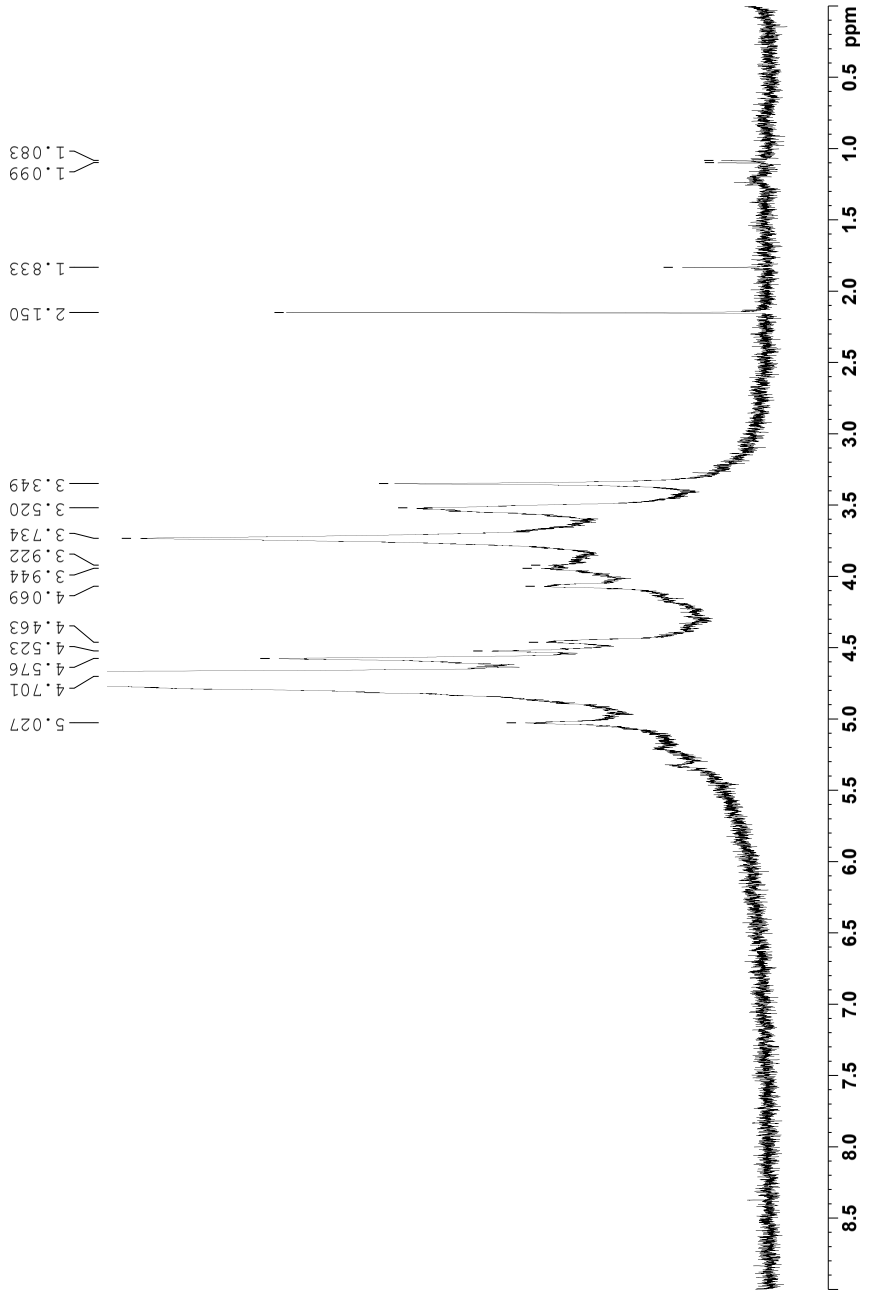

Figure 7.6: ^{1}H NMR spectrum of κ-carrageenan. The spectrum is made using the TopSpin software package (Bruker, USA).

Extracted EPS

The chemical properties of the extracted EPS are expected to affect the rheology of the resulting hydrogel. Therefore, the most important results from Chapter 6 are summarized in Table 7.1. Some striking differences are observed between the contents of the different sludge EPS, such as the relatively low polysaccharide-to-protein ratio in the EPS from the salt-adapted granule. In contrast, the floccular sludges show the highest polysaccharide-to-protein ratio. The most striking difference, however, is the amount of fatty acids being almost twice as large in the EPS extracted from the salt-adapted floc, compared to the other sludges. The variable composition of different EPSs is expected to induce differences in the hydrogel formation and their rheological properties.

TABLE 7.1: Normalized surface area between the baseline and FTIR spectrum of EPS extracted from the different industrial sludges used in this work. Each area is represented as a percentage of the total area of the three peaks.

Sample name	Relative area fatty acids [%]	Relative area proteins [%]	Relative area polysaccharides [%]
Floc before salt adaptation	4	44	52
EBPR-granule	4	48	47
Salt-adapted floc	9	39	52
Salt-adapted granule	5	56	39

The composition of the extracted EPS can also be compared to that of the two model systems to gain a better insight into their differences and similarities. These are expected to be crucial in comparing the EPS's gelation to that of the model systems.

Comparing chemical characteristics of EPS and model systems

Comparing the FTIR spectra of the two model systems to those of the EPS from four different sludges (given in Figures 7.3 and 7.7, respectively) shows that the model systems' spectra contain narrower, more defined peaks compared to those of the extracted EPS. This indicates the more complex composition of the EPS. Some of the peaks of the extracted EPS also closely match those of the two model systems, specifically those around 1030, 1400, and 1600 cm^{-1} when compared to alginate and 1035 cm^{-1} for the spectrum of κ-carrageenan. The FTIR spectra of the EPS do not flatten out between 900 and 600 cm^{-1}, possibly indicating the presence of some bonds like sulfates, which show their characteristic peak at 842 cm^{-1}, as observed in the spectrum of κ-carrageenan.

Since the EPS are compared to two polysaccharides, the locations of these corresponding peaks are the typical bonds seen in polysaccharidic structures, like carboxylate ions and several bonds between oxygen and carbon. Conversely, the region between 900 and 600 cm^{-1} contains bonds between heavier atoms, like P−O

and S−O bonds [142]. These S−O bonds are also present in the sulphate groups of κ-carrageenan, which explains the presence of a peak in this region in the FTIR spectrum of κ-carrageenan. However, this is a relatively narrow peak, while those of the EPS are very broad. For this reason, it is difficult to assign specific bonds to this region for the EPS. On the other hand, all EPS exhibit a small peak around 1224 cm^{-1}, similar to κ-carrageenan, indicating the presence of sulfate groups [76]. However, a peak at 1222 cm^{-1} could indicate the presence of P−O-bonds [185]. Hence, either P−O, S−O bonds or both are expected to be present in the EPS.
The FTIR spectra of the extracted EPS also show other differences when compared to the two polysaccharides, like more pronounced peaks around 2900 cm^{-1}, as well as the more prominent peaks around 1650 and 1550 cm^{-1}, corresponding to the fatty acids and proteins in the extracted EPS, respectively. Hence, the composition of the extracted EPS is more complicated than that of the polysaccharides. Schambeck *et al.* have already acknowledged the greater complexity of EPS compared to alginate, caused by the presence of other biopolymers such as proteins [182]. Even though they realize EPS do not only contain polysaccharides, they still describe extracted EPS as alginate-like exopolymers (ALE) [182]. This term arose due to the similarities of EPS and alginate in their hydrogel behaviour and because both EPS and alginate can be extracted similarly, using heat and sodium carbonate [178].

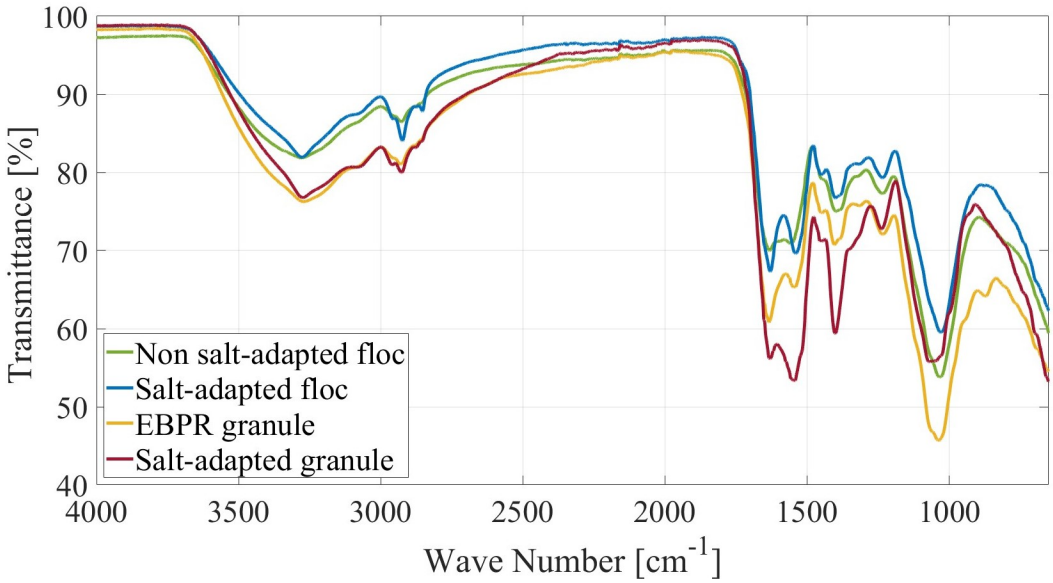

FIGURE 7.7: FTIR spectra of the EPS extracted from the different sludge samples used in this work.

The higher complexity of EPS is also observed in the different ^{1}H-NMR spectra (Figures 7.5 and 7.6 for the model systems, Figures 6.11, 6.13, 6.14, and 6.16 for the sludges), as the ^{1}H-NMR spectra of the EPS from the industrial sludges show broader peaks, spread out over a wider range. Peaks are not only observed between 4.4 and 3.2 ppm, as is the case for the polysaccharides, but all spectra also show

peaks between 2 and 1 ppm, corresponding to molecules other than polysaccharides. Due to their complex composition, the gelation mechanisms of EPS are expected to be more complex than those of the model systems.

7.2.2 Hypotheses for the rheology of EPS and model system hydrogels

Before determining the rheological properties of the hydrogels made from the model systems and the EPS, some hypotheses regarding their rheological behavior are proposed. The FTIR spectrum of sodium alginate, shown in Figure 7.3, exhibits prominent peaks at 1600 and 1400 cm^{-1}, both of which indicate the presence of carboxylate ions. These could induce ionic crosslinking by attracting cations, resulting in the formation of a physical crosslink. On the other hand, κ-carrageenan can induce similar crosslinks through its sulphate groups, showing peaks at 842 and 1224 cm^{-1}. The hydrogels of both model systems are expected to have different moduli, due to the different Coulomb interactions between the cations and the carboxylate groups of alginate and sulphate groups of κ-carrageenan. The moduli of the alginate hydrogels are expected to be the largest, as carboxylate ions are smaller than sulfate ions, resulting in stronger Coulomb forces in the sodium alginate hydrogels.

The composition of EPS is much more complex, containing many different functional groups, some of which are not present in any model systems (i.e., the N−H in the amide group). As these functional groups could have both positive and negative effects on the final hydrogel properties of the EPS, it is proposed that the EPS-based hydrogels are expected to have higher moduli due to the increased number of interactions enabled by the higher EPS complexity.

7.2.3 Rheological characterization

Model systems

Several sodium alginate hydrogels were made with 1 and 2.5 wt% alginate hydrogel bases and salt solutions containing 0.01 and 0.1 M $CaCl_2$. These amounts were based on the values used by Pagliaccia [157].
The frequency-dependent moduli of hydrogels are shown in Figure 7.8. The moduli of the gels are only weakly dependent on the frequency, irrespective of the gel composition. The storage modulus (G') of the hydrogel made with 2.5 wt% alginate and a 0.1 M $CaCl_2$ solution has a value of around 150,000 Pa at an angular frequency of 10 $\frac{\text{rad}}{\text{s}}$, which is approximately five times higher than the loss modulus (G''). This indicates rather solid-like, firm, and rigid behavior [134], which is also observed when handling the gel, as shown in Figure 7.9.

The same plot shows the dependence of the moduli on the salt and alginate concentration. Decreasing the alginate concentration in the hydrogel base from 2.5 to 1 wt% results in the moduli decreasing by a factor of 3.2 (red vs. blue data points in Figure 7.8). The value of G' of the 1 wt% alginate hydrogel, made with 0.1 M

$CaCl_2$ equals 46,000 Pa. Conversely, no significant change in the ratio of *G'* and *G"* is observed. Decreasing the salt concentration by 90 % results in moduli 3 to 4 times lower (green vs. blue data points in Figure 7.8), as the storage modulus *G'* of the hydrogel made with 2.5 wt% alginate and 0.01 M $CaCl_2$ equals 40,000 Pa at an angular frequency of 10 $\frac{\text{rad}}{\text{s}}$. Hence, the moduli appear to be dependent on both the salt and alginate concentrations, as both affect the crosslink density, resulting in changes in the observed moduli.

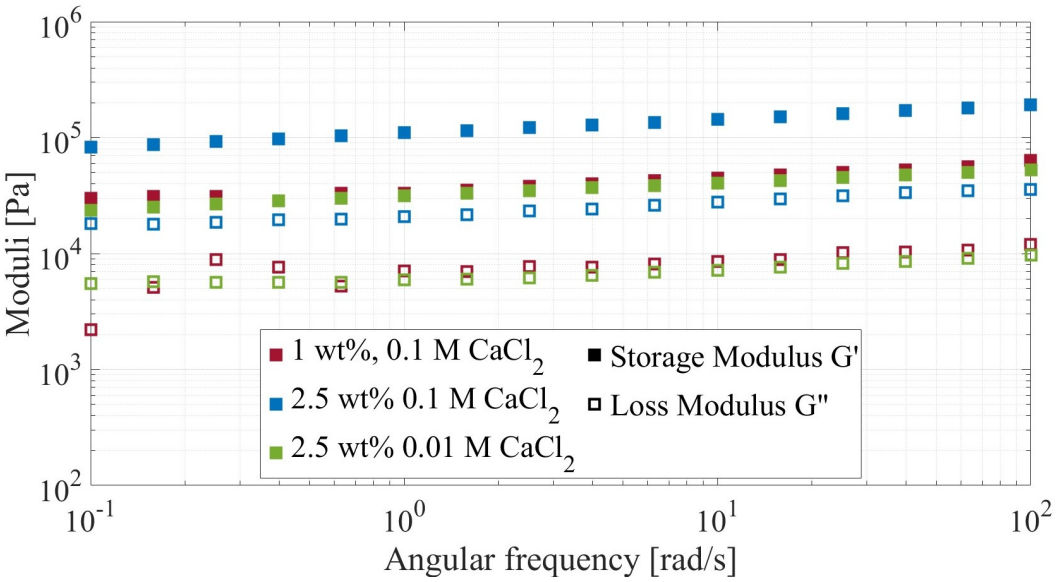

FIGURE 7.8: Frequency-dependent moduli of sodium alginate hydrogels, made with different salt concentrations in the crosslinking solution, obtained using an AR-G2 rheometer, with an oscillation strain of 0.01 % and decreasing angular frequency. The measurements are carried out at 20 °C.

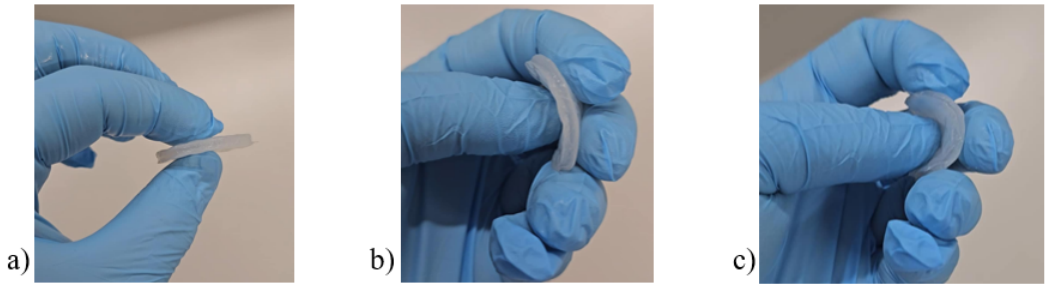

FIGURE 7.9: Visualization of the rigidity of the sodium alginate (2.5 wt%, 0.1 M $CaCl_2$) hydrogel. **a)** Pinching the gel gently results in very little deformation. **b)** Slightly bending the hydrogel does not have an effect on the hydrogel stability and feeling, as it remains intact. **c)** The hydrogel even resists severe bending, confirming its rigidity.

Liparoti *et al.* investigated the influence of varying sodium alginate concentrations on the rheological properties of hydrogels [125]. However, they prepared the hydrogel using a more conventional method, by submerging the hydrogel base directly in a salt bath containing 2.5 M $CaCl_2$ for 15 minutes, instead of letting it gelate in a mold using a dialysis membrane for 36 hours. In this manner, the authors were able to create hydrogel discs on which the rheological measurements are performed. Moreover, they used alginate concentrations between 3.2 and 9.5 wt% to form hydrogels, as well as $CaCl_2$ concentrations of 0.25 M and higher. They observed that the moduli are only slightly frequency-dependent, with the storage modulus of a hydrogel made with 3.2 wt% alginate and 0.25 M $CaCl_2$ at 10 $\frac{\text{rad}}{\text{s}}$ being equal to approximately 80.000 Pa [125], being only half of the value obtained in this work, despite using a higher salt concentration of 0.25 M. This difference can be attributed to the different preparation method of the hydrogel, which only allows crosslinking for 15 minutes, after which the gel beads are removed from the salt source. The method used in this work allows diffusion of ions throughout the entire hydrogel, ensuring a uniform crosslinking degree, which results in higher moduli [157]. They also determined the rheological properties of the alginate hydrogel, made with 2.5 wt% alginate and a 0.75 M $CaCl_2$ solution and observed an increase of the storage modulus at 10 $\frac{\text{rad}}{\text{s}}$ to around 200,000 Pa, representing a 2.5-fold increase. This is slightly less than the increase observed in this work, which could also be attributed to the differences in the hydrogel formation process.

Pagliaccia studied the effect of the Ca^{2+} concentration on the alginate hydrogels' mechanical properties, specifically the stiffness, characterized by the Young's modulus [157]. They observed an increase from 15 to 35 kPa in the Young's modulus when increasing the Ca^{2+} concentration from 0.01 to 0.1 M for 2.5 wt% alginate hydrogels. She attributed this increase in moduli to the formation of more crosslinks, resulting from more Ca^{2+} ions diffusing into the gel, which is enabled by the greater gradient between the gel and the environment [157].

Next, several κ-carrageenan hydrogels are made with a 1 wt% hydrogel base and salt solutions containing in total 0.1 M crosslink-inducing ions (0.1 M $CaCl_2$, 0.1 M KCl and 0.06 M KCl together with 0.04 M $CaCl_2$). The ratio of KCl and $CaCl_2$ is based on the ions present in EPS extracted from salt-adapted granular sludge and was determined using an ion chromatogram (data not shown).
Figure 7.10 shows the moduli of the three aforementioned hydrogels as a function of the angular frequency. Independent of the salts used, the moduli appear to be relatively frequency-independent. The hydrogel made with 1 wt% of κ-carrageenan and 0.1 M $CaCl_2$ exhibits a storage modulus slightly larger than 10,000 Pa at an angular frequency of 10 $\frac{\text{rad}}{\text{s}}$. Hardly any difference in the moduli is observed when changing the type of salt from $CaCl_2$ to KCl. Hence, the crosslink strength is comparable for both cations. However, when combining the two salts at the same total concentration, the storage modulus approximately doubles to a value slightly larger than 20,000 Pa. The storage modulus of the 1 wt% κ-carrageenan hydrogel, made with 0.1 M $CaCl_2$

at 10 $\frac{\text{rad}}{\text{s}}$, which is slightly larger than 10,000 Pa, is approximately four times smaller than that of the alginate gel made with the same salt and alginate concentration, which has a storage modulus of around 40,000 Pa at the same frequency.

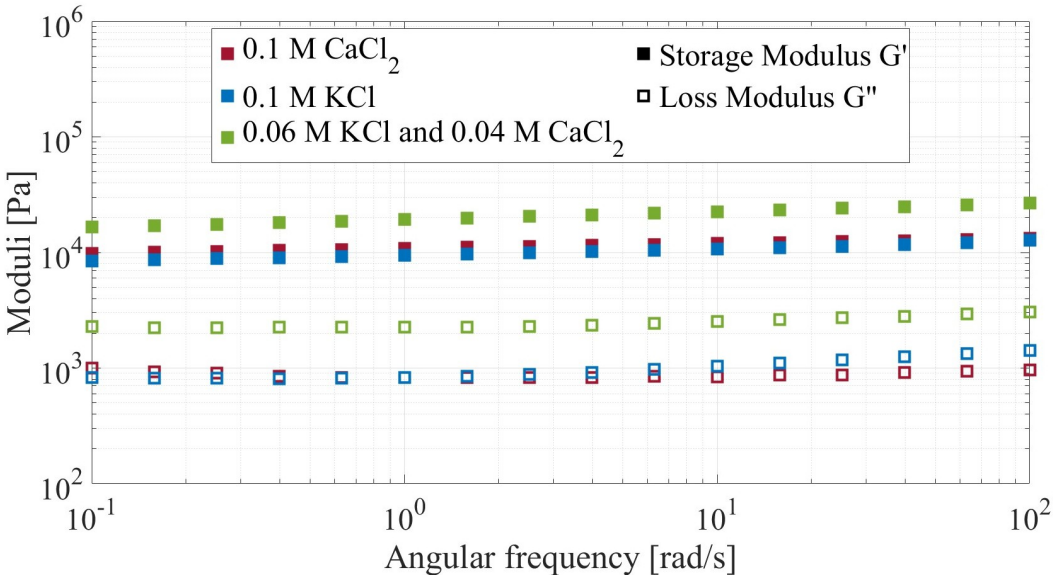

FIGURE 7.10: Frequency-dependent moduli of a hydrogel made with 1 wt% κ-carrageenan and salt solutions, containing either 0.1 M $CaCl_2$, 0.1 M KCl or 0.04 M $CaCl_2$ and 0.06 M KCl. The data is obtained using an AR-G2 rheometer, with an oscillation strain of 0.01 % and decreasing angular frequency. The measurements are carried out at 20 °C.

.

As already mentioned, the gelation of κ-carrageenan is a two-step process, requiring both heating (and subsequent cooling down) and ions to induce crosslinking [26]. During cool-down, the coil configuration of the κ-carrageenan polymers transforms into a helical structure, which aggregates under the influence of different cations (like K^+ and Ca^{2+}) to induce physical crosslinks [148, 208]. It is already known that K^+ ions are preferred for the gelation of κ-carrageenan, as they can form a bridge between sulphate groups and D-galactose residues, while Ca^{2+} bridges two sulphate groups directly [208].

Thrimawithana *et al.* investigated the effect of ion concentrations on hydrogels containing 0.4 w/v% κ-carrageenan and observed moduli largely independent of the angular frequency [208]. Hermansson *et al.* studied the effect of different K^+ and Ca^{2+} concentrations on κ-carrageenan hydrogels [88]. They observed the synergistic effect of the two types of ions, as the moduli showed a significant increase when both ions were added to one hydrogel. When combining the two ions, the hydrogel has a microstructure containing two types of linkages: a finer molecular network formed by the Ca^{2+} ions, as well as longer superstrands induced by the K^+ ions. Using a single type of cation only results in a fine molecular structure, with few superstands

visible in the K^+-based hydrogel and none in the Ca^{2+}-hydrogel. Because of this, hydrogels formed with a single type of cation have similar moduli [88], as observed in Figure 7.10. To ensure the highest moduli for the hydrogels made of EPS, salt solutions containing both KCl and $CaCl_2$ at a high concentration of 0.1 M are used to enable a possible synergistic effect between the two ions in the hydrogel formation of the extracted EPS.

Extracted EPS

First, different hydrogels were made using hydrogel bases containing 2 wt% of EPS, due to the limited availability of the material. This appeared to be more challenging than expected, as only the EPS from salt-adapted granular sludge could form hydrogels at 2 wt% EPS content, as shown in Figure 7.11a. The gel maintained its cylindrical shape, but also exhibited some permanent deformations at the top, caused by only gently tapping it with a spatula while removing it from the mold. Although the gel retains its shape, it appears rather fragile. The attempt to form a hydrogel using 2 wt% of the EPS extracted from the EBPR-granule clearly failed, as shown in Figure 7.11c, as the hydrogel was unable to maintain its cylindrical shape. Hence, it is clear that 2 wt% is not sufficient to form stable hydrogels, which is why the EPS concentration for the further hydrogels was increased to 5 wt%. As expected, increasing the EPS concentration to 5 wt% results in a well-sustained cylindrical shape of the hydrogel, as shown in Figure 7.11b, which displays the hydrogel made with 5 wt% EPS from salt-adapted granular sludge. Gelation at a concentration of 5 wt% was also possible for the EPS extracted from the EBPR-granule, as shown in Figure 7.11d. This gel had the firmest feeling of all hydrogels and was also able to maintain its cylindrical shape. Pagliaccia also observed that a concentration of at least 2.5 wt% is needed to form a stable hydrogel of EPS extracted from aerobic granular sludge [157]. However, as each EPS extraction only results in a limited amount of EPS, hydrogels with concentrations much larger than 5 wt% could not be made. For this reason, the hydrogels made of EPS from floccular sludges were also made using a 5 wt% hydrogel base. These hydrogels showed some peculiar results, as the hydrogel made using the non-salt-adapted floccular sludge (Figure 7.11e) has a much more slime-like appearance compared to that of the salt-adapted floccular sludge (Figure 7.11f), which looks more water-like. These two hydrogels were also unable to maintain their cylindrical shape when removed from of the mold. The slime-like gel appears less fragile than the watery hydrogel made with 5 wt% EPS from salt-adapted floccular sludge, while also feeling stiffer.

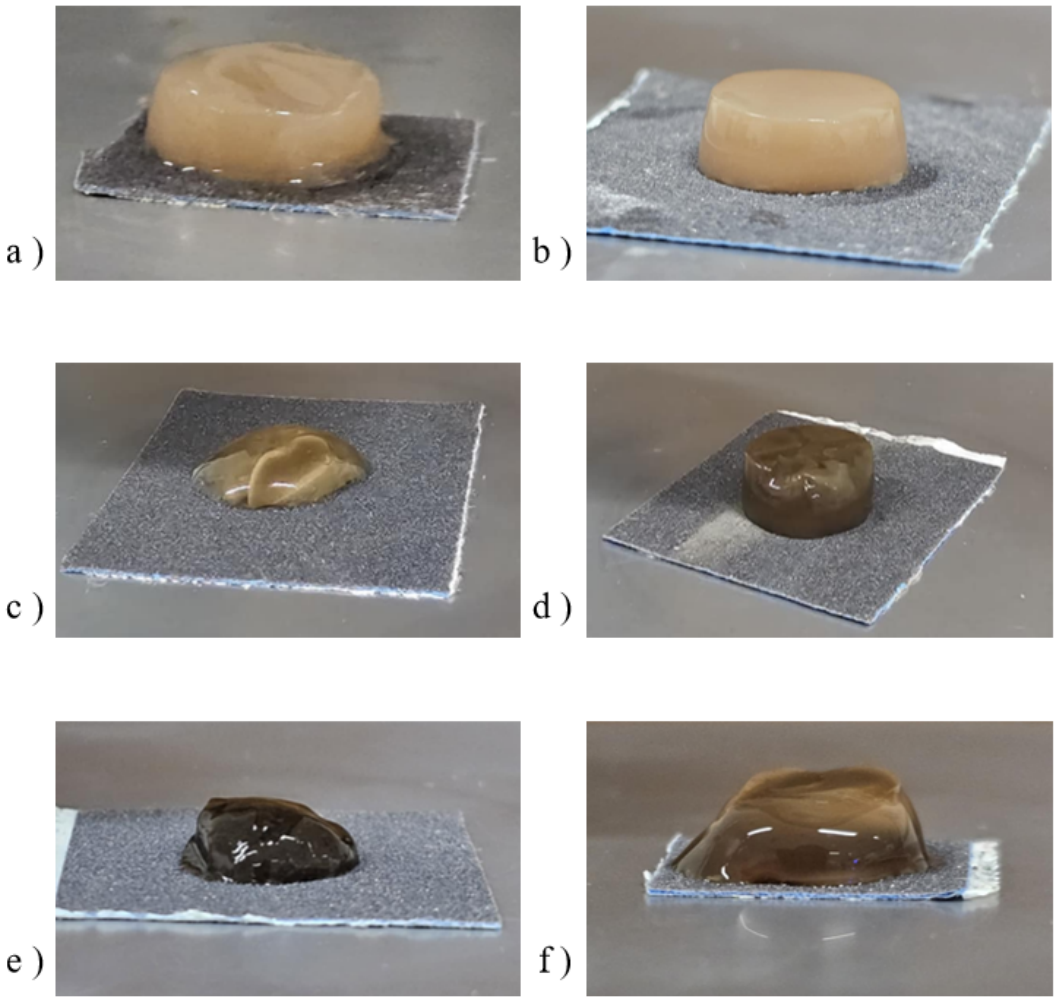

FIGURE 7.11: Hydrogels made from EPS extracted from different sludge sources, using different concentrations. **a)** 2 wt% EPS from salt-adapted granular sludge **b)** 5 wt% EPS from salt-adapted granular sludge **c)** 2 wt% EPS from EBPR-granular sludge **d)** 5 wt% EPS from EBPR-granular sludge **e)** 5 wt% of non-salt-adapted floccular sludge **f)** 5 wt% of salt-adapted floccular sludge

.

Figure 7.12 shows the moduli of the hydrogels made with 2 and 5 wt% of EPS extracted from the EBPR granule plotted as a function of the angular frequency. The moduli are plotted for angular frequencies between 0.1 and 10 $\frac{\text{rad}}{\text{s}}$, as inertial effects start to dominate the actual rheological behavior at higher angular frequencies, due to the need for higher strains during the measurements. For this reason, all frequency sweeps performed on hydrogels made from extracted EPS are only plotted between 0.1 and 10 $\frac{\text{rad}}{\text{s}}$. Independent of the amount of EPS used, the moduli of the hydrogel are only slightly frequency dependent. As expected, the hydrogel made with 5 wt% EPS shows the greatest moduli, with the storage modulus *G'* being

equal to 450 Pa at an angular frequency of 10 $\frac{\text{rad}}{\text{s}}$. At the same frequency, the loss modulus *G"* equals 50 Pa, approximately 9 times smaller than *G'*. This indicates the more solid-like behavior of the hydrogel, as expected from its appearance, as shown in Figure 7.11d. Even though the 5 wt% gel maintains its shape well, its moduli are still only a few percent of those of the model systems' gels.
The 2 wt% gel exhibits moduli that are mostly frequency-independent, with a storage modulus equal to 70 Pa at an angular frequency of 10 $\frac{\text{rad}}{\text{s}}$, which is 7.5 times lower than that of the 5 wt% hydrogel. This was expected based on its appearance (Figure 7.11c). Even though the "gel" resembles a liquid, the storage modulus is a factor of 4 to 5 larger than the loss modulus, which equals approximately 15 Pa at 10 $\frac{\text{rad}}{\text{s}}$, indicating its more solid-like rheological behavior. Comparing these results to the moduli of the model systems' hydrogel from Figures 7.8 and 7.10 shows that even the moduli of the hydrogel made with 5 wt% EPS are two orders of magnitude smaller than those of the hydrogels made from the model systems.

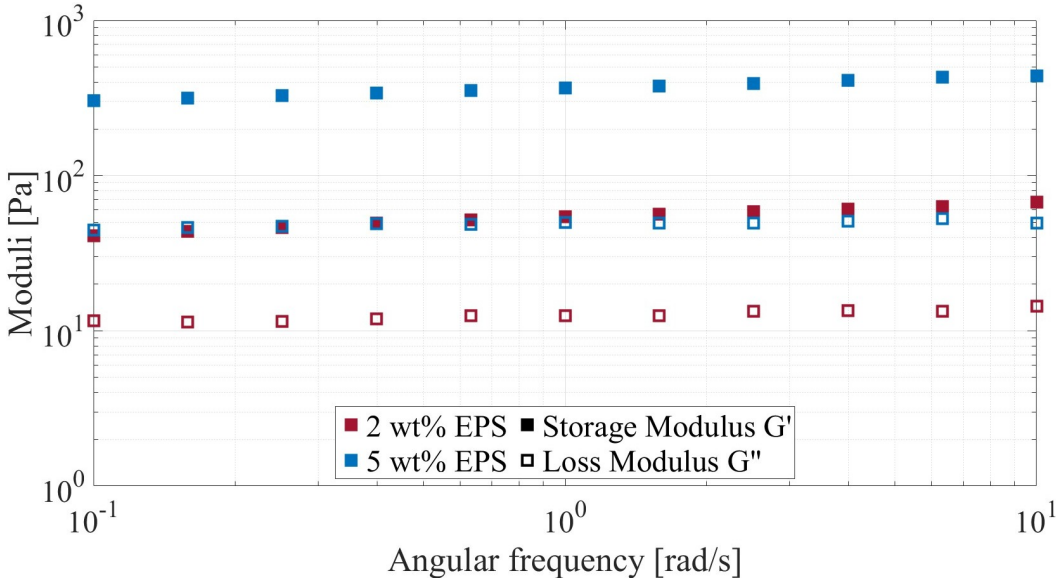

FIGURE 7.12: Frequency-dependent moduli of a hydrogel made with 2 wt% and 5 wt% EPS extracted from EBPR granular sludge, using the heat and sodium carbonate extraction method, obtained using a Discovery HR3 rheometer, with an oscillation strain of 5 % and decreasing angular frequency. The measurements are carried out at 20 ℃.

Figure 7.13 compares the hydrogels made using 5 wt% of EPS from both salt-adapted and non salt-adapted floccular sludge. Both hydrogels have relatively frequency-independent moduli. Salt adaptation does not appear to affect the hydrogels' rheology, as both storage and loss moduli exhibit extensive overlap. For both hydrogels, the storage modulus is around 180 Pa at 10 $\frac{\text{rad}}{\text{s}}$, while the loss modulus is between 30 and 40 Pa, 4 to 6 times smaller than *G'*, indicating the solid-like behavior of both hydrogels. The differences in their chemical composition, as shown in Table 7.1 (primarily a greater polysaccharide content), and their appearance, as shown in Figures 7.11e and 7.11f, are not reflected in the rheological characteristics of their hydrogels.

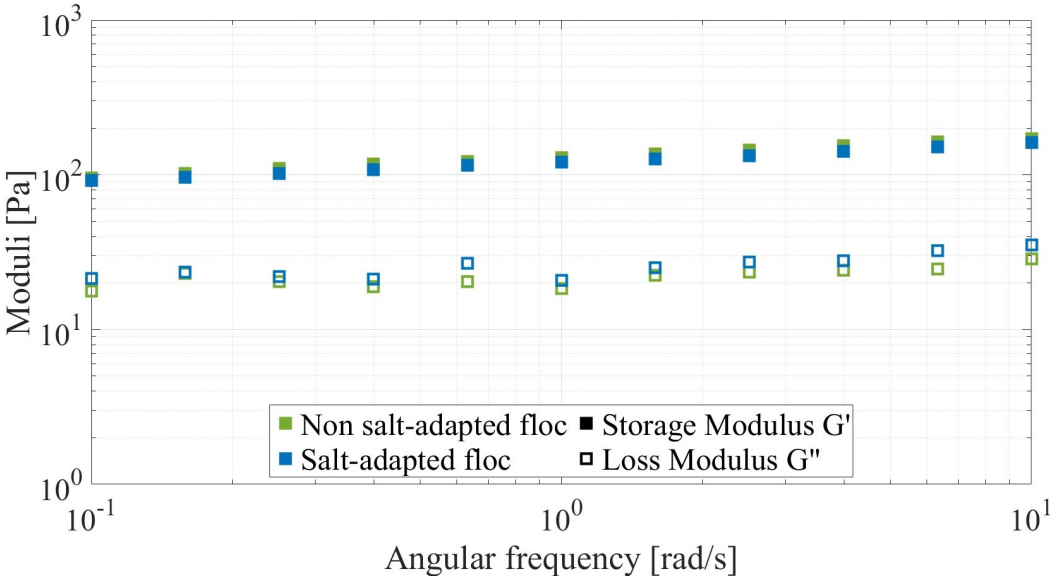

FIGURE 7.13: Frequency-dependent moduli of hydrogels made with 5 wt% of non salt-adapted and salt-adapted floccular sludge, obtained using a Discovery HR3 rheometer, with an oscillation strain of 5 % and decreasing angular frequency. The measurements are carried out at 20 ℃.

A comparison is made between the storage and loss moduli of hydrogels made of both salt-adapted floccular and granular sludge in Figure 7.14. Both hydrogels show relatively frequency-independent moduli, with the hydrogel made using EPS from the salt-adapted granular sludge having storage moduli approximately 1.5 times larger than those of the salt-adapted floccular sludge (236 Pa compared to 162 Pa). The loss moduli, on the other hand, almost overlap, indicating the more solid-like behavior of the hydrogel made from EPS derived from salt-adapted granular sludge, compared to that of the salt-adapted floccular sludge, which could also be observed from their appearance in Figure 7.11. These values are slightly smaller than those of the 5 wt% EBPR-granule EPS hydrogels, shown in Figure 7.12 and slightly larger than those made using floccular sludge, shown in Figure 7.13.

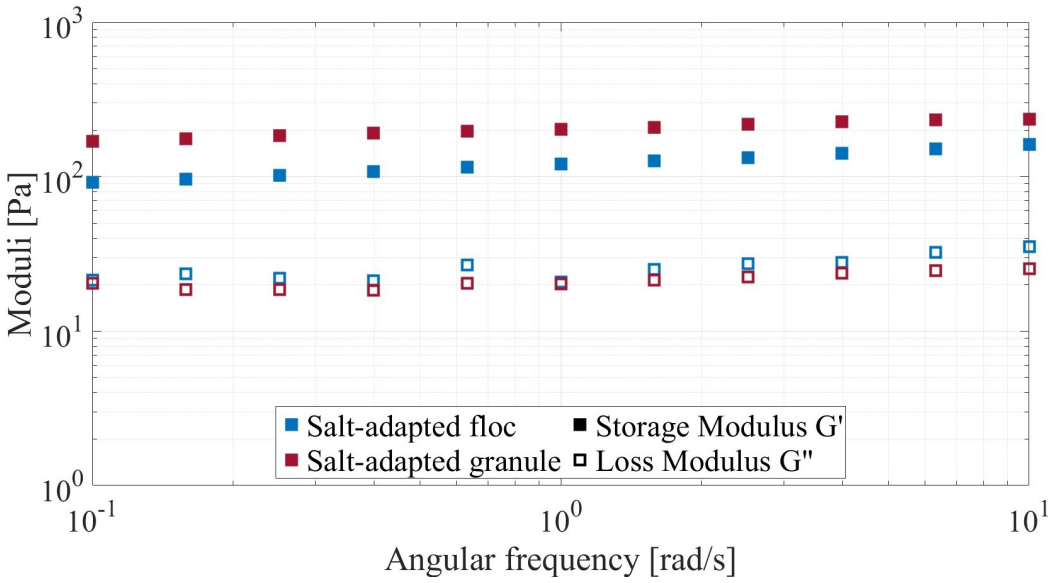

FIGURE 7.14: Frequency dependent moduli of hydrogels made with 5 wt% salt-adapted floccular and granular sludge, obtained using a Discovery HR3 rheometer, with an oscillation strain of 5 % and decreasing angular frequency. The measurements are carried out at 20 ℃.

Finally, Figure 7.15 compares the moduli of hydrogels made with EPS from the two granular sludges. Both hydrogels have very similar frequency-dependent behavior, with the hydrogel made with EPS from the EBPR granule having both larger storage moduli (*G'*) (450 Pa compared to 220 Pa at 10 $\frac{\text{rad}}{\text{s}}$) and loss moduli (*G"*) (50 Pa compared to 25 Pa at 10 $\frac{\text{rad}}{\text{s}}$). Both hydrogels have *G'* that are almost an order of magnitude larger than *G"*, indicating their more solid-like behavior, corresponding to the observations with the naked eye. The two hydrogels have a very similar degree of solid-like behavior, as the ratio of *G'* and *G"* is approximately the same for both.

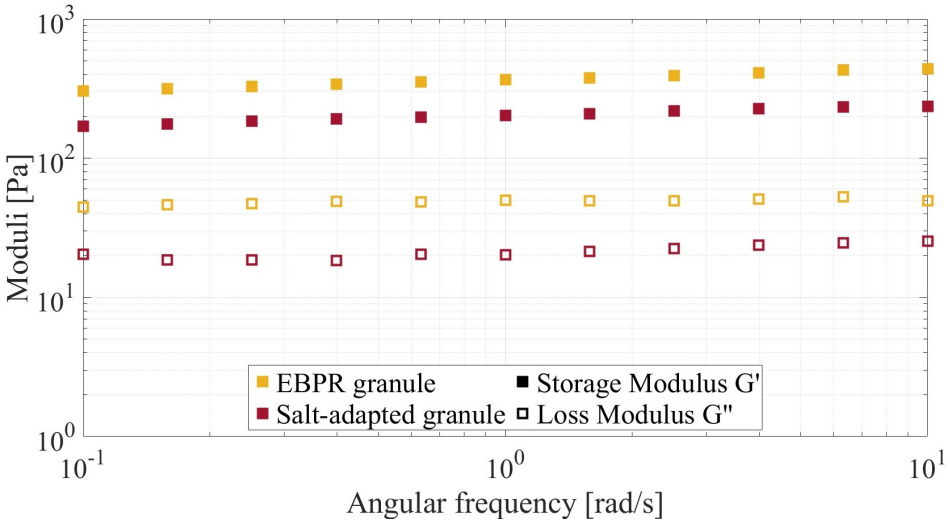

FIGURE 7.15: Frequency dependent moduli of hydrogels made with 5 wt% of non salt-adapted and salt-adapted floccular sludge, obtained using a Discovery HR3 rheometer, with an oscillation strain of 5 % and decreasing angular frequency. The measurements are carried out at 20 °C.

Figure 7.16 shows the rheological properties of the four different EPS-based hydrogels. The hydrogel made with EPS from the non salt-adapted EBPR granule shows the largest moduli, while those from the two floccular sludges result in the lowest moduli. Hydrogels made from granular sludge EPS have larger *G'*. Except for the EBPR granule, the *G"* of the different hydrogels are similar.

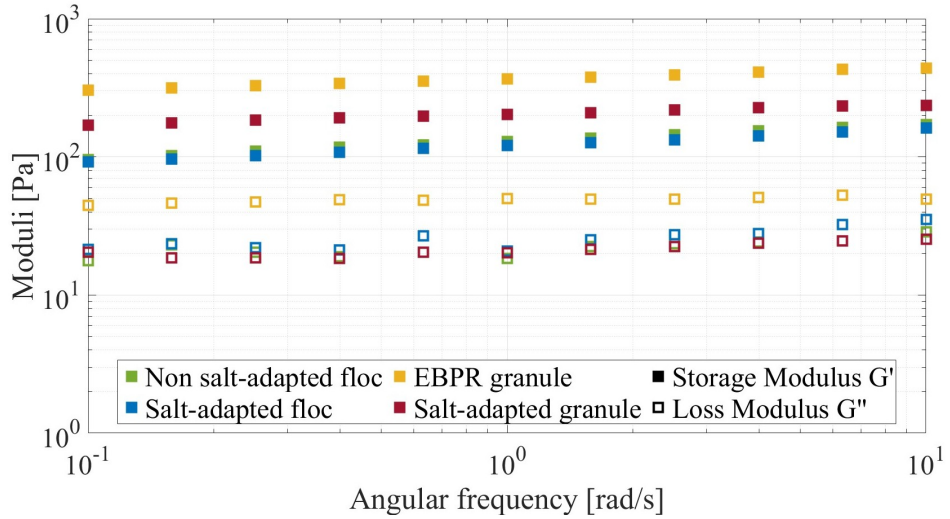

FIGURE 7.16: Frequency dependent moduli of hydrogels made with 5 wt% EPS, extracted from four different industrial sludge samples, obtained using a Discovery HR3 rheometer, with an oscillation strain of 5 % and decreasing angular frequency. The measurements are carried out at 20 °C.

7.3 Discussion

Understanding the effects of the EPS composition on the resulting hydrogel properties is of utmost importance for hydrogel applications. However, as the EPS composition is expected to be dependent on many external factors, it is unlikely that the EPS composition is constant over time [182]. Therefore, it is important to study the effect of the differences in chemical characteristics on hydrogel rheology and gelation.

Based on the relationships between the chemical characteristics and the gelation and rheological properties of the model systems, an attempt is made to reveal similar relationships for the EPS.

Linking rheology to chemical characterization: model systems

Alginate undergoes gelation by including Ca^{2+} ions into two antiparallel alginate molecules, more specifically into their guluronic acid regions. Repeating this process results in a shape similar to an egg-box [79]. Only the guluronic acid blocks can incorporate cations, mannuronic acid blocks cannot, such that the hydrogel's mechanical properties depend on the ratio of these two blocks in the alginate used [28]. Schambeck *et al.* linked the two blocks to different wavenumbers in the FTIR spectrum. Guluronic acid shows peaks between 1397 and 1232 cm^{-1}, while the mannuronic acid peak sits closer to 826 and 818 cm^{-1} [182]. When looking at the FTIR spectrum of sodium alginate in Figure 7.3, a prominent peak is observed in the region of the guluronic acid. In contrast, the peak of the mannuronic acid residues is only barely visible, indicating the higher density of the guluronic acid in the sodium alginate molecule. The high density of guluronic acid blocks in the alginate, compared to mannuronic acid, explains the high moduli observed in Figure 7.8.

As mentioned before, κ-carrageenan forms hydrogels in a completely different manner, having the ability to use both monovalent ions, like K^+, and divalent ions, like Ca^{2+} [208]. Both ions induce a coil-helix transition during the cooling of κ-carrageenan and then bind to specific sites within the molecule, inducing aggregation of these coils and subsequent gel formation. Apart from this fine network, K^+ can also induce superstrands, which are supramolecular structures, further increasing the stiffness of the hydrogel [88]. Ca^{2+} ions only have the ability to form intermolecular bridges between sulphate groups. In contrast, K^+ can form intermolecular bridges between sulfate groups of two different molecules, which is followed by attracting the oxygen from the anhydro-bridge, inducing a second attraction [208]. These bonds show their characteristic peaks in the FTIR spectra of κ-carrageenan at 843 and 1224 cm^{-1}, 928−933, and 1070 cm^{-1}, respectively [76, 207]. Also in the case of κ-carrageenan, these peaks are clearly visible in Figure 7.3.

The alginate gels (Figure 7.8) show greater moduli than the gels made of κ-carrageenan (Figure 7.10), even when both K^+ and Ca^{2+} ions are combined. The synergistic effect of the superstrands and the microstructure is not able to generate hydrogels

stiffer than those made of alginate. Hence, the physical crosslinks in the alginate hydrogels appear stiffer than those in κ-carrageenan gels.

Linking rheology to chemical characterization: extracted EPS

Linking the rheological properties of EPS hydrogels to their chemical compositions is not straightforward, as the gelation mechanism of EPS is expected to be as complex as its composition [59, 158]. Even literature shows uncertainty about which biopolymers induce gelation, as different authors have varying perspectives on the subject [157]. Some authors believe that proteins are essential for hydrogel formation [121], while others have observed no significant changes in hydrogel properties when changing the protein content [188]. Proteins are expected to be essential for the gelation because they contribute to the granulation process, which, in essence, forms a granular hydrogel [129, 189]. On the other hand, Schambeck *et al.* concluded that uronic carbohydrates control the gelation of EPS hydrogels [182]. Flemming and Wingender attributed the gelation ability of EPS to polysaccharides, proteins, and extracellular DNA, being the most important factors determining the EPS hydrogel properties [63]. Finally, Felz *et al.* even suggest that the gelation of EPS is not only caused by the complexation of ions in the EPS molecules, but also by the presence of several functional groups in the EPS, indicating the complex nature of EPS hydrogel formation [59]. To the best of the author's knowledge, no conclusive theory has been established or accepted that links the EPS composition to their rheological properties. Therefore, a comparison is made between the most important theories, linking the gelling behavior to the chemical composition. Two general remarks on the hydrogel formation are discussed first.

First, Lotti *et al.* investigated the effect of the EPS concentration in the hydrogel base on the final properties of the hydrogel. They concluded that a concentration greater than 17.5 wt% is required to form a stable hydrogel from EPS of anammox sludge [134]. Only such highly concentrated EPS could form an extensive 3D network, as an increase in moduli of three to four orders of magnitude is observed when the concentration is increased from 10 to 17.5 wt% [134]. To achieve such concentrations in this work, at least 200 mg of EPS is required, which could not be achieved with the current extraction methods. However, 5 wt% EPS already appeared sufficient to make a hydrogel for most sludge types. Nevertheless, the observed moduli in this work are still very low. Higher EPS concentrations are expected to result in higher moduli [134], possibly improving the measured rheological characteristics.

When comparing the moduli of the EPS hydrogel, it is clear that the EPS from granular sludge result in hydrogels with superior moduli than those made of floccular sludge EPS. Seviour also noticed a difference in the hydrogel properties of EPS from granular and floccular sludge, with only the EPS from granular sludge showing a clear sol-gel transition between pH values of 9 and 12. By lowering the pH closer to the operational pH of a wastewater treatment plant (6-8.5), a strong gelation was observed for the EPS from granular sludge, which was not observed for the

hydrogels made of floccular sludge EPS [188]. Schambeck *et al.* also compared the gelation behavior of both floccular and granular sludges and observed that hydrogels made of EPS from granular sludge have a higher storage modulus compared to those made from floccular sludges [182]. As already mentioned, they describe the EPS as alginate-like exopolymers (ALE), suggesting that the hydrogel formation of EPS is comparable to that of alginate. As alginate mainly forms crosslinks using guluronic acid blocks, a higher mannuronic acid content results in weaker hydrogels. Hence, they expect that floccular sludge produces more mannuronic acid-like EPS [182]. However, even though they consider the EPS as ALE, they also confirm that the EPS contain components other than polysaccharides, having a great variety of functional groups. This could enable the use of EPS in more applications as a biomaterial [123, 182]. However, it is also likely that the complex EPS composition results in a more complex gelation mechanism [59].

Felz hypothesizes that gelation is not only induced by ionic crosslinks between the carboxylic acid groups, as is the case for alginate, but also by other charged side groups, such as phosphates and sulphates, and hydrogen bonds [59]. He demonstrated this by comparing the resistance of EPS-based and alginate hydrogels to the complexing agent EDTA. EPS-based hydrogels appeared to be the most resistant, which is likely caused by these other bonding mechanisms shielding the ions in the hydrogel from the complexing agent [59]. EPS hydrogels also have a lower stiffness when using transition metals as opposed to earth alkali metals to induce ionic crosslinks, which is opposite to the behavior of alginate hydrogels. Both observations demonstrate a clear difference in gelation between alginate and EPS. Yet, a complete proof of Felz's hypothesis is lacking so far [59]. In one of their later papers, Felz *et al.* state that glycosaminoglycans (polysaccharides containing hexosamine and uronic acid as repeating units) may be a key component in the stabilization of EPS hydrogels. They are present in the extracellular matrix of mammalian cells and can form gels by binding chemically to proteins, attracting water and ions, and ultimately supporting the extracellular matrix [60].

Unlike Felz, Schambeck *et al.* do provide methods to link the rheological characteristics to the chemical characteristics, specifically the FTIR spectrum. As they assume that EPS gelation is similar to that of alginate, one can examine the mannuronic and guluronic acid peaks to link the chemical behavior of the EPS to the hydrogel rheology. The guluronic acid peak typically sits between 1397 and 1232 cm^{-1}, while the mannuronic acid peaks are situated at 826 and 818 cm^{-1} [182]. The FTIR spectra from the previous chapter are shown in Figure 7.17, with the blue rectangles indicating the regions corresponding to guluronic (G) and mannuronic (M) acid. Zooming in on the two characteristic regions provides additional information on the gelation of the extracted EPS. All FTIR spectra show no peak in the mannuronic acid region, while peaks are only observed at the borders of the guluronic acid region. These are the largest for the salt-adapted granule, followed by the EBPR granule, while those of the two floccular sludges appear the smallest. From this, the salt-adapted granular sludge is expected to show the largest moduli, which is

not observed in Figure 7.16. On the other hand, the two floccular sludges show the smallest moduli, as expected from the FTIR spectra. This shows that assuming the EPS behave like alginate provides some, yet not a complete insight into the gelation and rheological behavior of the EPS. Therefore, other components, such as proteins and lipids, are also expected to play a role in the gelation mechanism of EPS; however, they are not covered in the behavior of alginate. Another weakness of this method is the broadness of the guluronic acid region, showing overlap with peaks from bonds that are not present in alginate, such as the amide III peak at 1303 cm^{-1} and the phosphate peak at 1240 cm^{-1} [185].

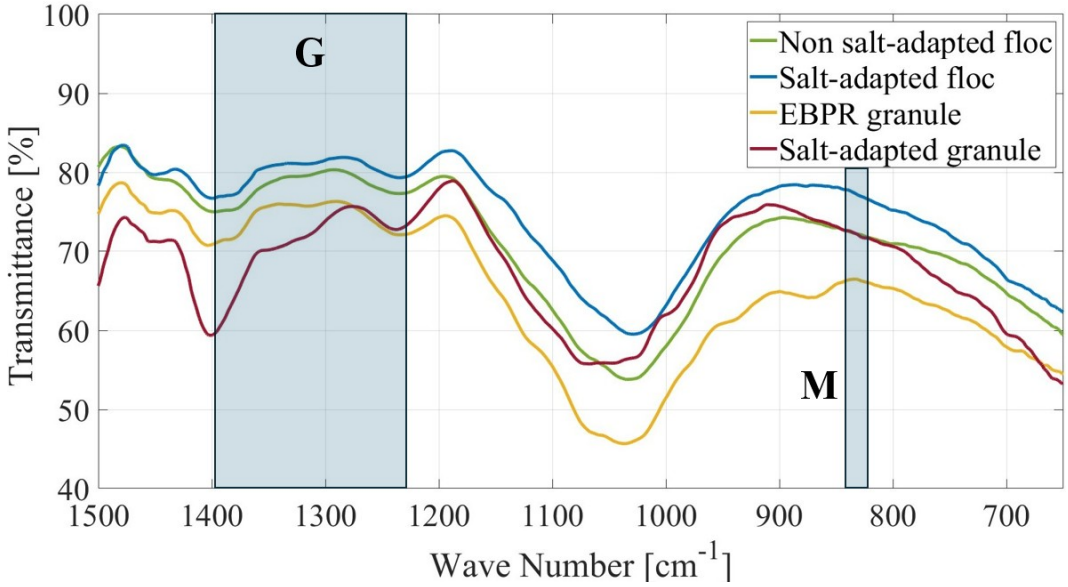

FIGURE 7.17: FTIR spectra of the EPS extracted from the different sludge samples used in this work. The indicated regions are characteristic for guluronic (G) and mannuronic (M) acid [182].

Maddela *et al.* investigated the fouling capacity of EPS from several bacterial strains to see which chemical bonds induced the most fouling in a membrane bioreactor [139]. They examined the gelation ability of the different EPSs and correlated it with specific characteristic wavenumbers corresponding to the gel-inducing chemical bonds, primarily focusing on polysaccharides and proteins. They observed that peaks at 1020 cm^{-1} (uronic acids) and 1250 cm^{-1} (O-acetyl) were present in the FTIR spectra of EPS from highly fouling bacterial strains. Also peaks at 920 cm^{-1} (α-1-4-glycosidic links) and 1550 cm^{-1} (amide II) were linked to membrane fouling. Similar values were also determined by Campo *et al.* as crucial for EPS gelation [25]. Glycosidic links are essential in forming polysaccharides, as they link sugar monomers to form a long chain, which is crucial in the gelation of EPS. The other three peaks were observed to correlate directly with the fouling rate. As these bonds indicate the ability to form gel structures, these four characteristic peaks could be used to link the rheology of EPS hydrogels to their chemical characteristics [139].

A closer look at these regions in the FTIR spectra of the different extracted EPS is provided in Figure 7.18. In the region around 920 cm^{-1}, a slight bend is only visible in the curves of the two granular sludges, while all four spectra show a broad peak around 1020 and 1250 cm^{-1}. The peak at 1020 cm^{-1} appears to be the largest for the EBPR-granule, while those of the other three are similar in size. On the other hand, the peak at 1250 cm^{-1} appears slightly larger for the EPS from the salt-adapted sludge. Finally, all four spectra show a peak around 1550 cm^{-1}, with that of the non salt-adapted floc being the smallest and that of the salt-adapted granule being the largest. Overall, it can be concluded that the salt-adapted granule shows the most prominent peaks at these four wavenumbers, with the EBPR-granule coming in second place, followed by the salt-adapted and non salt-adapted floccular sludge, which comes in last place. From these observations, one would conclude that the greatest moduli should be observed for the salt-adapted granular sludge, which is not the case.

The main drawback of the study by Maddela *et al.* is that it only identifies the components with their characteristic peak positions without providing the mechanism of their gelation, which is currently unknown [139]. Hence, it is clear that the gelation of hydrogels cannot solely be explained by the characteristic peaks of four bonds known to produce gelating EPS. As Felz mentioned, EPS gelation is expected to be more complex than ionic crosslinks alone [59]. Hydrogen bonds or entanglements between the different EPS could be responsible for these rheological characteristics. However, this must be confirmed in further research.

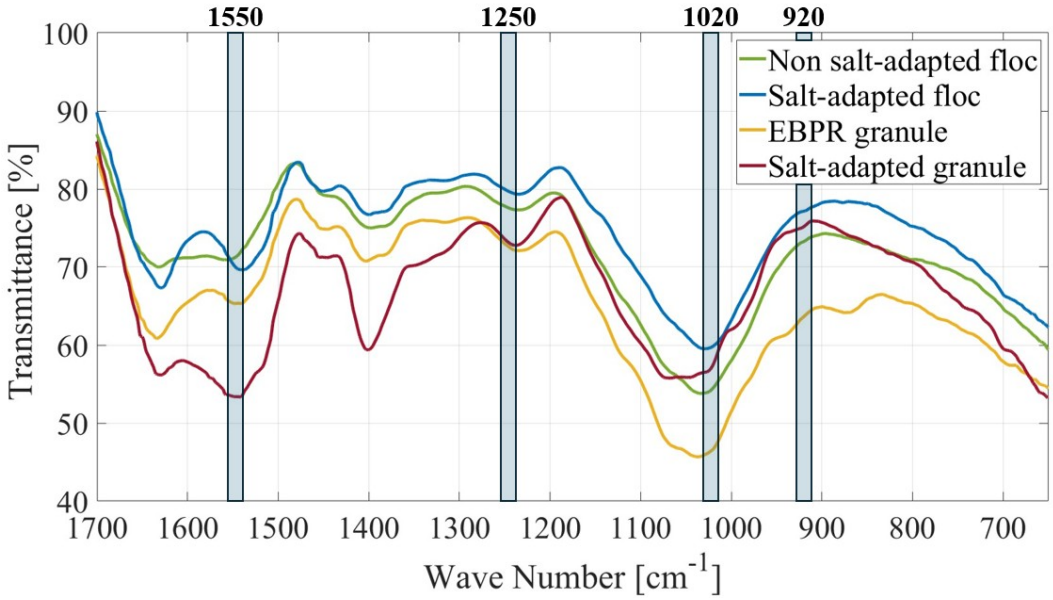

FIGURE 7.18: FTIR spectra of the EPS extracted from the different sludge samples used in this work. The indicated regions are characteristic for guluronic (G) and mannuronic (M) acid [182].

Contradicting the rheological properties observed in Figure 7.16, Felz and Maddela *et al.* conclude that hydrogels made of EPS from the salt-adapted granule should yield the highest moduli. Also the later work of Felz, in which he states that glycosaminoglycans are the biomolecules contributing the most to granule stabilization, would lead to this conclusion [60]. This is because the characteristic wavenumbers of the glycosaminoglycans overlap with those discussed by Maddela and Felz, as the peak at 1020 cm^{-1} corresponds to the uronic acids [139], while the peaks at 1550 (N−H) and 1050 cm^{-1} are characteristic for the hexosamines present in the glycosaminoglycans [185].

In this regard, it should be noted that due to the limited amount of material available, only one hydrogel could be prepared from each type of EPS, resulting in rheological measurements based on a single hydrogel in this work. Repeating the experiments to verify the similarity of the rheological is therefore advisable, especially considering the numerous factors contributing to variability in the EPS composition. The moduli obtained in this work are also relatively low due to the low EPS concentration used for the hydrogel formation. More concentrated EPS hydrogel bases would result in hydrogels with greater moduli and crosslink density [134], making the differences in rheological characteristics more pronounced. Hence, repeating the experiments and using higher EPS concentrations in the hydrogel base is recommended to ensure that the obtained rheological data truly represents the gelation behavior of the EPS.

As a final attempt to link the rheological properties of the EPS hydrogel to their chemical characteristics, the FTIR, Raman and NMR spectra of the four different sludges are considered, along with the relative areas presented in Table 7.1. At first sight, Table 7.1 does not show a clear pattern in which the values increase or decrease according to the order EBPR-granule, salt-adapted granule, floccular sludges, which is the order of decreasing moduli in Figure 7.16. Both granular sludges have a smaller polysaccharide-to-protein ratio than the floccular sludges. A higher protein content might, therefore, positively affect the rheological properties. On the other hand, this should result in the hydrogel made of EPS from the salt-adapted granule having the highest moduli due to their smallest polysaccharide-to-protein ratio, which is not observed. From the observation that the two floccular sludges have similar moduli, one could conclude that the polysaccharides are the most significant factor contributing to the rheological characteristics of EPS hydrogels, with lower polysaccharide content resulting in higher moduli. However, this does not correspond to the observations made for the two granular sludges. No trend is observed for the fatty acids either, such that no conclusions can be drawn from the FTIR spectra.

No conclusions can be drawn from the Raman spectra of the different sludges, shown in Figure 7.19, either, as the four spectra essentially overlap in the region above 1050 cm^{-1}, while the peaks below this value appear almost identical. All four sludges exhibit peaks around 490, 600, 800 and 1050 cm^{-1}, indicating the presence of some typical bonds found in EPS, as listed in Table C.2 in Appendix C.1.2.

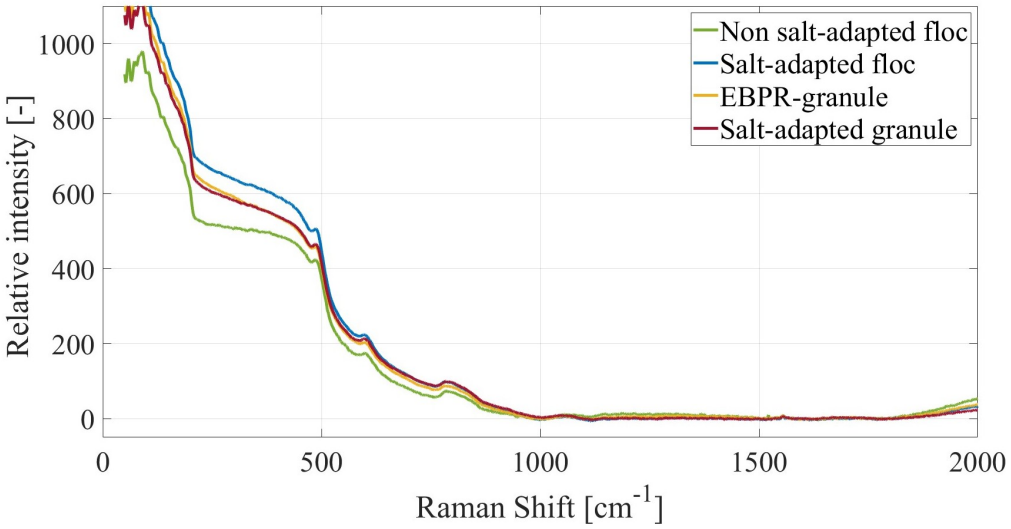

FIGURE 7.19: Raman spectra of the EPS extracted from the different sludge samples.

The ^{1}H-NMR spectra, given in Figures 6.11, 6.13, 6.14, and 6.16, show significant differences between the different spectra, ranging from the NMR spectrum of the EPS from the EBPR granule, which only exhibits very slight peaks to that of the salt-adapted granular sludge having much more precise and narrow peaks. This spectrum also shows peaks at NMR shifts greater than 6.5 ppm, which are not present in the other three spectra. In general, each spectrum has its distinctive features and shape, such that the spectra contain too many differences to draw valuable conclusions.

7.4 Conclusions

EPS extracted from four different sludge samples were compared to two model systems: sodium alginate and κ-carrageenan, both polysaccharides.

NMR, FTIR and Raman spectroscopy were performed on both model systems. The Raman and FTIR spectra exhibited peaks at locations consistent with those reported in the literature, indicating the presence of distinct functional groups in the two model system biopolymers. The most significant differences between the spectra of the two polysaccharides were the FTIR peak at 842 cm^{-1} in the κ-carrageenan spectrum, caused by the sulphate groups and the Raman peaks at 1305 and 1414 cm^{-1} in the sodium alginate spectrum, indicating that carboxylate groups are only present in sodium alginate, which are both confirmed by the Lewis-structures of the two polysaccharides.

Hydrogels of the two model systems were made under different conditions. Increasing the salt concentration in the crosslinking solution and the polysaccharide concentration in the hydrogel base leads to increased moduli of alginate hydrogels,

as the crosslinking density increases. For the κ-carrageenan, a synergistic effect is observed between potassium and calcium ions, as hydrogels display higher moduli when combining both ions.

In the next step, the gelation mechanisms of the two model systems' hydrogels were explained. Alginate hydrogels are formed according to the egg-box model, in which divalent ions (like Ca^{2+}) are included between the guluronic acid blocks of the alginate molecules. This principle does not work with monovalent ions like K^+.
On the other hand, the gelation of κ-carrageenan is a two-step process that requires both cooling and the presence of cations. These cations can be both monovalent and multivalent. During cooling, the κ-carrageenan molecules are known to form helix structures, with the cations creating physical crosslinks by inducing the aggregation of these coils. Both K^+ and Ca^{2+} can induce this aggregation. Conversely, only K^+ has the ability to form superstrands in the hydrogel, further enhancing its stiffness. This results in the aforementioned synergistic effect of K^+ and Ca^{2+} on the moduli of κ-carrageenan hydrogels.

Next, the hydrogel formation process of the extracted EPS was described. Different authors have varying views on this issue, making the discussion of the gelation even more complex. It is expected that the gelation of EPS hydrogels is caused not only by ionic crosslinks but also by other intermolecular interactions such as hydrogen bonds, entanglements, and others. Three authors provided FTIR peaks corresponding to chemical bonds associated with the EPS gelation behavior. However, when comparing the peaks of the different sludges to the proposed models, no conclusive results could be obtained, confirming the complexity of the EPS gelation process. Comparing the chemical tests of the different extracted EPS to those of the two model systems did not yield new insights either.

Chapter 8

Conclusions and future prospects

To finalize this work, an overview of the most important conclusions is provided, followed by future prospects that contain recommendations for future research.

8.1 Conclusions

High-quality water is a scarce resource that must be preserved at all costs, requiring the treatment of wastewater streams from various industrial processes and municipal sources prior to their discharge into the environment. The key step in this treatment is often biological wastewater treatment, in which sludge is added to remove carbon-, nitrogen- and phosphorus-based pollutants from the wastewater. This process can be performed under both aerobic and anaerobic conditions, while the sludge morphology can also vary between different wastewater treatment plants. In this regard, floccular and granular sludge are distinguished. Independent of the type of sludge or conditions, excess waste sludge is always produced, with only municipal wastewater treatment producing up to 45 million tons of excess sludge per year. Until now, no commercial use was found for this waste stream, as it is mostly incinerated or disposed of. Therefore, a possible application for this sludge must be considered.

Waste sludge consists of different components, of which the extracellular polymeric substances (EPS) show the highest potential for valorization. EPS are a mixture of different biological polymers, mainly proteins and polysaccharides. Their composition depends on numerous factors, such as the components in the influent wastewater stream, time, etc. Therefore, it is important to characterize the chemical composition of extracted EPS, as most applications have specific requirements for the EPS used. The EPS cannot be used directly either, as they are contained inside the waste sludge, such that extraction is the first step in any application.

Literature has not yet proposed a standardized extraction protocol. Multiple authors have attempted various extraction protocols, each obtaining different results. Hence, the EPS composition depends on the extraction method used, which was also concluded in this work. For this reason, it is of utmost importance to standardize the

extraction protocol when studying EPS. A valuable extraction method has a high yield of the extracted EPS, results in an EPS sample representative of the EPS in the sludge, obtains a pure EPS fraction, minimizes its inorganic content and avoids cell lysis. This last criterion is important in the study of EPS, as the contamination of EPS with intracellular components is undesired. For this reason, four different extraction protocols are performed on pellets of *Aspergillus oryzae*, used as a model system for (salt-adapted) sludge aggregates. The four extraction protocols used in this work include extraction using (1) heat and sodium carbonate, (2) NaCl, (3) urea and (4) urea and NaCl. A comparison of these four methods revealed that the NaCl extraction was more favorable, while the heat and sodium carbonate extraction generated the highest amount of cell lysis. However, because the heat and sodium carbonate method has been used most frequently in the literature, this method was selected as the one used for the remaining extractions. However, it is important to note that the term extracellular polymeric substances (EPS) is not 100 % correct when using this extraction protocol, as the EPS likely also contains some intracellular molecules. Hence, the extracted material is more accurately referred to as EPS-based material.

To determine the usability of the extracted EPS for specific applications, they must be chemically characterized. This characterization can be performed at different levels of complexity, ranging from identifying specific types of molecules to determining the exact composition of molecules. More general tests include hydrophobicity tests and colorimetric assays, while more complex tests include 3D-EEM, Raman, FTIR and NMR spectroscopy. The EPS composition is expected to be very complex, containing biomolecules such as proteins, polysaccharides, lipids, DNA, uronic acids, and humic acids, making their characterization more challenging. Some of these molecules interfere with each other during characterization, further complicating this process. Raman, FTIR, and NMR can be used to determine the EPS's molecular fingerprints, which contribute to the understanding of their composition. Hence, these three characterization techniques were applied to EPS extracted from four different sludge sources. Both floccular and granular sludges, as well as both salt-adapted and non salt-adapted sludges were covered in this work. Their fingerprints were compared to each other and to the EPS extracted from three pure cultures: *Azoarcus communis*, *Dietzia maris*, and *Aspergillus oryzae*. For all sources of EPS, the FTIR spectra appeared to be the primary source of information, as most studies in the literature also used this technique to characterize EPS. Using these spectra, ratios of proteins, polysaccharides and fatty acids could be determined, which were then compared to the literature. NMR and Raman spectroscopy, as well as thermogravimetric analysis, were employed to confirm the observations made using FTIR spectroscopy. It was concluded that: (1) EPS are strain-dependent, as the EPS of *Azoarcus communis* and *Dietzia maris* contained different biomolecules at different concentrations, (2) EPS from sludge samples display a larger polysaccharide-to-protein ratio compared to the pure cultures, (3) salt adaptation results in greater polysaccharide-to-protein ratios, as the salting in of the proteins induces an increase in their solubility (4) salt-adapted granular sludge has a higher protein content than salt-adapted floccular

sludge and (5) the EPS produced by an aerobic salt-adapted fungus are less complex than that of anaerobic granular salt-adapted sludge, due to the higher microbial complexity of the sludge granule. Hence, the composition of the extracted EPS clearly depends on the sludge source.

In the final step, these characterization results can be used for various potential applications of the EPS. These range from replacing fossil-fuel-based polymers, taking advantage of their polymeric character of EPS, to using them as hydrogels, benefiting from their gelation mechanisms. As the EPS composition varies over time and depends on many external conditions, understanding the mechanisms of their gelation is crucial, as well as the effects of changes in EPS composition on these mechanisms. Here, a two-faceted approach can be used: (1) looking directly at the results of the chemical tests and (2) linking the chemical and rheological behavior of the EPS to those of two model systems, sodium alginate and κ-carrageenan. Both model systems exhibit distinct gelation mechanisms, using different chemical bonds that interact with specific cations to form physical crosslinks. Rheological measurements were performed on hydrogels made of these model systems at different polysaccharide concentrations in the hydrogel base and salt concentrations in the crosslinker solution. These results were linked to the gelation mechanisms of the two model systems. Next, an attempt was made to compare the chemical characteristics and rheological observations of hydrogels made of EPS from different sources with the gelling behavior of EPS. This gelation was expected to be more complex than that of the model systems, as the EPS gelation was assumed to be dependent not only on ionic crosslinking but also on other intermolecular effects, such as hydrogen bonds. This was examined by comparing the rheological and chemical characteristics of the EPS to two theories proposed in the literature. No direct trends were observed between the chemical and rheological characteristics of the EPS, confirming the proposed hypothesis of a more complex gelation mechanism.

8.2 Future prospects

Extracellular polymeric substances (EPS) clearly show potential for application in various industrial fields as a new biological resource. However, further steps are required to unlock their full potential and improve their understanding.

Firstly, a standardized extraction method must be established, as the composition of the extracted EPS depends on the extraction protocol. In this work, four extraction protocols have been compared, which is only a small subset of all the extraction protocols currently explained and studied in the literature. A more profound systematic comparison of current extraction protocols results in a firmer theoretical basis for standardizing the extraction method. Different fields of application might yield different optimal extraction protocols, as the criteria for optimal extraction depend on the application. Low amounts of cell lysis are more important for fundamental studies on EPS, whereas more application-oriented criteria, like a high yield and a low price of the extraction, must be considered for industrial applications.

From Chapter 6, it was clear that the current chemical characterization techniques are insufficient to characterize the EPS composition completely. Although Raman spectroscopy should be suitable for characterizing different chemical bonds in the extracted EPS, it was observed that the resolution was often insufficient to observe significant differences in EPS content. In this regard, FTIR spectroscopy showed more promising results, as it is able to distinguish between different chemical bonds in the extracted EPS more effectively, allowing for the identification of specific types of biomolecules and their respective ratios. However, this method is also limited due to the complexity of EPS, resulting in the (partial) overlap of some peaks. On the other hand, different biomolecules (i.e., two different proteins) may contain the same type of bonds, resulting in the limited characterization ability of FTIR. In this regard, NMR shows greater potential, as it can distinguish between hydrogen atoms based on their electron environment. This could enable differentiation to the molecular level. However, also in this case, the complex and unknown composition of EPS increases the difficulty of identifying different EPS components from an NMR spectrum. This problem can be resolved as follows. By experimentally determining the NMR spectra of some pure biopolymers, a larger spectral database can be established, acting as a reference for an EPS sample of unknown composition. By first analyzing the extracted EPS using proteomics and glycomics, some candidate biopolymers could be selected, of which the NMR spectra can then be compared to the spectrum of the extracted EPS to draw more definitive conclusions.

Chapter 7 demonstrated one of the many potential applications of EPS extracted from different sludges as hydrogels. Other applications include using the EPS as a hydrophobic coating for paper, or to make objects more fire-retardant. However, for most of them, the usability of EPS has only been proven on a lab scale. To scale up these processes, some further research is required on topics like: (1) how to transport sludge from the wastewater treatment plant to the facility where the EPS

are extracted, (2) how to upscale the extraction protocol to an industrial level[1], (3) what is the shelf-life of industrial sludge, how long can it be stored before the EPS are extracted, (4) what is the shelf-life of the extracted EPS, before their application, (5) do the EPS degrade over time when used in specific applications, (6) are there limitations to the use of the EPS, like regulations. These parameters are important as EPS essentially arises from microbiological material, which can form a health or biological hazard. Even though the usability of EPS has been demonstrated at a proof-of-concept level, upgrading to a full industrial scale still requires some technical information, to which little attention has been paid yet.

[1]The scalability of the extraction protocol depends of course on the required chemical species. When examining the four extraction protocols, discussed in Section 5, the heat and sodium carbonate extraction shows the most potential for upscaling due to the low amount of Na_2CO_3 required to perform it, compared to the other three extraction protocols, making it more economically viable. The low amount of Na_2CO_3 also results in the EPS being less contaminated, reducing the purification requirements. It should be noted as well that the composition of the extracted EPS is expected to differ after scaling up due to the dependence of the EPS composition on the extraction protocol's parameters. This should be verified experimentally as well.

Appendices

Appendix A

Materials and methods: Additional figures

A.1 Hydrogel molds: Technical drawings

A.1.1 Model system hydrogels

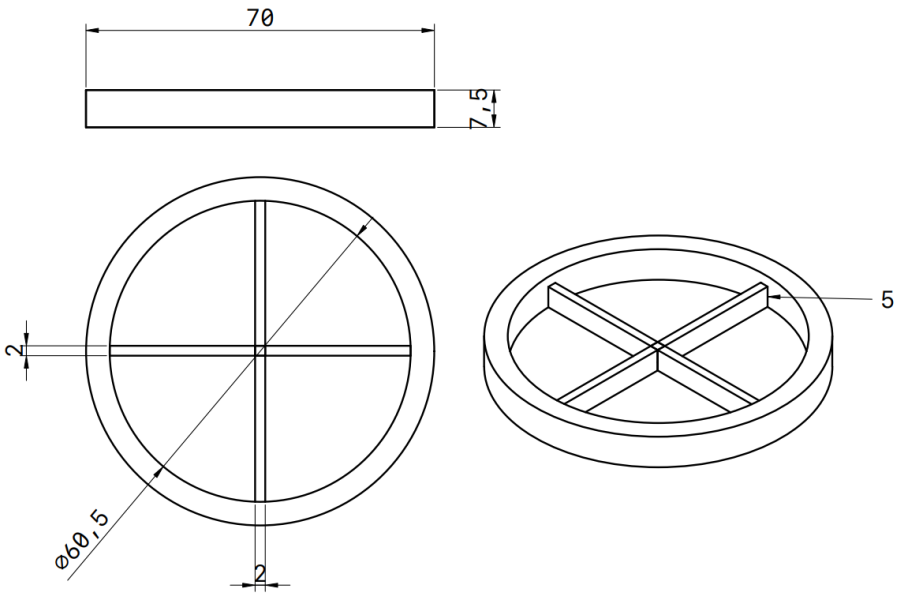

FIGURE A.1: Technical drawing of the cap of the 3D-printed mold, in which the hydrogels of the model systems are made. The dimensions are given in mm.

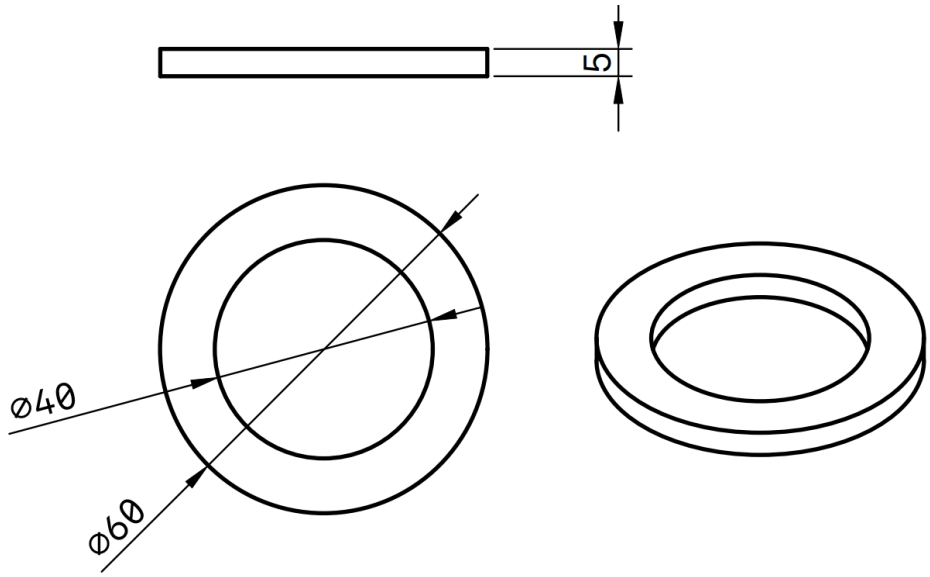

Figure A.2: Technical drawing of the cylinder of the 3D-printed mold, in which the hydrogels of the model systems are made. The dimensions are given in mm.

A.1.2 EPS hydrogels

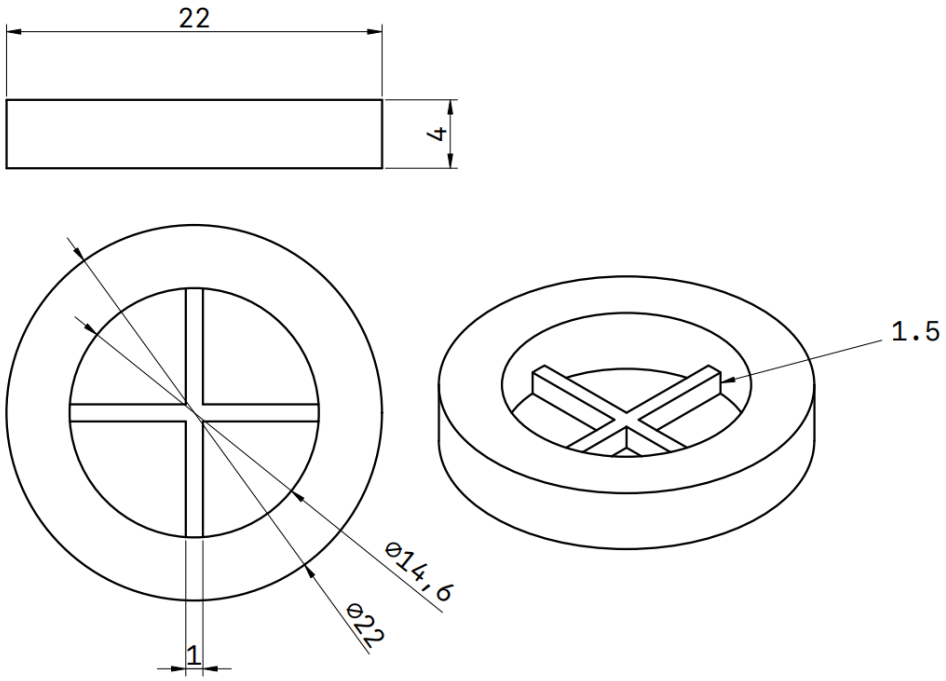

Figure A.3: Technical drawing of the cap of the 3D-printed mold, in which the hydrogels of EPS are made. The dimensions are given in mm.

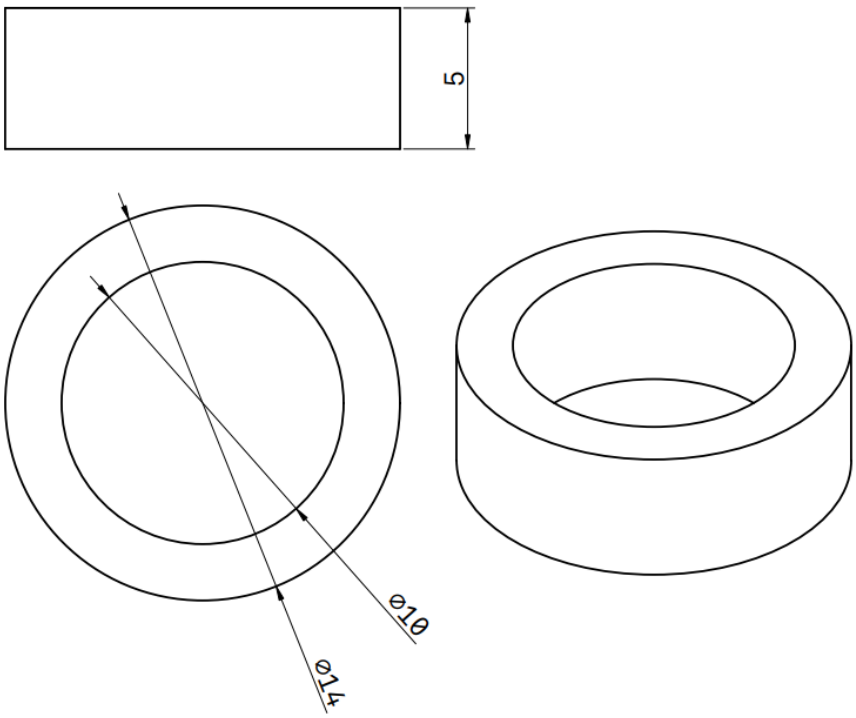

FIGURE A.4: Technical drawing of the cylinder of the 3D-printed mold, in which the hydrogels of EPS are made. The dimensions are given in mm.

A.2 Amplitude sweeps hydrogels

It is important that the frequency sweeps, discussed in this work, are all measured in the linear viscoelastic regime (LVER) of the material. In this region, the material response to a sinusoidal deformation is also a sinusoidal wave, with a different amplitude and phase shift. The border of the LVER can be determined using the 5 % rule, that states that the border of the LVER is located at the oscillation strain, where the moduli deviate 5 % or more from the values at low strain (constant moduli should be observed at the lowest oscillation strains). During a frequency sweep, the applied oscillation must be selected such that it sits in the LVER of the material. Hence, amplitude sweeps must be performed for the different hydrogels made.

A.2.1 Model systems' hydrogels

For the model systems' hydrogel, the oscillation strain during the frequency sweeps was set to 0.01 %. Figures A.5 and A.6 show that this strain clearly falls in the LVER of the material, as both figures show constant moduli at an oscillation strain of 0.01 %. Using the aforementioned 5 % rule, the border of the LVER is determined to be 0.64 % for both alginate and κ-carrageenan hydrogels, which is significantly larger than the strain of 0.01 % used during the frequency sweeps.

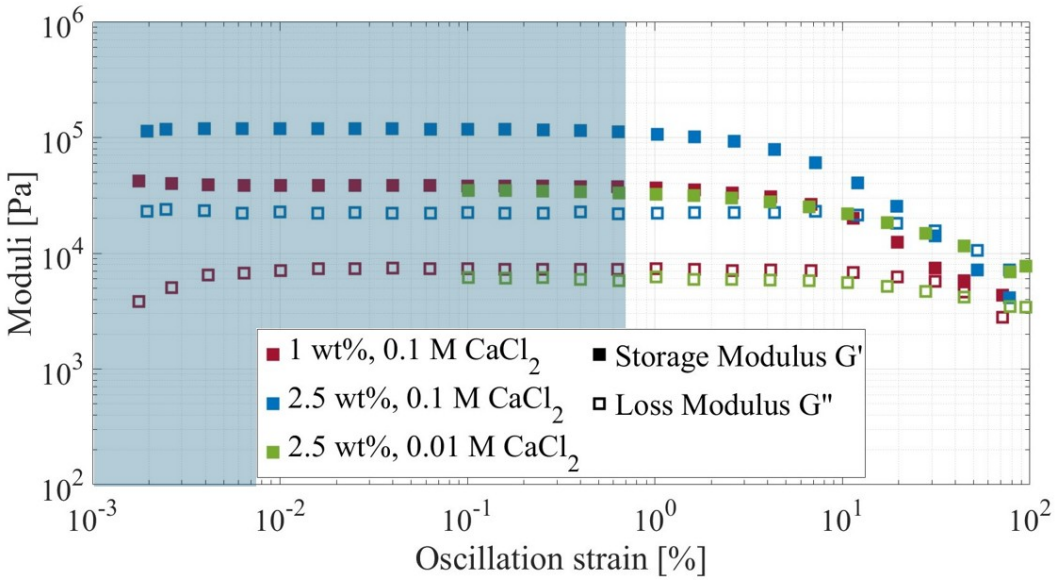

Figure A.5: Amplitude sweep of the different hydrogels made using sodium alginate. The amplitude sweep uses an angular frequency of 1 $\frac{\text{rad}}{\text{s}}$ and increasing oscillation strain. The light-blue box indicates the linear visco-elastic regime (LVER).

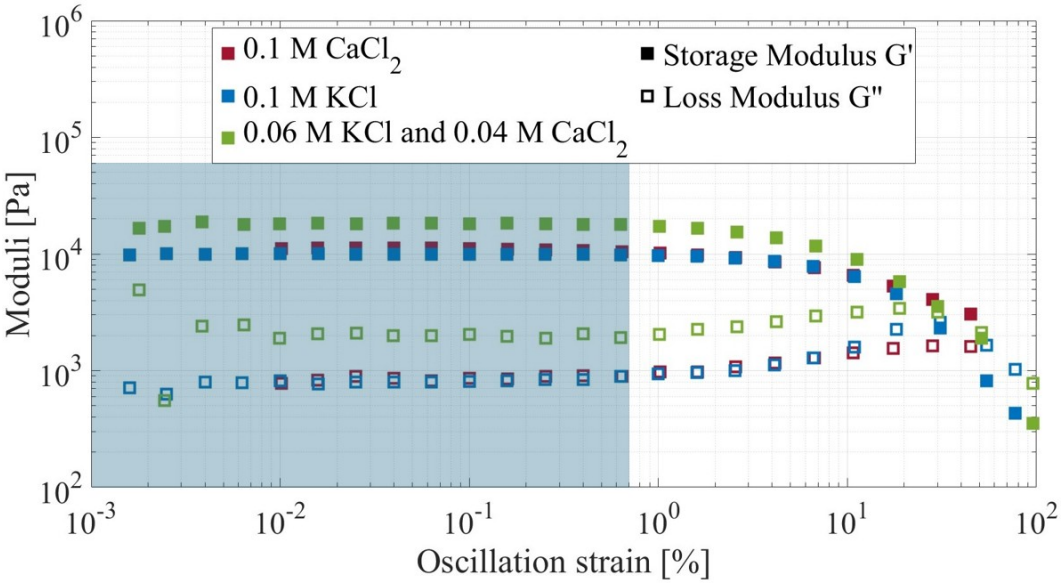

Figure A.6: Amplitude sweep of the different hydrogels made using κ-carrageenan. The amplitude sweep uses an angular frequency of 1 $\frac{\text{rad}}{\text{s}}$ and increasing oscillation strain. The light-blue box indicates the linear visco-elastic regime (LVER).

A.2.2 EPS-based hydrogels

For the EPS-based hydrogels, the oscillation strain was set to 5 %, as lower values led to a poor signal-to-noise ratio. The amplitude sweep, given in Figure A.7 shows that only the hydrogel made of EPS from the salt-adapted floc shows more or less constant moduli at oscillation strains between 1 and 10 %. For the other two hydrogels, 5 % sits just outside the LVER, as its border is located around 4 %. However, it should be noted that the definition of the LVER is more empirical, rather than backed up by theoretical concepts. If ,for example, a 10 % rule would have been used instead of the 5 % rule, the oscillation strain of 5 % would have been located inside the LVER. Hence, the frequency sweeps at an oscillation strain of 5 % are still acceptable.

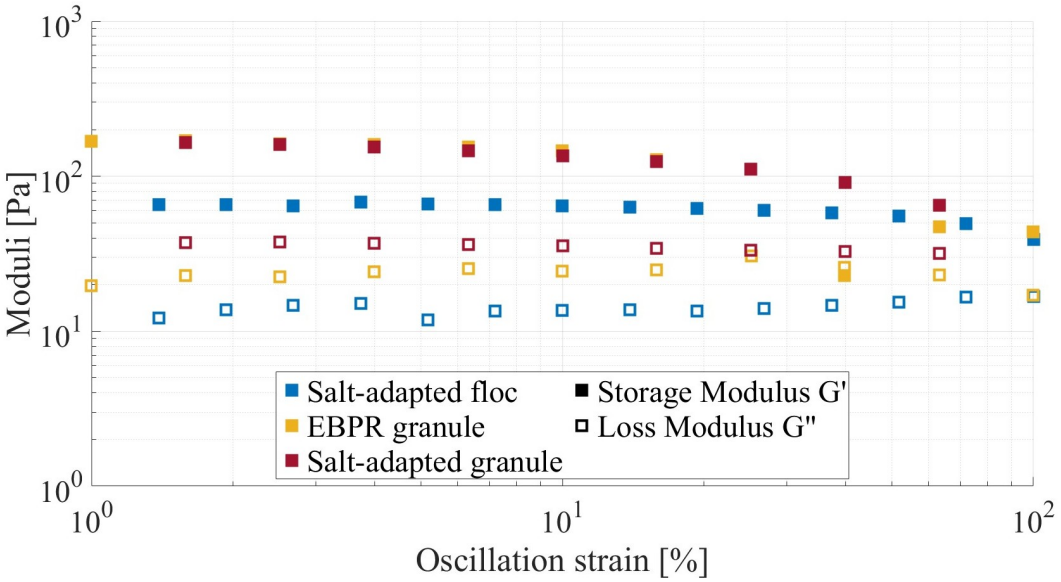

FIGURE A.7: Amplitude sweep of the different EPS-based hydrogels. The amplitude sweep uses an angular frequency of 10 $\frac{\text{rad}}{\text{s}}$ and increasing oscillation strain.

Appendix B

EPS extraction: Additional figures and calculations

B.1 Determination total and volatile solids

Table B.1 shows the numerical values of parameters needed to determine the TS and VS values per gram of wet biomass for the *Aspergillus oryzae*. For this determination, two samples are taken to determine it. The total solids of the samples is equal to the weight of the sample after drying at 105℃ for two hours. The volatile solids equals the difference between the total solids and the mass of the sample after burning the sample at 550℃ for two hours. It includes the organic components present in the initial sample.

Table B.1: Determination of the amount of volatile solids per gram of wet pellets of *Aspergillus oryzae*.

	Sample 1	Sample 2
Total wet mass [mg]	472.98	408.06
Total dried mass (after 105℃) [mg]	14.63	13.75
Total burnt mass (after 550℃) [mg]	6.14	5.14
Total solids [mg]	14.63	13.75
Volatile solids [mg]	8.49	8.61
Volatile solids per gram biomass [mg/g]	17.95	21.1

B.2 NMR spectra of EPS of *Aspergillus oryzae*, extracted via different extraction methods

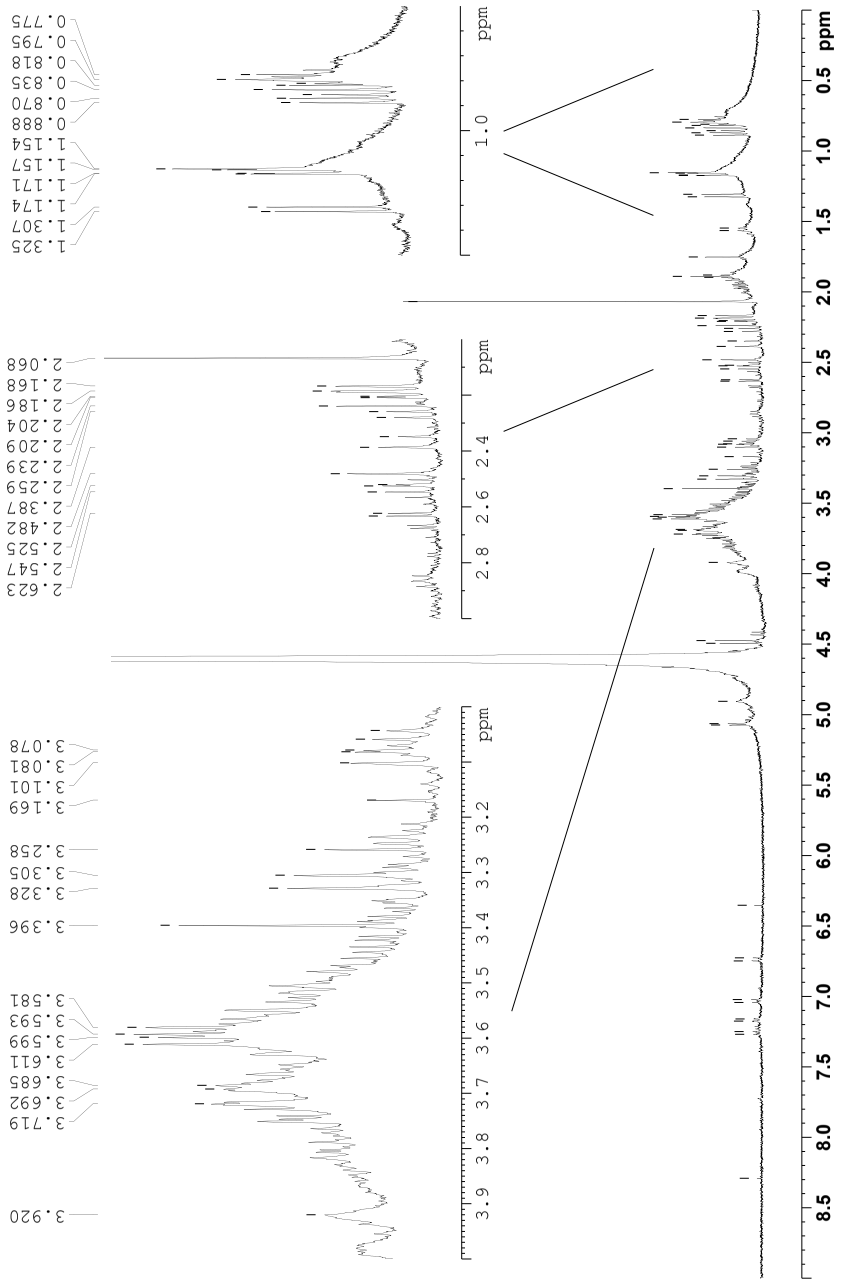

Figure B.1: ^{1}H NMR-spectrum of EPS extracted from *Aspergillus oryzae*, using sodium chloride. The spectrum is made using the TopSpin software package (Bruker, United States of America).

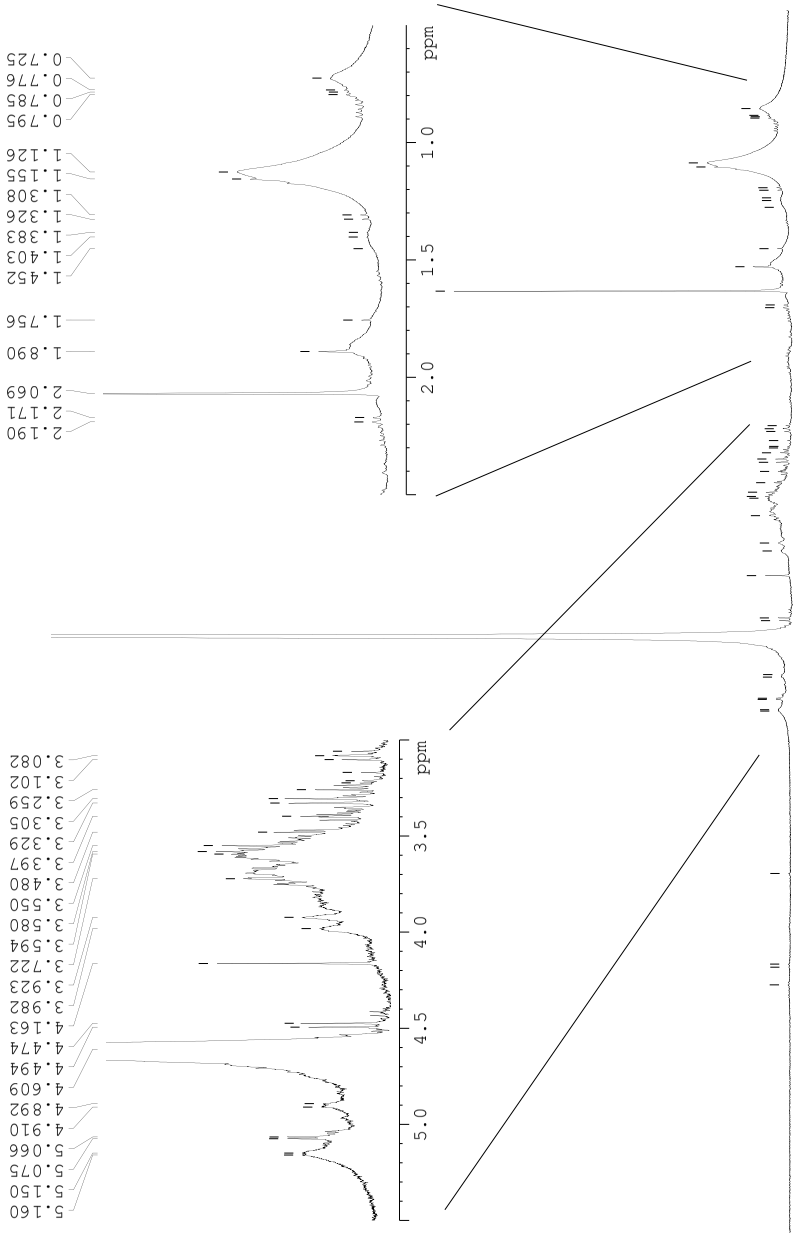

FIGURE B.2: ^{1}H NMR-spectrum of EPS extracted from *Aspergillus oryzae*, using urea and sodium chloride. The spectrum is made using the TopSpin software package (Bruker, United States of America).

B.3 pH calculation of heat and sodium carbonate extraction solution

This section discusses the determination of the pH of the solution, used in the heat and sodium carbonate extraction. The concentration of sodium carbonate in this solution is equal to $0.5\frac{\text{g}}{\text{L}}$. This has to be converted to molarity first:

$$0.5\ \frac{g}{L} \cdot 0.009434\ \frac{mol}{g} = 0.00472\ \frac{mol}{L} = 0.00472\ M \tag{B.1}$$

With this concentration, the pH can be determined using the ion product of water, and the base constant K_b of the carbonate ion. Assuming all sodium carbonate dissolves in the water, the initial concentration of carbonate in water is equal to 0.00742 M. Assuming the ion product of water K_w at 80 °C sits around $2 \cdot 10^{-13}$ [96] and assuming the acid constant K_a of HCO_3^- is approximately equal to that at 25 °C ($5.55 \cdot 10^{-11}$), the following expression is obtained for K_b:

$$K_b = \frac{K_w}{K_a} = \frac{2 \cdot 10^{-13}}{5.55 \cdot 10^{-11}} = 0.00360 \tag{B.2}$$

This constant is the equilibrium constant of the following chemical reaction:

$$CO_3^{2-} + H_2O <=> HCO_3^- + OH^- \tag{B.3}$$

Assuming that the reaction reaches its equilibrium, the concentration of OH^- ($[OH^-]$) can be determined by determining the conversion of the chemical reaction. When creating a conversion table for the chemical reaction and assuming the liquid volume stays constant during the reaction, the equilibrium $[OH^-]$, which is set equal to x, can be determined by solving the equation:

$$K_b = 0.00360 = \frac{x^2}{0.00472 - x} \tag{B.4}$$

Solving this equation for x, results in x being equal to 0.002698 M, such that the concentration of OH^- also equals this value. Now, the H^+ concentration can be determined via the value of K_w at 80 °C:

$$[H^+] = \frac{2 \cdot 10^{-13}}{0.002698} = 7.41 \cdot 10^{-11} \tag{B.5}$$

Applying the definition of the pH, results in:

$$pH = -log([H^+]) = -log(7.41 \cdot 10^{-11}) = 10.13 \tag{B.6}$$

This results in the pH being approximately 10.13. This appears to be a good approximation for the reality, as the pH of the solution used in this extraction was determined to be 10.01 ± 0.09 by Le *et al.* [111].

Appendix C

EPS characterisation: Additional figures and tables

C.1 Characteristic tables

C.1.1 FTIR Spectrometry

Table C.1: Characteristic wavenumber of different functional groups in Fourier Transform Infrared Spectroscopy. The table is split into 4 regions corresponding to a type of biological macromolecule. Taken from Schmitt and Flemming (1998) [185].

Region	Wavenumber (cm^{-1})	Functional group
Fatty acid region	3400	OH of water
	2956	CH_3 asym. stretch
	2920	CH_2 asym. stretch
	2870	CH_3 sym. stretch
	2850	CH_2 sym. stretch
Protein region	1745/1735	>C=O stretch, Ester, fatty acids
	1705	>C=O stretch, Ester, carboxylic groups
	1652-1648	Amide I, (C=O) different conformation
	1550-1548	Amide II, N-H, C-N and structure of proteins
	1460-1454	C-H bend. from CH_2
Mixed region	1400-1398	C-O bend. from carboxylate ions
	1303	Amide III (C-N)
	1240	P=O from phosphate
	1222	P-O
	1114	C-O-P, P-O-P
Polysaccharide region	1085	Ring vibrations
	1052	C-O, C-O-C from polysaccharides

C.1.2 Raman Spectrometry

Table C.2 shows the characteristic frequencies of chemical bonds often present in EPS and assigns them to possible chemical bonds. In this table, the term carbohydrates is used. Carbohydrates is the collective term for monosaccharides, oligosaccharides, and polysaccharides, with the monosaccharides being the monomeric units to build up the other two. Oligosaccharides contain up to 10 monosaccharide monomers, polysaccharides contain more than 10 monosaccharides [137].

TABLE C.2: Characteristic frequencies of different functional groups in Raman Spectroscopy. Each functional group is also linked to a certain component of EPS. Adapted from Elleuch *et al.* (2025) [55].

Frequency (cm^{-1})	Functional group	Macromolecules containing it
408-495	PO_4	Carbohydrates
603-695	C-S stretching and C-C twisting / SO_4	Carbohydrates / Proteins
1000-1010	C-C aromatic ring stretching (Phe)	Proteins
1030-1130	C-N stretching or symmetric dioxy stretching of phosphate backbone	Carbohydrates / Proteins / Nucleic acids
1314-1345	δ(CH) / amide III	Carbohydrates / Proteins
~2600	SH	
2800-3000	CH stretching	Lipids / Proteins
3100-3500	H_2O / OH^-	

C.1.3 NMR tables

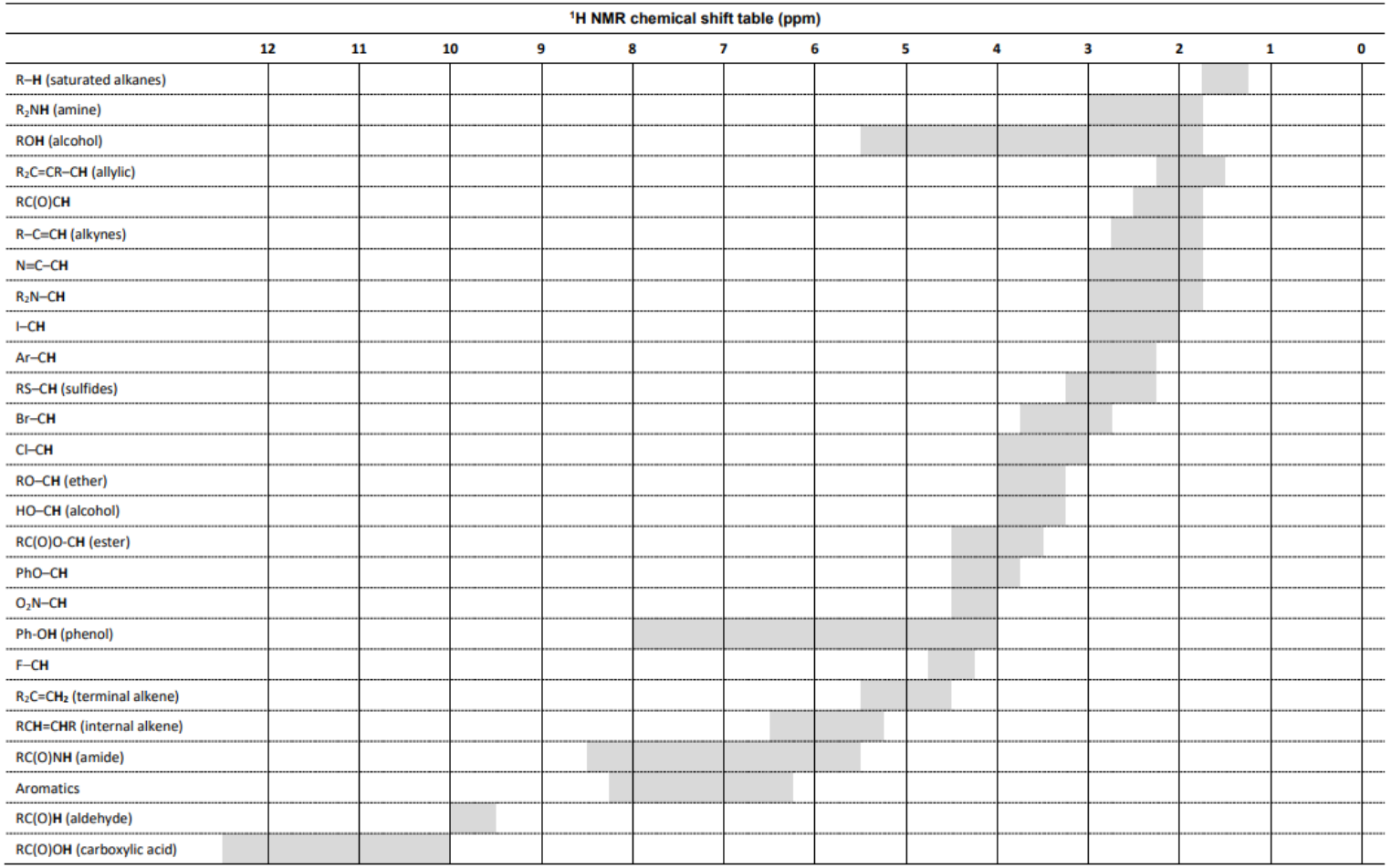

FIGURE C.1: Common chemical bonds with their respective chemical shift (in ppm) in a ^{1}H NMR-spectrum. Taken from Steurs (2024) [202].

Appendix D

EPS comparison: Additional figures

D.1 FTIR spectra

D.1.1 FTIR spectra EPS from pure cultures

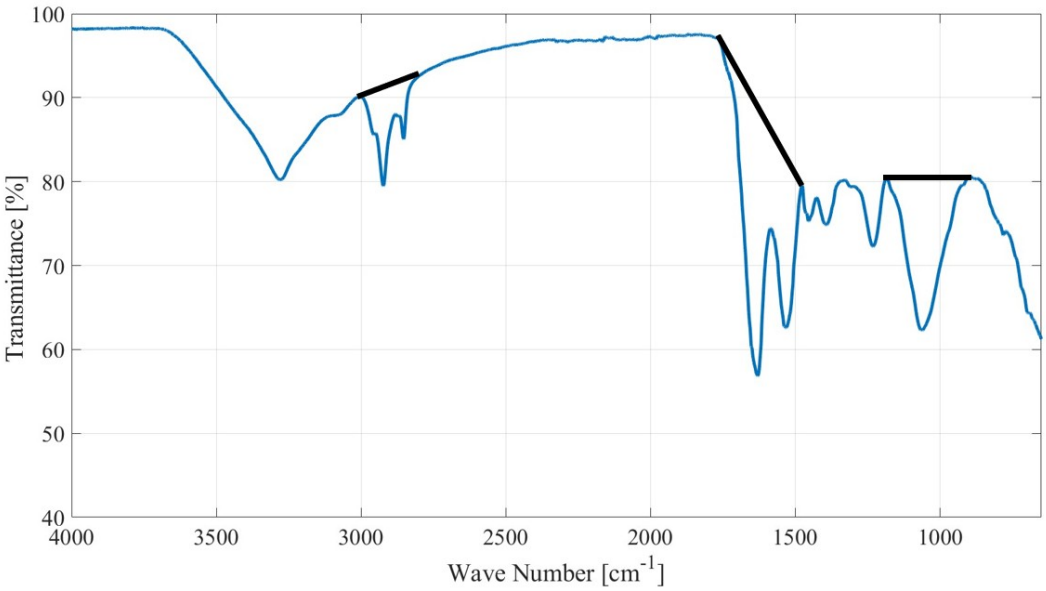

FIGURE D.1: FTIR spectrum of EPS extracted from *Azoarcus communis*, with the black lines representing the baselines used for the numerical determination of the intensity of peaks, representing a different types of biomolecules.

D.2 Raman spectra

D.2.1 Raman spectra EPS from sludges

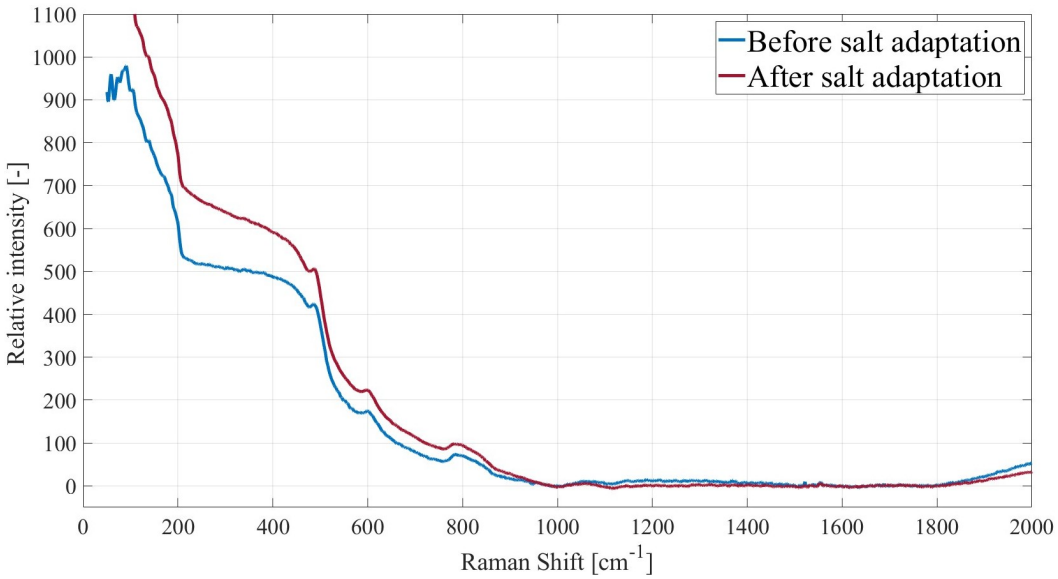

FIGURE D.2: Raman spectrum of EPS extracted from floccular sludge, before and after adaptation to to 5 $\frac{g}{L}$ Na^+, extracted using the heat and sodium carbonate extraction method

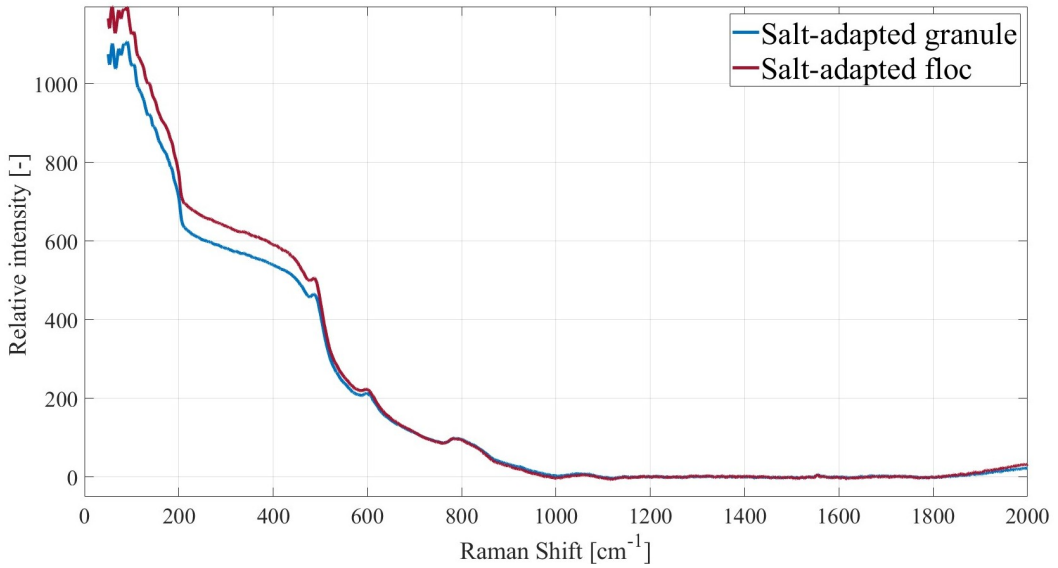

FIGURE D.3: Raman spectrum of EPS extracted from salt-adapted granular and salt-adapted floccular sludge, using the heat and sodium carbonate extraction method

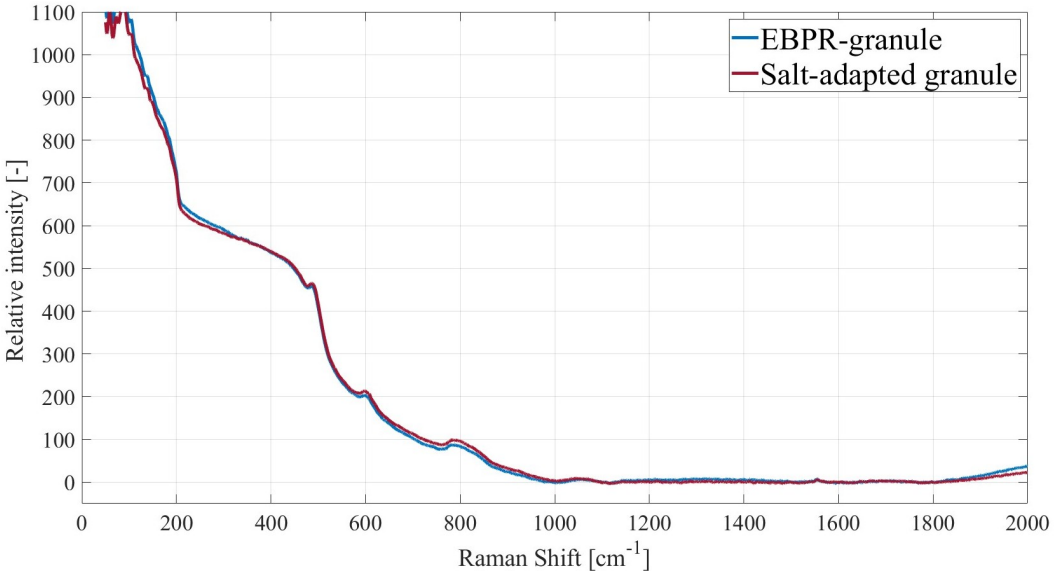

FIGURE D.4: Raman spectrum of EPS extracted from salt-adapted and EBPR granular sludge, obtained using the heat and sodium carbonate extraction method

D.3 Thermogravimetric analyses of the EPS from industrial sludges

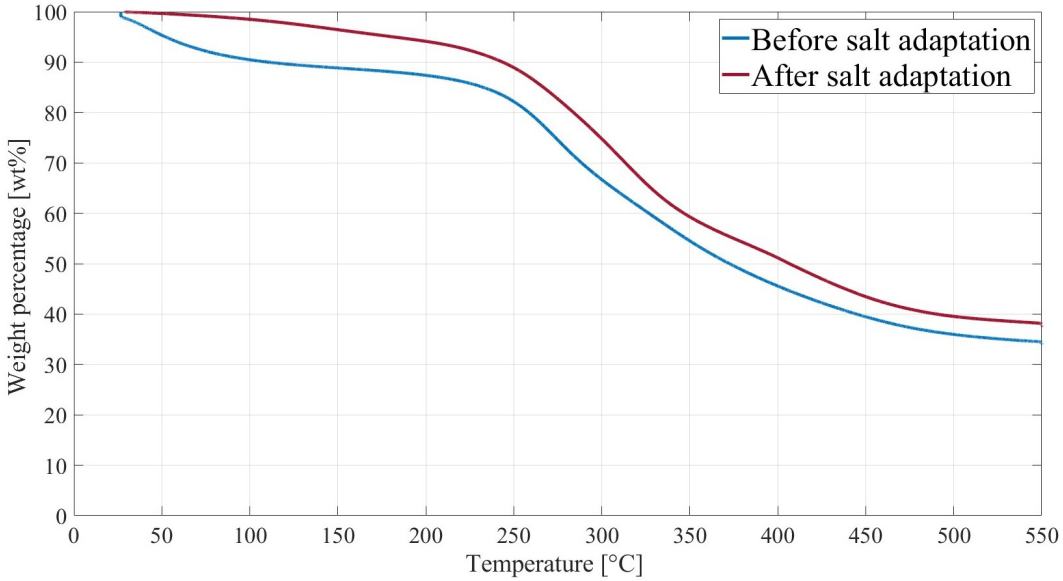

FIGURE D.5: Thermogravimetric analyses of EPS extracted from floccular sludge, before and after salt adaptation, using the heat and sodium carbonate extraction method.

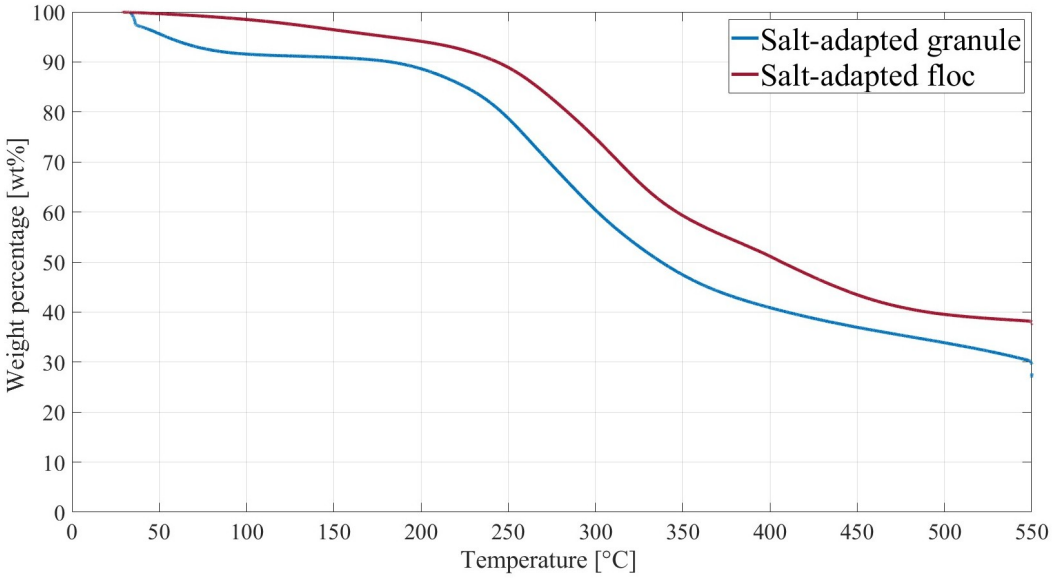

Figure D.6: Thermogravimetric analyses of EPS extracted from salt-adapted granular and floccular sludge using the heat and sodium carbonate extraction method.

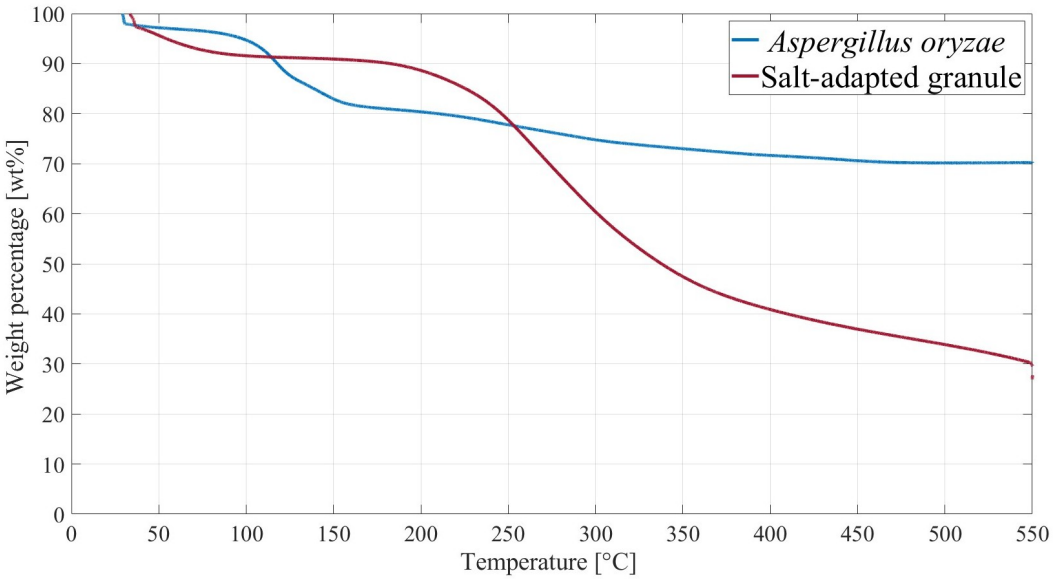

Figure D.7: Thermogravimetric analyses of EPS extracted from *Aspergillus oryzae* and salt-adapted granular sludge, using the heat and sodium carbonate extraction method.

D.4 Statements Generative AI

Use of Generative AI

I did use generative AI assistance tools during the writing process of my thesis, most often for mere language assistance.

I did use the generative AI assistance tools ChatGPT as well as Google Gemini.

Generative AI was **NOT** used as a search engine to learn about a particular topic**.**

Generative AI was **NOT** used for carrying out a literature review.

Generative AI was **NOT** used for short-form input assistance.

Google Gemini and ChatGPT **were used for generating programming code.** The general code made to generate the different plots was completely self-made. However, the slight adaptations to general plots in Matlab (setting the font to Times New Roman, adding the multicolumn legends to the rheology plots) were made based on some tips and tricks provided by the Generative AI. Apart from this, no *Generative AI* was used to generate code.

Generative AI was **NOT** used to generate new research ideas.

Generative AI was **NOT** used to generate visuals.

No other uses of *Generative AI* are applicable to the content of this thesis.

The text/code/ images in this thesis are my own (unless otherwise specified) and generative AI has only been used in accordance with the KU Leuven guidelines and appropriate references have been added. I have reviewed and edited the content as needed and I take full responsibility for the content of the thesis.

Bibliography

[1] C. Abeygunawardana, T. C. Williams, J. S. Sumner, and J. P. Hennessey. Development and Validation of an NMR-Based Identity Assay for Bacterial Polysaccharides. *Analytical Biochemistry*, 279(2):226–240, Mar. 2000. DOI: 10.1006/abio.1999.4470.

[2] S. S. Adav and D.-J. Lee. Extraction of extracellular polymeric substances from aerobic granule with compact interior structure. *Journal of Hazardous Materials*, 154(1-3):1120–1126, June 2008. DOI: 10.1016/j.jhazmat.2007.11.058.

[3] S. S. Adav, D.-J. Lee, and J.-H. Tay. Extracellular polymeric substances and structural stability of aerobic granule. *Water Research*, 42(6-7):1644–1650, Mar. 2008. DOI: 10.1016/j.watres.2007.10.013.

[4] T. Agustina, H. Ang, and V. Vareek. A review of synergistic effect of photocatalysis and ozonation on wastewater treatment. *Journal of Photochemistry and Photobiology C: Photochemistry Reviews*, 6(4):264–273, Dec. 2005. DOI: 10.1016/j.jphotochemrev.2005.12.003.

[5] K. M. Alkaabi, A. Yafea, and S. S. Ashraf. Effect of pH on Thermal- and Chemical-Induced Denaturation of GFP. *Applied Biochemistry and Biotechnology*, 126(2):149–156, 2005. DOI: 10.1385/abab:126:2:149.

[6] American Public Health Association (APHA). *Standard Methods for the Examination of Water and Wastewater*. American Public Health Association, Washington, D.C., 20th edition, 2012.

[7] M. Arienzo, E. Christen, W. Quayle, and A. Kumar. A review of the fate of potassium in the soil-plant system after land application of wastewaters. *Journal of Hazardous Materials*, 164(2-3):415–422, May 2009. DOI: 10.1016/j.jhazmat.2008.08.095.

[8] N. R. Babij, E. O. McCusker, G. T. Whiteker, B. Canturk, N. Choy, L. C. Creemer, C. V. D. Amicis, N. M. Hewlett, P. L. Johnson, J. A. Knobelsdorf, F. Li, B. A. Lorsbach, B. M. Nugent, S. J. Ryan, M. R. Smith, and Q. Yang. NMR Chemical Shifts of Trace Impurities: Industrially Preferred Solvents Used in Process and Green Chemistry. *Organic Process Research & Development*, 20(3):661–667, Feb. 2016. DOI: 10.1021/acs.oprd.5b00417.

[9] A. S. Bal and N. N. Dhagat. Upflow anaerobic sludge blanket reactor–a review. *Indian journal of environmental health*, 43:1–82, Apr. 2001.

[10] B. Balasubramanian, S. Ilavenil, A.-D. N.A., P. Agastian, and K. C. Choi. Isolation and characterization of Aspergillus sp. for the production of extracellular polysaccharides by response surface methodology. *Saudi Journal of Biological Sciences*, 26(3):449–454, Mar. 2019. DOI: 10.1016/j.sjbs.2018.10.015.

[11] A. Bateman. The structure of a domain common to archaebacteria and the homocystinuria disease protein. *Trends in Biochemical Sciences*, 22(1):12–13, Jan. 1997. DOI: 10.1016/s0968-0004(96)30046-7.

[12] R. Benedict and D. Carlson. Aerobic heterotrophic bacteria in activated sludge. *Water Research*, 5(11):1023–1030, Nov. 1971. DOI: 10.1016/0043-1354(71)90036-4.

[13] M. Boleij, M. Pabst, T. R. Neu, M. C. M. van Loosdrecht, and Y. Lin. Identification of Glycoproteins Isolated from Extracellular Polymeric Substances of Full-Scale Anammox Granular Sludge. *Environmental Science and Technology*, 52(22):13127–13135, Oct. 2018. DOI: 10.1021/acs.est.8b03180.

[14] M. Boleij, T. Seviour, L. L. Wong, M. C. van Loosdrecht, and Y. Lin. Solubilization and characterization of extracellular proteins from anammox granular sludge. *Water Research*, 164:114952, Nov. 2019. DOI: 10.1016/j.watres.2019.114952.

[15] S. Bolisetty, M. Peydayesh, and R. Mezzenga. Sustainable technologies for water purification from heavy metals: review and analysis. *Chemical Society Reviews*, 48(2):463–487, 2019. DOI: 10.1039/c8cs00493e.

[16] U. Bose, J. A. Broadbent, A. Juhasz, S. Karnaneedi, E. B. Johnston, S. Stockwell, K. Byrne, V. Limviphuvadh, S. Maurer-Stroh, A. L. Lopata, and M. L. Colgrave. Protein extraction protocols for optimal proteome measurement and arginine kinase quantitation from cricket acheta domesticus for food safety assessment. *Food Chemistry*, 348:129110, June 2021. DOI: 10.1016/j.foodchem.2021.129110.

[17] A. Bou-Sarkis, B. Pagliaccia, A. Ric, N. Derlon, E. Paul, Y. Bessiere, and E. Girbal-Neuhauser. Effects of alkaline solvents and heating temperatures on the solubilization and degradation of gel-forming Extracellular Polymeric Substances (EPS) extracted from aerobic granular sludge. *Biochemical Engineering Journal*, 185:108500, July 2022. DOI: 10.1016/j.bej.2022.108500.

[18] E. Brauchle, A. Knopf, H. Bauer, N. Shen, S. Linder, M. Monaghan, K. Ellwanger, S. Layland, S. Brucker, A. Nsair, and K. Schenke-Layland. Noninvasive Chamber-Specific Identification of Cardiomyocytes in Differentiating Pluripotent Stem Cells. *Stem Cell Reports*, 6(2):188–199, Feb. 2016. DOI: 10.1016/j.stemcr.2015.12.007.

[19] R. B. Brown and J. Audet. Current techniques for single-cell lysis. *Journal of The Royal Society Interface*, 5(2), Apr. 2008. DOI: 10.1098/rsif.2008.0009.focus.

[20] C. Buenaño Vargas, M. C. Gagliano, L. M. Paulo, A. Bartle, A. Graham, H. P. J. van Veelen, and V. O'Flaherty. Acclimation of microbial communities to low and moderate salinities in anaerobic digestion. *Science of The Total Environment*, 906:167470, Jan. 2024. DOI: 10.1016/j.scitotenv.2023.167470.

[21] G. S. Bumbrah and R. M. Sharma. Raman spectroscopy - Basic principle, instrumentation and selected applications for the characterization of drugs of abuse. *Egyptian Journal of Forensic Sciences*, 6(3):209–215, Sept. 2016. DOI: 10.1016/j.ejfs.2015.06.001.

[22] J. T. Bunce, E. Ndam, I. D. Ofiteru, A. Moore, and D. W. Graham. A Review of Phosphorus Removal Technologies and Their Applicability to Small-Scale Domestic Wastewater Treatment Systems. *Frontiers in Environmental Science*, 6, Feb. 2018. DOI: 10.3389/fenvs.2018.00008.

[23] K. D. Burch, B. Han, J. Pichtel, and T. Zubkov. Removal efficiency of commonly prescribed antibiotics via tertiary wastewater treatment. *Environmental Science and Pollution Research*, 26(7):6301–6310, Jan. 2019. DOI: 10.1007/s11356-019-04170-w.

[24] K. Burton. A study of the conditions and mechanism of the diphenylamine reaction for the colorimetric estimation of deoxyribonucleic acid. *The Biochemical journal*, 62:315–323, Feb. 1956.

[25] R. Campo, E. Carretti, C. Lubello, and T. Lotti. Recovery of structural extracellular polymeric substances (sEPS) from aerobic granular sludge: Insights on biopolymers characterization and hydrogel properties for potential applications. *Journal of Environmental Management*, 324:116247, Dec. 2022. DOI: 10.1016/j.jenvman.2022.116247.

[26] V. L. Campo, D. F. Kawano, D. B. d. Silva, and I. Carvalho. Carrageenans: Biological properties, chemical modifications and structural analysis - A review. *Carbohydrate Polymers*, 77(2):167–180, June 2009. DOI: 10.1016/j.carbpol.2009.01.020.

[27] F. Cao, I. Bourven, P. N. Lens, E. D. van Hullebusch, Y. Pechaud, and G. Guibaud. Hydrophobic features of EPS extracted from anaerobic granular sludge: an investigation based on DAX-8 resin fractionation and size exclusion chromatography. *Applied Microbiology and Biotechnology*, 101(8):3427–3438, Dec. 2016. DOI: 10.1007/s00253-016-8053-z.

[28] L. Cao, W. Lu, A. Mata, K. Nishinari, and Y. Fang. Egg-box model-based gelation of alginate and pectin: A review. *Carbohydrate Polymers*, 242:116389, Aug. 2020. DOI: 10.1016/j.carbpol.2020.116389.

[29] E. Cetin, K. Aleksanyan Magden, Y. Zhou, and G. Yilmaz. Effect of hydrodynamic conditions on the formation and structure of aerobic granular sludge performing enhanced biological phosphorus removal. *Water and Environment Journal*, 36(1):56–66, Oct. 2021. DOI: 10.1111/wej.12754.

[30] R. Chan and V. Chen. The effects of electrolyte concentration and ph on protein aggregation and deposition: critical flux and constant flux membrane filtration. *Journal of Membrane Science*, 185(2):177–192, Apr. 2001. DOI: 10.1016/s0376-7388(00)00645-1.

[31] L. Chen, Q. Hu, X. Zhang, Z. Chen, Y. Wang, and S. Liu. Effects of salinity on the biological performance of anaerobic membrane bioreactor. *Journal of Environmental Management*, 238:263–273, May 2019. DOI: 10.1016/j.jenvman.2019.03.012.

[32] W. Chen, P. Westerhoff, J. A. Leenheer, and K. Booksh. Fluorescence excitation-emission matrix regional integration to quantify spectra for dissolved organic matter. *Environmental Science and Technology*, 37(24):5701–5710, Nov. 2003. DOI: 10.1021/es034354c.

[33] W.-H. Chen, Y.-S. Chu, J.-L. Liu, and J.-S. Chang. Thermal degradation of carbohydrates, proteins and lipids in microalgae analyzed by evolutionary computation. *Energy Conversion and Management*, 160:209–219, Mar. 2018. DOI: 10.1016/j.enconman.2018.01.036.

[34] Y.-P. Chen, P. Zhang, J.-S. Guo, F. Fang, X. Gao, and C. Li. Functional groups characteristics of EPS in biofilm growing on different carriers. *Chemosphere*, 92(6):633–638, July 2013. DOI: 10.1016/j.chemosphere.2013.01.059.

[35] S. Chong, T. K. Sen, A. Kayaalp, and H. M. Ang. The performance enhancements of upflow anaerobic sludge blanket (UASB) reactors for domestic sludge treatment - A State-of-the-art review. *Water Research*, 46(11):3434–3470, July 2012. DOI: 10.1016/j.watres.2012.03.066.

[36] L. A. Cole. *Evolution of Chemical, Prokaryotic, and Eukaryotic Life*, pages 93–99. Elsevier, Amsterdam, 2016. DOI: 10.1016/b978-0-12-809685-7.00013-7.

[37] S. Comte, G. Guibaud, and M. Baudu. Relations between extraction protocols for activated sludge extracellular polymeric substances (EPS) and complexation properties of Pb and Cd with EPS. *Enzyme and Microbial Technology*, 38(1-2):246–252, Jan. 2006. DOI: 10.1016/j.enzmictec.2005.06.023.

[38] Council of the European Union. Wastewater treatment, 2024. https://www.consilium.europa.eu/en/policies/wastewater-treatment/,[Accessed on 11/11/2024.

[39] I. Cumpstey. Chemical modification of polysaccharides. *ISRN Organic Chemistry*, 2013:1–27, Sept. 2013. DOI: 10.1155/2013/417672.

[40] S. Dababat, G. Enaime, M. Wichern, and M. Lübken. Aerobic Granular Sludge: Perspectives for Excess Sludge Management and Resource Recovery. *Chemie Ingenieur Technik*, 95(12):1881–1896, Oct. 2023. DOI: 10.1002/cite.202300093.

[41] P. d'Abzac, F. Bordas, E. Joussein, E. van Hullebusch, P. Lens, and G. Guibaud. Characterization of the Mineral Fraction Associated to Extracellular Polymeric Substances (EPS) in Anaerobic Granular Sludges. *Environmental Science and Technology*, 44(1):412–418, Dec. 2009. DOI: 10.1021/es901912g.

[42] Q. Dai, L. Ma, N. Ren, P. Ning, Z. Guo, L. Xie, and H. Gao. Investigation on extracellular polymeric substances, sludge flocs morphology, bound water release and dewatering performance of sewage sludge under pretreatment with modified phosphogypsum. *Water Research*, 142:337–346, Oct. 2018. DOI: 10.1016/j.watres.2018.06.009.

[43] L. de Bruin, M. de Kreuk, H. van der Roest, C. Uijterlinde, and M. van Loosdrecht. Aerobic granular sludge technology: an alternative to activated sludge? *Water Science and Technology*, 49(11-12):1–7, June 2004. DOI: 10.2166/wst.2004.0790.

[44] M. de Kreuk, J. Heijnen, and M. van Loosdrecht. Simultaneous COD, nitrogen, and phosphate removal by aerobic granular sludge. *Biotechnology and Bioengineering*, 90(6):761–769, Apr. 2005. DOI: 10.1002/bit.20470.

[45] M. De Kreuk, B. McSwain, S. Bathe, S. Tay, N. Schwarzenbeck, and P. Wilderer. Discussion outcomes. *Aerobic granular sludge*, pages 155–169, 2005.

[46] C. A. de Lemos Chernicharo. *Anaerobic reactors*. Number 4 in Biological Wastewater Treatment Series. IWA Publishing, London, 2007.

[47] V. M. Dembitsky and M. Srebnik. Natural halogenated fatty acids: their analogues and derivatives. *Progress in Lipid Research*, 41(4):315–367, July 2002. DOI: 10.1016/s0163-7827(02)00003-6.

[48] A. Demirbas, G. Edris, and W. M. Alalayah. Sludge production from municipal wastewater treatment in sewage treatment plant. *Energy Sources, Part A: Recovery, Utilization, and Environmental Effects*, 39(10):999–1006, apr 2017. DOI: 10.1080/15567036.2017.1283551.

[49] K. I. Draget, G. Skjåk-Bræk, and O. Smidsrød. Alginate based new materials. *International Journal of Biological Macromolecules*, 21(1-2):47–55, Aug. 1997. DOI: 10.1016/s0141-8130(97)00040-8.

[50] C.-D. Dubé and S. R. Guiot. Characterization of the protein fraction of the extracellular polymeric substances of three anaerobic granular sludges. *AMB Express*, 9(1), Feb. 2019. DOI: 10.1186/s13568-019-0746-0.

[51] M. Dubois, K. Gilles, J. K. Hamilton, P. A. Rebers, and F. Smith. A colorimetric method for the determination of sugars. *Nature*, 168(4265):167–167, July 1951. DOI: 10.1038/168167a0.

[52] A. K. Dwivedi. Researches in water pollution: A review. *International Research Journal of Natural and Applied Sciences*, 4(1):118–142, 2017.

[53] M. Eggersdorfer and A. Wyss. Carotenoids in human nutrition and health. *Archives of Biochemistry and Biophysics*, 652:18–26, Aug. 2018. DOI: 10.1016/j.abb.2018.06.001.

[54] H. El Farissi, R. Lakhmiri, A. Albourine, M. Safi, and O. Cherkaoui. Removal of RR-23 dye from industrial textile wastewater by adsorption on cistus ladaniferus seeds and their biochar. 7, 11 2017.

[55] J. Elleuch, M. Drira, I. Ghribi, F. Hadjkacem, G. Pierre, C. Causserand, H. Khemakhem, P. Michaud, I. Fendri, and S. Abdelkafi. Amphora coffeiformis extracellular polymeric substances and their potential applications in lead removal. *Antonie van Leeuwenhoek*, 118(3), Feb. 2025. DOI: 10.1007/s10482-024-02057-6.

[56] K. Ellis. Slow sand filtration as a technique for the tertiary treatment of municipal sewages. *Water Research*, 21(4):403–410, Apr. 1987. DOI: 10.1016/0043-1354(87)90187-4.

[57] H. H. P. Fang and X. S. Jia. Extraction of extracellular polymer from anaerobic sludges. *Biotechnology Techniques*, 10(11):803–808, Nov. 1996. DOI: 10.1007/bf00154662.

[58] G. Feijoo, M. Soto, R. Mendez, and J. M. Lema. Sodium inhibition in the anaerobic digestion process: Antagonism and adaptation phenomena. *Enzyme and Microbial Technology*, 17(2):180–188, Feb. 1995. DOI: 10.1016/0141-0229(94)00011-f.

[59] S. Felz. *Structural Extracellular Polymeric Substances from Aerobic Granular Sludge*. PhD thesis, Delft University of Technology, 2019. DOI: 10.4233/UUID:93E702D1-92B2-4025-AB57-6D2C141ED14D.

[60] S. Felz, H. Kleikamp, J. Zlopasa, M. C. van Loosdrecht, and Y. Lin. Impact of metal ions on structural EPS hydrogels from aerobic granular sludge. *Biofilm*, 2:100011, Dec. 2020. DOI: 10.1016/j.bioflm.2019.100011.

[61] C. Feng, T. Lotti, R. Canziani, Y. Lin, C. Tagliabue, and F. Malpei. Extracellular biopolymers recovered as raw biomaterials from waste granular sludge and potential applications: A critical review. *Science of The Total Environment*, 753:142051, Jan. 2021. DOI: 10.1016/j.scitotenv.2020.142051.

[62] R. Ferrentino, M. Langone, L. Fiori, and G. Andreottola. Full-Scale Sewage Sludge Reduction Technologies: A Review with a Focus on Energy Consumption. *Water*, 15(4):615, Feb. 2023. DOI: 10.3390/w15040615.

[63] H.-C. Flemming and J. Wingender. The biofilm matrix. *Nature Reviews Microbiology*, 8(9):623–633, Aug. 2010. DOI: 10.1038/nrmicro2415.

[64] D. Focht and A. Chang. *Nitrification and Denitrification Processes Related to Waste Water Treatment*, pages 153–186. Elsevier, Amsterdam, 1975. DOI: 10.1016/s0065-2164(08)70428-3.

[65] A. Foglia, C. Akyol, N. Frison, E. Katsou, A. L. Eusebi, and F. Fatone. Long-term operation of a pilot-scale anaerobic membrane bioreactor (anmbr) treating high salinity low loaded municipal wastewater in real environment. *Separation and Purification Technology*, 236:116279, Apr. 2020. DOI: 10.1016/j.seppur.2019.116279.

[66] K. Frank. *Microbiology in Clinical Pathology*, pages 3237–3268. Elsevier, Amsterdam, 2014. DOI: 10.1016/b978-0-12-386456-7.06304-8.

[67] B. Frølund, R. Palmgren, K. Keiding, and P. H. Nielsen. Extraction of extracellular polymers from activated sludge using a cation exchange resin. *Water Research*, 30(8):1749–1758, Aug. 1996. DOI: 10.1016/0043-1354(95)00323-1.

[68] M. Gagliano, S. Ismail, A. Stams, C. Plugge, H. Temmink, and J. Van Lier. Biofilm formation and granule properties in anaerobic digestion at high salinity. *Water Research*, 121:61–71, Sept. 2017. DOI: 10.1016/j.watres.2017.05.016.

[69] M. C. Gagliano, T. R. Neu, U. Kuhlicke, D. Sudmalis, H. Temmink, and C. M. Plugge. EPS Glycoconjugate Profiles Shift as Adaptive Response in Anaerobic Microbial Granulation at High Salinity. *Frontiers in Microbiology*, 9:1423, July 2018. DOI: 10.3389/fmicb.2018.01423.

[70] D. Gao, L. Liu, H. Liang, and W.-M. Wu. Aerobic granular sludge: characterization, mechanism of granulation and application to wastewater treatment. *Critical Reviews in Biotechnology*, 31(2):137–152, Oct. 2010. DOI: 10.3109/07388551.2010.497961.

[71] R. Geetha Bai and R. Tuvikene. Potential Antiviral Properties of Industrially Important Marine Algal Polysaccharides and Their Significance in Fighting a Future Viral Pandemic. *Viruses*, 13(9):1817, Sept. 2021. DOI: 10.3390/v13091817.

[72] R. Gehr. Removal of extracellular material techniques and pitfalls. *Water Research*, 17(12):1743–1748, 1983. DOI: 10.1016/0043-1354(83)90195-1.

[73] K. V. Gernaey, M. C. van Loosdrecht, M. Henze, M. Lind, and S. B. Jorgensen. Activated sludge wastewater treatment plant modelling and simulation: state of the art. *Environmental Modelling and Software*, 19(9):763–783, Sept. 2004. DOI: 10.1016/j.envsoft.2003.03.005.

[74] A. G. Geyik and F. Cecen. Variations in extracellular polymeric substances (EPS) during adaptation of activated sludges to new feeding conditions. *International Biodeterioration and Biodegradation*, 105:137–145, Nov. 2015. DOI: 10.1016/j.ibiod.2015.08.021.

[75] R. Gheorghita Puscaselu, A. Lobiuc, M. Dimian, and M. Covasa. Alginate: From food industry to biomedical applications and management of metabolic disorders. *Polymers*, 12(10):2417, Oct. 2020. DOI: 10.3390/polym12102417.

[76] E. Gomez-Ordonez and P. Ruperez. FTIR-ATR spectroscopy as a tool for polysaccharide identification in edible brown and red seaweeds. *Food Hydrocolloids*, 25(6):1514–1520, Aug. 2011. DOI: 10.1016/j.foodhyd.2011.02.009.

[77] G. Gonzalez-Gil, L. Thomas, A.-H. Emwas, P. N. L. Lens, and P. E. Saikaly. NMR and MALDI-TOF MS based characterization of exopolysaccharides in anaerobic microbial aggregates from full-scale reactors. *Scientific Reports*, 5(1), Sept. 2015. DOI: 10.1038/srep14316.

[78] G. Goswami, S. Chaudhuri, and D. Dutta. Studies on the stability of a carotenoid produced by a novel isolate using low cost agro-industrial residue and its application in different model systems. *LWT - Food Science and Technology*, 63(1):780–790, Sept. 2015. DOI: 10.1016/j.lwt.2015.03.017.

[79] G. T. Grant, E. R. Morris, D. A. Rees, P. J. Smith, and D. Thom. Biological interactions between polysaccharides and divalent cations: The egg-box model. *FEBS Letters*, 32(1):195–198, May 1973. DOI: 10.1016/0014-5793(73)80770-7.

[80] G. Guibaud, S. Comte, F. Bordas, S. Dupuy, and M. Baudu. Comparison of the complexation potential of extracellular polymeric substances (EPS), extracted from activated sludges and produced by pure bacteria strains, for cadmium, lead and nickel. *Chemosphere*, 59(5):629–638, Apr. 2005. DOI: 10.1016/j.chemosphere.2004.10.028.

[81] S. R. Guiot, A. Pauss, and J. W. Costerton. A structured model of the anaerobic granule consortium. *Water Science and Technology*, 25(7):1–10, Apr. 1992. DOI: 10.2166/wst.1992.0133.

[82] J. Guo, J. Zhou, D. Wang, C. Tian, P. Wang, M. Salah Uddin, and H. Yu. Biocalalyst effects of immobilized anthraquinone on the anaerobic reduction of azo dyes by the salt-tolerant bacteria. *Water Research*, 41(2):426–432, Jan. 2007. DOI: 10.1016/j.watres.2006.10.022.

[83] X. Guo, J. Liu, and B. Xiao. Evaluation of the damage of cell wall and cell membrane for various extracellular polymeric substance extractions of activated sludge. *Journal of Biotechnology*, 188:130–135, Oct. 2014. DOI: 10.1016/j.jbiotec.2014.08.025.

[84] X. Guo, Y. Miao, B. Wu, L. Ye, H. Yu, S. Liu, and X.-x. Zhang. Correlation between microbial community structure and biofouling as determined by analysis of microbial community dynamics. *Bioresource Technology*, 197:99–105, Dec. 2015. DOI: 10.1016/j.biortech.2015.08.049.

[85] J. Gupta, R. Rathour, C. L. Dupont, D. Kaul, and I. S. Thakur. Genomic insights into waste valorized extracellular polymeric substances (EPS) produced by Bacillus sp. ISTL8. *Environmental Research*, 192:110277, Jan. 2021. DOI: 10.1016/j.envres.2020.110277.

[86] M. Hamoda, I. Al-Ghusain, and N. Al-Mutairi. Sand filtration of wastewater for tertiary treatment and water reuse. *Desalination*, 164(3):203–211, Apr. 2004. DOI: 10.1016/s0011-9164(04)00189-4.

[87] S. He, L. Feng, W. Zhao, J. Li, Q. Zhao, and L. Wei. Composition and molecular structure analysis of hydrophilic/hydrophobic extracellular polymeric substances (EPS) with impacts on sludge dewaterability. *Chemical Engineering Journal*, 462:142234, Apr. 2023. DOI: 10.1016/j.cej.2023.142234.

[88] A.-M. Hermansson, E. Eriksson, and E. Jordansson. Effects of potassium, sodium and calcium on the microstructure and rheological behaviour of kappa-carrageenan gels. *Carbohydrate Polymers*, 16(3):297–320, Jan. 1991. DOI: 10.1016/0144-8617(91)90115-s.

[89] M. J. Higgins and J. T. Novak. Characterization of exocellular protein and its role in bioflocculation. *Journal of Environmental Engineering*, 123(5):479–485, May 1997. DOI: 10.1061/(asce)0733-9372(1997)123:5(479).

[90] P.-N. Hong, R. Honda, M. Noguchi, and T. Ito. Optimum selection of extraction methods of extracellular polymeric substances in activated sludge for effective extraction of the target components. *Biochemical Engineering Journal*, 127:136–146, Nov. 2017. DOI: 10.1016/j.bej.2017.08.002.

[91] T. Hong, J.-Y. Yin, S.-P. Nie, and M.-Y. Xie. Applications of infrared spectroscopy in polysaccharide structural analysis: Progress, challenge and perspective. *Food Chemistry: X*, 12:100168, Dec. 2021. DOI: 10.1016/j.fochx.2021.100168.

[92] N. Horan and C. Eccles. Purification and characterization of extracellular polysaccharide from activated sludges. *Water Research*, 20(11):1427–1432, Nov. 1986. DOI: 10.1016/0043-1354(86)90142-9.

[93] B. Hu, L. Du, and S. Matsukawa. NMR study on the network structure of a mixed gel of kappa and iota carrageenans. *Carbohydrate Polymers*, 150:57–64, Oct. 2016. DOI: 10.1016/j.carbpol.2016.04.112.

[94] L. Hulshoff Pol, S. de Castro Lopes, G. Lettinga, and P. Lens. Anaerobic sludge granulation. *Water Research*, 38(6):1376–1389, Mar. 2004. DOI: 10.1016/j.watres.2003.12.002.

[95] S. Ismail, C. de La Parra, H. Temmink, and J. van Lier. Extracellular polymeric substances (EPS) in upflow anaerobic sludge blanket (UASB) reactors operated under high salinity conditions. *Water Research*, 44(6):1909–1917, Mar. 2010. DOI: 10.1016/j.watres.2009.11.039.

[96] H. Iwamura. Organic reactions in sub- and supercritical water in the absence of any added catalyst. *The Journal of Research Institute of Science and Technology, Nihon University*, 132:1–9, 01 2014.

[97] P. U. Iyare, S. K. Ouki, and T. Bond. Microplastics removal in wastewater treatment plants: a critical review. *Environmental Science: Water Research and Technology*, 6(10):2664–2675, 2020. DOI: 10.1039/d0ew00397b.

[98] P. Jaibiba, S. Naga Vignesh, and S. Hariharan. *Working principle of typical bioreactors*, pages 145–173. Elsevier, Amsterdam, 2020. DOI: 10.1016/b978-0-12-821264-6.00010-3.

[99] H.-L. Jiang, J.-H. Tay, and S. T.-L. Tay. Changes in structure, activity and metabolism of aerobic granules as a microbial response to high phenol loading. *Applied Microbiology and Biotechnology*, (5):602–608, May 2004.

[100] P. B. Jordal, M. S. Dueholm, P. Larsen, S. V. Petersen, J. J. Enghild, G. Christiansen, P. Hø jrup, P. H. Nielsen, and D. E. Otzen. Widespread Abundance of Functional Bacterial Amyloid in Mycolata and Other Gram-Positive Bacteria. *Applied and Environmental Microbiology*, 75(12):4101–4110, June 2009. DOI: 10.1128/aem.02107-08.

[101] D. Kalita, P. Konwar, D. Sahu, S. Baruah, and S. Barua. *Fluoropolymer nanocomposites: introduction, fundamental properties, and high-performance applications*, pages 79–120. Elsevier, Amsterdam, 2023. DOI: 10.1016/b978-0-323-95335-1.00023-2.

[102] I. Karakas, S. B. Sam, E. Cetin, E. Dulekgurgen, and G. Yilmaz. Resource recovery from an aerobic granular sludge process treating domestic wastewater. *Journal of Water Process Engineering*, 34:101148, Apr. 2020. DOI: 10.1016/j.jwpe.2020.101148.

[103] K. Kaviyarasan. Application of UASB Reactor in Industrial Wastewater Treatment - A Review. volume 5, 2014. ISSN: 2229-5518.

[104] J. Keller and K. Hartley. Greenhouse gas production in wastewater treatment: process selection is the major factor. *Water Science and Technology*, 47(12):43–48, June 2003. DOI: 10.2166/wst.2003.0626.

[105] N. K. Kim, N. Mao, R. Lin, D. Bhattacharyya, M. C. van Loosdrecht, and Y. Lin. Flame retardant property of flax fabrics coated by extracellular polymeric substances recovered from both activated sludge and aerobic granular sludge. *Water Research*, 170:115344, Mar. 2020. DOI: 10.1016/j.watres.2019.115344.

[106] P. J. A. Kleinman, A. N. Sharpley, R. W. McDowell, D. N. Flaten, A. R. Buda, L. Tao, L. Bergstrom, and Q. Zhu. Managing agricultural phosphorus for water quality protection: principles for progress. *Plant and Soil*, 349(1-2):169–182, July 2011. DOI: 10.1007/s11104-011-0832-9.

[107] T. Kobayashi, K. Abe, K. Asai, K. Gomi, P. R. Juvaddi, M. Kato, K. Kitamoto, M. Takeuchi, and M. Machida. Genomics of aspergillus oryzae. *Bioscience, Biotechnology, and Biochemistry*, 71(3):646–670, Mar. 2007. DOI: 10.1271/bbb.60550.

[108] K. Krysiak-Baltyn, R. Cavalida, B. Thwaites, P. J. Reeve, P. J. Scales, B. Van den Akker, L. Ong, G. J. Martin, A. D. Stickland, and S. L. Gras. Comparison of physical characteristics and dewatering behaviour between granular and floccular sludges generated from the same sewage source. *Journal of Water Process Engineering*, 29:100785, June 2019. DOI: 10.1016/j.jwpe.2019.100785.

[109] P. Larsen, J. L. Nielsen, D. Otzen, and P. H. Nielsen. Amyloid-Like Adhesins Produced by Floc-Forming and Filamentous Bacteria in Activated Sludge. *Applied and Environmental Microbiology*, 74(5):1517–1526, Mar. 2008. DOI: 10.1128/aem.02274-07.

[110] W. C. Lay, Y. Liu, and A. G. Fane. Impacts of salinity on the performance of high retention membrane bioreactors for water reclamation: A review. *Water Research*, 44(1):21–40, Jan. 2010. DOI: 10.1016/j.watres.2009.09.026.

[111] T. M. Le, Y. Lin, W.-Q. Zhuang, K. Jayaraman, and N. K. Kim. Effects of Extraction Methods on the Thermal Stability of Extracellular Polymeric Substances-Based Biomaterials from Wastewater Sludge. *Environmental Science & Technology*, 59(8):4165–4177, Feb. 2025. DOI: 10.1021/acs.est.4c10329.

[112] S. Le Borgne, D. Paniagua, and R. Vazquez-Duhalt. Biodegradation of organic pollutants by halophilic bacteria and archaea. *Microbial Physiology*, 15(2-3):74–92, 2008. DOI: 10.1159/000121323.

[113] K. Y. Lee and D. J. Mooney. Alginate: Properties and biomedical applications. *Progress in Polymer Science*, 37(1):106–126, Jan. 2012. DOI: 10.1016/j.progpolymsci.2011.06.003.

[114] N. M. Lee and T. Welander. Reducing sludge production in aerobic wastewater treatment through manipulation of the ecosystem. *Water Research*, 30(8):1781–1790, Aug. 1996. DOI: 10.1016/0043-1354(96)00059-0.

[115] O. Lefebvre and R. Moletta. Treatment of organic pollution in industrial saline wastewater: A literature review. *Water Research*, 40(20):3671–3682, Dec. 2006. DOI: 10.1016/j.watres.2006.08.027.

[116] O. Lefebvre, S. Quentin, M. Torrijos, J. J. Godon, J. P. Delgenes, and R. Moletta. Impact of increasing nacl concentrations on the performance and community composition of two anaerobic reactors. *Applied Microbiology and Biotechnology*, 75(1):61–69, May 2007. DOI: 10.1007/s00253-006-0799-2.

[117] J. Lei, X. Zhang, Y. Liu, X. Wang, G. Li, T. Feng, and H. Zhong. Adsorption Characteristics between Different Sizes of Microplastics and EPS Fractions of Anaerobic Granular Sludge. *Polish Journal of Environmental Studies*, 33(3):2141–2148, Jan. 2024. DOI: 10.15244/pjoes/173167.

[118] G. Lettinga, A. F. M. van Velsen, S. W. Hobma, W. de Zeeuw, and A. Klapwijk. Use of the upflow sludge blanket (usb) reactor concept for biological wastewater treatment, especially for anaerobic treatment. *Biotechnology and Bioengineering*, 22(4):699–734, Apr. 1980. DOI: 10.1002/bit.260220402.

[119] J. Li, K. F. See, and J. Chi. Water resources and water pollution emissions in China's industrial sector: A green-biased technological progress analysis. *Journal of Cleaner Production*, 229:1412–1426, Aug. 2019. DOI: 10.1016/j.jclepro.2019.03.216.

[120] N. Li, D. Wei, S. Wang, L. Hu, W. Xu, B. Du, and Q. Wei. Comparative study of the role of extracellular polymeric substances in biosorption of ni(ii) onto aerobic/anaerobic granular sludge. *Journal of Colloid and Interface Science*, 490:754–761, Mar. 2017. DOI: 10.1016/j.jcis.2016.12.006.

[121] W.-W. Li and H.-Q. Yu. Insight into the roles of microbial extracellular polymer substances in metal biosorption. *Bioresource Technology*, 160:15–23, May 2014. DOI: 10.1016/j.biortech.2013.11.074.

[122] S. J. Lim and T.-H. Kim. Applicability and trends of anaerobic granular sludge treatment processes. *Biomass and Bioenergy*, 60:189–202, Jan. 2014. DOI: 10.1016/j.biombioe.2013.11.011.

[123] Y. Lin, K. Nierop, E. Girbal-Neuhauser, M. Adriaanse, and M. van Loosdrecht. Sustainable polysaccharide-based biomaterial recovered from waste aerobic granular sludge as a surface coating material. *Sustainable Materials and Technologies*, 4:24–29, July 2015. DOI: 10.1016/j.susmat.2015.06.002.

[124] Y. M. Lin, L. Wang, Z. M. Chi, and X. Y. Liu. Bacterial alginate role in aerobic granular bioparticles formation and settleability improvement. *Separation Science and Technology*, 43(7):1642–1652, May 2008. DOI: 10.1080/01496390801973805.

[125] S. Liparoti, V. Speranza, and F. Marra. Alginate hydrogel: The influence of the hardening on the rheological behaviour. *Journal of the Mechanical Behavior of Biomedical Materials*, 116:104341, Apr. 2021. DOI: 10.1016/j.jmbbm.2021.104341.

[126] H. Liu and H. H. Fang. Extraction of extracellular polymeric substances (EPS) of sludges. *Journal of Biotechnology*, 95(3):249–256, May 2002. DOI: 10.1016/s0168-1656(02)00025-1.

[127] L. Liu, D.-W. Gao, M. Zhang, and Y. Fu. Comparison of ca2+ and mg2+ enhancing aerobic granulation in sbr. *Journal of Hazardous Materials*, 181(1-3):382–387, Sept. 2010. DOI: 10.1016/j.jhazmat.2010.05.021.

[128] M. Liu, J. J. Gill, R. Young, and E. J. Summer. Bacteriophages of wastewater foaming-associated filamentous gordonia reduce host levels in raw activated sludge. *Scientific Reports*, 5(1), Sept. 2015. DOI: 10.1038/srep13754.

[129] X. Liu, J. Liu, D. Deng, R. Li, C. Guo, J. Ma, and M. Chen. Investigation of extracellular polymeric substances (EPS) in four types of sludge: Factors influencing EPS properties and sludge granulation. *Journal of Water Process Engineering*, 40:101924, Apr. 2021. DOI: 10.1016/j.jwpe.2021.101924.

[130] X. Liu, Q. Pei, H. Han, H. Yin, M. Chen, C. Guo, J. Li, and H. Qiu. Functional analysis of extracellular polymeric substances (EPS) during the granulation of aerobic sludge: Relationship among EPS, granulation and nutrients removal. *Environmental Research*, 208:112692, May 2022. DOI: 10.1016/j.envres.2022.112692.

[131] Y. Liu and H. H. P. Fang. Influences of Extracellular Polymeric Substances (EPS) on Flocculation, Settling, and Dewatering of Activated Sludge. *Critical Reviews in Environmental Science and Technology*, 33(3):237–273, July 2003. DOI: 10.1080/10643380390814479.

[132] Y. Liu and J.-H. Tay. State of the art of biogranulation technology for wastewater treatment. *Biotechnology Advances*, 22(7):533–563, Sept. 2004. DOI: 10.1016/j.biotechadv.2004.05.001.

[133] S. Lorenzen. The isolated effect of particle surface charge on filter cake properties. *The PhD Series of the Faculty of Engineering and Science*, 2016. DOI: 10.5278/VBN.PHD.ENGSCI.00185.

[134] T. Lotti, E. Carretti, D. Berti, C. Montis, S. Del Buffa, C. Lubello, C. Feng, and F. Malpei. Hydrogels formed by anammox extracellular polymeric substances:

structural and mechanical insights. *Scientific Reports*, 9(1), Aug. 2019. DOI: 10.1038/s41598-019-47987-8.

[135] O. H. Lowry, N. Rosebrough, A. L. Farr, and R. J. Randall. Protein measurement with the folin phenol reagent. *Journal of Biological Chemistry*, 193(1):265–275, Nov. 1951. DOI: 10.1016/s0021-9258(19)52451-6.

[136] H. Lu, K. Chandran, and D. Stensel. Microbial ecology of denitrification in biological wastewater treatment. *Water Research*, 64:237–254, Nov. 2014. DOI: 10.1016/j.watres.2014.06.042.

[137] L. Lundqvist. *Structural and interaction studies of polysaccharides by NMR spectroscopy*. PhD thesis, Swedish University of Agricultural Sciences, 2015.

[138] F. A. MacLeod, S. R. Guiot, and J. W. Costerton. Layered structure of bacterial aggregates produced in an upflow anaerobic sludge bed and filter reactor. *Applied and Environmental Microbiology*, 56(6):1598–1607, June 1990. DOI: 10.1128/aem.56.6.1598-1607.1990.

[139] N. R. Maddela, Z. Zhou, Z. Yu, S. Zhao, and F. Meng. Functional Determinants of Extracellular Polymeric Substances in Membrane Biofouling: Experimental Evidence from Pure-Cultured Sludge Bacteria. *Applied and Environmental Microbiology*, 84(15), Aug. 2018. DOI: 10.1128/aem.00756-18.

[140] A. Mahardika, A. B. Susanto, R. Pramesti, H. Matsuyoshi, B. B. Andriana, Y. Matsuda, and H. Sato. Application of imaging Raman spectroscopy to study the distribution of Kappa carrageenan in the seaweed Kappaphycus alvarezii. *Journal of Applied Phycology*, 31(2):1383–1390, Sept. 2018. DOI: 10.1007/s10811-018-1618-8.

[141] J. Mallevialle, P. E. Odendaal, and M. R. Wiesner. *Water treatment membrane processes*. McGraw-Hill Professional, New York City, 1996.

[142] A. T. Mansour, A. E. Alprol, K. M. Abualnaja, H. S. El-Beltagi, K. M. A. Ramadan, and M. Ashour. The Using of Nanoparticles of Microalgae in Remediation of Toxic Dye from Industrial Wastewater: Kinetic and Isotherm Studies. *Materials*, 15(11):3922, May 2022. DOI: 10.3390/ma15113922.

[143] M. Mecozzi, M. Pietroletti, M. Scarpiniti, R. Acquistucci, and M. E. Conti. Monitoring of marine mucilage formation in Italian seas investigated by infrared spectroscopy and independent component analysis. *Environmental Monitoring and Assessment*, 184(10):6025–6036, Oct. 2011. DOI: 10.1007/s10661-011-2400-4.

[144] J. N. Meegoda, B. Li, K. Patel, and L. B. Wang. A review of the processes, parameters, and optimization of anaerobic digestion. *International journal of environmental research and public health*, 15, Oct. 2018. DOI 10.3390/ijerph15102224.

[145] L. Mertens. Can bioaugmentation with aerobic fungal pellets enhance the start-up of an anaerobic digester treating saline wastewater with a non-saline-acclimated inoculum? Master's thesis, KULeuven, 2025.

[146] U. Metzger, U. Lankes, K. Fischpera, and F. H. Frimmel. The concentration of polysaccharides and proteins in EPS of Pseudomonas putida and Aureobasidum pullulans as revealed by 13C CPMAS NMR spectroscopy. *Applied Microbiology and Biotechnology*, 85(1):197–206, Oct. 2009. DOI: 10.1007/s00253-009-2218-y.

[147] T. Mino, M. van Loosdrecht, and J. Heijnen. Microbiology and biochemistry of the enhanced biological phosphate removal process. *Water Research*, 32(11):3193–3207, Nov. 1998. DOI: 10.1016/s0043-1354(98)00129-8.

[148] E. R. Morris, D. A. Rees, and G. Robinson. Cation-specific aggregation of carrageenan helices: Domain model of polymer gel structure. *Journal of Molecular Biology*, 138(2):349–362, Apr. 1980. DOI: 10.1016/0022-2836(80)90291-0.

[149] J. D. Munoz Sierra, M. J. Oosterkamp, W. Wang, H. Spanjers, and J. B. van Lier. Comparative performance of upflow anaerobic sludge blanket reactor and anaerobic membrane bioreactor treating phenolic wastewater: Overcoming high salinity. *Chemical Engineering Journal*, 366:480–490, June 2019. DOI: 10.1016/j.cej.2019.02.097.

[150] S. Naidoo and A. Olaniran. Treated Wastewater Effluent as a Source of Microbial Pollution of Surface Water Resources. *International Journal of Environmental Research and Public Health*, 11(1):249–270, Dec. 2013. DOI: 10.3390/ijerph110100249.

[151] NASA. Why europa: Ingredients for life, 2022. https://europa.nasa.gov/why-europa/ingredients-for-life/#:~:text=Scientists%20say%20we%20should%20look,life%20takes%20time%20to%20develop. [Accessed: 11 November 2024].

[152] L. N. Nguyen, A. Q. Nguyen, and L. D. Nghiem. *Microbial Community in Anaerobic Digestion System: Progression in Microbial Ecology*, pages 331–355. Springer Singapore, Nov. 2018. DOI: 10.1007/978-981-13-3259-31-5.

[153] S.-Q. Ni, N. Sun, H. Yang, J. Zhang, and H. H. Ngo. Distribution of extracellular polymeric substances in anammox granules and their important roles during anammox granulation. *Biochemical Engineering Journal*, 101:126–133, Sept. 2015. DOI: 10.1016/j.bej.2015.05.014.

[154] Y. Nie, Z. Wang, W. Wang, Z. Zhou, Y. Kong, and J. Ma. Bio-flocculation of microcystis aeruginosa by using fungal pellets of aspergillus oryzae: Performance and mechanism. *Journal of Hazardous Materials*, 439:129606, Oct. 2022. DOI: 10.1016/j.jhazmat.2022.129606.

[155] P. H. Nielsen, A. M. Saunders, A. A. Hansen, P. Larsen, and J. L. Nielsen. Microbial communities involved in enhanced biological phosphorus removal from wastewater-a model system in environmental biotechnology. *Current Opinion in Biotechnology*, 23(3):452–459, June 2012. DOI: 10.1016/j.copbio.2011.11.027.

[156] O. Nowak. Optimizing the use of sludge treatment facilities at municipal wwtps. *Journal of Environmental Science and Health, Part A*, 41(9):1807–1817, Sept. 2006. DOI: 10.1080/10934520600778986.

[157] B. Pagliaccia. *Insights on the recovery, characterization and valorization of Extracellular Polymeric substances (EPS) from granular sludge applied in innovative wastewater treatment systems*. PhD thesis, Universite de Toulouse, 2022.

[158] B. Pagliaccia, R. Campo, E. Carretti, M. Severi, C. Lubello, and T. Lotti. Towards resource recovery-oriented solutions in agriculture exploiting structural extracellular polymeric substances (sEPS) extracted from aerobic granular sludge (AGS). *Chemical Engineering Journal*, 485:149819, Apr. 2024. DOI: 10.1016/j.cej.2024.149819.

[159] B. Pagliaccia, E. Carretti, M. Severi, D. Berti, C. Lubello, and T. Lotti. Heavy metal biosorption by Extracellular Polymeric Substances (EPS) recovered from anammox granular sludge. *Journal of Hazardous Materials*, 424:126661, Feb. 2022. DOI: 10.1016/j.jhazmat.2021.126661.

[160] L. Passauer, T. Hallas, E. Baucker, G. Ciesielski, S. Lebioda, and U. Hamer. Biodegradation of hydrogels from oxyethylated lignins in model soils. *ACS Sustainable Chemistry and Engineering*, 3(9):1955–1964, Aug. 2015. DOI: 10.1021/acssuschemeng.5b00139.

[161] M. Patziger, H. Kainz, M. Hunze, and J. Jozsa. Influence of secondary settling tank performance on suspended solids mass balance in activated sludge systems. *Water Research*, 46(7):2415–2424, May 2012. DOI: 10.1016/j.watres.2012.02.007.

[162] S. Peng, A. Hu, J. Ai, W. Zhang, and D. Wang. Changes in molecular structure of extracellular polymeric substances (EPS) with temperature in relation to sludge macro-physical properties. *Water Research*, 201:117316, Aug. 2021. DOI: 10.1016/j.watres.2021.117316.

[163] T. Peng, Y. Wang, J. Wang, F. Fang, P. Yan, and Z. Liu. Effect of different forms and components of EPS on sludge aggregation during granulation process of aerobic granular sludge. *Chemosphere*, 303:135116, Sept. 2022. DOI: 10.1016/j.chemosphere.2022.135116.

[164] O. Pidoux, J.-N. Argenson, V. Jacomo, and M. Drancourt. Molecular identification of a dietzia maris hip prosthesis infection isolate. *Journal of Clinical Microbiology*, 39(7):2634–2636, July 2001. DOI: 10.1128/jcm.39.7.2634-2636.2001.

[165] D. Pooja, P. Kumar, P. Singh, and S. Patil. *Sensors in Water Pollutants Monitoring: Role of Material*. Springer Singapore, 2020. DOI: 10.1007/978-981-15-0671-0.

[166] C. Proikakis, N. Mamouzelos, P. Tarantili, and A. Andreopoulos. Swelling and hydrolytic degradation of poly(d,l-lactic acid) in aqueous solutions. *Polymer Degradation and Stability*, 91(3):614–619, Mar. 2006. DOI: 10.1016/j.polymdegradstab.2005.01.060.

[167] M. Pronk, M. de Kreuk, B. de Bruin, P. Kamminga, R. Kleerebezem, and M. van Loosdrecht. Full scale performance of the aerobic granular sludge process for sewage treatment. *Water Research*, 84:207–217, Nov. 2015. DOI: 10.1016/j.watres.2015.07.011.

[168] J. Prosser. *Autotrophic Nitrification in Bacteria*. Elsevier, Amsterdam, 1990. DOI: 10.1016/s-2911(08)60112-5.

[169] S. Ramakrishnan and R. K. Prud'homme. Effect of solvent quality and ions on the rheology and gelation of κ-carrageenan. *Journal of Rheology*, 44(4):885–896, July 2000. DOI: 10.1122/1.551119.

[170] K. Rasmussen, C. Reilly, Y. Li, and R. S. Jones. Realtime imaging of antibiofilm effects using cp oct. *Biotechnology and Bioengineering*, 113(1):198–205, Sept. 2015. DOI: 10.1002/bit.25701.

[171] C. Reddy, R. Ghai, Rashmi, and V. Kalia. Polyhydroxyalkanoates: an overview. *Bioresource Technology*, 87(2):137–146, Apr. 2003. DOI: 10.1016/s0960-8524(02)00212-2.

[172] E. Reid, X. Liu, and S. Judd. Effect of high salinity on activated sludge characteristics and membrane permeability in an immersed membrane bioreactor. *Journal of Membrane Science*, 283(1-2):164–171, Oct. 2006. DOI: 10.1016/j.memsci.2006.06.021.

[173] X. Ren, D. Yu, S. Han, and Y. Feng. Thermolysis of recombinant escherichia coli for recovering a thermostable enzyme. *Biochemical Engineering Journal*, 33(1):94–98, Jan. 2007. DOI: 10.1016/j.bej.2006.09.017.

[174] M. Rigoulet, C. Bouchez, P. Paumard, S. Ransac, S. Cuvellier, S. Duvezin-Caubet, J. Mazat, and A. Devin. Cell energy metabolism: An update. *Biochimica et Biophysica Acta (BBA) - Bioenergetics*, 1861(11):148276, Nov. 2020. DOI: 10.1016/j.bbabio.2020.148276.

[175] R. Risi, L. Manti, G. Perna, M. Lasalvia, V. Capozzi, I. Delfino, and M. Lepore. X-ray radiation-induced effects in human mammary epithelial cells investigated by raman microspectroscopy. In J. Popp, W. Drexler, V. V. Tuchin, and D. L. Matthews, editors, *Biophotonics: Photonic Solutions for Better Health Care III*, volume 8427, page 84272E. SPIE, June 2012. DOI: 10.1117/12.921389.

[176] L. Rizzo, A. Fiorentino, and A. Anselmo. Advanced treatment of urban wastewater by uv radiation: Effect on antibiotics and antibiotic-resistant e. coli strains. *Chemosphere*, 92(2):171–176, June 2013. DOI: 10.1016/j.chemosphere.2013.03.021.

[177] R. Rupert, K. F. Rodrigues, V. Y. Thien, and W. T. L. Yong. Carrageenan From Kappaphycus alvarezii (Rhodophyta, Solieriaceae): Metabolism, Structure, Production, and Application. *Frontiers in Plant Science*, 13, May 2022. DOI: 10.3389/fpls.2022.859635.

[178] S. Saji, A. Hebden, P. Goswami, and C. Du. A Brief Review on the Development of Alginate Extraction Process and Its Sustainability. *Sustainability*, 14(9):5181, Apr. 2022. DOI: 10.3390/su14095181.

[179] M. Sajjad and K. S. Kim. Extraction of extracellular polymeric substances from activated sludge using sodium oxalate. *International Journal of Environmental Science and Technology*, 13(7):1697–1706, May 2016. DOI: 10.1007/s13762-016-1004-5.

[180] H. Sanawar, I. Pinel, N. Farhat, S. Bucs, J. Zlopasa, J. Kruithof, G. Witkamp, M. van Loosdrecht, and J. Vrouwenvelder. Enhanced biofilm solubilization by urea in reverse osmosis membrane systems. *Water Research X*, 1:100004, Dec. 2018. DOI: 10.1016/j.wroa.2018.10.001.

[181] C. M. Santegoeds, L. R. Damgaard, G. Hesselink, J. Zopfi, P. Lens, G. Muyzer, and D. de Beer. Distribution of sulfate-reducing and methanogenic bacteria in anaerobic aggregates determined by microsensor and molecular analyses. *Applied and Environmental Microbiology*, 65(10):4618–4629, Oct. 1999. DOI: 10.1128/aem.65.10.4618-4629.1999.

[182] C. M. Schambeck, E. Girbal-Neuhauser, L. Böni, P. Fischer, Y. Bessière, E. Paul, R. H. R. da Costa, and N. Derlon. chemical and physical properties of alginate-like exopolymers of aerobic granules and flocs produced from different wastewaters. *Bioresource Technology*, 312:123632, Sept. 2020. DOI: 10.1016/j.biortech.2020.123632.

[183] T. Schmid, A. Messmer, B.-S. Yeo, W. Zhang, and R. Zenobi. Towards chemical analysis of nanostructures in biofilms II: tip-enhanced Raman spectroscopy of alginates. *Analytical and Bioanalytical Chemistry*, 391(5):1907–1916, Apr. 2008. DOI: 10.1007/s00216-008-2101-1.

[184] I. Schmidt, O. Sliekers, M. Schmid, E. Bock, J. Fuerst, J. G. Kuenen, M. S. Jetten, and M. Strous. New concepts of microbial treatment processes for the nitrogen removal in wastewater. *FEMS Microbiology Reviews*, 27(4):481–492, Oct. 2003. DOI: 10.1016/s0168-6445(03)00039-1.

[185] J. Schmitt and H.-C. Flemming. FTIR-spectroscopy in microbial and material analysis. *International Biodeterioration and Biodegradation*, 41(1):1–11, Jan. 1998. DOI: 10.1016/s0964-8305(98)80002-4.

[186] A. Schmoldt, H. F. Benthe, and G. Haberland. Digitoxin metabolism by rat liver microsomes. *Biochemical pharmacology*, 24:1639–1641, Sept. 1975.

[187] T. Seviour, N. Derlon, M. S. Dueholm, H.-C. Flemming, E. Girbal-Neuhauser, H. Horn, S. Kjelleberg, M. C. van Loosdrecht, T. Lotti, M. F. Malpei, R. Nerenberg, T. R. Neu, E. Paul, H. Yu, and Y. Lin. Extracellular polymeric substances of biofilms: Suffering from an identity crisis. *Water Research*, 151:1–7, Mar. 2019. DOI: 10.1016/j.watres.2018.11.020.

[188] T. Seviour, M. Pijuan, T. Nicholson, J. Keller, and Z. Yuan. Gel-forming exopolysaccharides explain basic differences between structures of aerobic sludge granules and floccular sludges. *Water Research*, 43(18):4469–4478, Oct. 2009. DOI: 10.1016/j.watres.2009.07.018.

[189] G.-P. Sheng, H.-Q. Yu, and X.-Y. Li. Extracellular polymeric substances (EPS) of microbial aggregates in biological wastewater treatment systems: A review. *Biotechnology Advances*, 28(6):882–894, Nov. 2010. DOI: 10.1016/j.biotechadv.2010.08.001.

[190] B. Shivu, S. Seshadri, J. Li, K. A. Oberg, V. N. Uversky, and A. L. Fink. Distinct beta-Sheet Structure in Protein Aggregates Determined by ATR-FTIR Spectroscopy. *Biochemistry*, 52(31):5176–5183, July 2013. DOI: 10.1021/bi400625v.

[191] K.-Y. Show and D.-J. Lee. *Anaerobic Treatment Versus Aerobic Treatment*, pages 205–230. Elsevier, Amsterdam, 2017. DOI: 10.1016/b978-0-444-63665-2.00008-4.

[192] K.-Y. Show, Y. Yan, H. Yao, H. Guo, T. Li, D.-Y. Show, J.-S. Chang, and D.-J. Lee. Anaerobic granulation: A review of granulation hypotheses, bioreactor designs and emerging green applications. *Bioresource Technology*, 300:122751, Mar. 2020. DOI: 10.1016/j.biortech.2020.122751.

[193] B. J. Singh, A. Chakraborty, and R. Sehgal. A systematic review of industrial wastewater management: Evaluating challenges and enablers. *Journal of Environmental Management*, 348:119230, Dec. 2023. DOI: 10.1016/j.jenvman.2023.119230.

[194] C. M. Singleton, F. Petriglieri, K. Wasmund, M. Nierychlo, Z. Kondrotaite, J. F. Petersen, M. Peces, M. S. Dueholm, M. Wagner, and P. H. Nielsen. The novel genus, candidatus phosphoribacter, previously identified as tetrasphaera, is the dominant polyphosphate accumulating lineage in ebpr wastewater treatment plants worldwide. *The ISME Journal*, 16(6):1605–1616, Feb. 2022. DOI: 10.1038/s41396-022-01212-z.

[195] S. Sivaprakasam, S. Mahadevan, S. Sekar, and S. Rajakumar. Biological treatment of tannery wastewater by using salt-tolerant bacterial strains. *Microbial Cell Factories*, 7(1), Apr. 2008. DOI: 10.1186/1475-2859-7-15.

[196] T. Solov'eva, V. Davydova, I. Krasikova, and I. Yermak. Marine compounds with therapeutic potential in gram-negative sepsis. *Marine Drugs*, 11(6):2216–2229, June 2013. DOI: 10.3390/md11062216.

[197] W. Song, S. Ding, L. Zhou, N. Li, Y. Zhang, H. Li, J. Ding, and J. Lu. The performance of co-immobilized strains isolated from activated sludge combined with scenedesmus quadricauda to remove nutrients and organics in black odorous water. *Bioresource Technology*, 345:126571, Feb. 2022. DOI: 10.1016/j.biortech.2021.126571.

[198] A. Sonune and R. Ghate. Developments in wastewater treatment methods. *Desalination*, 167:55–63, 2004.

[199] D. T. Sponza. Investigation of extracellular polymer substances (EPS) and physicochemical properties of different activated sludge flocs under steady-state conditions. *Enzyme and Microbial Technology*, 32(3-4):375–385, Mar. 2003. DOI: 10.1016/s0141-0229(02)00309-5.

[200] O. V. Stepanenko, O. V. Stepanenko, I. M. Kuznetsova, V. V. Verkhusha, and K. K. Turoverov. Sensitivity of superfolder gfp to ionic agents. *PLoS ONE*, 9(10):e110750, Oct. 2014. DOI: 10.1371/journal.pone.0110750.

[201] G. Steurs. personal communication.

[202] G. Steurs. Advanced NMR Spectroscopy: NMR Data Tables. page 10, 2024.

[203] D. Sudmalis, M. Gagliano, R. Pei, K. Grolle, C. Plugge, H. Rijnaarts, G. Zeeman, and H. Temmink. Fast anaerobic sludge granulation at elevated salinity. *Water Research*, 128:293–303, Jan. 2018. DOI: 10.1016/j.watres.2017.10.038.

[204] D. Sudmalis, S. Millah, M. Gagliano, C. Butre, C. Plugge, H. Rijnaarts, G. Zeeman, and H. Temmink. The potential of osmolytes and their precursors to alleviate osmotic stress of anaerobic granular sludge. *Water Research*, 147:142–151, Dec. 2018. DOI: 10.1016/j.watres.2018.09.059.

[205] D. Sudmalis, T. Mubita, M. Gagliano, E. Dinis, G. Zeeman, H. Rijnaarts, and H. Temmink. Cation exchange membrane behaviour of extracellular polymeric substances (EPS) in salt adapted granular sludge. *Water Research*, 178:115855, July 2020. DOI: 10.1016/j.watres.2020.115855.

[206] G. P. Szekeres and J. Kneipp. Sers probing of proteins in gold nanoparticle agglomerates. *Frontiers in Chemistry*, 7, Jan. 2019. DOI: 10.3389/fchem.2019.00030.

[207] M. G. Tecson, D. H. Camacho, V. D. Ebajo, and L. V. Abad. Structural investigation of degradation products of irradiated kappa-carrageenan. *Radiation Physics and Chemistry*, 194:110015, May 2022. DOI: 10.1016/j.radphyschem.2022.110015.

[208] T. Thrimawithana, S. Young, D. Dunstan, and R. Alany. Texture and rheological characterization of kappa and iota carrageenan in the presence of counter ions. *Carbohydrate Polymers*, 82(1):69–77, Aug. 2010. DOI: 10.1016/j.carbpol.2010.04.024.

[209] X. Tian, Z. Shen, Z. Han, and Y. Zhou. The effect of extracellular polymeric substances on exogenous highly toxic compounds in biological wastewater treatment: An overview. *Bioresource Technology Reports*, 5:28–42, Feb. 2019. DOI: 10.1016/j.biteb.2018.11.009.

[210] United States Environmental Protection Agency. Effluent guidelines, 2024. https://www.epa.gov/eg, [Accessed on 11/11/2024].

[211] R. Van den Broeck. *Activated sludge mixed liquor characteristics versus membrane fouling in MBRs*. PhD thesis, KULeuven, 2011.

[212] B. Van der Bruggen. *Waste Water Treatment Technology Part I: Legislation in Flanders and Primary Waste Water Technology*. Acco Leuven, 2018.

[213] J. Van Dierdonck. *Impact of Influent Characteristics on Activated Sludge Bioflocculation in Lab-scale Systems*. PhD thesis, KULeuven, 2013.

[214] K. van Leeuwen, E. de Vries, S. Koop, and K. Roest. The energy and raw materials factory: Role and potential contribution to the circular economy of the netherlands. *Environmental Management*, 61(5):786–795, Jan. 2018. DOI: 10.1007/s00267-018-0995-8.

[215] J. B. van Lier, F. P. van der Zee, C. T. M. J. Frijters, and M. E. Ersahin. Celebrating 40 years anaerobic sludge bed reactors for industrial wastewater treatment. *Reviews in Environmental Science and Biotechnology*, 14(4):681–702, Aug. 2015. DOI: 10.1007/s11157-015-9375-5.

[216] Vlaamse Milieu Maatschappij. Wet op de bescherming van de oppervlaktewateren tegen verontreiniging, 2024. https://www.vmm.be/wetgeving/

wet-op-de-bescherming-van-de-oppervlaktewateren-tegen-verontreiniging [Accessed on 11/11/2024].

[217] I. Vyrides, H. Santos, A. Mingote, M. J. Ray, and D. C. Stuckey. Are compatible solutes compatible with biological treatment of saline wastewater? batch and continuous studies using submerged anaerobic membrane bioreactors (sambrs). *Environmental Science and Technology*, 44(19):7437–7442, Sept. 2010. DOI: 10.1021/es903981k.

[218] M. Wagner, N. P. Ivleva, C. Haisch, R. Niessner, and H. Horn. Combined use of confocal laser scanning microscopy (CLSM) and Raman microscopy (RM): Investigations on EPS - Matrix. *Water Research*, 43(1):63–76, Jan. 2009. DOI: 10.1016/j.watres.2008.10.034.

[219] D. Wang, N. Dong, S. Hui, and Y. Niu. Analysis of urea pyrolysis products in 132.5-190degreesc. *Energy Procedia*, 158:2170–2175, Feb. 2019. DOI: 10.1016/j.egypro.2019.01.616.

[220] J. Wang and H. Chen. Catalytic ozonation for water and wastewater treatment: Recent advances and perspective. *Science of The Total Environment*, 704:135249, Feb. 2020. DOI: 10.1016/j.scitotenv.2019.135249.

[221] Z. Wang, Z. Wu, and S. Tang. Extracellular polymeric substances (EPS) properties and their effects on membrane fouling in a submerged membrane bioreactor. *Water Research*, 43(9):2504–2512, May 2009. DOI: 10.1016/j.watres.2009.02.026.

[222] C. Wei, F. Zhang, Y. Hu, C. Feng, and H. Wu. Ozonation in water treatment: the generation, basic properties of ozone and its practical application. *Reviews in Chemical Engineering*, 33(1):49–89, July 2016. DOI: 10.1515/revce-2016-0008.

[223] Y. Wei, R. T. Van Houten, A. R. Borger, D. H. Eikelboom, and Y. Fan. Minimization of excess sludge production for biological wastewater treatment. *Water Research*, 37(18):4453–4467, Nov. 2003. DOI: 10.1016/s0043-1354(03)00441-X.

[224] D. T. Welsh. Ecological significance of compatible solute accumulation by microorganisms: from single cells to global climate. *FEMS Microbiology Reviews*, 24(3):263–290, July 2000. DOI: 10.1111/j.1574-6976.2000.tb00542.x.

[225] M. K. Winkler, R. Kleerebezem, W. O. Khunjar, B. de Bruin, and M. C. van Loosdrecht. Evaluating the solid retention time of bacteria in flocculent and granular sludge. *Water Research*, 46(16):4973–4980, Oct. 2012. DOI: 10.1016/j.watres.2012.06.027.

[226] Y. Xiao and D. J. Roberts. A review of anaerobic treatment of saline wastewater. *Environmental Technology*, 31(8):1025–1043, jul 2010. DOI: 10.1080/09593331003734202.

[227] W. Xing, M. Yin, Q. Lv, Y. Hu, C. Liu, and J. Zhang. *Oxygen Solubility, Diffusion Coefficient, and Solution Viscosity*, pages 1–31. Elsevier, Amsterdam, 2014. DOI: 10.1016/b978-0-444-63278-4.00001-x.

[228] H.-Y.-Y. Yao, J.-Q. Wang, J.-Y. Yin, S.-P. Nie, and M.-Y. Xie. A review of NMR analysis in polysaccharide structure and conformation: Progress, challenge and perspective. *Food Research International*, 143:110290, May 2021. DOI: 10.1016/j.foodres.2021.110290.

[229] D. P. Zagklis and G. Bampos. Tertiary Wastewater Treatment Technologies: A Review of Technical, Economic, and Life Cycle Aspects. *Processes*, 10(11):2304, nov 2022. DOI: 10.3390/pr10112304.

[230] S. A. Zahra, R. Persiani, M. K. Dueholm, M. van Loosdrecht, P. H. Nielsen, T. W. Seviour, and Y. Lin. Rethinking characterization, application, and importance of extracellular polymeric substances in water technologies. *Current Opinion in Biotechnology*, 89:103192, Oct. 2024. DOI: 10.1016/j.copbio.2024.103192.

[231] N. S. Zaidi, K. Muda, and M. Sillanpaa. Effects of extra-cellular polymeric substances towards physical properties of biomass under magnetic field exposure. *International Journal of Environmental Science and Technology*, 16(7):3801–3808, July 2018. DOI: 10.1007/s13762-018-1897-2.

[232] W. Zeng, F. Li, C. Wu, R. Yu, X. Wu, L. Shen, Y. Liu, G. Qiu, and J. Li. Role of extracellular polymeric substance (EPS) in toxicity response of soil bacteria Bacillus sp. S3 to multiple heavy metals. *Bioprocess and Biosystems Engineering*, 43(1):153–167, Sept. 2019. DOI: 10.1007/s00449-019-02213-7.

[233] L. Zhang, X. Lin, Z. Zhang, G.-H. Chen, and F. Jiang. Elemental sulfur as an electron acceptor for organic matter removal in a new high-rate anaerobic biological wastewater treatment process. *Chemical Engineering Journal*, 331:16–22, Jan. 2018. DOI: 10.1016/j.cej.2017.08.055.

[234] S. Zhang, S. Wakai, N. Sasakura, H. Tsutsumi, Y. Hata, C. Ogino, and A. Kondo. Pyruvate metabolism redirection for biological production of commodity chemicals in aerobic fungus aspergillus oryzae. *Metabolic Engineering*, 61:225–237, Sept. 2020. DOI: 10.1016/j.ymben.2020.06.010.

[235] J. Zheng, C. Su, J. Zhou, L. Xu, Y. Qian, and H. Chen. Effects and mechanisms of ultraviolet, chlorination, and ozone disinfection on antibiotic resistance genes in secondary effluents of municipal wastewater treatment plants. *Chemical Engineering Journal*, 317:309–316, June 2017. DOI: 10.1016/j.cej.2017.02.076.

[236] Y. N. Zhou, J. Li, J. Li, and S. Wei. Dewaterability of aerobic granular sludge. *Applied Mechanics and Materials*, 90-93:2944–2948, Sept. 2011. DOI: 10.4028/www.scientific.net/amm.90-93.2944.

[237] L. Zhu, H.-y. Qi, M.-l. Lv, Y. Kong, Y.-w. Yu, and X.-y. Xu. Component analysis of extracellular polymeric substances (EPS) during aerobic sludge granulation using FTIR and 3D-EEM technologies. *Bioresource Technology*, 124:455–459, Nov. 2012. DOI: 10.1016/j.biortech.2012.08.059.

[238] J. Zlopasa, E. Koenders, and S. Picken. Using bio-based polymers for curing cement-based materials. In *AMS 14 Proceedings of the Int. Conference on Ageing of Materials and Structures*, pages 220–226, 2014.

[239] V. Zorraquino, D. Toubiana, D. Yan, and E. Blumwald. Draft Genome Sequence of the Nitrogen-Fixing Endophyte Azoarcus communis SWub3. *Microbiology Resource Announcements*, 7(13), Oct. 2018. DOI: 10.1128/mra.01080-18.

[240] E. Zuriaga-Agusti, A. Bes-Pia, J. Mendoza-Roca, and J. Alonso-Molina. Influence of extraction methods on proteins and carbohydrates analysis from MBR activated sludge flocs in view of improving EPS determination. *Separation and Purification Technology*, 112:1–10, July 2013. DOI: 10.1016/j.seppur.2013.03.048.